REPORT DOCUMENTATION PAGE

Form Approved
OMB No. 0704-0188

The public reporting burden for this collection of information is estimated to average 1 hour per response, including the time for reviewing instructions, searching existing data sources, gathering and maintaining the data needed, and completing and reviewing the collection of information. Send comments regarding this burden estimate or any other aspect of this collection of information, including suggestions for reducing the burden, to Department of Defense, Washington Headquarters Services, Directorate for Information Operations and Reports (0704-0188), 1215 Jefferson Davis Highway, Suite 1204, Arlington, VA 22202-4302. Respondents should be aware that notwithstanding any other provision of law, no person shall be subject to any penalty for failing to comply with a collection of information if it does not display a currently valid OMB control number.

PLEASE DO NOT RETURN YOUR FORM TO THE ABOVE ADDRESS.

1. REPORT DATE *(DD-MM-YYYY)*	2. REPORT TYPE	3. DATES COVERED *(From - To)*
27-03-2009	FINAL	22-01-2007 - 21-07-2009

4. TITLE AND SUBTITLE

Mission-Adaptable Chemical Sensor (MACS)

5a. CONTRACT NUMBER

W911NF-07-C-0009

5b. GRANT NUMBER

5c. PROGRAM ELEMENT NUMBER

6. AUTHOR(S)

Dr. Keith Reiss

5d. PROJECT NUMBER

51461-EL-DRP

5e. TASK NUMBER

5f. WORK UNIT NUMBER

7. PERFORMING ORGANIZATION NAME(S) AND ADDRESS(ES)

Smart Transitions, LLC
10461 White Granite Drive, Suite 103
Oakton VA 22124

8. PERFORMING ORGANIZATION REPORT NUMBER

9. SPONSORING/MONITORING AGENCY NAME(S) AND ADDRESS(ES)

U.S. Army Research Office
P.O. Box 12211
Research Triangle Park, NC 27709-2211

10. SPONSOR/MONITOR'S ACRONYM(S)

DARPA/STO

11. SPONSOR/MONITOR'S REPORT NUMBER(S)

12. DISTRIBUTION/AVAILABILITY STATEMENT

Approved for public release; distribution unlimited.

13. SUPPLEMENTARY NOTES

The views, opinions and/or findings contained in this report are those of the author(s) and should not be construed as an official Department of the Army position, policy or decision, unless so designated by other documentation.

14. ABSTRACT

MACS (Mission Adaptable Chemical Sensor) commenced as a concept for creating a complex chemical signatures potentially targeting illicit operations of interest, notably irregular or covert manufacturing sites of WMDs, IEDs, or drugs. In order to do this, the initial CONOPS was for the placement of a MACS in a very low altitude UAV. The CONOPS further would permit autonomous guidance within the sensory area of interest by permitting MACS software to adjust the mission waypoints so as to home in on the source of a particular "disturbance," or a plume containing the signature elements. As DARPA embraced the concept of MACS, the mission capabilities became more general. Not only would the initial mission concept remain a distinct possibility, but many others as well. What is the MACS concept? The answer is essentially twofold: (1) to produce a system that can ingest a relatively small quantity of air at 1 atm pressure that is then assayed within a core submillimeter wave precision spectrometer-based sensor; and to surround the basic spectrometer with a flexible set of subsystems that will provide great flexibility and thus "mission adaptability."

15. SUBJECT TERMS

spectrometry, chemical weapons, illicit drugs

16. SECURITY CLASSIFICATION OF:			17. LIMITATION OF ABSTRACT	18. NUMBER OF PAGES	19a. NAME OF RESPONSIBLE PERSON
a. REPORT	b. ABSTRACT	c. THIS PAGE			Dr. Keith Reiss
U	U	U	UU	217	19b. TELEPHONE NUMBER *(Include area code)* 703-346-4751

Mission-Adaptable Chemical Sensor (MACS)

Final Report

Prepared for the Defense Advanced Programs Agency,
Strategic Technologies Office

Dr. Frank Patten

27 March 2009

Under Contract:

W911NF-070C-0009

Smart Transitions, LLC
10461 White Granite Drive
Suite 103
Oakton, VA 22124

Table of Content

1 Executive Summary

MACS (Mission Adaptable Chemical Sensor) commenced as a concept for creating a complex chemical signatures potentially targeting illicit operations of interest, notably irregular or covert manufacturing sites of WMDs, IEDs, or drug processing. In order to accomplish this, the initial CONOPS was for the placement of a MACS in a very low altitude UAV. The CONOPS further would permit autonomous guidance within the sensory area of interest by permitting MACS software to adjust the mission waypoints so as to home in on the source of a particular "disturbance." The disturbance in this case would be the abundance of a plume containing the signature elements. As DARPA embraced the concept of MACS, the mission capabilities became more general. Not only would the initial mission concept remain a distinct possibility, but many others as well as shown by Figure 1.1.

Figure 1.1. Some potential MACS missions.

What is the MACS concept? The answer is essentially two fold: (1) to produce a system that can ingest a relatively small quantity of air[1] 1 atm pressure that is then assayed within a core submillimeter wave precision spectrometer-based sensor; and to surround the basic spectrometer with a flexible set of subsystems that will provide great flexibility and thus "mission adaptability."

Rotational spectroscopy (Figure 1.2) is the key to providing maximum selectivity in the identification of individual gas species and also, fortuitously, also provides a regime of optimum sensitivity. And although ideal for the purposes envisioned, has not until MACS become a real

[1] The system can also ingest a non atmospheric sample at any pressure from a flask. This represents a completely different scenario from the main line scenario mentioned in the text.

world capability for a miniature sensor. The conventional academic laboratories have been operating with rather large and impractical systems, possibly fully tube dependent and utilizing cold detectors. MACS, on the other hand, must be fully solid state and so far, with room temperature detection. The trades in sensitivity (namely noise reduction via incoherent spectral integration and other factors such as detector cooling) may yet suggest improvements that may alter the Phase 1 system result (which has no detector cooling).

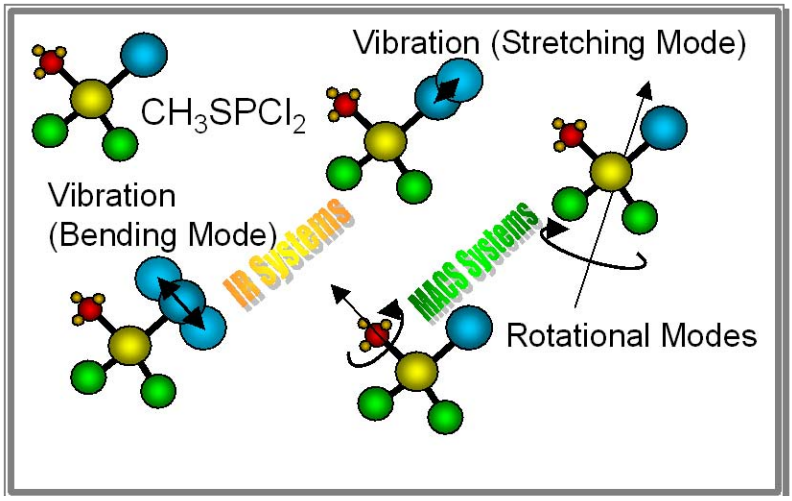

Figure 1.2. Classical sensors employing spectroscopy for gases are IR systems; MACS looks at the less energetic and far more signature rich rotational transitions.

The standard approach within the university laboratory has no need for a front end, and yet this becomes the most significant aspect of the program to miniaturize the system and to provide preconcentration of the atmospheric sample with perhaps 100,000X gains accruing. In operating the tiny THz spectrometer sample cell system at the optimum pressure (about 10 mT where the pressure and Doppler broadening are about equivalent) we find a best point in the playoff between sensitivity and selectivity. Less pressure and we lose sensitivity; more sample (i.e., pressure) and our lines broaden and we commence to lose specificity. Rotational lines at atmosphere have line widths of approximately 5 GHz which simply jumbles the lines into energy absorption bands that carry virtually no useful information; and yet at our MACS operating pressure they are about 3 MHz. Our resolution is about 1/33 of a line width. Therefore we are easily capable of rendering precise frequency measurements associated with the signal processing of the resultant spectra rendered from scans of various portion s of the overall 60 GHz operational band pass of the system (in the 200 GHz regime).

The system operates from the standpoint of superior frequency knowledge that permits computations to render precise matches between library spectra (i.e., the ROM-based digital spectra and derivative products [peak frequencies and line widths]) and the empirical spectra when properly adjusted by concentration proportionality factors. The match between a library line and an empirical line when taken together with the library sample call concentration and the preconcentration gain for the empirical line and its measured intensity facilitate the system's assay capability. That is, the rendering of the input atmospheric concentration of each detected species.

The Phase 1 system embraced several important physical and performance objectives; namely to produce an integrated system in a 1 cubic foot box and be able to differentiate 30 gases in a mixture and detect down to a 100 ppt sensitivity level with very high PDF and very low PFA (0.9999 and 0.0001, respectively). These objectives and more were met by the Phase 1 system, which is covered in detail within this report.

In addition to the technical objectives and achievements, the program plan includes activities of the MAG (MACS Advisory Group) intended primarily to attract and familiarize elements of various potential user communities with the existence and future potentials of MACS derivative

systems. The ultimate objective is recognized as the production of new US sensor system capability, and the methodology we have employed has been dependent upon several targeted applied research efforts to provide answers and optimizations for aspects of this system development that were not available or yet suitable for integration into a sensor product. Future phases of the program will successively lead to the production of field activity demonstration systems that can lead directly to production.

In conceiving the notion of a point sensor employing rotational spectroscopy as the key element in detection and classification, we assembled a team of experts that for Phase 1 would be responsible for adapting laboratory scale technologies into a very small package. In general, ST leads the systems engineering and central electronics; OSU leads the development of the spectroscopic techniques; and likewise Battelle leads in the development of preconcentration techniques. The entire team then converts the techniques selected into not a breadboard, but a working prototype

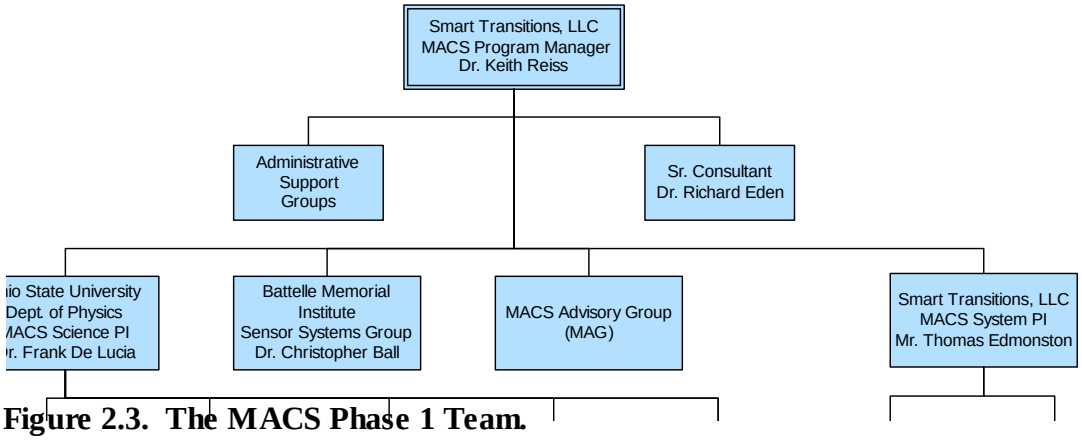

Figure 2.3. The MACS Phase 1 Team.

2 MACS System Architecture

As shown in the functional block diagram (Figure 2.1), the functions of MACS were divided into three subsystems the Sample Acquisition And Processing module (SAPM); the sample cell and terahertz generation electronic (simply know as the THz module); and the core electronics consisting of the remaining functions such as power generation and distribution, central computing, and the frequency management system (FMS) that functions as a base-band spectrometer. The interfaces between these subsystems are robust and straightforward to allow the units to be built and tested by discrete development teams and integrated near the end of the program. Specifically the interfaces are power, serial communications and a few isolated RF connections.

The MACS systems architecture was driven primarily by the requirements to fit within a 1 cubic foot chassis, a required sensitivity of better than 100 PPT, and an 18 month development cycle. These somewhat mutually exclusive requirements caused the team to choose a high probability of success design utilizing COTS components to the largest extent possible. The core spectrometer and THz module are the two segments of MACS where COTS components were not available and required OSU and ST to execute significant development efforts. A more custom design approach on the follow-on system would result in a system with similar performance but significantly lower power consumption and size.

The resulting design is a rack mountable instrument fitting in a 3U high (5.25") 17 inch wide chassis approximately 19.4 inches deep. The unit is powered from standard US wall power (120 VAC). The front panel has a power button, touch screen display, two USB ports, and the gas inlet port. The touch screen display provides a Graphical User Interface for a user to interact with the unit. The USB ports allow the user to connect a keyboard, mouse or memory stick device. The rear panel has an IEC power connector, VGA output connector, pumping exhaust port, and direct injection proportional valve. A standard power cord attaches to the IEC connector and connects MACS to a 15 amp wall outlet. The exhaust port vents the analyte under test at the end of the cycle and therefore may be connected to "house exhaust" to satisfy OSHA requirements. The direct injection valve can be used to bypass the sorbent system during system testing or for bleeding air into the sample cell.

The following high level steps represent a single cycle of the spectrometer system:

1. The SAPM is activated reducing the pressure in the THz module to less than 1 millitorr removing any residual sample and readying the system for spectroscopy.
2. The gas sample is pulled across a sorbent bed, used to collect and concentrate analytes while allowing bulk atmosphere such as nitrogen, oxygen, and carbon dioxide to pass.
3. The inlet valve is closed and the pressure in the sorbent collection chamber is reduced to less than 1 millitorr to eliminate the rest of the bulk atmospherics.
4. The sorbent chamber is isolated from the pumping system and the transfer valve is opened. Heat is applied to the sorbent to cause trapped analytes to be released into the sample cell.
5. Pressure in the sample cell to adjusted to 10 millitorr by pumping out excess sample or bleeding in additional atmosphere automatically as each scenario dictates. This is the optimum pressure for spectroscopy where the pressure and Doppler broadening are about equal whereby minimizing line widths and maximizing the instruments' specificity.

6. The CC now instructs the FMS to generate the sweep frequencies required by the THz module. This is a swept receiver configuration where the two frequencies maintain a 10.7 MHz offset (at final frequency) throughout the sweep. The specific sweep frequencies are a function of the "scenario" being executed by the user. This could be a full band sweep in the case of building a library or possibly a segmented search of the strongest line of each analyte in the library. In the latter case a single line detection would cause the CC to expand the search to include additional lines of the suspected analyte to improve the probability of detection. Frequency modulation is applied to allow first or second derivative detection.
7. The FMS frequencies are multiplied by 24 using microwave diodes to produce approximately 1 mW of power in the 210 to 270 GHz band. A wire grid polarizer allows this power to be adjusted to prevent saturation of the system. As the system sweeps analytes contained in the sample cell are excited and at analyte specific frequencies the millimeter wave energy is absorbed. This provides a unique signature for each analyte.
8. The FMS detects the power of the 10.7 MHz intermediate frequency provided by the THz module at 600 K samples per second providing for a power verses swept frequency display. Additionally signal processing is performed to selectively capture the frequency modulation information (digital lock-in function) at the 1x or 2x rate to recover the first or second derivative respectively. Detection of the derivatives helps reduce the effects of base-line variations due to VSWR and other effects not associated with rotational absorption.
9. The demodulated absorption data is transferred from the FMS to the CC via a high speed 32 bit parallel buss where it is further processed to provide accurate frequency registration and amplitude calibration.
10. These "normalized" sweeps are then passed to the analysis engine (contained within the CC) where line detections are compared to library information and specific chemical detections are determined. Additionally this module assesses the concentration levels of the detected analyte at the inlet port.
11. Detections and concentration levels are displayed on the front panel

This total process takes less than 7 minutes and is ready to repeat immediately allowing for persistent monitoring of an environment.

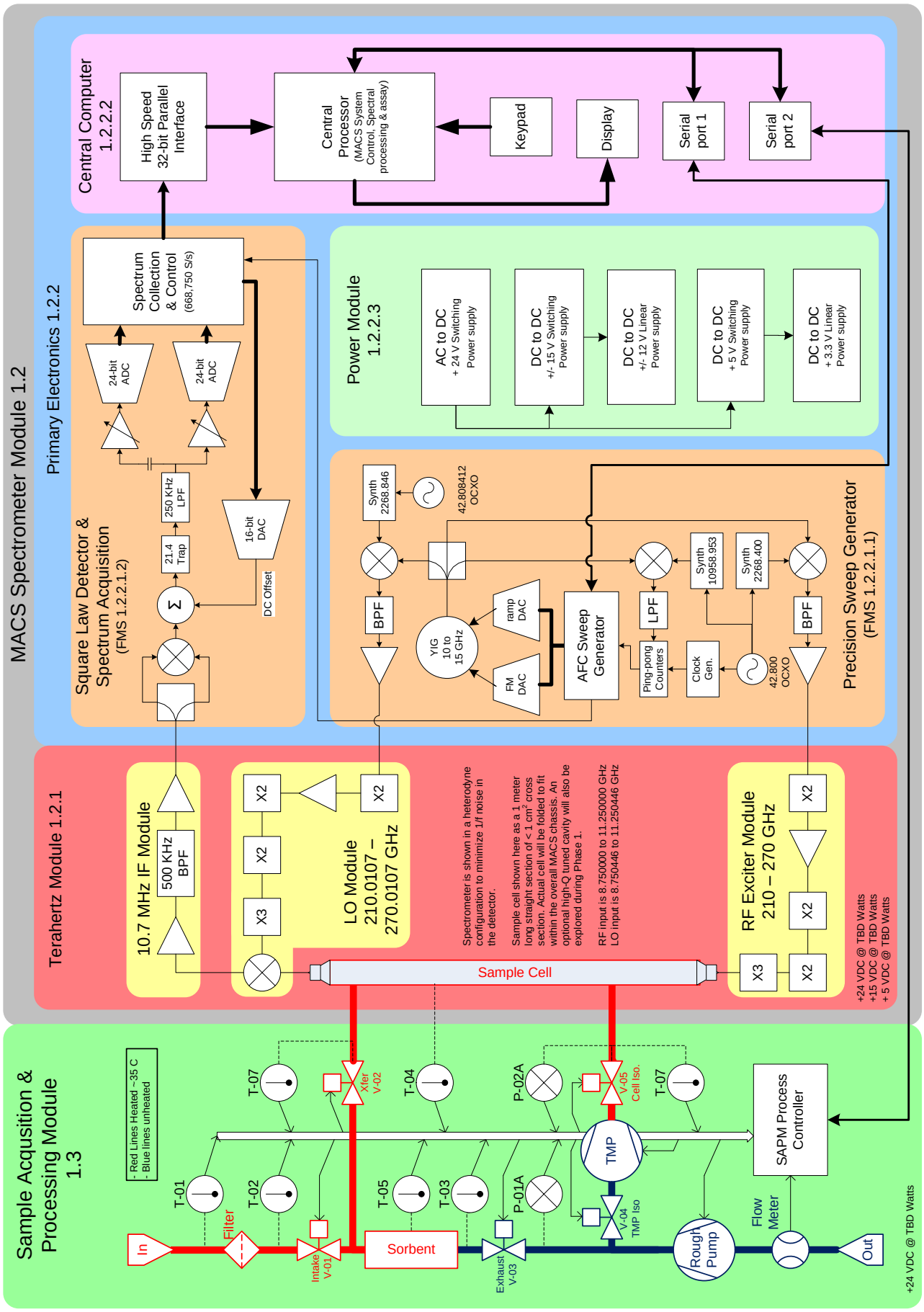

Figure 2.1. MACS1 Functional diagram.

3 SAPM (Sample Acquisition and Processing Module)

The Sample Acquisition and Processing Module (SAPM) is a sub-system responsible for the following functionality in the MACS system:

- Collection of air samples over a pre-defined collection cycle (~several minutes)
- Separation of trace analytes from major atmospheric constituents
- Accumulation of analytes over collection cycle
- Evacuation of the THz spectroscopy cell
- Transfer of collected analytes to the evacuated cell for spectral interrogation
- Communication of SAPM status to the MACS central computer
- Introduction of make-up air or direct inject of sample gases (for testing purposes).

The SAPM is composed of two primary sub-systems. The SAPM Base Module (SBM) includes a pumping system to pull air samples through the system and to evacuate the THz cell, tubing and valves to connect various components, pressure sensors to monitor the manifold and THz cell pressures, heaters to control manifold and cell temperatures, and electronics and software to control operations and communicate with the MACS central computer. The SAPM Mission Module (SMM) contains the sorbent-based pre-concentrator (3D sorbet tube or 2D sorbent disk) and heaters to enable desorption of the concentrated analytes. The SMM can be configured for specific missions via the choice of sorbent materials, which can preferentially adsorb certain classes of materials better or worse than other sorbents.

Figure 3.1 shows overview of the general SAPM configuration, including pumps, valves, pressure sensors, interface to the THz cell, and sample inlet and outlet. This figure primarily shows the SBM, with the SMM embedded on the interior of the SBM. The rest of this section describes the design trades conducted early in the program that identified some of the SAPM components (Section 3.1), an overview of the system operation (Section 3.2), research and development activities that will lead to Phase 2 improvements (Section 3.3), SAPM design specifications and engineering drawings (Section 3.4), and an overview of SAPM performance (Section 3.5).

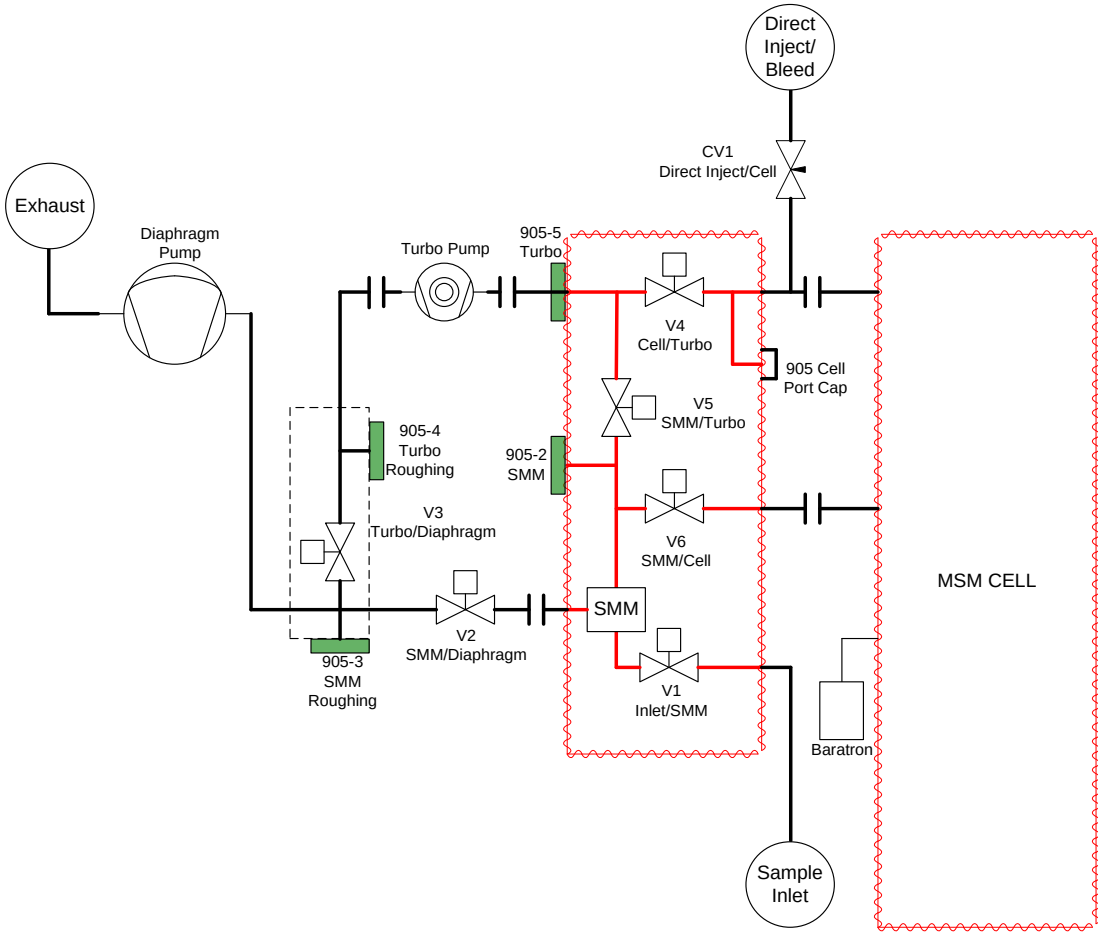

Figure 3.1. Overview of SAPM configuration (red indicates heated components)

3.1 Summary of Trades and R&D Leading to Design

This section describes the two main trade studies that were conducted in the early stages of the SAPM development. These studies involve the selection of appropriate pumping (Section 3.1.1) and pre-concentrator (Section 3.1.2) technologies.

3.1.1 Pump Selection

The choice of vacuum technology components for the SAPM was a critical engineering decision with significant impact on the process development schedule, system size, and specification of other system parameters (e.g. tube sizes and evacuation time). The specifications driving vacuum equipment selection were mainly cell pressure (<10 mTorr prior to sample injection) and overall system size (1 ft^3). Early on, turbomolecular pumps were identified as leading candidates for their established use in analytical systems, compact design, high effective pumping speed, and electrical compatibility. Initially a miniature unit from Creare was investigated. Creare does not specialize in vacuum products; they are a R&D company that sells a pump they developed for NASA. While the turbo itself was small (12 in^3), they do not offer a complete solution which includes a turbo controller and backing pump (both larger components that must be considered). They are extremely expensive ($60,000 each). They are not mass produced, and it is unknown how many they have sold or what reliability can be expected. Battelle assessed that the Creare pump would be a risk for process development, but a candidate for future miniaturization phases.

The search for a turbo pump system extended to include more traditional vacuum products companies such as BOC Edwards, Welch, Alcatel, Shimadzu, and Varian. The common problems with products from these companies are 1) large, external turbo controllers 2) large backing pumps. For example, the smallest solution from Edwards is a turbo pump, controller, and backing pump at 100 in^3, 259 in^3, and 437 in^3, respectively. The volume of these components alone is nearly 800 in^3, or 46% of the entire system allotment.

During the search for suitable pumps, both Battelle and the OSU team separately came across a product from Pfeiffer Vacuum. Advertised as the world's smallest mass produced drag pump and on the market since 2000, they use an integrated controller and compact backing pump for a complete miniature vacuum solution. The TPD 011 turbo pump with controller measures 4.65" X 6.63" X 6.75" = 208 in^3 and the MVP 006 backing pump is 7.09" X 3.92" X 4.17" = 116 in^3. The total volume is 324 in^3 which is roughly 19% of the overall system.

A study of pipe and orifice losses and evacuation time convinced Battelle that the performance of the Pfeiffer pump system was adequate. The turbo pump has an ultimate pressure of 10^{-5} mbar, rated flow of 10 L/s, and maximum backing pressure of 25 mbar. The pump has a magnetic bearing on the high vacuum side and a lubricated bearing on the low vacuum side. The lubricant was assessed as a potential trace contaminant, but found not to be a significant source of contaminant gases. Battelle was unable to assess the system effects of vibration and magnetic fields caused by the turbopump before development. The backing pump has an ultimate pressure of <2 mbar and rated flow of 6 L/min.

In summary, the MACS system size requirement severely limited our options for vacuum pump components, and the Pfeiffer system was judged to be the quickest path to a demonstration system.

3.1.2 Pre-Concentrator Technology

In order to achieve the ambitious performance specification of 100 ppt sensitivity, the use of some kind of pre-concentrator technology during air sample acquisition was required. Battelle reviewed several technology options, an analysis of which is presented in Table 3.1. The use of both three-dimensional (tubes) and two-dimensional (surface) sorbent configurations were selected and pursued for development. Through the development of an initial breadboard system, many of the "cons" for the sorbent technologies were eliminated or mitigated. For example, Battelle showed that the trapped chemicals could be desorbed and flowed directly to the evacuated THz cell without requiring the use of a carrier gas. Also, procedures and system interlocks were developed to eliminate exposure of the sorbent material to ambient air while at elevated temperatures.

Table 3.1. Analysis of pros and cons of candidate concentrator technologies

Technology	Pros	Cons
Sorbents	1. Established Technology. 2. Many different sorbents for variety of chemicals 3. Commercially available, off the shelf. 4. Properties well characterized for many different classes of compounds.	1. No "one-size fits all" sorbent. 2. 3-D sorbent tubes may need purge gas. 3. Sensitive to O_2 and H_2O when at elevated temperatures. 4. High thermal capacity (requires more energy to heat and cool). 5. Limited lifetime.
PLOT Columns	1. Commercially available. 2. May require little or not purge gas to assist in desorption. 3. Low thermal capacity. 4. Small footprint.	1. Unproven technology for concentrating samples. 2. Limited number of stationary phases. 3. May have low break-through values. 4. Sensitive to O_2 and H_2O when at elevated temperatures. 5. Limited lifetime.
Membranes	1. Very selective for small molecules. 2. Some commercially available.	1. Many unable to discriminate atmospheric gases from target analytes. 2. Propensity to become fouled. 3. May have lower surface area than sorbents – may have lower processing capacity. 4. Not amenable to most classes of chemicals.
2-D Ion Trap	1. Use well known ion trap technologies to select and concentrate target analyte ions. 2. May allow for examination of some analytes with no dipoles. 3. Trap only target analytes under vacuum conditions.	1. Unproven/unknown technology for THz spectroscopy. 2. Requires re-examination of all target analytes. 3. May not generate sufficient ion current to be detected by THz spectroscopy. 4. ???
2-D Sorbents	1. Desorb analytes in or at the THz cell. 2. May eliminate need for purge gas. 3. Custom replacement part that will require future purchases.	1. Requires up-front engineering – no off the shelf product. 2. Loading capacity may lower that some 3-D sorbent tubes. 3. Sensitive to O_2 and H_2O when at elevated temperatures. 4. Limited lifetime.

3.2 Explanation of System Operation

The concept of operation for the SAPM was designed to acquire an air sample, desorb trace constituents into the THz cell, and evacuate system components. The sequence of operations is shown graphically in Figures 3.2-3.9. Before the sequence begins, we assume that all components are already operational and have reached a suitable state of equilibrium. First, the system is prepared for measurement by evacuating the THz cell to below 1 mTorr (Figures 3.2 and 3.3). Next, the air sample is drawn through the SMM (either sorbent tube or disk) by means of the diaphragm pump (Figure 3.4). The total volume of air processed is equal to the pumping speed of the pump (1.2 L/s with inlet filter, 4 L/s maximum) times the duration of the sample acquisition. After sample acquisition is complete, the SMM is pumped first by the diaphragm pump (Figure 3.5) and then by the turbomolecular pump (Figure 3.6). The trace-level gases trapped from the air sample are then desorbed into the THz cell by heating the sorbent to 250°C (Figure 3.7). While the THz spectroscopic measurement is being conducted, the SMM may be pumped down again (Figure 3.8). Finally, the cell is evacuated (Figure 3.9), and if the SMM temperature has relaxed below 50°C, then the sample acquisition process starts over again with a new air sample.

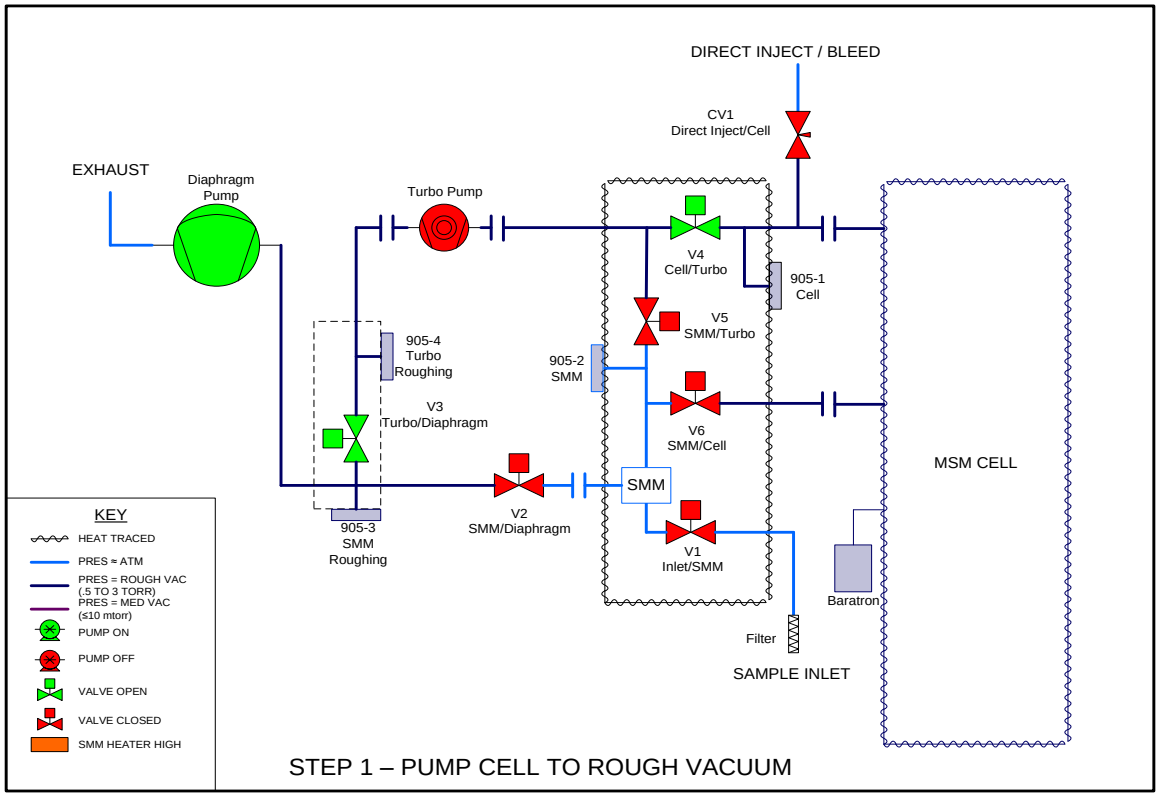

Figure 3.2. Evacuation of the THz cell (MSM) via the diaphragm pump

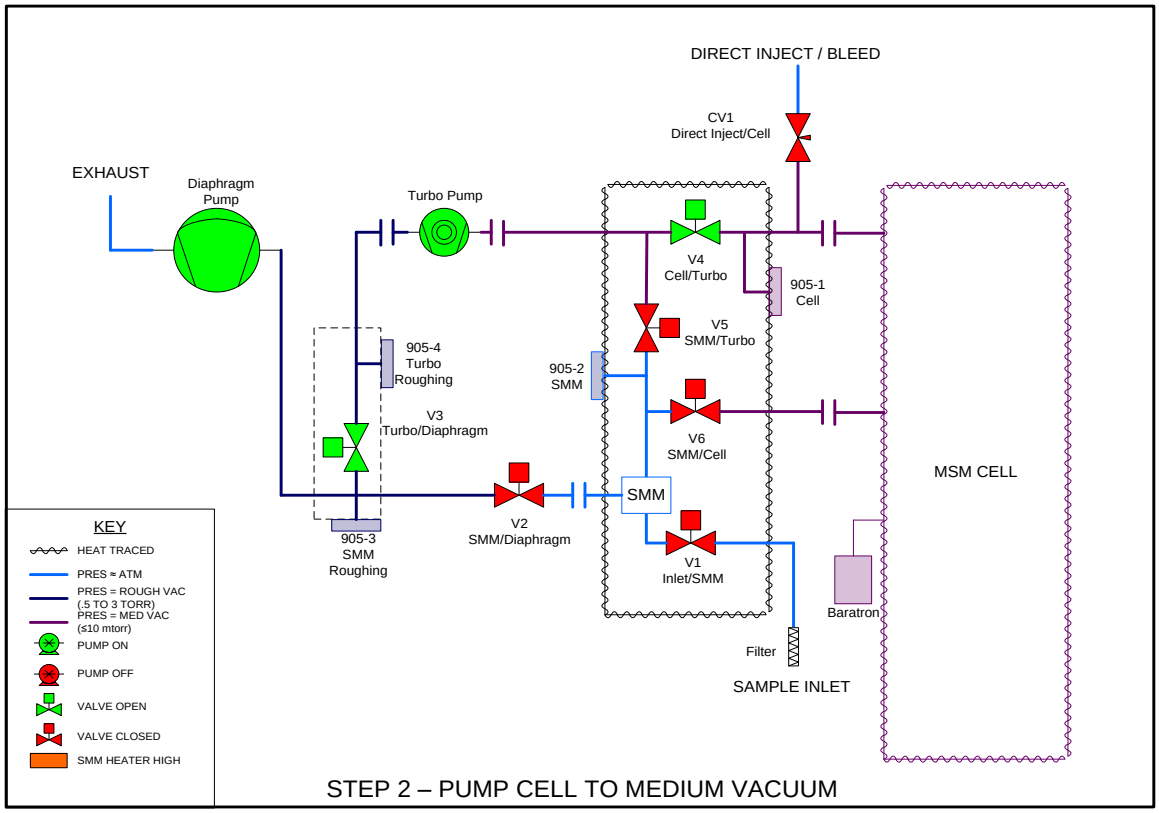

Figure 3.3. Complete evacuation of the THz cell via the turbo pump (below 1 mTorr)

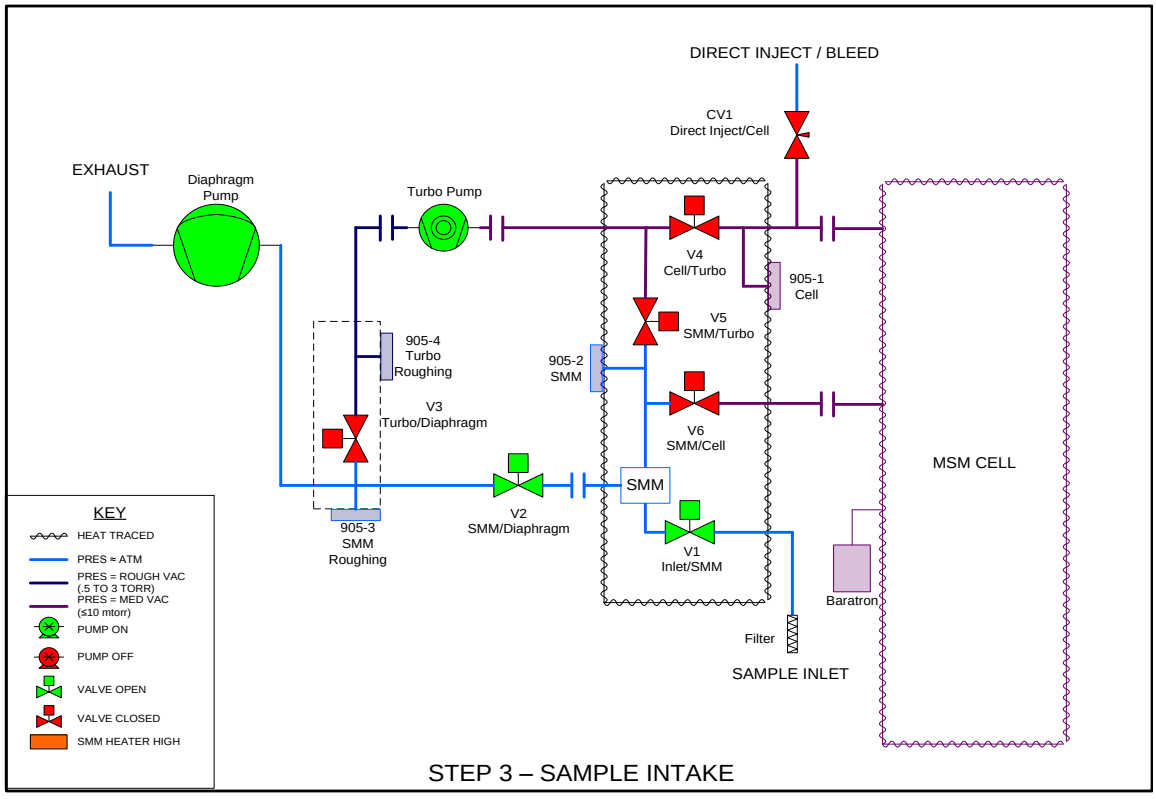

Figure 3.4. Flow of air sample through SMM via the diaphragm pump

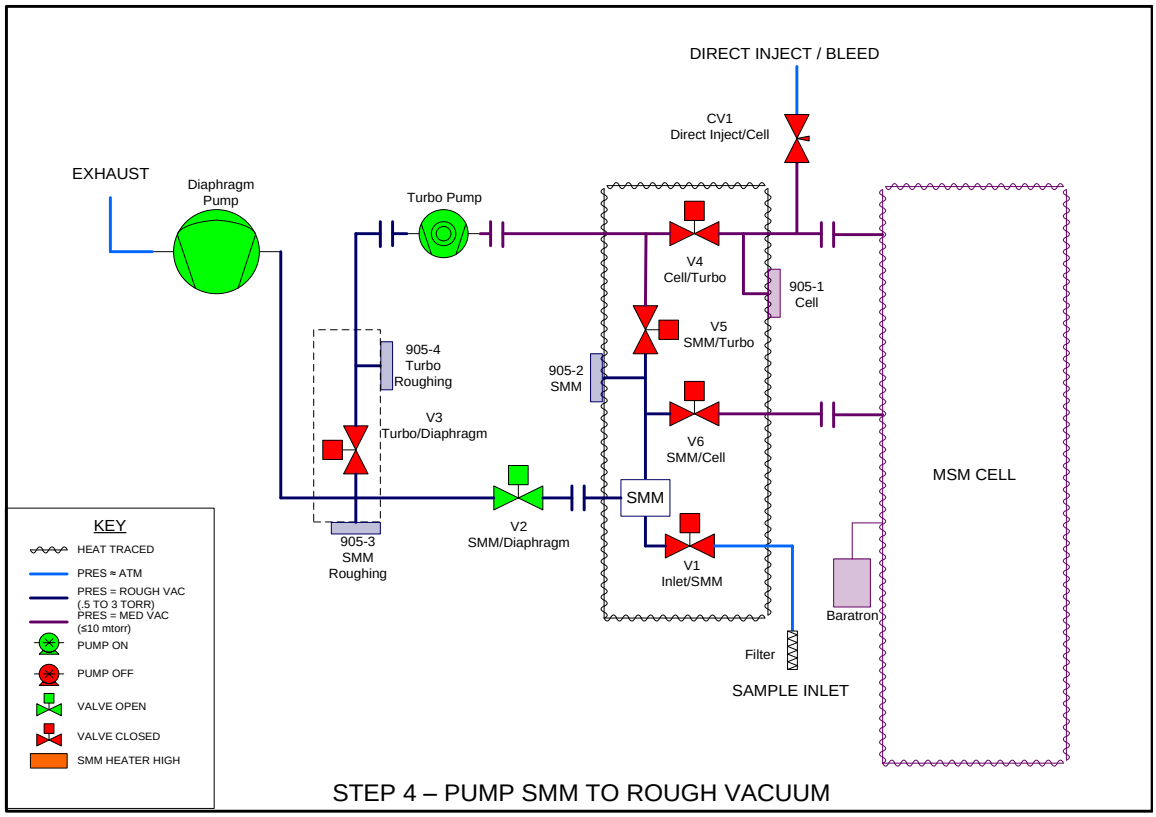

Figure 3.5. Completion of acquisition and evacuation of SMM via the diaphragm pump

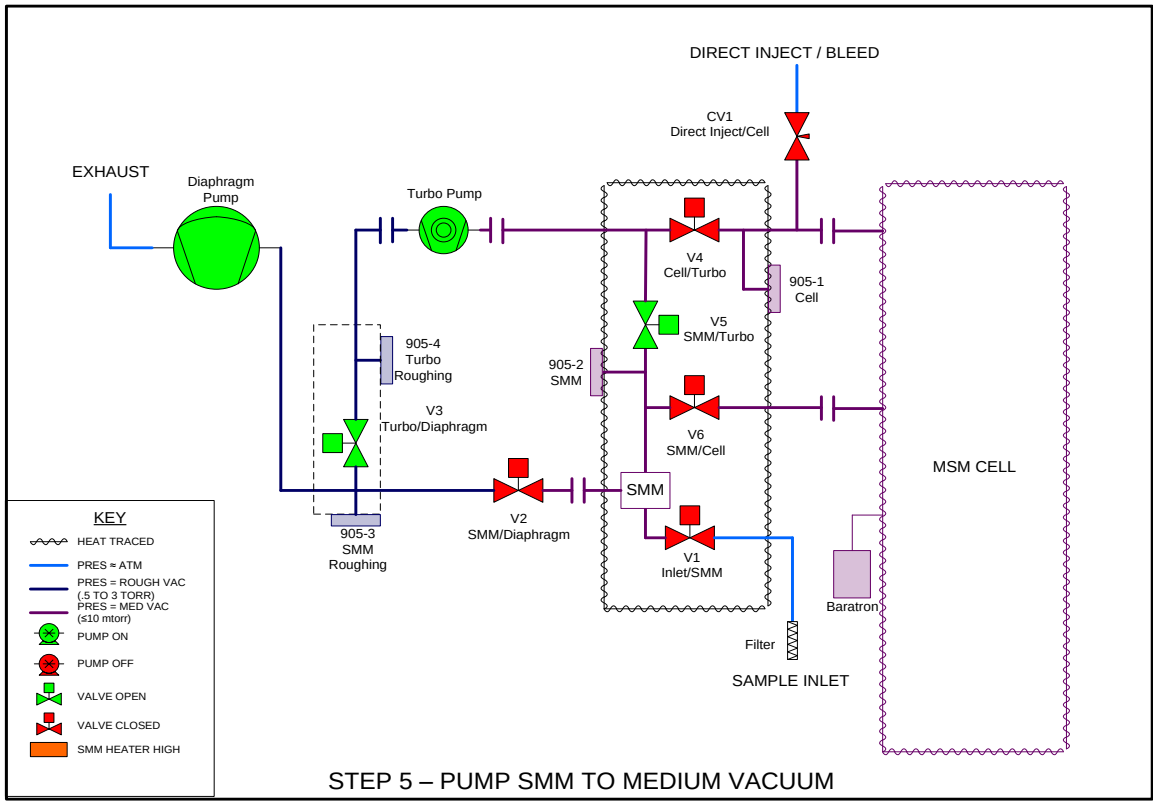

Figure 3.6. Complete evacuation of the SMM via the turbo pump

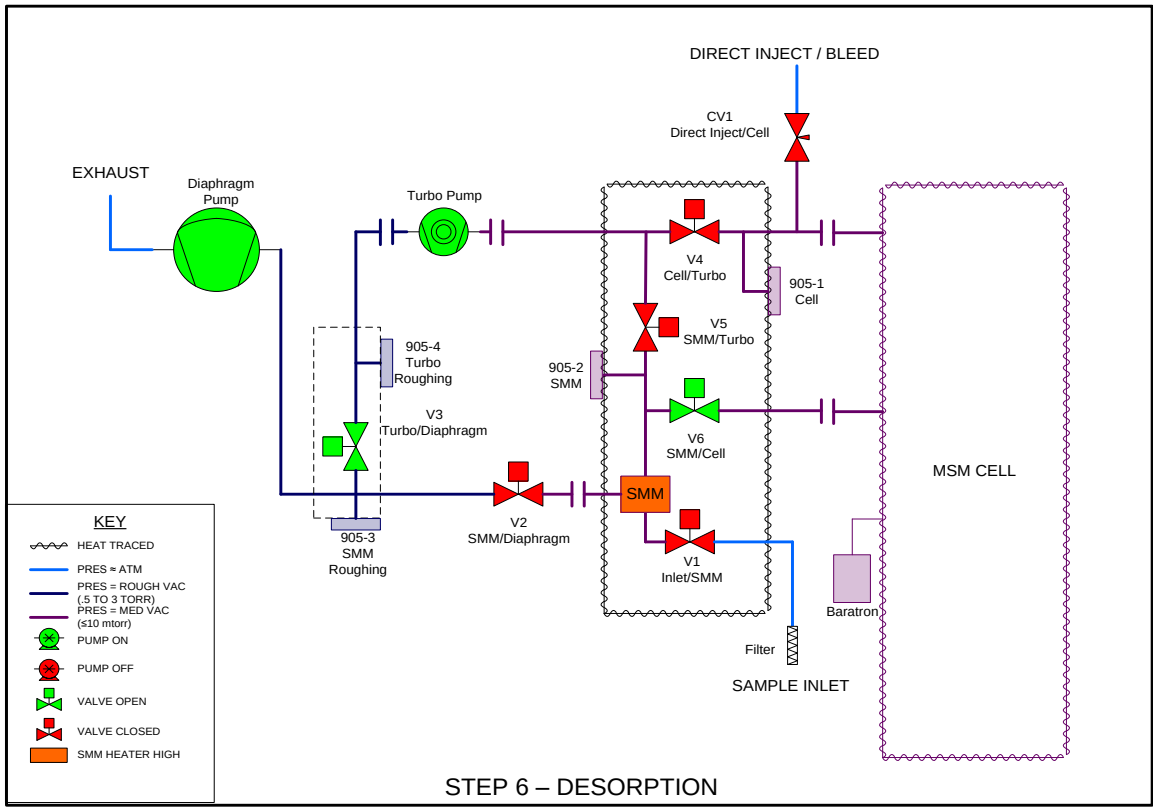

Figure 3.7. Desorption of captured trace gases into the THz cell

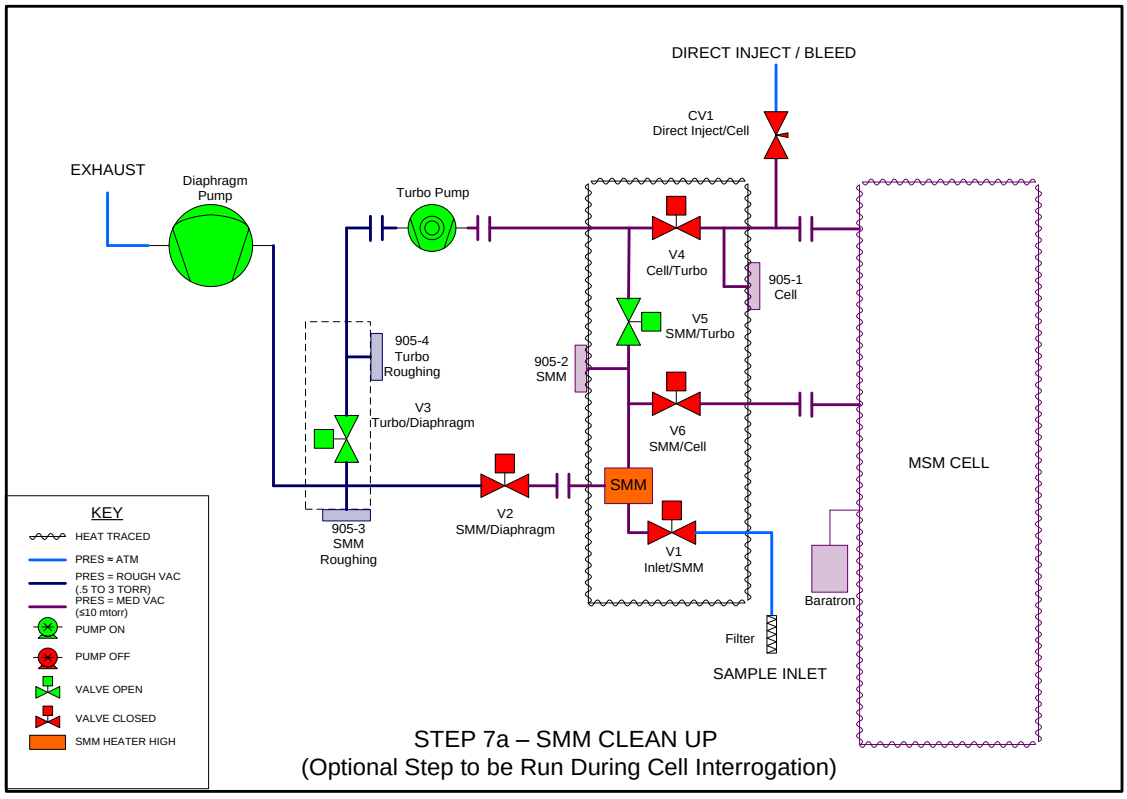

Figure 3.8. Optional evacuation of SMM during THz spectroscopic measurement

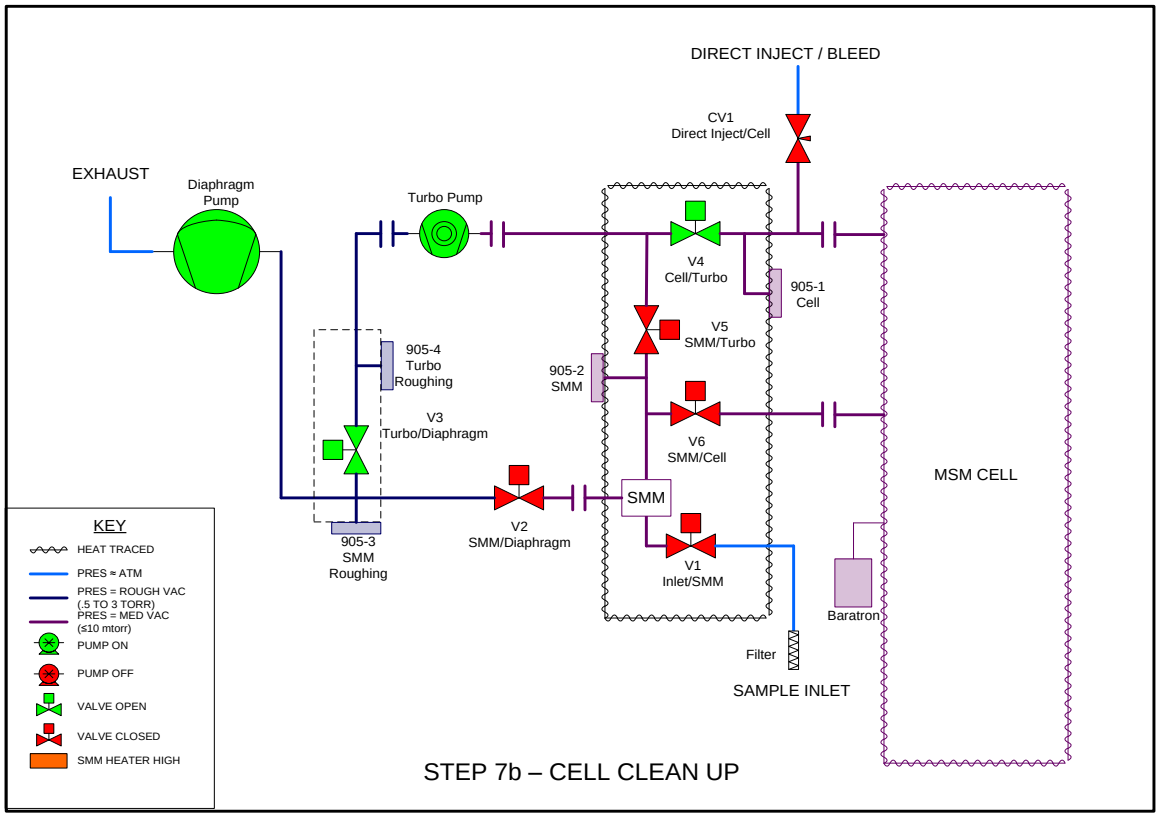

Figure 3.9. Completion of THz measurement and evacuation of THz cell

3.3 R&D Leading to Phase 2 Improvements (Size, Volume, Cost, Speed, Performance)

Much of Battelle's effort in developing the SAPM focused on engineering design and optimization of the pumps, manifolds, valves, pressure transducers, heaters, and associated electronics. Additionally, Battelle focused on characterizing the performance of common sorbent materials against candidate MACS analytes. The major R&D efforts that will enable significant Phase 2 improvements involved radical improvements to the standard sorbent tube technology (Section 3.3.1) and identifying a suitable path forward for reducing overall system size, weight, and power consumption (Section 3.3.2).

3.3.1 2D Sorbent R&D

The objective of this effort was to develop a two-dimensional (2D) concentrator that meets performance requirements (>10^5 concentration) within the required MACS operation cycle (~5 minutes to acquire and process air sample).

The 2D concentrator was developed to address potential limitations in standard concentrator designs. Standard concentrators are based on well-known packed-bed sorbent tubes used to collect and concentrate trace targeted constituents (analytes) from air. In practice, a measured volume of air is drawn through a tube containing a packed bed of sorbent material at ambient temperature. The targeted analytes are retained by the sorbent material. Most atmospheric gases

are not retained and pass through the sorbet bed. When the desired amount of air has passed through the sorbent, an inert gas is introduced flowing in the opposite direction, and the tube is rapidly heated causing the analytes to be desorbed back into the gas phase where they are swept away (purged) by the inert gas. Depending on the relative absorption efficiencies, and relative volumes of initial air collected and reversed gas flow, trace constituents in air can be concentrated to arbitrarily high levels.

Design constraints on the MACS system, however, limit the use of this strategy to achieve the desired detection sensitivity. In particular, because of the pressure limitations of the terahertz (THz) cell, no purge gas can be used to carry desorbed analytes to the detector. Instead, analytes would be desorbed into a vacuum and migrate into the cell driven only by molecular diffusion. The packed-bed design of the sorbent collector that enhances capture of analyte molecules was expected to inhibit their free diffusion back through the packed bed to the THz cell.

A 2D sorbent bed would eliminate the 3D tortuous path that a desorbed analyte must negotiate as it diffuses from the sorbent to the THz cell and reduce the chances that the analyte will be re-sorbed. By placing a 2D sorber as close as possible to the THz cell, by facing the 2D sorbent-coated surface of the sorber toward the cell opening, and by engineering the connection (including the valve) to the cell to enhance molecular diffusion, the amount of collected analyte that will be transferred into the cell for detection can be maximized.

In addition, a 2D concentrator would reduce the system dead volume that would need to be evacuated during each collect/desorb cycle, thus decreasing overall cycle time and increasing system sensitivity. Finally, the 2D concentrator will have significantly less thermal mass than a sorbent tube, thus reducing the power required to heat the concentrator rapidly for desorption and reducing the cool-down time during each cycle.

The 2D concentrator design was based on the assumption that no carrier gas can be used to move desorbed analyte molecules from the sorbent to the THz cell because of total pressure limitations in the cell. To address this design constraint, the sorbent was configured with the highest area/volume ratio as possible (to reduce possible secondary sorption of analyte). In the current embodiment of the 2D concentrator, the sorbent is configured as a near monolayer of sorbent particles on a flat surface. To optimize the path of the desorbed analyte molecules to the cell, the sorbent-covered surface will face the access port to the THz cell, will be positioned as close as possible to the cell, and the connecting hardware (valves, tubing) will have the largest possible diameter. In addition, dead volume between the concentrator and the cell has been minimized. The concentrator is built on a 0.020-in thick quartz plate to minimize thermal mass, thus decreasing both the heat and cooling cycle times. The concentrator resistive heater is laid directly onto the quartz plate to reduce thermal mass associated with the heater. A 1-inch diameter quartz substrate is used to increase the available area for sorbent loading. The sorbent is applied to the surface opposite the heater by a suitable adhesive.

The current design of the heater element is shown in Figures 3.10 and 3.11. The metal selected for the heating element is titanium. Line widths at the center will be 25 μm grading over a series of 47 concentric circles to 1200 μm at the edge of the heater area. The estimated total resistance of the heater is approximately 24 □. Battelle uses standard cleanroom photolithographic

processes to form the heater pattern in a thin film coating of titanium on the 1-inch diameter fused silica discs. The heater pattern consists of a radial mesh pattern with a center electrode and a circular outer electrode. A precision chrome-on-glass photomask containing the heater design was purchased from a vendor. Battelle applied a thin coating of UV-light sensitive photoresist on to one surface of the 1-inch disc, then brought the photomask into intimate contact with the photoresist-coated part for a UV exposure step. The exposed regions of photoresist became cross-linked and rendered insoluble. The unexposed regions of the pattern were developed away in an aqueous developer. We applied a thin film coating of vacuum-deposited titanium metal on the patterned discs. The discs were immersed in a solvent to remove or "lift-off" the unwanted titanium located on photoresist patterned areas. The metal left was the patterned titanium radial mesh and electrodes firmly affixed to the fused silica discs.

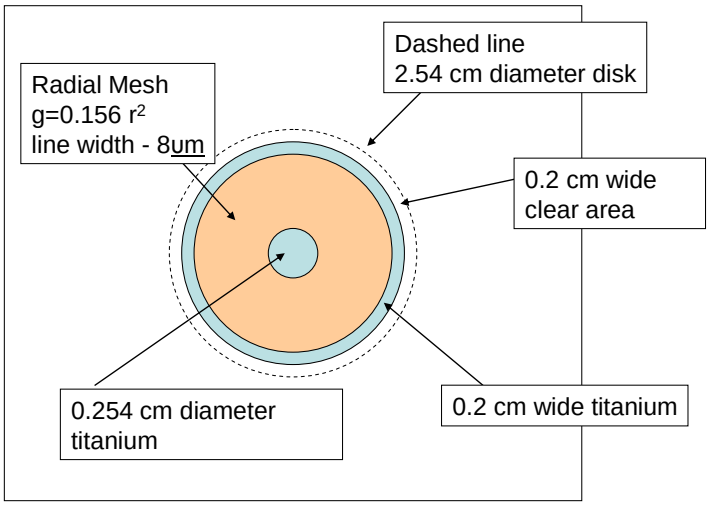

Figure 3.10. High level design of the integrated heater and quartz substrate

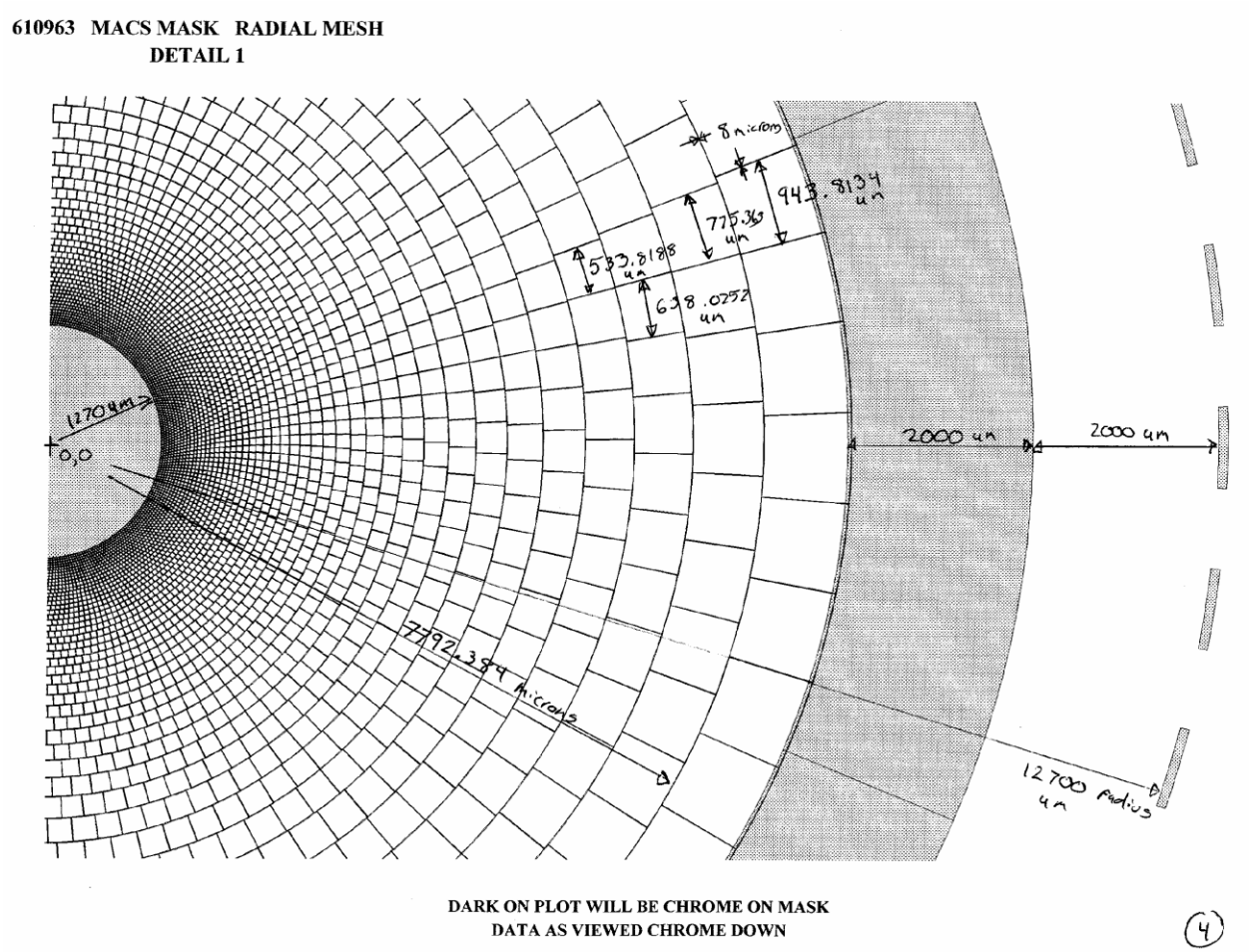

Figure 3.11. Detail of titanium mesh heater design

The sorbent material was attached to the quartz substrate by a suitably chosen adhesive material. Based on the literature and our experience, three commercially-available adhesives were considered: sodium silicate, poly(dimethylsiloxane) [PDMS], and polyimide. PDMS was selected for further development because it is heat and oxidatively stable at the expected operating temperatures, provides a non-brittle coating, and is expected to provide additional strength to the 2D concentrator substrate. In addition, PDMS is a sorbing material, thus contributing to the overall collecting capacity of the 2D concentrator. Development to date has used a spin-coated adhesive layer ~ 0.001 inches thick. This is adequate to secure adhere the individual sorbent grains without blinding too much of the active surface.

The PDMS adhesive is prepared by a two-part thermal cure process in xylene solvent. Curing is accomplished by heating at 150°C for 1.5 hours. Thorough removal of xylene solvent and any other volatiles will be confirmed by GC-MS analysis of cured adhesive. If xylene or any other outgassed compound is detected, an additional evacuation step will be added to the PDMS curing procedure. Outgassing of the adhesive is not expected to be a factor if the curing process is conducted according to the manufacturer's process.

There are many commercially-available sorbets that can be considered for the SAPM mission module. We selected a limited number based on a literature review of materials known to effectively sorb the TICs of interest. Limited testing (using 3D, packed-bed tubes only) has been conducted on Carbosieve G and SIII, Carbotrap C and F, and Carboxen 1000, 1016, 1018, and 569. Based on initial results, most subsequent testing was conducted with Carboxen 1000. Currently we are using a 40/60 mesh product (0.025 - 0.017 inch diameter) for the sorbent material. These small sorbent grains are applied by dropping or pressing them into the adhesive before it is thermally cured. Non-adhered grains are removed by tapping the substrate to remove excess grains. Figure 3.12 shows an example of sorbent grains attached to a polyimide adhesive layer on a test substrate.

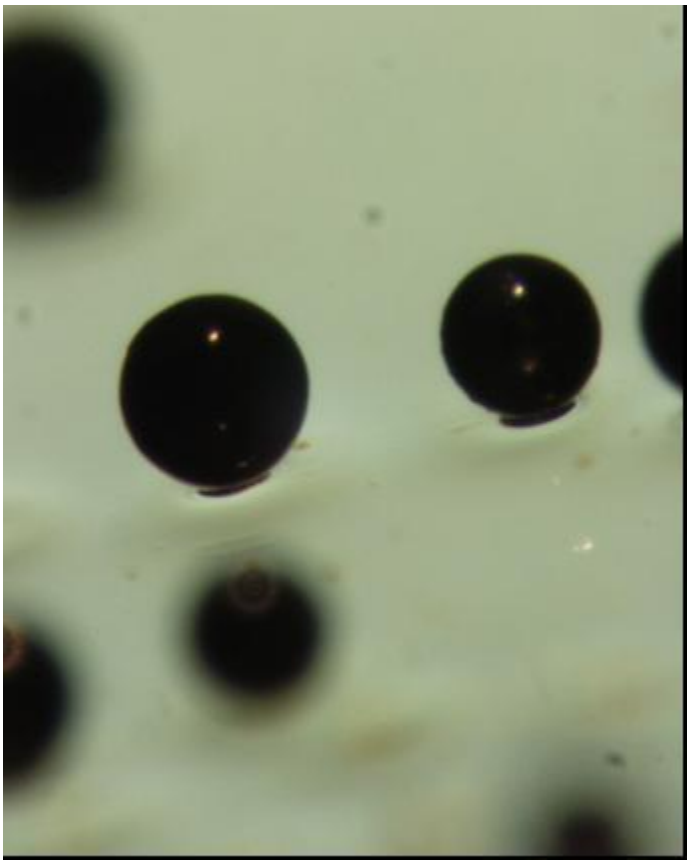

Figure 3.12. Microscopy image of sorbent grains attached to a test surface with polyimide adhesive

The design for the 2D housing has an axial inlet flow toward the center of the sorbent-coated side of the concentrator with radial outlets to shape and distribute the gas flow, as shown in Figure 3.13. Design features in the inlet path and within the cell are incorporated to ensure a turbulent flow regime to optimize mass transfer to the concentrator surface. Computational fluid dynamics (CFD) modeling (FLUENT) was used to visualize the air flow at the concentrator surface. The design balances air velocity (increases in which increase turbulence), pressure drop, and contact time (increases in which require a lower air velocity). Key adjustable parameters are the flow channel height and length/height ratio, shown in Figure 3.14.

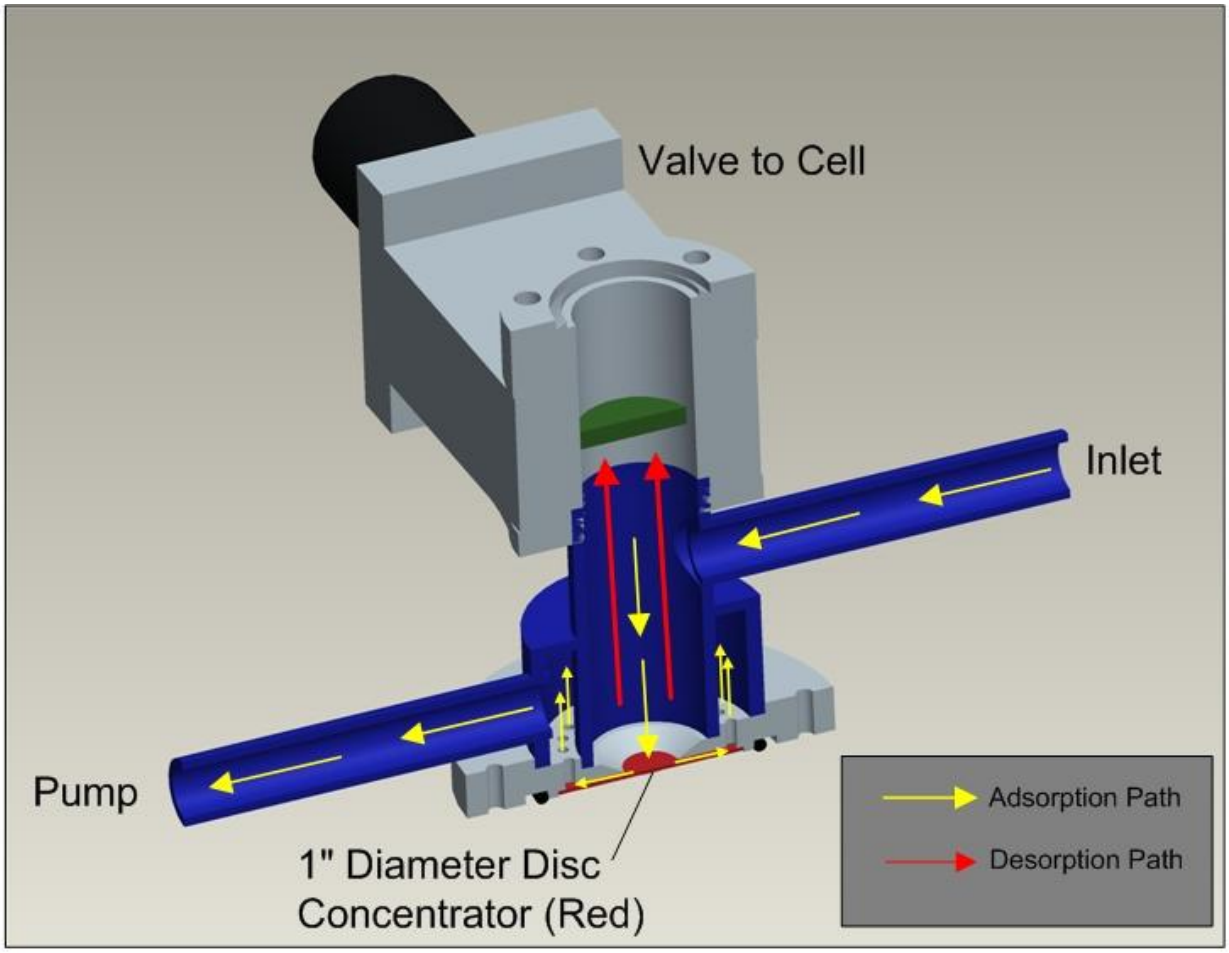

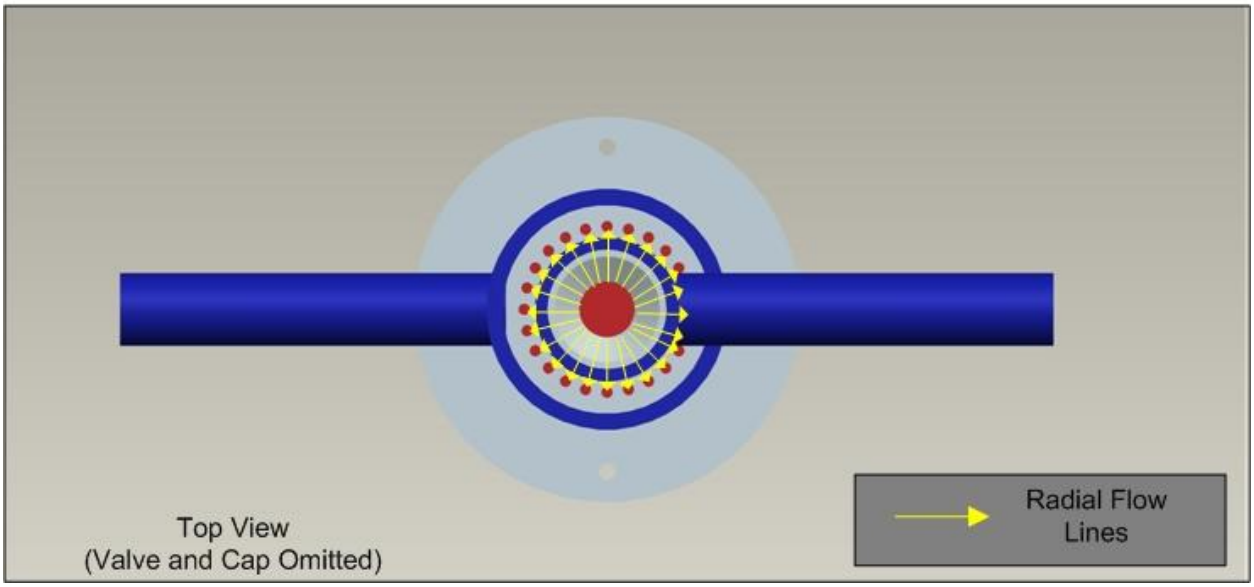

Figure 3.13. 2D concentrator housing showing single axial inlet and multiple radial outlets

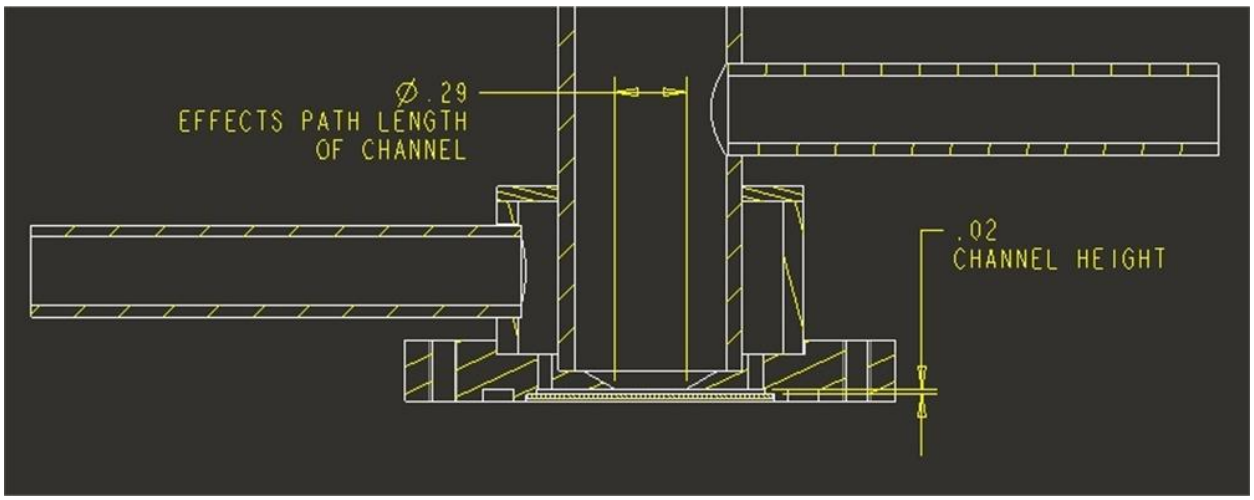

Figure 3.14. 2D concentrator housing showing critical flow dimensions

The CFD modeling effort considered several design options for the 2D concentrator housing shown in Figures 3.13 and 3.14. In a preliminary set of runs, a variety of dimensions were explored for the channel height (gap above the 2D concentrator disk) and the diameter of the tube connecting the disk to the cell. In all cases, the configuration was assumed to be axisymmetric, which simplified the calculations considerably. Mass transfer at the disk surface was approximated by assuming no mass-transfer resistance at the surface (tracer gas concentration set to 0). A total of four configurations were modeled for two air flow rates (1 L/min and 5 L/min) and two flow directions (forward and reverse). Figure 3.15 shows an example of the graphical output from one of the modeling runs. Figure 3.16 shows the estimated absorption efficiency based on each housing design and air flow configuration. These results assumed that the sorbent disk collected 100% of tracer material that was incident upon it.

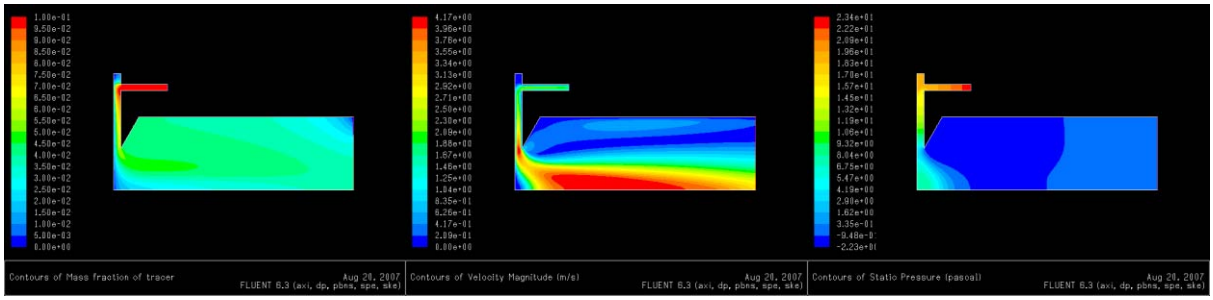

Figure 3.15. Graphical depiction of CFD modeling output, including static pressure (left), velocity magnitude (center), and tracer mass fraction (right)

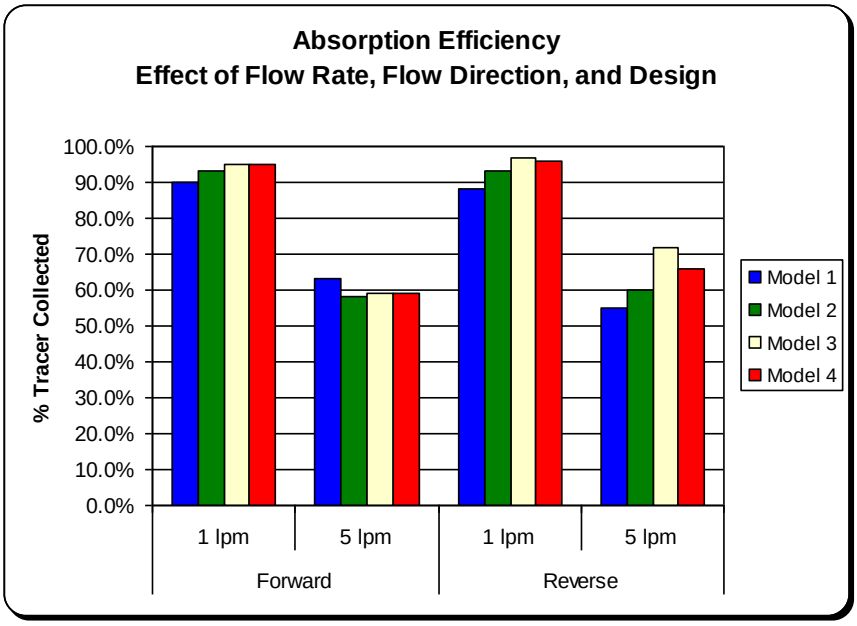

Figure 3.16. Efficiency by which various 2D housing design and flow configurations collect tracer gas materials onto the surface of the sorbent disk

Based on the outcome of these preliminary calculations, a set of recommendations were developed to serve as the basis for a refined set of calculations. These recommendations include the use of 1/16" axial holes in holder, a 0.03" gap above disc, and reverse flow direction. The primary variable tested in the refined set of calculations was the tube diameter linking the sorbent surface to the cell. A range of diameters were considered, including 1/16", 1/8", 3/16", 1/4", and 0.334" (maximum diameter). Figure 3.17 shows a summary of the results of these calculations. Based on these results, Battelle selected a diameter of 1/8" for the opening directly above the sorbent disk. This selection was based on maximizing absorption efficiency, minimizing desorption time, and optimizing the pressure drop (shown in Figure 3.18).

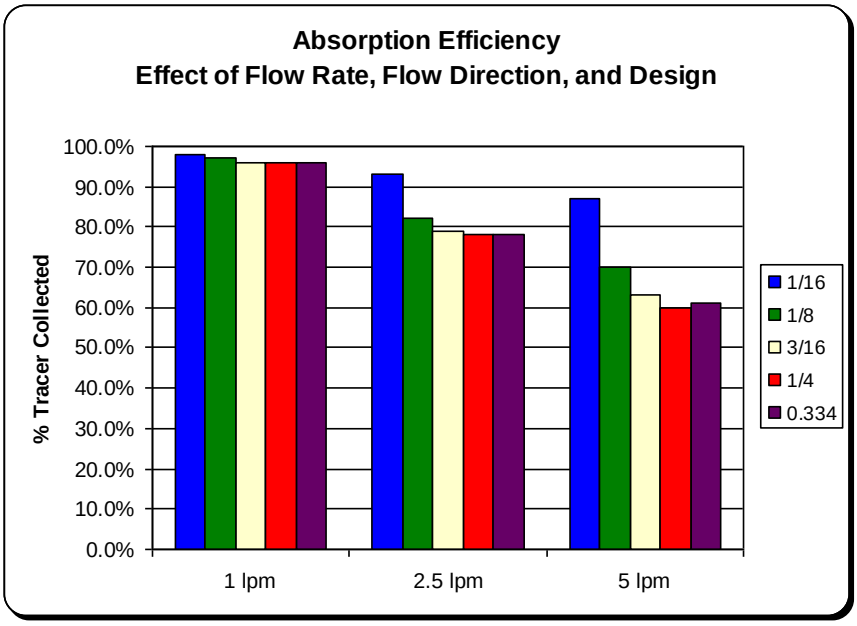

Figure 3.17. Refined efficiency by which various 2D housing design and flow configurations collect tracer gas materials onto the surface of the sorbent disk

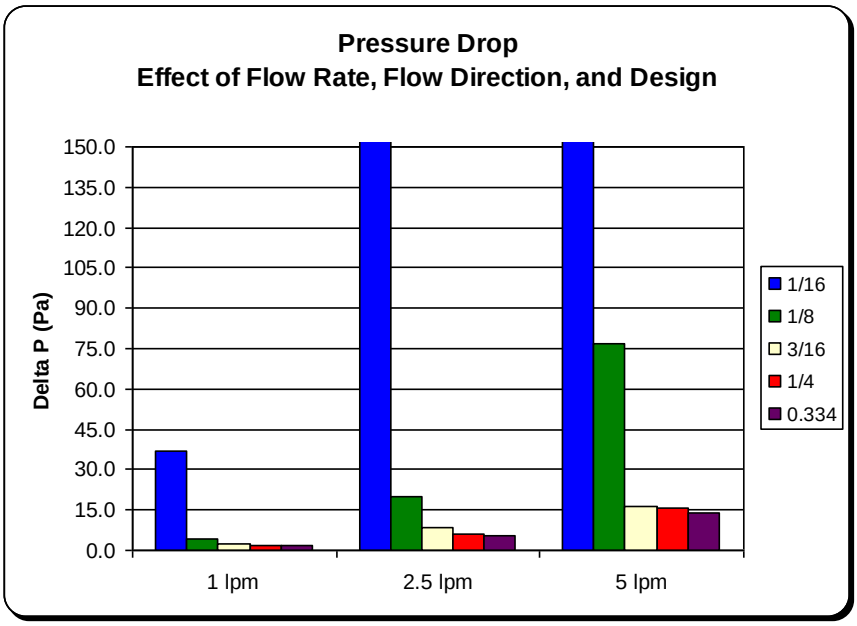

Figure 3.18. Pressure drop associated with various 2D housing design and flow configurations

Tests of the 2D concentrator system were conducted and are presented in Section 3.5.2. In the end, the final deliverable SAPM system incorporated 3D sorbent tubes rather than 2D sorbent disks. Battelle chose this path because the schedule and budget did not permit as much testing of the system as would be required to demonstrate system performance. The 3D sorbent tubes, while not ideal from a power and timing perspective, were known to perform based on sorbent testing described in Section 3.5.1. The R&D associated with the 2D system, however, is quite

valuable for work to be performed under Phase 2. The 2D system requires significantly less power to heat (for desorption) and significantly less time to cool (in preparation for subsequent sample acquisitions). In addition, the 2D system may be configured to handle multiple sorbent materials or may be multiplexed for increased sensitivity or specificity.

3.3.2 Reduced System Volume, Weight, and Power

Battelle has also focused on how to reduce the volume, weight, and power consumption of the SAPM under Phase 2. The primary driver is the pumping system, which occupies over half of the SAPM volume and consumes well over half of the total power (~20 W each). Table 3.2 summarizes the dimensions of the key SAPM components, including the pumpes. The current pumping system, manufactured by Pfeiffer, is a combination of a diaphragm pump (Part No.) and turbomolecular pump (Part No.). While these COTS pumps are among the smallest on the market, they provide higher levels of performance and are much larger than is required for the MACS system. As a result, they serve a dual purpose in the SAPM by evacuating the cell to pressures below 1 mTorr and drawing the air sample through the system at 1-5 L/min. An ideal solution would be to incorporate a single, miniaturized mechanical pump, but none is available on the open market.

Table 3.2. Summary of SAPM component sizes

Equipment List							
	ID Tag	Manufacturer	Model	Envelope Size, in	Envelope Volume, in^3	Actual Volume, in^3	Packaging Efficiency
System	SAPM-1	Battelle		13.5 X 10 X 5	675	**217.8**	**32.3%**
Pumps	DIAPHRAGM PUMP	Pfeiffer	MVP 006	7.1 X 4.2 X 3.9	116.3	70.6	**60.7%**
	TURBO PUMP	Pfeiffer	TPD 011	6.6 X 4.6 X 4.2	127.5	55	**43.1%**
Valves	V1 - INLET/SMM	CKD	GFVB25-2-O-B2CS-3	1.9 X 1.7 X 0.9	2.9	2.1	**72.4%**
	V2 - SMM/DIAPHRAGM	CKD	GFVB25-2-O-B2CS-3	1.9 X 1.7 X 0.9	2.9	2.1	**72.4%**
	V3 - TURBO/DIAPHRAGM	CKD	GFVB25-2-O-B2CS-3	1.9 X 1.7 X 0.9	2.9	2.1	**72.4%**
	V4 - CELL/TURBO	CKD	GFVB55-2-O-B2CS-5	2.9 X 2.5 X 1.7	12.3	8.4	**68.3%**
	V5 - SMM/TURBO	CKD	GFVB55-2-O-B2CS-5	2.9 X 2.5 X 1.7	12.3	8.4	**68.3%**
	V6 - SMM/CELL	CKD	GFVB55-2-O-B2CS-5	2.9 X 2.5 X 1.7	12.3	8.4	**68.3%**
	CV1 - DIRECT INJECT / BLEED	Pfeiffer	RME 005	1.8 X 0.8 X 1.3	1.9	1	**52.6%**
Manifold	HIVAC MANIFOLD	Battelle	N/A	1.8 X 1.3 X 1.1	2.6	2.2	**84.6%**
	SMM OUTLET MANIFOLD	Battelle	N/A	1.7 X 1.1 X 0.4	0.7	0.5	**71.4%**
	DIAPHRAGM PUMP MANIFOLD	Battelle	N/A	7.5 X 2.3 X 1.73	29.8	15.9	**53.4%**

In the late stages of Phase 1, the MACS team became aware of miniaturized pumps that were developed by Raytheon Sarcos for DARPA. The most relevant pump system is a combination of dual piston pumps and a molecular drag pump. This system occupies a little more than 13 in^3, weighs approximately 1 lb, and draws 7 W of power. The Phase 2 SAPM can be shrunk significantly if this pump system is viable and within a suitable price range (they have to be custom built by Raytheon Sarcos). This system will only be able to evacuate the cell; it does not have sufficient capacity to draw the air sample through the sorbent. Battelle has identified several COTS miniature diaphragm pump options that can pull the air samples at 3-4 L/min. Generally, these pumps occupy less than 8 in^3, weigh less than 0.5 lb, and draw less than 10 W.

With the combination of the Raytheon Sarcos pumps and the COTS miniature diaphragm pumps, Battelle believes that the overall SAPM size and power can be reduced substantially (1/6 of the Phase 1 volume, less than 1/5 of the weight, and less than 1/3 of the power).

Another way that the overall SAPM volume and weight can be reduced is to re-engineer the SAPM manifold, currently fabricated from blocks of stainless steel, and investigate additional valving options. While not as significant as the pumps, the valves are quite large due to the requirements on tubing/manifold channel dimensions. Battelle hopes to balance these requirements and determine if other valve options are available that can provide size, weight, and power improvements.

As described above in Section 3.3.1, the 2D sorbent system, which Battelle intends to implement fully under Phase 2, will provide additional power savings due to the smaller thermal mass of the sorbent disk compared to the 3D sorbent tube. Less power will be required to heat the sorbent disk in order to desorb trapped molecules, and less time will be required to heat and cool the disk, offering improvements in the time scale of SAPM operations.

3.4 Module Design Specifications and Engineering Drawings

The design requirements for the SAPM system are derived from the overall MACS system requirements. These include the following explicit system requirements, with derived requirements listed as sub-bullets:

- MACS volume = 1 ft^3 (1728 in^3)
  - Final SAPM allocation was 699 in^3
- Detection sensitivity = 100 ppt
  - Minimum SAPM concentration factor of 10^4
  - SAPM flow rate of at least 1 L/min
  - THz base cell pressure < 1 mTorr
  - THz operational cell pressure ~ 10 mTorr
- Measurement cycle time = 10 min
  - SAPM cycle time ~5 min
  - SAPM flow rate of at least 1 L/min
- MACS weight = 30 lb
  - Final SAPM weight was 23 lb
- MACS power consumption = 25 W
  - Final average SAPM power consumption = 80 W

To meet these explicit and derived system requirements, Battelle developed the system shown schematically in Figure 3.1. An annotated photograph of this layout is shown in Figure 3.19. The SAPM is comprised of two major sub-systems, the SBM and SMM. The SBM includes all electronic and mechanical components necessary to acquire an air sample, evacuate the THz cell, and communicate with the MACS central computer. The SMM includes the sorbent-based pre-concentrator system that extracts trace gas constituents from the bulk air sample. Each sub-system is described in further detail in the following sub-sections.

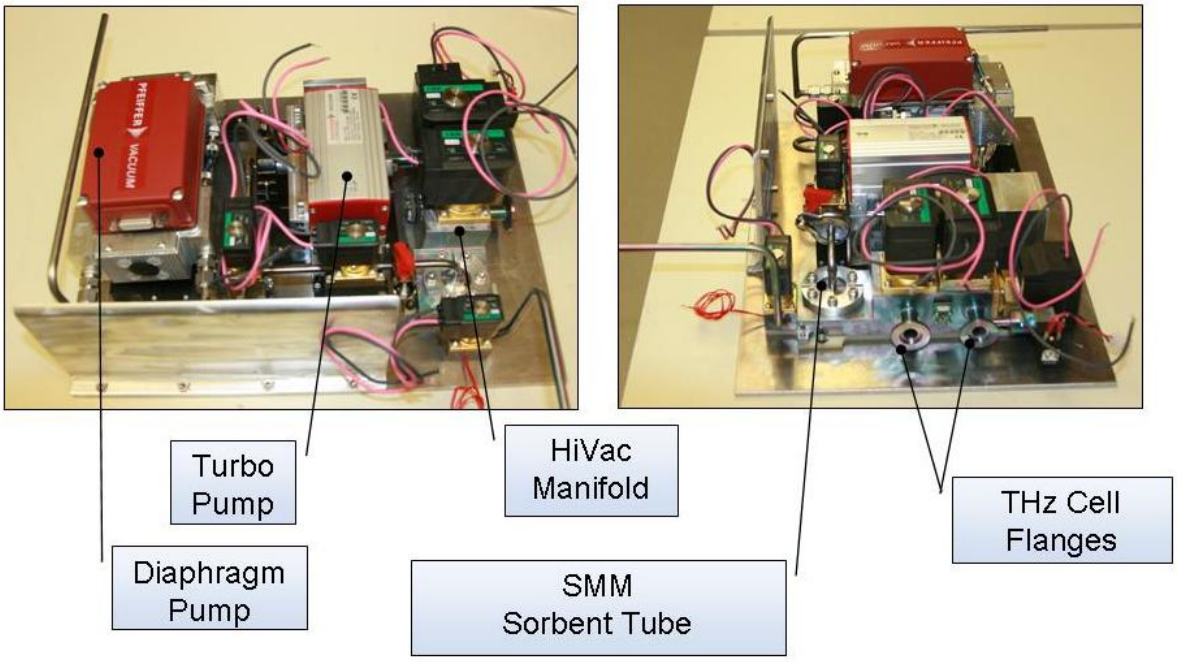

Figure 3.19. Annotated photograph of the SAPM system

3.4.1 SBM Mechanical System

The SBM mechanical system was designed, developed, and tested to help meet the aforementioned design requirements. The details of the SBM mechanical components and mechanical drawings are provided in Appendix 3.1.

3.4.2 SBM Electronic System

The SBM electronic system was designed, developed, and tested to help meet the aforementioned design requirements. A Circuit Card Assembly (CCA) controls the interface to the SAPM for the central computer and controls the collection and processing of samples. It interfaces with the pressure transducers, THz stepper motor, SMM, heaters, and valves. The CCA incorporates the following components:

- Freescale microprocessor
  - 16-Bit CPU12X, 512K Byte Flash, 20K Byte RAM, 4K EEPROM
- SAPM controller firmware for the Freescale microprocessor
  - Written in C with C++ style commenting
  - Firmware is updateable through debug port
  - Function-based code
- Firmware
  - Inputs: Micropirani gauges, baratron gauge, thermocouples
  - Outputs: Diaphragm pump, turbo pump, valves, heaters, stepper motor
- SAPM flexibility provided through excess capability within the controller

The details of the SBM electronic components and several mounting plate drawings are provided in Appendix 3.2. In addition, the Serial Control Interface document is provided in Appendix 3.3 and the CCA Requirement Specification document is provided in Appendix 3.4.

3.4.3 SMM Design

Two SMM concepts were designed and tested for the SAPM: the 3D sorbent tube and the 2D sorbent disk. Only the 3D sorbent tube was implemented in the final deliverable; additional development of the 2D system is required before implementation. Numerous sorbent materials were tested, as described in Section 3.5. Mechanical drawings for the 3D sorbent tube and the 2D sorbent disk housing are provided in Appendix 3.5.

3.5 Module Performance (Measures and Results)

3.5.1 SAPM System Performance Verification

Numerous tests were conducted to characterize the performance of the SAPM to verify that the SAPM, and ultimately the integrated MACS system, will meet the performance requirements. A summary of the results of these tests are presented in this section.

- Verification of low cell pressure – tests conducted at Battelle and at Ohio State verified that the SAPM pump system could achieve cell pressures below 1 mTorr. In these tests, both types of pressure sensors would zero-out. The Baratron goes down to 0.1 mTorr before it zeroes. The micropirani goes down to 0.01 mTorr before it zeroes. At the low end of the pressure scale for either gauge, the accuracy of the pressure measurement is questionable. Battelle deems that it is safe to assume that the ultimate cell pressure is below 10^{-4} Torr. The turbo pump is rated down to $4x10^{-5}$ Torr.

- Verification of SAPM air sample flow rates – an in-line TSI flow meter (range of 0.01-20 L/min) was used to monitor the air sample flow rate through the sorbent system. Without a filter on the SAPM inlet, the flow rate was measured to be as high as 5.2 L/min. With a 2 □ m filter in place at the inlet, the flow rate was reduced to 1.2 L/min.

- Estimate of SAPM system power consumption – the Battelle team estimated the overall power consumption of the SAPM system over the course of a typical measurement cycle. Figure 3.20 presents estimates of the power consumption for individual components and the overall SAPM system over time. The typical average power consumed is 80-100 W, with peak power of approximately 150 W.

- Verification of sorbent heater performance – 3D and 2D sorbent heaters were tested to demonstrate that the ultimate temperature was obtainable and to measure the heating/cooling time scale.

    - 3D sorbent tube – the heater achieved temperatures above 250°C. Figure 3.21 shows an example of the timing of the heat cycle. Less than one minute is

required to achieve 160°C, though more than 2 minutes is required for the sorbent tube to cool to the original starting temperature.

- 2D sorbent disk – the heater achieved temperatures above 250°C. Figure 3.22 shows an example of the timing of the heat cycle. Current estimates indicate that the 2D sorbent disk takes about 15 seconds to achieve 200°C at 24 VDC, and 20 seconds to achieve 250°C. The disk takes about 1 minute to cool to an operational temperature (<50°C).

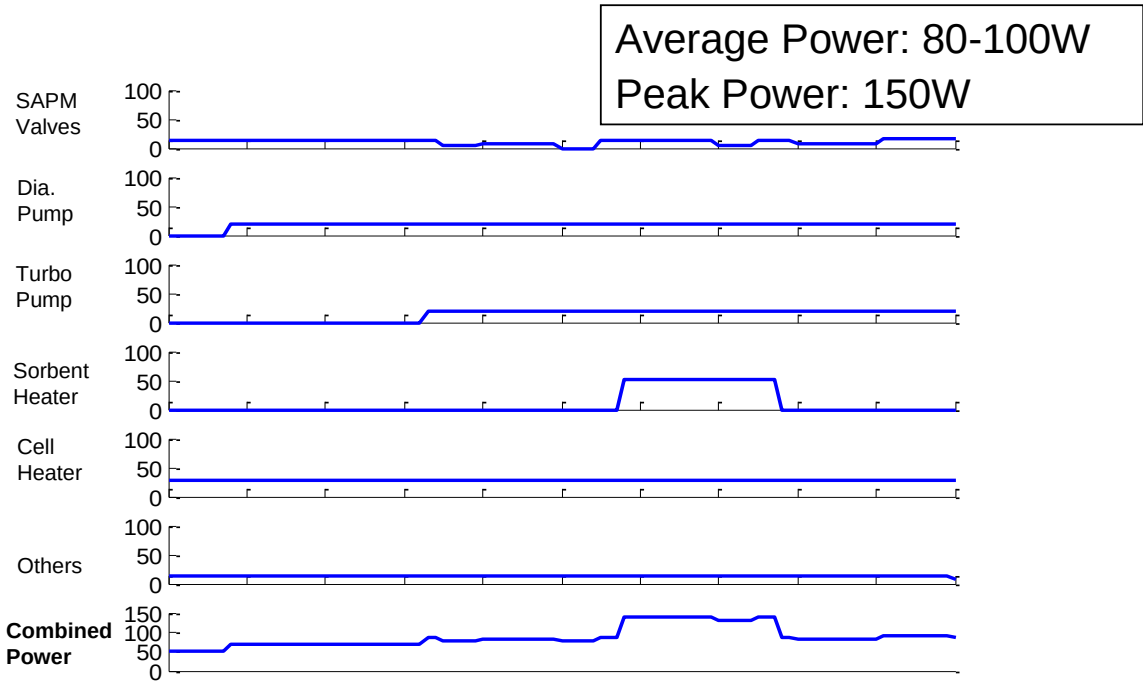

Figure 3.20. Estimate of SAPM power consumption over time during a measurement sequence

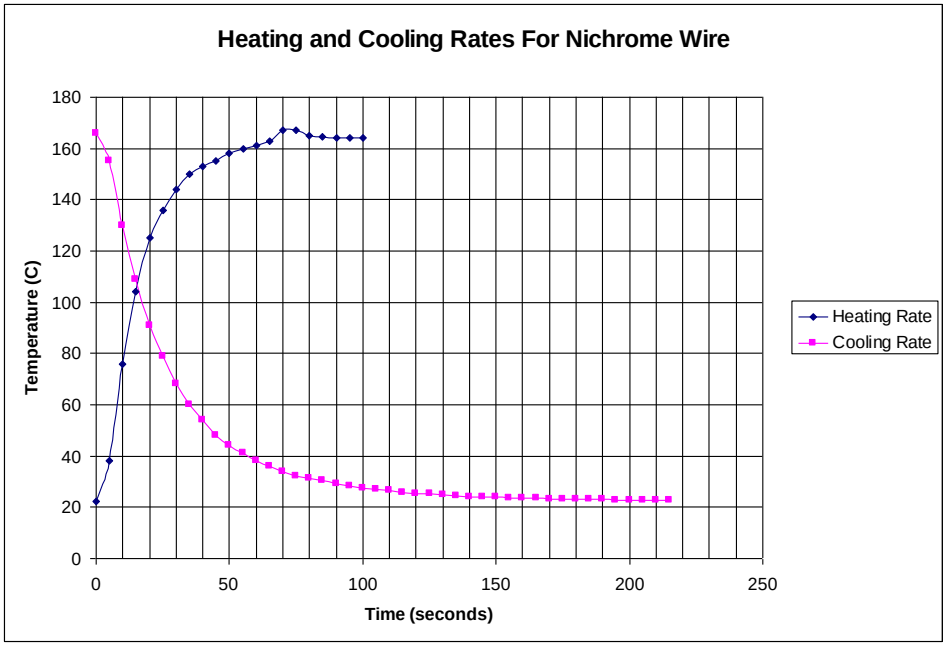

Figure 3.21. Example thermal profile for a nichrome wire heated sorbent tube

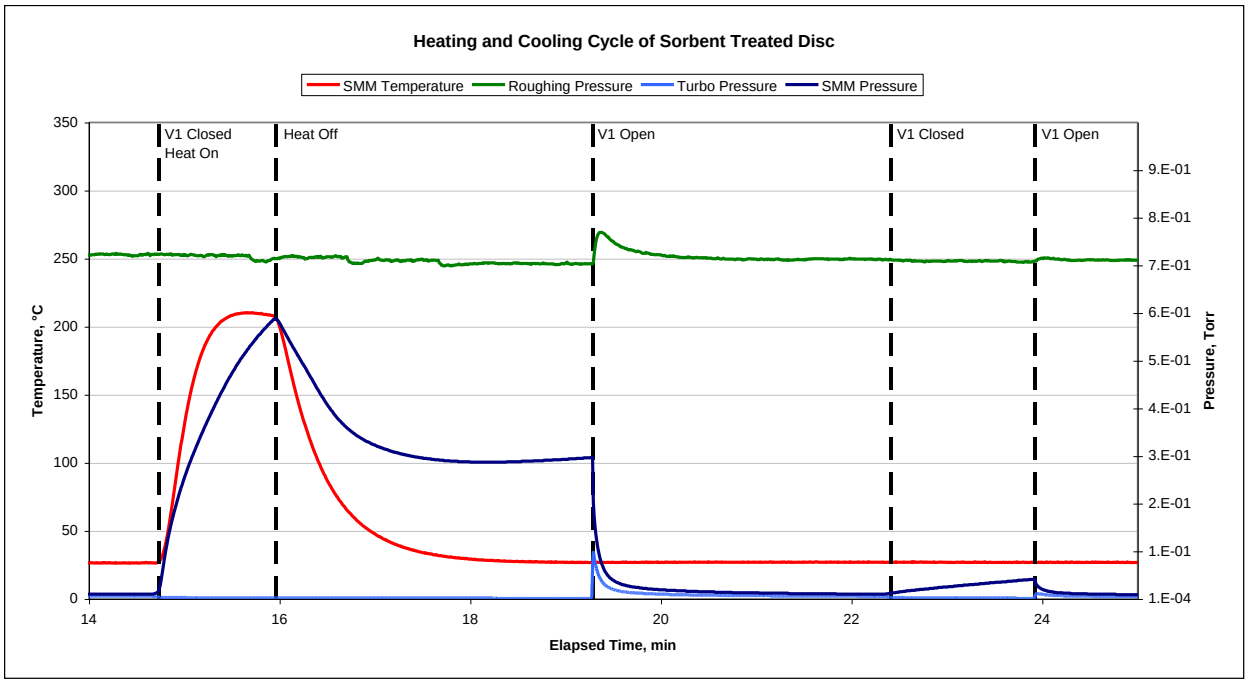

Figure 3.22. Example thermal profile for a 2D sorbent disk

3.5.2 Sorbent performance testing

The objective for the laboratory investigation of gas-phase concentrators is to identify a suitable method for concentrating trace-level analytes in air while excluding concomitant gases such as nitrogen, oxygen, and water vapor. Once concentrated, the target analytes will be liberated into a spectrometer for analysis.

The concentrator technology for the sample acquisition and processing module (SAPM) is a critical component of the MACS system. Experimental evaluations of commercially available sorbents are being conducted to identify and characterize a variety of sorbents that will achieve the stated goals for the SAPM. The SAPM must collect and concentrate up to 30 analytes from air with at least one analyte to be detected at a concentration of 100 pptv. The ideal concentrator will process large volumes of air, and selectively retain desired target analytes while excluding all nonessential gasses such as nitrogen, oxygen, water, etc. Analytes selected for these tests were identified as being of interest to one or more Government agencies or that are simulants for highly toxic compounds.

All experiments involving sorbent testing have been conducted on a modified gas chromatograph mass spectrometer (GC/MS) system. A test system, shown schematically in Figure 3.23, was constructed and used for all sorbent tests to date. The sorbent tube is a 0.25 in Sulfinert treated stainless steal tube packed with ~10 mg of sorbent. Spring clips and deactivated glass wool are used to keep the sorbent material in the tube. The active sorbent bed depth is ≤ 1 mm.

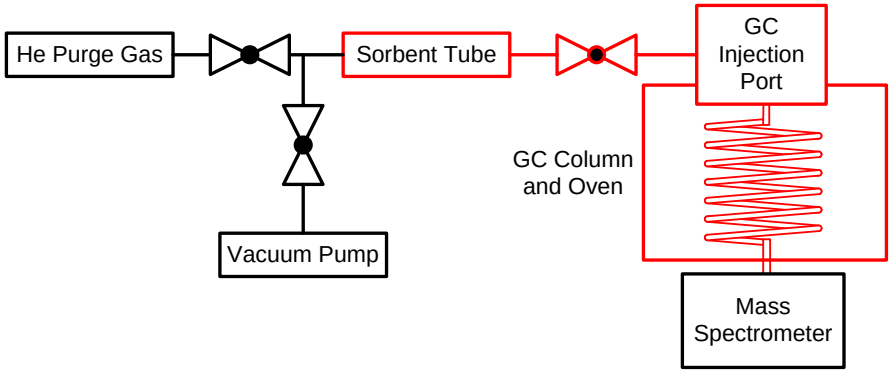

Figure 3.23. Block diagram for MACS SAPM test system

Using established procedures, sorbent tubes were spiked typically with ~500 ng of analyte diluted off line in an air mixture. Starting with neat material, target analytes were serially diluted in glass bottles caped with Teflon lined septa until a desired concentration was achieved. A gas-tight glass syringe was used to withdraw 100 µL of gas sample standard which was then slowly spiked into the inlet gas stream of the sorbent tube. The resultant mixture represents an analyte concentration of 30 ppbv in 10 L of atmosphere. During and after spiking, a total of 10 L of clean air is pulled through the sorbent tube (~1 L/min) to simulate a 10 L collection volume.

The loaded sorbent tube was removed and transferred to an inlet manifold system attached to the injection port of a GC/MS, shown in Figure 3.23. A Restek RTX-1701 GC column (0.25 mm ID, 1.0 µm film, 30 m length) was installed into the GC oven. The GC injection port was equipped with a split/splitless injection port with a quartz inlet liner deactived using an in-house hexamethyldisilazane deactivation process. The inlet was operated in the split mode with a split flow of 23 mL/min and a column flow rate of 1 mL/min.

The sorbent tube and plumbing were evacuated for 5.0 min using a foreline pump. The base pressure as measured on a thermocouple pressure gauge located on the inlet housing of the foreline pump was ~9×10^{-2} torr. The actual pressure in the sorbent tube was unknown but is expected to be higher. During this time, the sorbent tube was maintained at a constant temperature (room temperature, 50 °C, or 100 °C). The transfer lines and injection port were heated to ~130 °C and 220 °C, respectively.

To desorb, the valve to the vacuum pump was closed and the sorbent tube was heated rapidly to ~250 °C. A helium purge gas (UHP grade) was used to facilitate the transfer of analyte from the sorbent tube, through the gas chromatograph, and to the mass spectrometer. The desorbed analyte flowed into the GC injection port and onto the GC column. The initial temperature of the GC oven was 50 °C and was held there for 10.0 min. The oven was then heated at 25 °C min^{-1} to 250 °C and held for 24 min. The mass spectrometer, calibrated daily with directly injected analytes, was operated in the full scan mode with a typical mass range of *m/z* 10 to *m/z* 300.

To date, eleven sorbents and two porous layer open tubular (PLOT) columns have been assessed using approximately 60 sorbent/analyte combinations. The sorption/desorption efficiencies for each target analyte were determined along with the exclusivity of the sorbent for target analytes and atmospheric components. Using these methods, independent quantification of the sorption and desorption efficiencies cannot be readily determined; the reported efficiencies are the product of the individual sorption and desorption efficiencies. Blank-corrected results of these analyses are summarized in Appendix 3.6.

The PLOT columns failed to retain acetonitrile, which was selected as the initial test analyte for the system, and were not evaluated further. Carboxen 1000 was able to selectively trap a wide range of compounds, with varying sorption/desorption efficiencies. To date, 28 compounds have shown sorption/desorption efficiencies greater than 10% for Carboxen 1000 while 17 analytes have shown recoveries ≥ 85%. Some analytes exhibit recoveries greater than 100% and this is believed to be due to the ubiquitous natures of these compounds in the lab air. Though not evaluated to date, it is anticipated that using humidified zero air (high purity air consisting N_2, O_2, H_2O, etc) would bring these recoveries to nearly 100%.

Not all chemicals exhibited high sorption/desorption efficiencies on Carboxen 1000. It is not clear if these analytes were retained and not desorbed or if they were not retained at all. To achieve high sensitivities on the MACS system for analytes that exhibit low recoveries on Carboxen 1000, different strategies such as sampling more air or using of different sorbent material will need to be examined. Both scenarios are feasible but have not been done for all analytes shown in Appendix 3.6. The maximum flow rate through the sorbent tube while maintaining high capture efficiencies has not been evaluated.

The sorption/desorption efficiency reproducibility was evaluated. Six replicate measurements were made using acetonitrile and Carboxen 1000. For this study, the mean recovery was 160% with a 3.1% RSD. These data suggest that reproducible results can be achieved using sorbents in a 3D device. Long term stability measurements have not been made but will be attempted.

Penetration of acetonitrile through a packed 3D sorbent tube (breakthrough) was studied. Using ~10 mg of Carboxen 1000 (effective depth ≤ 1 mm) a linear response (R^2 = 0.99990) up to a ~12,000 ng spike is obtained (Figure 3.24). This suggests that little breakthrough had occurred and indicates that anticipated collection amounts will be effectively collected. However, at 50,000 ng, the response is less than predicted (dotted line) suggesting that some breakthrough had occurred.

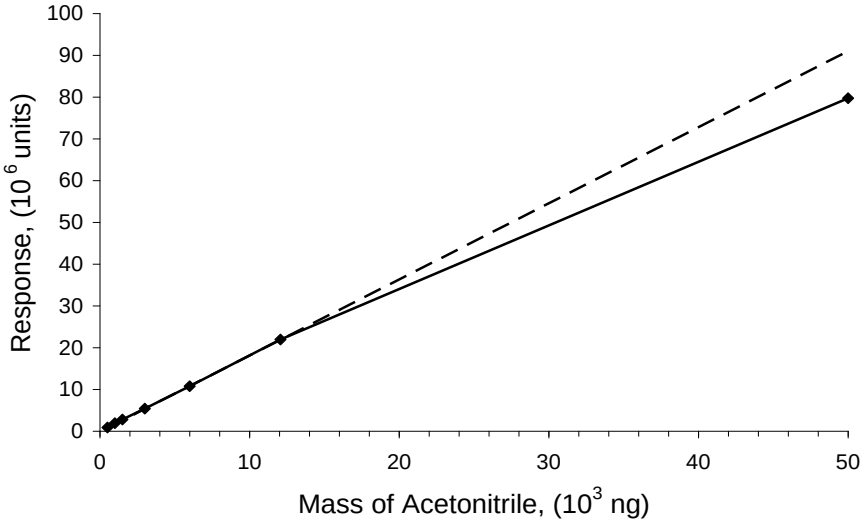

Figure 3.24. Experimental evaluation (solid line) of acetonitrile breakthrough as challenged on Carboxen 1000. Dashed line is theoretical value assuming linear response.

The sorbent data were also evaluated in terms of partial pressures and the ability to exclude atmospheric gasses. Using acetonitrile as an example, a 500-ng gas phase spike would correspond to a theoretical partial pressure of ~ 2.38 mtorr in a 100-mL vessel at 40 °C. The pressure of the sorbent tube, as measured on the inlet manifold of a mechanical foreline pump following a 5 min pump-down time, was ~9×10^{-2} torr. The actual pressure in the sorbent tube was not measured but is likely higher than this value. This pressure is ~9× greater than the maximum allowable pressure of the spectrometer.

Based on the GC/MS data from the sorption/desorption experiments, the derived partial pressures for the atmospheric components for acetonitrile retained on Carboxen 1000 are shown in Table 3.3. The sorbent tube was maintained at three different temperatures during evacuation. At 25 °C, the sum of partial pressures for N_2, O_2, CO_2, and H_2O is 7×10^{-1} torr. Elevating the sorbent tube to 50 °C and 100 °C decreased the pressure to 5.7×10^{-1} and 2.8×10^{-1} torr, respectively. The results for other analytes retained on Carboxen 1000 are similar (to within a factor of two). Other sorbents that effectively retained acetonitrile were no better at excluding atmospheric gases than Carboxen 1000.

Table 3.3. Partial pressures of acetonitrile and other atmospheric gas components

	Acetonitrile	*N_2*	*O_2*	*CO_2*	*H_2O*
ρ, mtorr, 25 °C	*2.75*	*323.3*	*12.0*	*11.5*	*368.6*
ρ, mtorr, 50 °C	*2.99*	*162.9*	*108.2*	*13.9*	*282.6*
ρ, mtorr, 100 °C	*2.13*	*137.3*	*46.5*	*4.4*	*87.7*

Acetonitrile, with a boiling point of ~ 82 °C, was effectively retained when the sorbent tube was placed under vacuum and heated to 100 °C. The atmospheric gases, however, were more effectively removed at higher temperatures. This suggests that some gains may be made by evacuating the sorbent tube at an elevated temperature prior to desorption.

4 TM (THz Module)

4.1 Summary of Trades and R&D Leading to Design

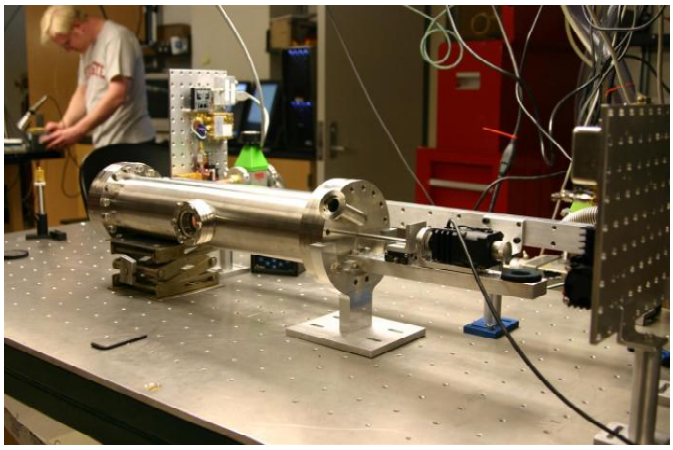

Figure 4.1.1. Cavity test beds used for cell analyses.

The trade space leading to the THz Module (TM) was very large. We adopted the strategy of finding a low risk path to satisfy the 18 month GNG criteria, while at the same time laying the foundation for an enhanced Phase 2 system. Elements of the TM include the spectroscopic cell, the x 24 multiplier chain and mixer chain to translate the X-band drive to 210 – 270 GHz, the transfer optics, a wire grid power adjustment, and the IF signal chain. In general, the trade space of each of these interacts with the trade space of the group as a whole.

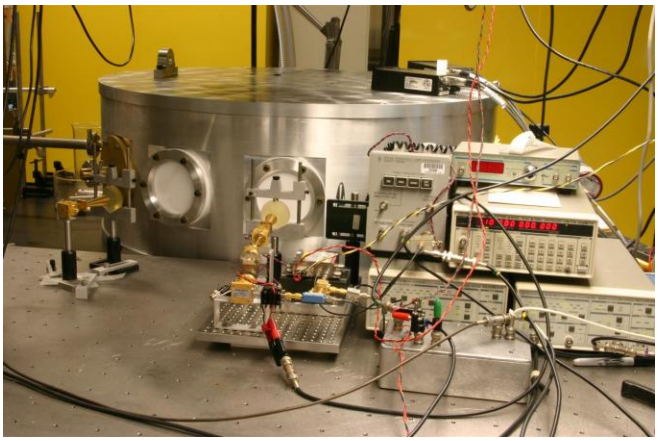

Figure 4.1.2. Test system for the development of the spectroscopy and hardware for the Terahertz

Cell strategies can be separated into two categories: Those that use resonant cavities and those that do not. While the former can lead to significantly increased effective path lengths, considerations of molecular saturation, bandwidth, and analysis speed led to the selection of the non-resonant approach. This decision was solidified by analysis that showed that we would be able to meet the GNG without the system complexity (and risk) that a cavity system would introduce. Figure 4.1.1 shows one of the test beds for this work.

In order to separate the molecular signatures from noise and system systematics, some kind of modulation is required. In THz spectroscopy, the most widely used and proved in Frequency Modulatition (FM). This approach takes advantage of the fact that the spectral linewidth is much narrower in frequency than the systematic variations in the background which are due to standing waves, source and detector response, etc. First derivative FM discriminates against the broader system features according to the ratio of the their width relative to the linewidth, whereas second derivative discriminates

according to the square of the ratio. There are other technical considerations and in the end we used both according to the task at hand.

Another form of modulation is molecular modulation, usually via the Stark Effect. This has traditionally been used primarily at low frequencies where second order Stark Effects are bigger. However, we were able to show experimentally and theoretically that for large molecules highly favorable first order Stark Effects will occur in larger molecules. These larger molecules will be a focus of Phase 2. Accordingly, we adopted FM for the Phase 1 as the low risk path, but explored the first order Stark Effects to lay a foundation for Phase 2. Figure 4.1.2 shows the test system that was used for this and other spectroscopic studies.

4.2 Explanation of System Operation

Figure 4.2.1 shows the TM in the context of the overall system. The receiver accepts a 20 dbm signal from the FMS/Synthesizer that is offset from the transmit signal by 10.7 MHz/24 to provide a local oscillator. The THz transmitter accepts a 20 dbm signal from the FMS/Synthesizer and multiplies it x24 to produce 1 mW in the 210 - 270 GHz frequency band. This power is subsequently attenuated (to minimize molecular saturation) by a programmable wire grid polarizer. The output from the transmitter is transmitted through a 1 m folded cell and detected by the receiver module. The mixer in the receiver has a noise temperature of <3000K and produces a 10.7 MHz IF signal to the ST detector and digitizer. The output of the IF is then detected and processed either by the digital signal processing of the FMS or by a digital lock-in card. Gas is provided to this cell, its pressure monitored, evacuated by the SAPM.

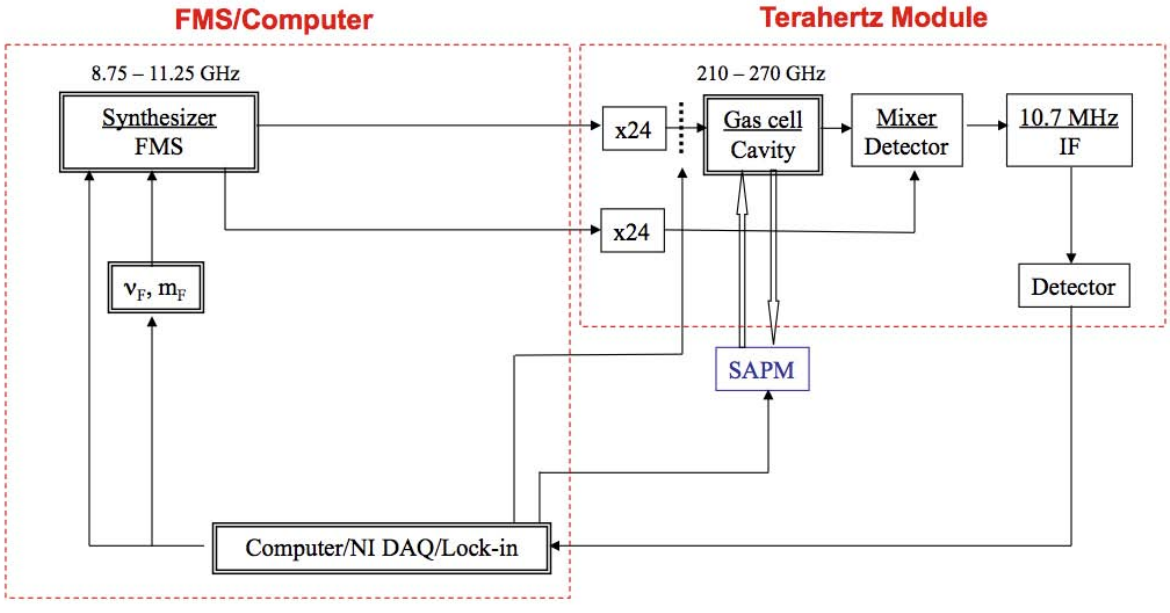

Figure 4.2.1. Elements of the THz Module in the context of a simplified overall MACS system - to show interfaces.

4.3 R&D Leading to Phase 2 Improvements (Size, Volume, Cost, Speed, Performance)

Most of this work was carried out by VDI, some of it in collaboration with OSU. This research was focused on four items: (1) The reduction of broadband noise in the broadly tunable RX/TX systems necessary for MACS, (2) Strategies and designs for reduced size and power in these RX/TX systems, (3) Improved reliability of the frequency multipliers, and (4) Development and delivery of fixed bias, broadly tunable systems for a 600 GHz channel for a Phase 2 MACS.

(1) Broadband Noise: From the beginning of the program, it was recognized that there were two fundamental unknowns that had the potential to severely impact the MACS concept. One of these was the impact of broad band noise as it progressed through the highly non-linear multiplier chains of both the RX and TX. This was of particular concern because we needed to use a heterodyne detector to detect a small change in a large amount of spectrometer excitation power. To our knowledge, this had never been done in the context of broadband tunable systems. For example, similar RX systems are typically used to detect small amounts of power (not small changes in a large amount of power) in radar, imaging, or radio astronomy applications.

Indeed, it was initially found that the RX and TX systems that had been used successfully when independent had significant extra noise when used in the configuration required by MACS. However, VDI (working in conjunction with the amplifier vendor) successfully eliminated the excess noise, and in doing so removed the biggest fundamental worry about the viability of the MACS spectrometer concept. Although this issue will continue to be important in the ongoing development of MACS prototypes, this Phase 1 effort has demonstrated that this is a solvable problem that will not impact the performance of the final MACS systems.

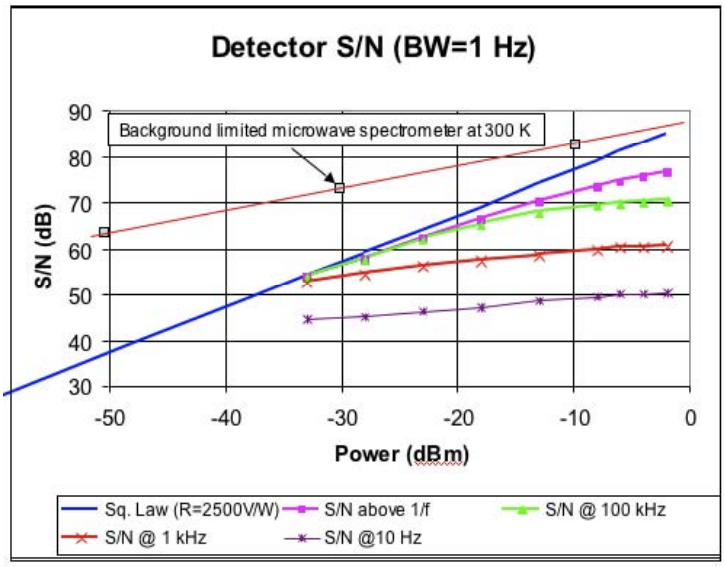

Figure 4.3.1. Relation between measured amplifer noise as a function of signal recovery frequency and power in comparison to the Townes limit.

Figure 4.3.1 summaries some of this work.

(2) Reduced Size and Power: Because of the nature of the small market for THz technology, systems have been developed by mixing and matching subunits (amplifiers, multipliers, mixers, etc.) – each of which occupies its own waveguide block (see Figure 4.3.3 below). If larger

quantities of a particular THz system are required, integration into a single block would not only save considerable space (virtually all of the block volume is related to the need for input and output waveguide and flanges), but also reduce losses and increase efficiency. Accordingly, VDI undertook the design of such a system that could be used for a Phase 2 system. This is shown in Figure 4.3.2. Furthermore, VDI has recently developed several integrated multiplier chains, including a x3x3 multiplier that is presently in volume production for the ALMA program (~150 units). The successful production of these integrated multiplier chains demonstrates that the concept shown in Figure 2 can be realized in the Phase 2 MACS program.

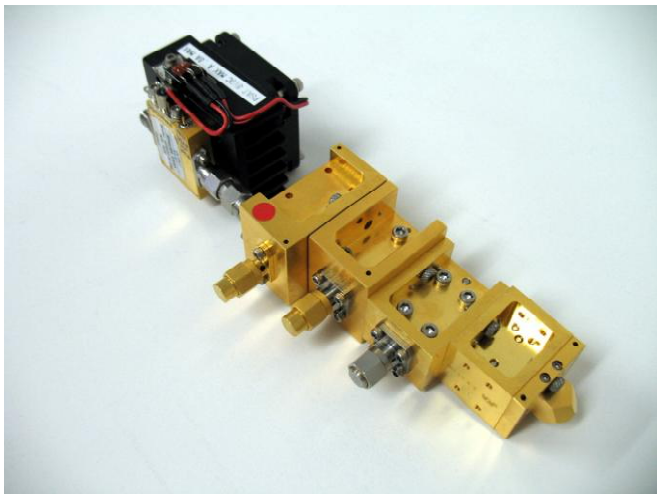

Figure 4.3.3. 575 - 650 broadband source.

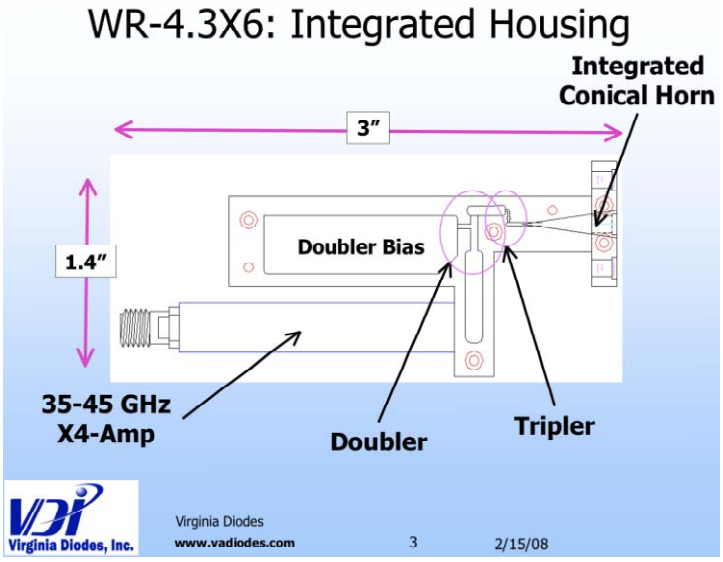

Figure 4.3.2. Size and form of integrated VDI system.

Figure 4.3.2 shows the size reduction that this approach can achieve.

(3) Multiplier Reliability: The reliability of the frequency multipliers is a primary concern for the final MACS systems. In Phase 1, several of the multipliers were damaged during use at OSU. Although VDI was able to rapidly repair these components, it was critical to identify the cause of the failures, and develop improved components with greater reliability. Initially the failures were surprising, since the same multiplier design is often used at higher power levels with good reliability. However, through the Phase 1 effort, VDI determined that an additional failure

mechanism must be considered for MACS-type operation. Specifically, it was found that continuous frequency sweeping of the system causes a fairly rapid modulation of the power dissipated in the multiplier diode chips. It was the resulting thermal transients that caused the failures experienced in Phase 1, rather than an increased peak temperature. Failures due to thermal transients are well documented in the semiconductor industry, and VDI has recently learned that such failures occur in multipliers where the input power is modulated. It has now been demonstrated that frequency sweeping can also cause similar thermal transients. VDI is presently developing design strategies to reduce this problem in the MACS multipliers, and a new design of the critical WR12x2 frequency doubler is under development.

(4) Broadband High Frequency Source: VDI developed and delivered a broadband, rapidly tunable, high frequency Transmit/Receive system suitable for MACS. This 600 GHz channel was originally considered a part of the Phase 1 system, but was deferred to Phase 2 to allow greater Phase 1 emphasis on achieving reduced system size. The new system developed in Phase 1 is fundamentally better than previous 600 GHz systems because the broad tuning band was achieved without any manual or computer controlled adjustment of the bias of the various multipliers as the frequency is swept. Rather, the new system has the same fixed bias and fast tunability as the 210-270 GHz systems used in the Phase 1 prototype. Additionally, this development will be very important for Phase 2 because the smaller diffraction higher sensitivity at 600 GHz provides a path to both smaller and more sensitive systems.

5 FMS (Frequency Management System)

The Frequency Management System (FMS) is one of the key technologies of the MACS system. The main objectives of the FMS are (a) To provide LO and RF signals to the THz module, which are then multiplied up in frequency by 24 and then used for the spectroscopy, (b) To provide precise frequency knowledge of the current THz output frequency to the MACS system for both frequency output control (in order to perform the spectroscopy we need precise frequency knowledge to within 100 kHz at 300 GHz system operation) and in the data recovery, (c) To perform frequency sweeps across bands of frequencies – different chemical species exhibit different absorption characteristics over different excitation frequencies, and (d) The perform data processing on the received power spectrum input from the THz module, including all filtering, averaging, derivatives, and data formatting.

5.1 Summary of Trades and R&D Leading to Design

The primary system concerns (apart from the functionality listed above) were (a) Size (b) Power (c) Ability to lock to a given frequency quickly and to perform sweeps. Some of the tradeoffs are explained in the next section.

5.2 Explanation of System Operation

The FMS consists of two PCBs (RF and Digital) along with a YIG-tuned oscillator.
The block diagram of the RF module is shown here.

Dual Band RF Module rev 2.2

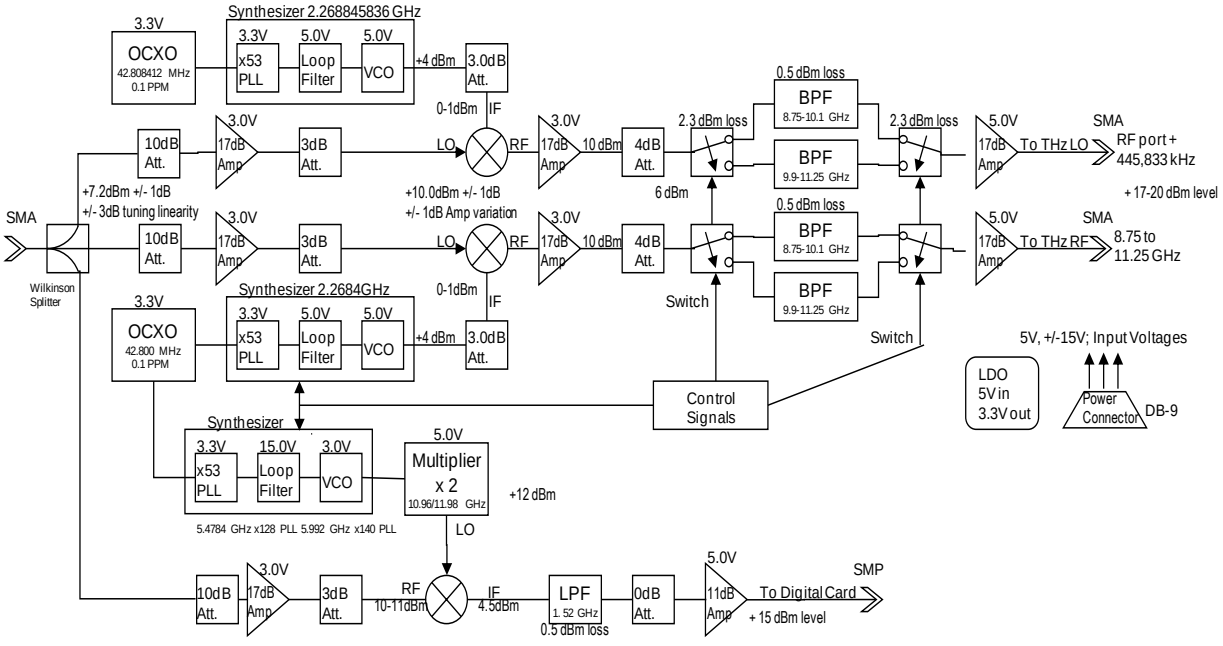

Given the heterodyne receiver architecture, the FMS was responsible for generating the RF and LO outputs fed to the THz module. Because the output of the x24 THz module was in the range of 210-270 GHz, the input frequencies to the THZ module needed to be in the range of 8.75-

11.25GHz. Unfortunately, there was no low cost, small form factor synthesizer module which could produce these frequencies with low noise and quick lock time (accuracy was NOT an issue) and so we decided to use a combination of frequency synthesizers and RF mixers to create the RF and LO signals.

Specifically, the architecture consisted of two ovenized crystal oscillators (OCXO) accurate to within 50 ppb. The OCXOs had slightly differing output frequencies, such that when multiplied up by the synthesizers and THz module, the final frequency difference would equal 10.7 MHz, used by our heterodyne receiver. These OCXO signals are first multiplied up in frequency by a PLL/synthesizer chip. Then, these signals are mixed with the YIG tuned oscillator to create the desired RF and LO frequencies.

This proposed architecture created a number of issues, the biggest of which was creating a spur-free signal for the spectroscopy, specifically by eliminating undesired mixer products before they entered the THz module. This was accomplished by (a) Bandpass filtering the mixer outputs to pass only the desired LO or RF output frequency, (b) Carefully selecting the synthesizer output frequency so that there would be few or no mixer products in the passband, and (c) dividing up the passband into a high band and a low band to support the needed filtering. The bandpass filters and band switches are shown in the block diagram.

Appropriate signal power levels needed to be achieved for the different modules on the RF card, and thus amplifiers (some variable gain) and attenuators were placed throughout the main signal path to achieve the desired signal levels throughout the card. An important requirement of the card was achieving a constant power output over the whole band – this required creating precise trace lengths, impedances, and terminations for the 8.75-11.25 GHz signals.

The YIG-tuned oscillator output often varies over time with changes in temperature, vibration, normal drift, etc. Thus, in order to maintain a highly accurate output frequency, the FMS needed a control loop, to make changes to the YIG input voltage in order to have it oscillate at the desired output frequency.

To accurately record the current output frequency, we adopted the following strategy. Because we only needed 1.35 GHz of frequency knowledge, we could mix the current output frequency down from 8.75-10.1GHz or 9.9-11.25 GHz bands down to 0.05-1.4 GHz. Specifically, this is accomplished by a 3rd synthesizer, a x2 multiplier chip, a 3rd mixer, and a low pass filter, all shown at the bottom of the block diagram. The 0.05-1.4 GHz signal is then sent to the digital card to be counted by the fast ECL counters (capable of counting up to 1.5 GHz) and FPGA.

Two counters (known as ping pong counters) on the digital card alternate counting the current output frequency. Every millisecond, one counter is read by the microcontroller on the digital PCB while the other counter is counting. The counters alternate functions every millisecond so that an accurate (to 1 kHz) count could be maintained. The millisecond boundary is known to be accurate because it is derived from the 42.8MHz OCXO. (Note: Eventually, the boundary was changed to approx 1.53 ms.)

If a count was found to be lower than expected, the microcontroller outputs a new value into a 32-bit DAC on the digital card. The DAC output was filtered and sent to the main coil driver of the YIG-tuned oscillator to adjust the frequency to the desired value.

The block diagram of the digital card is shown below. The counters are shown on the lower left of the diagram.

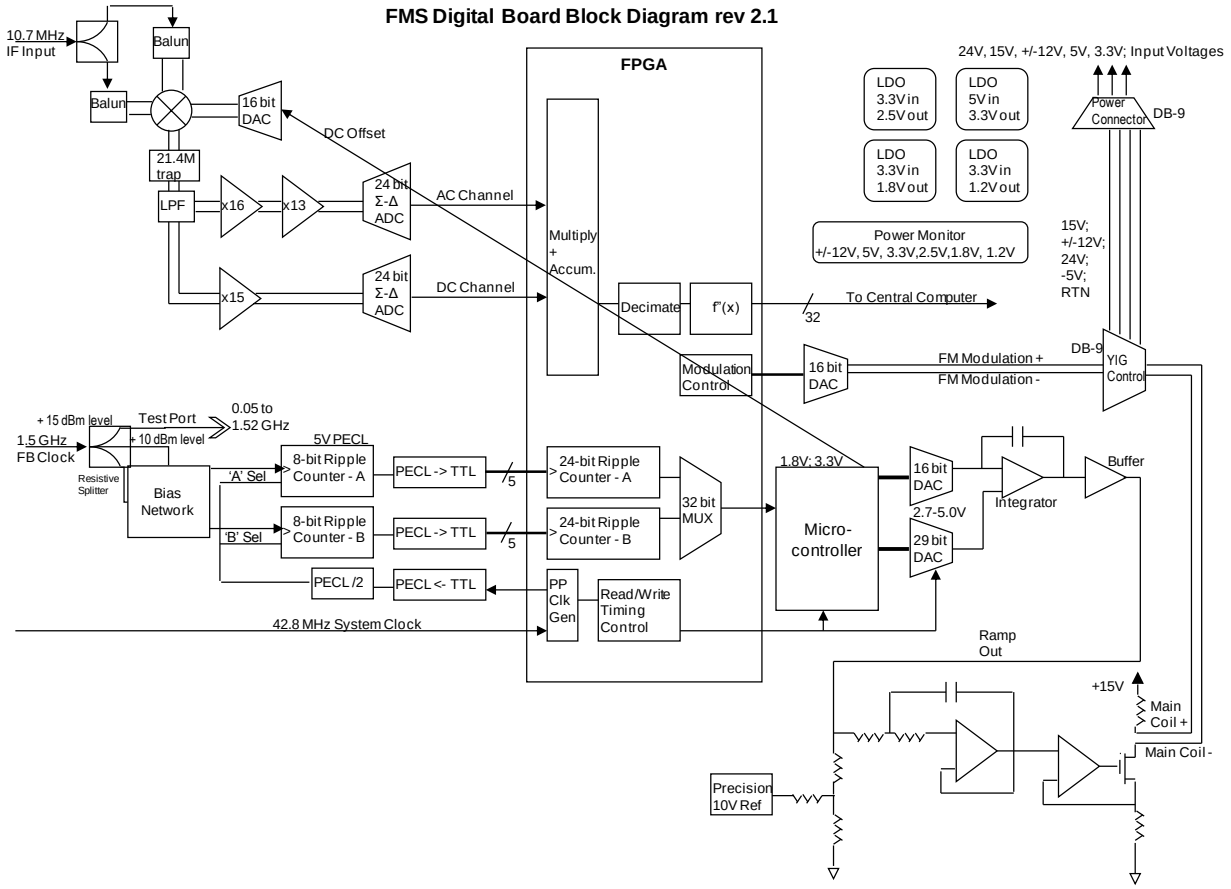

To perform the frequency sweep, an integrator op-amp with reset switch mechanism was used on the digital card. The microcontroller controls a 16 bit DAC whose output voltage controls the rate of charge accumulation in a capacitor connected to the integrator op amp. The output of the integrator op-amp is summed with the 32-bit DAC output to sweep the YIG output frequency over time. Sweeps can be repeated by discharging the capacitor (closing the switch) and recharging the capacitor (switch open).

The final section of the digital card is the receiver section. The 10.7 MHz IF signal comes into the card and is immediately passed through a variable attenuator followed by an amplifier. The goal is the get a maximum input voltage at the square law detector chip so as to maximize the input range of the chip. The key component of the receiver is a square law detector (self multiplier or self mixer), which multiples the input signal by itself to produce a DC component and a 21.4 MHz component. The 21.4 MHz component is tuned out using the tunable trap, and the DC signal component is passed along to 2 ADC chips. One ADC is called the DC ADC which is used to measure the current average IF power. This information is coupled with the AC ADC, which is used to measure changes in the IF input power. Together, the DC and AC ADCs provide MACS with the information necessary to characterize the chemical under test.

As mentioned earlier, the FPGA performs the data processing on the IF spectrum. Data from the ADCs is read by the FPGA, which averages the data, and optionally takes first and second derivatives of the input data. Data is transmitted back to the central computer over a 32 bit bus.

Lastly, the FPGA and microcontroller control frequency modulation. The frequency modulation is used to cause small changes in the output frequency, causing changes in the input power spectrum. These changes in input power are processed by taking the first and second derivatives of the power spectrum in the FPGA; this information (about the rate of power change) often more accurately characterizes a chemical than does the regular power spectrum data.

5.3 R&D Leading to Phase 2 Improvements (Size, Volume, Cost, Speed, Performance)

One of the requirements for Phase 2 is to perform spectroscopy both at 210-270 GHz and at 540-660 GHz. Unfortunately, this means a base frequency (before the THz module) of 8.75-13.75 GHz.

With this new requirement, filtering undesired spurs from 8.75-13.75 GHz will introduce more system complexity and require more space and possibly power. In order to avoid these issues, a simpler (but more costly) architecture is being adopted. This architecture requires the use of two YIG-tuned oscillators to generate the RF and LO signals.

The following paragraphs are taken from Dr. Richard C. Eden, describing the phase 2 proposed improvements.

Power reductions in the MACS Phase II precision frequency generation system could be afforded both by component selection and by altering the basic architecture. A major element of power is the main coil dissipation in the YIG-tuned oscillator. This can be greatly reduced by going to a YIG-tuned oscillator design incorporating a permanent magnet, such that the oscillation frequency with no applied coil current is at mid-band, instead of at f_{osc}=0 as in the normal electromagnet design, as used in the MACS Phase I frequency generation system. For example, consider the 8.75GHz to 11.25GHz (10.00±1.25GHz) YIG-tuned oscillator output frequency sweep that goes into the x24 multiplier chain to produce the final 210GHz to 270GHz (240±30GHz) submillimeter wave output sweep. For comparison purposes, imagine that the YIG coil sensitivity and resistance were unity (1 amp/GHz and 1 ohm), then with the conventional electromagnet coil YIG-tuned oscillator, the DC power at the 10GHz band center would be $P_{DC}=I_{coil}^2R_{coil}$=100W, and the average power over the 8.75GHz to 11.25GHz sweep would be 100.52W. On the other hand, if the permanent magnet YIG-tuned oscillator produces 10.00GHz with I_{coil}=0, then the DC coil power at the 10GHz band center would be zero, and the average power over the 8.75GHz to 11.25GHz sweep would be only 0.5208W, 193x less average coil power than the electromagnet version. In addition to reducing coil power, the permanent magnet version of the YIG-tuned oscillator is less sensitive to small percentage variations in the coil drive current. For example, while a 0.0001% variation in I_{coil} in a conventional electromagnet YIG-tuned oscillator produces a 0.0001% frequency variation (e.g., 11KHz at f=11GHz), with the permanent magnet version, the same 0.0001% variation in I_{coil} produces a much smaller frequency variation, (e.g., 1.0KHz at f=11GHz).

In the MACS Phase I system, another substantial power element involved the high-frequency ECL input stages of the two "ping-pong counter" frequency divider chains used for the frequency base and to implement the frequency-locked loop. This power dissipation could be reduced greatly by going to a faster FPGA such that fewer ECL stages are required because the FPGA divider stages can operate at much higher frequencies. This would certainly be done if it is decided to retain the frequency-locked loop architecture for Phase II, but there are good

arguments for changing to a phase-locked loop approach for the MACS Phase II precision frequency generation system which would not use the ping-pong counters at all.

One of the most serious concerns with the MACS Phase I system has proven to be the sensitivity of the YIG-tuned oscillator frequency to external environmental effects such as temperature and magnetic fields, and particularly to mechanical stresses and vibration. The frequency-locked loop, which has an update rate of about 1ms, handles drift and very low frequency disturbances quite well, and can significantly suppress error frequencies up to about 60Hz, is of little value for higher frequency interferers. This is dealt with quite effectively in the MACS Phase I system by vibration-isolating the YIG-tuned oscillator and turning off major interference sources such as the vacuum roughing pump while scans are in progress. However, this will be more difficult in the MACS Phase II system, both because it is more compact (bringing interfering sources closer to the YIG), and because it is intended for operation in more hostile field environments where the external vibration levels could be quite significant. Hence a more robust frequency generation system is desired for the MACS Phase II system.

The loop update rate (the ping-pong count period) in the MACS Phase I system was limited by the trade-off between the need for frequency precision (which favors a longer count period so that more cycles can be counted) and the desire to access the count data more rapidly (for purposes of updating the frequency-locked loop). The count period of about 1ms was selected as a good compromise, but as noted above, does not allow for very effective suppression of higher frequency (>100Hz) interferers by the FLL. An alternative approach which avoids this trade-off is the use of a phase-locked loop (PLL) architecture for the YIG-tuned oscillator frequency control. In a PLL, the corrective signal is developed in proportion to the error in phase between the generated signal and a reference signal, which occurs much more quickly than does a measurable frequency error. This allows for much more effective feedback control of the output signal (to reduce frequency/phase errors) with a PLL than is possible with an FLL.

The PLL was considered, of course, for the original implementation of the MACS Phase I system. However, at the time, the only practical hardware available to implement a PLL-controlled FCS was a classical analog frequency synthesizer architecture, in which a variable-modulus divider is used to divide down the VCO (e.g., YIG-tuned oscillator) output for phase comparison with a fixed precision reference frequency (where the phase error signal from that comparison is loop filtered and applied back to the frequency control input of the VCO [e.g., YIG coil]). This architecture proved inadequate for meeting all of the MACS Phase I system goals because the settling time of the synthesizer feedback loop is too slow to meet high scan rate requirements. We also considered advanced feed-forward/feedback PLL architectures that might be implemented with FPGAs that would allow extension of the PLL concept to high scan rates, but the fundamental requirement for a time interpolation capability between the fixed frequency FPGA clock and the essentially continuously variable signal output frequency makes the concept difficult to realize without some specialized mixed-signal circuitry not available on an FPGA (and, of course, the design cost for a custom chip would be prohibitive).

Fortunately, in the interim since the initiation of the MACS Phase I design, a commercial chip has become available that can serve to get around this problem and make a PLL approach workable for MACS Phase II. This key component is the direct digital synthesizer (DDS) chip, such as the Analog Devices AD9912 1GHz clock rate DDS. The analog anti-aliasing filter on the DDS output resolves the time interpolation issue noted above. While the broadband spur levels from these DDS chips are too high to use them directly as the FMS source driving the x24 frequency multiplier chain (unless a narrowband tuned filter such as a YIG-tuned narrowband

bandpass filter is used), this DDS output should make an excellent reference frequency generator for a PLL frequency generation approach. While numerous detailed design implementations are possible for the DDS-referenced FCS, the basic approach is to utilize the ~400MHz output frequency range of the DDS chip to act as the frequency reference for the YIG-tuned oscillator. This is most conveniently done by using the DDS in a higher Nyquist band (e.g., in the 3rd Nyquist band, 1.0GHz to 1.5GHz nominal for the 1.0GHz clock rate DDS), possibly with an RZ (return-to-zero) comb generator circuit on the DAC output to enhance performance in higher Nyquist operation. One approach would be to simply frequency multiply this 1.05GHz to 1.45GHz output up to the YIG output frequency range of interest. While this would be simple and very low power, the process of frequency multiplication increases phase noise and spur levels, making a frequency translation approach more attractive from a performance standpoint.

Implementing the MACS Phase II frequency control system with a frequency translation approach based on a DDS reference means breaking the YIG-tuned oscillator swept frequency range into a series of overlapping sub-bands, each at least 400MHz wide (i.e., the 8.75-11.25GHz input range into the x24 frequency multiplier chain would be comprised of at least 7 overlapping sub-bands [probably at least 8 or 10]). The frequency translation for each sub-band would be different, in order to shift the YIG-tuned oscillator frequency down into the 1.05GHz to 1.45GHz DDS output range (or visa-versa) for phase comparison. This frequency translation source could itself be a selected comb generator harmonic of some fixed reference oscillator (which has the advantage of no generator settling time), or a standard frequency synthesizer (which would require settling time, unless a pair of these synthesizers were used in "ping-pong" operation). In either case, some settling time would be required for the DDS-referenced phase-locked loop when transitioning from one sub-band to another. However, in comparison to the overall scan times these sub-band transition times are insignificant, particularly in light of the fact that the sub-bands are overlapping so that there will be absolutely no cases of narrow frequency range scans in which it is necessary to change sub-bands to complete the narrow, high-rate scan.

Note that it would be possible to use the DDS reference signal itself, translated up to a higher frequency range, as the exciter input signal into the x24 frequency multiplier chains. Unfortunately, the spur level of the DDS signal is substantial, so that it would require use of a YIG-tuned narrowband bandpass filter to clean the signal up sufficiently for the application. While this would seem to get away from the requirement for a phase detector/phase-locked loop in the exciter design, in fact this is not the case. Because the very narrowband YIG-tuned filter is subject to the same coil drive current precision, hysteresis, and environmental (temperature, magnetic field and vibration) perturbations to its center frequency that a YIG-tuned oscillator is, there will be substantial random variations of the filter center frequency relative to the signal frequency. Uncorrected, such variations would lead to (very) undesired amplitude and phase modulations of the output signal which could very seriously degrade system performance. Fortunately, it is possible to phase-lock the narrowband YIG-tuned filter to the signal frequency by comparing the output phase to the input phase and feeding the error back to the YIG drive coil (in essence identical to what is done in a YIG-tuned oscillator phase-locked loop). Hence, a phase-locked loop is needed for either the YIG-tuned filter approach or the YIG-tuned oscillator implementation of the MACS Phase II frequency control system. Since we have confidence in the very low AM and low phase noise levels obtainable by phase-locking the YIG-tuned oscillator, this represents an attractive starting point for the MACS Phase II frequency control system.

The YIG-tuned oscillator phase-locked loop approach should provide excellent robustness for the MACS Phase II frequency control system because of the relatively low latency and high loop gains possible with this PLL approach (particularly in comparison to the MACS Phase I FLL). The FM coil of the YIG-tuned oscillator has a bandwidth measured to be about 1.5MHz, and even the main coil bandwidth is probably well over 10KHz when driven by a current source, so the loop bandwidth can be made large enough to very effectively suppress the environmental FM interference effects observed in the MACS Phase I system tests.

Requirements for spectral data acquisition are derived from the spectrometer sweep bandwidths and the required sample resolution. Doppler broadening of THz rotational spectroscopy results in linewidths of ~ 0.6 MHz at our preferred 10 mTorr pressure level. To de-convolve overlapping lines, data will be collected at one tenth the linewidth or 60 KHz. Since the high band channel has a 60 GHz maximum sweep width in one second, the highest sampling bandwidth will be 600 K samples recorded for each sweep ($60 \times 10^{9} \div 100 \times 10^{3}$). To provide for engineering margin a pair of 24-bit sigma-delta ADCs (one for the DC channel and one for the AC channel) operating at up to a 668,750 sample per second rate were been chosen for the MACS Phase 1 instrument. In the MACS Phase II system, particular focus will be made on maximizing the SNR for 1st or 2nd derivative measurements by optimizing the □ □ ADC sample rate, as well as optimizing the on-chip FIR filter in the ADC for operation as a modestly narrow bandpass filter to avoid aliasing of out-of-band noise, in conjunction with an FPGA-implemented very narrowband digital filter (e.g., long FIR filter) to minimize the noise-equivalent bandwidth in the measurements.

Some of the major power reduction items, as discussed in section III.4.3, include replacing the conventional electromagnet YIG-tuned oscillator with a much lower coil power permanent magnet version. Going from the MACS Phase I frequency-locked loop FMS to a DDS-based phase-locked loop approach will not only save power (by eliminating the need for the ECL ping-pong counter stages), but provide for much higher loop gain and bandwidth to greatly reduce frequency perturbations due to environmental effects like stray magnetic fields, temperature, and (especially) mechanical vibration/stress effects. This PLL FMS will also allow for more versatile, higher rate scans for faster overall system operation. The MACS Phase II system will also utilize a higher performance FPGA to support incorporation of more advanced digital signal processing functionality in order to achieve highly effective noise reduction in order to realize optimized SNR in the acquired scans, particularly in the FM-modulated first and second derivative waveform measurement modes.

5.4 Module Design Specifications and Engineering Drawings

Both the RF and Digital modules were approximately 4.75" tall and 8.75" long to fit within the required space of the MACS box. The power specifications are mentioned in the power section. Engineering drawings were produced in ORCAD software on 'D' sized paper, and therefore are not included in this report.

5.5 Module Performance (Measures and Results)

A graph of the input power versus ADC output is shown below. Every point on the X-axis from 1-14 represents a 3dB drop in input power, and the Y-axis plots the ADC output (on a log2

scale). From this graph, we can see that the receiver module to have approximately 40dB of dynamic range.

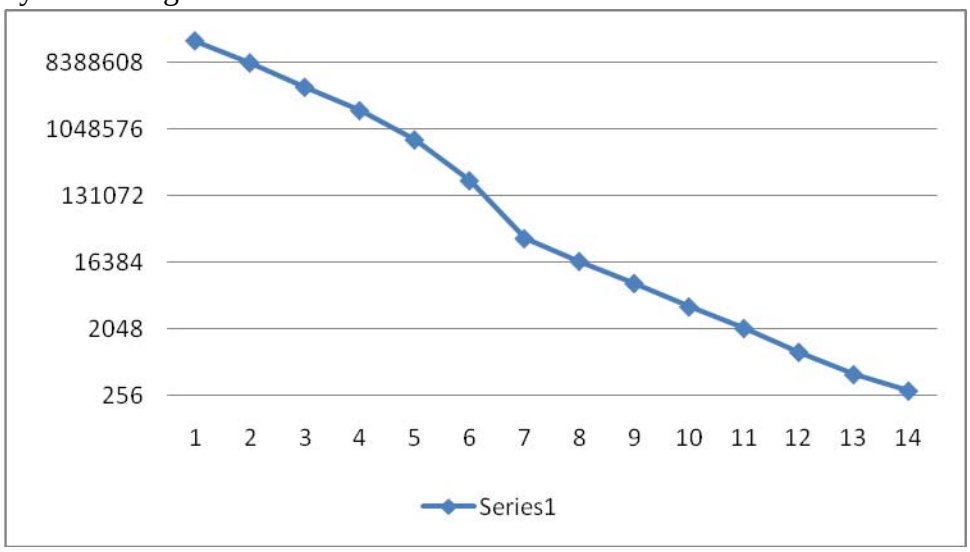

Based on the datasheets of every part in the receiver architecture, we found the dynamic range to be limited by the noise specifically in the square law detector (as opposed to thermal noise in the amplifiers).

Spectrum analyzer plots of the transmit power showed uneven output power between the low band and high band; within a given band though, the power output was within 0.5 dB of the mean.

The lowest concentration we were able to detect was probably in the hundreds of ppt, but we have no confirmed data on this as of yet. Advanced work with the FMS is covered in Appendix A5.2.

6 CC (Central Computer)

6.1 Summary of Trades and R&D Leading to Design

The main consideration when selecting the central computer hardware for the preliminary MACS phase was choosing a configuration that would provide hardware and software flexibility and accommodate unexpected problems or modifications to the other hardware modules. A standard Intel PC was chosen because it provided the most options for operating systems, software development platforms and available hardware modules for data IO between the FMS, the SAPM, and the outside world. Having a wide array of COTS products to chose from made this selection very economical in terms of $/MFLOP and $/GB for processing and storage, and also provided inexpensive software development options.

The highest bandwidth bus in the MACS system is the frequency and power measurement outputs from the FMS module. Each FMS data packet contains 8 words of 4 bytes each, which provide a single frequency measurement channel, 6 channels of power absorption data, and one debug channel. The data rate can be as high as 668.75 kHz, which results in a total bandwidth of 21.4 MB/s. To handle this data rate, the NI-6536 32 bit digital I/O board was chosen for the receive side. This module can handle a maximum data rate of 100MB/s, and includes onboard memory and DMA controllers, which allows for very reliable and simple data transfer.

In addition to the high bandwidth spectral data interface between the FMS and the central computer, the CC also needs a low bandwidth bi-directional interface with the SAPM controller and the FMS controller to configure and execute spectral sweeps. An RS-232 interface was selected for both these interfaces, because this would provide simple debugging allowed the SAPM and FMS modules to be tested and developed independently without any special support hardware or software.

A 7” touchscreen display was selected for the user interface. This choice provides the operator complete control without needed to add a keyboard or mouse, and is simple to program and reconfigure. A touch interface is familiar even to novice computer operators, and can easily be tailored to different applications.

A complete list of central computer hardware is provided in Appendix A6.1.

6.2 Explanation of System Operation

The central computer is responsible for collecting and correlating all spectral data, displaying scenario results and handling all operator interactions. In normal operation, the user selects a scenario to execute using the touch screen interface. The scenario then runs at the scheduled times defined in scenario script, and the CC commands the SAPM and FMS modules accordingly. First, the CC commands the SAPM over the CC to SAPM RS-232 port using the SAPM commands defined in Appendix A3.3. Once the SAPM has collected and transferred a sample to the THz module cell, the CC to FMS RS-232 link is used to configure and execute a spectral scan, using the FMS command protocol in appendix A5.1. Incoming spectral data then

arrives over the 32 bit parallel bus, and the NI-6536 digital I/O card collects this data until the CC reads and processes it. For the Phase 1 system, the decision was made that all incoming data would be immediately and permanently saved in a raw binary format, which allows for data review and reprocessing if higher up software modifications occur. The 750GB system hard drive is used to store this data, as well as chemical library files, and results from the spectral analysis and classification. This incoming spectral data is then analyzed by the system software described in Section 8. Depending on the defined scenario, the SSW will return concentration values for one or more analytes of interest. These results will be given to the user using the touch screen display.

In addition to the standard MACS operating configuration, external data ports on the MACS box have been added to allow engineering development and debugging. An external VGA connector allows the display output to be routed to a larger display, and external USB ports allow keyboard, mouse, and data drive connections to the system for software upgrades or data archiving. The USB interface can also be used to add new scenarios to the MACS unit, or to update or expand the MACS library files.

6.3 R&D Leading to Phase 2 Improvements (Size, Volume, Cost, Speed, Performance)

The main focus for CC improvements during MACS phase 2 is to simplify and improve interconnects between system components to lead to a more modular system design. These changes should also simplify the system software and make MACS more platform independent. One major improvement in system operation will be migrating away from the 32 bit parallel interface to an Ethernet link between the FMS and the CC. This single interface will also replace the RS-232 command link which will greatly simplify the interface between the two modules. Improvements to the FPGA software in phase 2 will shift more of the data filtering process from the CC to the FMS. This will reduce the system data rate to the point where the FMS output will always have a wide bandwidth margin that can be used when command and control is necessary. This change will eliminate the need for the digital I/O card, which was an expensive component with a large footprint. The digital I/O card also required a PCI-express slot, which limited motherboard selection. The current motherboard will be replaced with a similar motherboard that provides dual VGA and Ethernet controllers, which will provide dedicated external VGA and Ethernet ports. This Ethernet interface provides MACS with a very standard data interface that will allow a wide variety of operating systems and processors to interface with the FMS. By implementing a standard TCP/IP interface, different data ports can be assigned to each channel, allowing very easy parsing of command and control, debug messages, and output data. Another major advantage of this interface is it allows multiple MACS units to be controlled by a single external master computer. The master computer could collect spectral or scenario result data from multiple MACS units or download new scenario and library information.

The MACS phase 1 system did have some issues with system cooling in the CC unit, and these issues will be addressed in phase 2. As stated earlier, the elimination of the digital I/O daughter card makes the CC unit smaller. This extra space will be used to provide more effective heat transfer from the CC.

7 PM (Power Module)

7.1 Summary of Trades and R&D Leading to Design

At the preliminary and critical design reviews, we released the following projected power budget:

Element	24V Pwr	15V Pwr	-12V Pwr	12V Pwr	5V Pwr	3.3V Pwr	Sys Pwr	Comment	Basis
Central Processor				50.0				Weight estimated, 90% efficiency supply	Datasheet
Hard Disk				10.5					
Data Acquisition				3.6		2.5			Datasheet
Digital Card/ FMS		0.1	0.3	1.0	7.2	6.6		Custom PWB using COTS parts	Datasheet
RF Block/FMS			3.1	0.0	4.0	3.2		Custom PWB using COTS parts	Datasheet
YIG	24.0	12.8	0.8						Datasheet
Power Module							40.0	80% efficiency to produce 200W	Datasheet
System Display						7.4		AUO G150XG01	Datasheet
Thermal Control							5.0	Heat Sink, fans, etc.	Best Guess
System Keypad/Input							0.5		Best Guess
Pri. Electronics Subtotal	24.0	12.8	4.2	65.1	11.1	19.6	182.4		
Sample Cell (Cavity)								Existing Design	Engineering Estimate
RF Exciter module		1.0	1.0	18.0				Custom PWB using COTS parts	Engineering Estimate
LO/Detector module		1.0	1.0	18.0				Custom PWB using COTS parts	Engineering Estimate
IF Module		1.0	1.0	18.0				Custom PWB using COTS parts	Engineering Estimate
Miscellaneous Plumbing									Engineering Estimate
THz Subtotal	0.0	3.0	3.0	54.0	0.0	0.0	60.0		
Turbo Pump	115.0								Engineering Estimate
Diaphragm Pump	17.0								Engineering Estimate
Flowmeter	12.0								Engineering Estimate
Vacuum Valve Manifold	13.0							COTS Equipment	Engineering Estimate
Plumbing	13.0							Custom Design	Engineering Estimate
SAPM Subtotal	170.0						170.0	Sub-contract allocations	
Interconnects								Assumes 80% packaging efficiency	
Totals (metric)	**194.0**	**15.8**	**7.2**	**119.1**	**11.1**	**19.6**	**412.4**		
Totals (english)									

Amongst the critical design requirements were (a) The ability to provide more than 400W of system power at any given time, (b) The ability to provide up to 194W of power on the 24V power supply, due to a high instantaneous "turn on" current of the turbo pump. (c) The ability to provide for the different system level voltages (24V, +15V, +/-12V, 5V, 3.3V), (d) Small form factor, high power efficiency, and low noise.

Based on these considerations, and the research of several corporations, we decided on Vicor as the best solution to our needs. The PFC micro supply provided the requisite power, number of voltages, and had a very nice form factor which fit in our system. The main drawback of the PFC micro was high supply noise (this may have been the case with all alternatives), therefore we ended up purchasing noise reduction modules from Vicor to meet the power supply noise requirements.

7.2 Explanation of System Operation

The Vicor power supply module receives as its input 115V AC from an AC MAINS power source. The Vicor module converts the AC input to a DC output voltage, which is fed to 6

individual DC/DC modules which produce the 24V, 15V, +/-12V, 5V, and 3.3V output voltages. These voltages are fed through the noise reduction modules on the power supply distribution card (which in the system sits on top of the CPU module). The power supply distribution card has DB15 connectors to the individual system sub-modules: SAPM, THz, FMS (RF and Digital). Each connector has a standard pinout, used throughout the system, as shown here in this table:

Pin 1	+15V	Pin 6	GND	Pin 11	GND
Pin 2	GND	Pin 7	+5V	Pin 12	+3.3V
Pin 3	GND	Pin 8	+5V	Pin 13	GND
Pin 4	-12V	Pin 9	+24V	Pin 14	+12V
Pin 5	GND	Pin 10	GND	Pin 15	+12V

7.3 R&D Leading to Phase 2 Improvements (Size, Volume, Cost, Speed, Performance)

It is an important goal of phase 2 to reduce the size, power, and cost of the MACS system. The power supply basically must meet the system requirements, and once the power budget for phase 2 has been established, it is our intention to revisit the alternatives for power supply modules to increase the efficiency, and decrease the volume, cost, and noise specifications of our power supply module.

The major proposed upgrade for phase 2 is to provide a 28V DC input alternative alongside the 115V AC power supply option. This could be accomplished by using high voltage OR-ing diodes to take either the output of the AC/DC converter in the MACS box or to take the 28V input directly and feed it to the DC/DC power supply modules. Using a DC input would provide the MACS system with more flexibility of usage, less power consumed inside the system, and lower system noise.

7.4 Module Design Specifications and Engineering Drawings

The design guide (this is the relevant document) for the PFC Micro power supply module can be found at the following URL:

http://www.vicorpower.com/documents/design_guides/pfcmicro_designguide.pdf?src=vicoreurope

The datasheet for the MicroRAM output ripple attenuation module can be found at the following URL:

http://cdn.vicorpower.com/documents/datasheets/ds_microram.pdf

7.5 Module Performance (Measures and Results)

The modules provided adequate power, and the main figure of merit would be the voltage ripple for which we have no official measurement as of yet.

8 SSW (System Software)

8.1 The MACS Unser Interface

The MACS user interface is designed to operate completely from a touch screen interface, with minimal user interaction or understanding of the MACS system. In normal operation, an operator would select a pre-configured scenario from a list and execute it. Scenarios would typically be designed by experienced personnel to search for one or more chemical of interest. Design of these scenarios is covered in Section 8.2. Execution of a typical scenario that searches for one or more analytes of interest is described below.

Figure 8.1 shows the scenario selection tab of the MACS software. If additional scenarios are defined paging keys will appear that allow the user to scroll through the additional options. The selected scenario is shown in orange, and will begin execution when the GO button is pressed. The scenario can also be paused or cancelled.

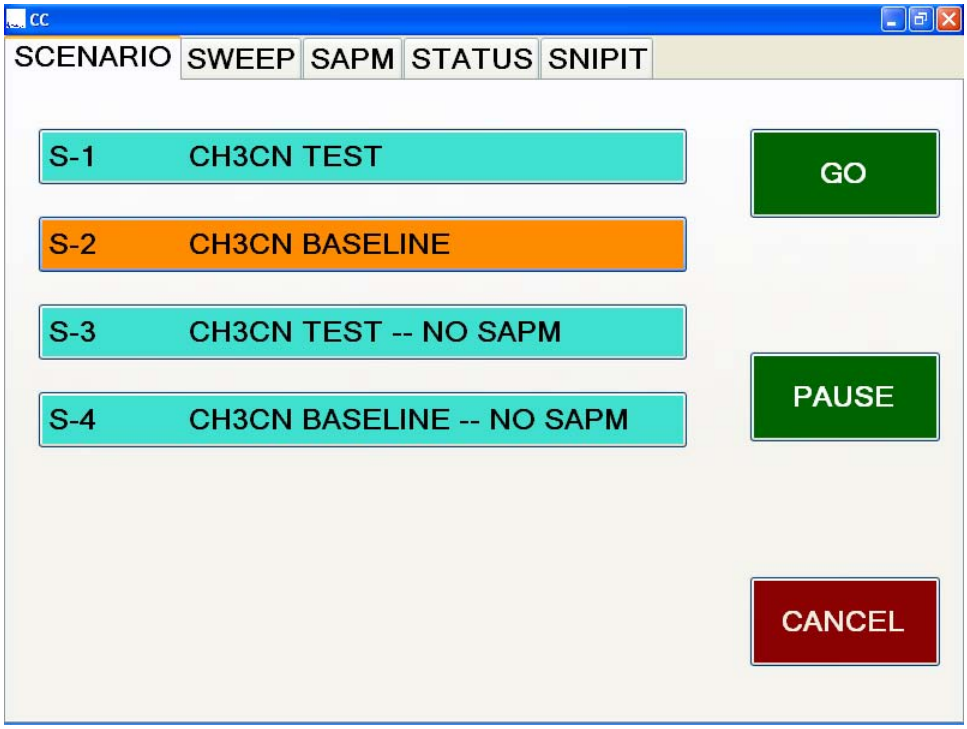

Figure 8.1. MACS Scenario selection Tab

Once a scenario is selected and executed, the MACS system will automatically command the SAPM module to collect a sample. The user can monitor the progress of the sample collection process by switching to the SAPM tab, which is shown in figure 8.2. In addition to automatic execution, a more experienced user can manually select different SAPM phases of operation by touching the stage buttons on the left hand side. These stages are carefully designed scripts that operate the SAPM without risking damage to the turbo molecular pump or the sorbent, both of which have strict operating guidelines. The turbo pump cannot operate at

pressures above 1 Torr, and the sorbents cannot be exposed to temperatures above 100 °C at high pressures, because it will rapidly oxidize. The SAPM stages are briefly described in Table 8.1. As the stages execute, the MACS software updates the user on system progress in the progress bar at the top of the screen.

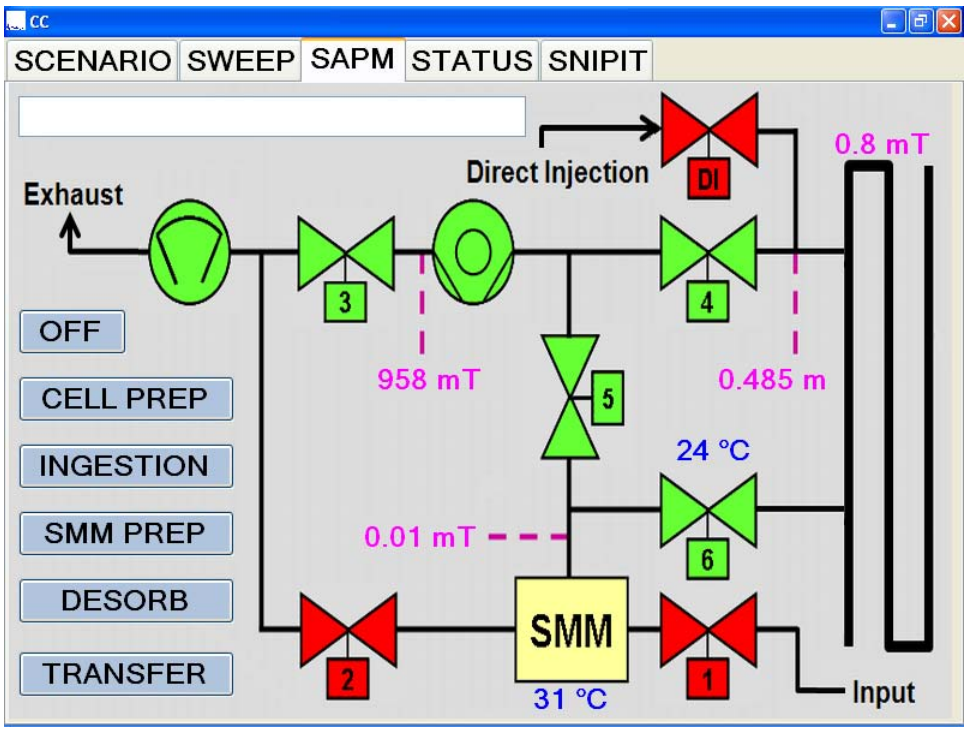

Figure 8.2. SAPM Status Tab

State	Function
OFF	Closes all valves and turns off the turbo and diaphragm pumps.
CELL PREP	Opens valves 3,4 and 5 and pumps the sample cell and SMM to a hard vacuum
INGESTION	Opens valves 1 and 2 so the diaphragm pump can pull air through the sorbent module (SMM). The sorbent traps chemicals of interest that are present in the atmosphere.
SMM PREP	The SMM area is pulled to a hard vacuum by opening valves 3 and 5.
DESORB	The SMM is heated to 200 °C to release chemicals trapped by the sorbent
TRANSFER	Valve 6 is opened to allow gasses released by the sorbent to diffuse into the sample cell

Table 8.1. SAPM Stage Descriptions

Once a sample has been transferred to the sample cell, it is scanned by the FMS at frequencies of interest defined by the scenario script. Typically multiple narrow frequency segments are scanned for each analyte of interest. These frequency segments are chosen at locations where the molecule has strong absorption peaks. The segments are scanned multiple times in a row, and the MACS software averages these results together to increase the signal to noise ratio. Each scan of the gas can be seen on the sweep tab, show in Figure 8.3. The MACS

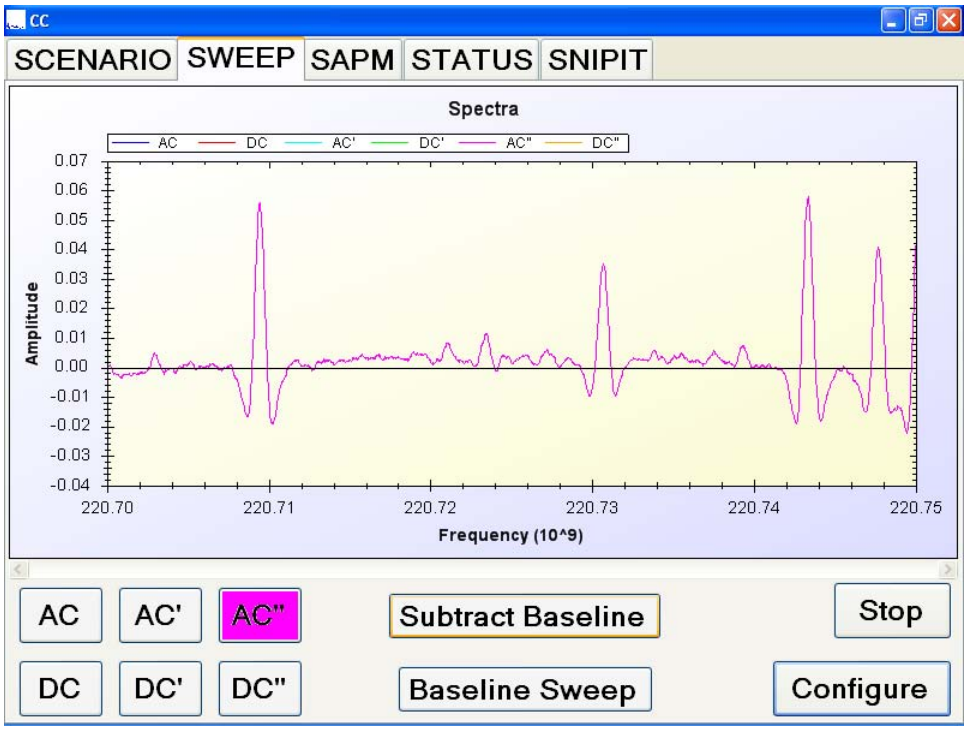

Figure 8.3. SWEEP Display Tab.

FMS has an AC coupled and a DC coupled channel that recovers the IF, and in addition to that can calculate the first or second derivative of the signal by applying the proper RF modulation. These six data channels can be toggled on or off using the buttons on the SWEEP tab. By default the typical channel of interest is selected automatically, so only advanced users would want to change this selection. The Baseline Sweep button indicates when the system is performing a sweep to calibrate out variations inherent to the system. Ideally, a sweep of an empty cell would yield a perfectly flat line, but power variations in the multiplier chain at different frequencies, imperfections in the cell walls and mirrors, and other minor effects cause some baseline variation. These features can be learned by performing a baseline sweep with an empty cell, and then this curve is subtracted from future data to give the best possible signal to noise ratio. For testing purposes, engineers can toggle the baseline subtraction on and off, or initiate a baseline sweep manually using the buttons on the SWEEP tab.

Operators can also abort the current MACS sweep by touching the Stop button. The Configure button can be used to set up and execute a manual scan of a desired frequency band. Again, this kind of operation is never necessary for normal operation, but can be used for testing or system demonstration. The sweep configuration screen is shown in Figure 8.4. The sweep can be configured either by entering a start and stop frequency or by selecting a center frequency and a span, much like a spectrum analyzer. Different scan rates can be selected using the slope key, and repeating the scan more than once can be done to improve signal to noise ratio. In general, slower scans provide higher resolution, and faster scans can be used when a very wide frequency range needs to be covered. Users can also select raw power, first derivative, or second derivative data under the Modulation section. The modulation rate and deviation can also be selected. For all controls that require a numeric input, touching the control brings up a keypad that allows easy input using the touch screen interface. This keypad is shown in Figure 8.5. Once the sweep is configured the system will perform the sweep as soon as the Execute button is pressed. The configuration can be cancelled by pressing the Cancel button.

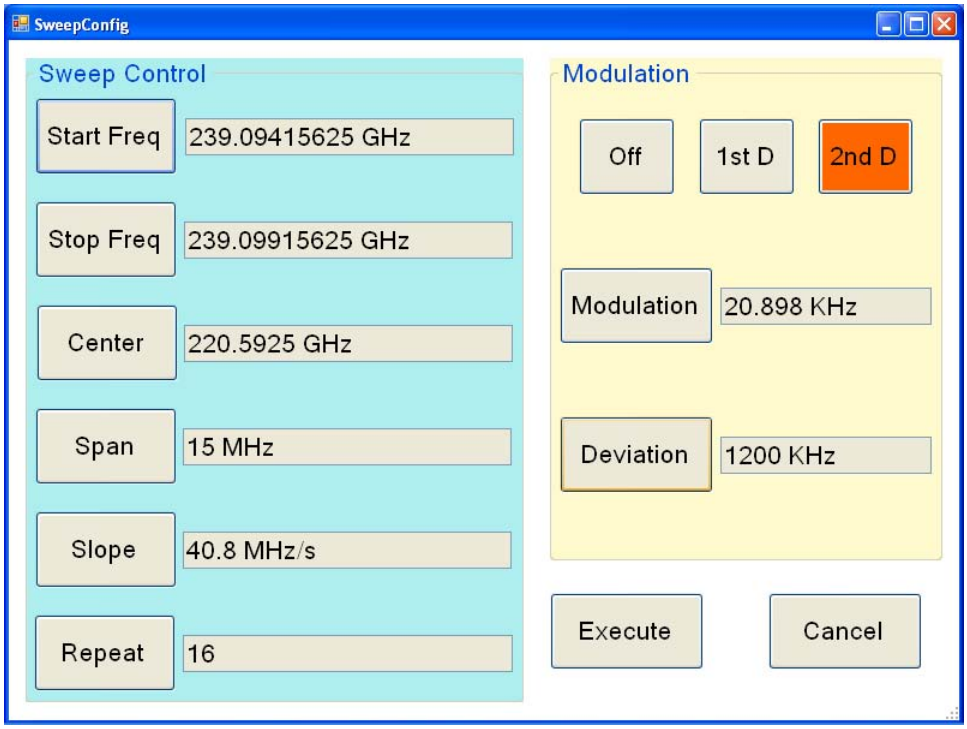

Figure 8.4. Sweep Configuration Tab

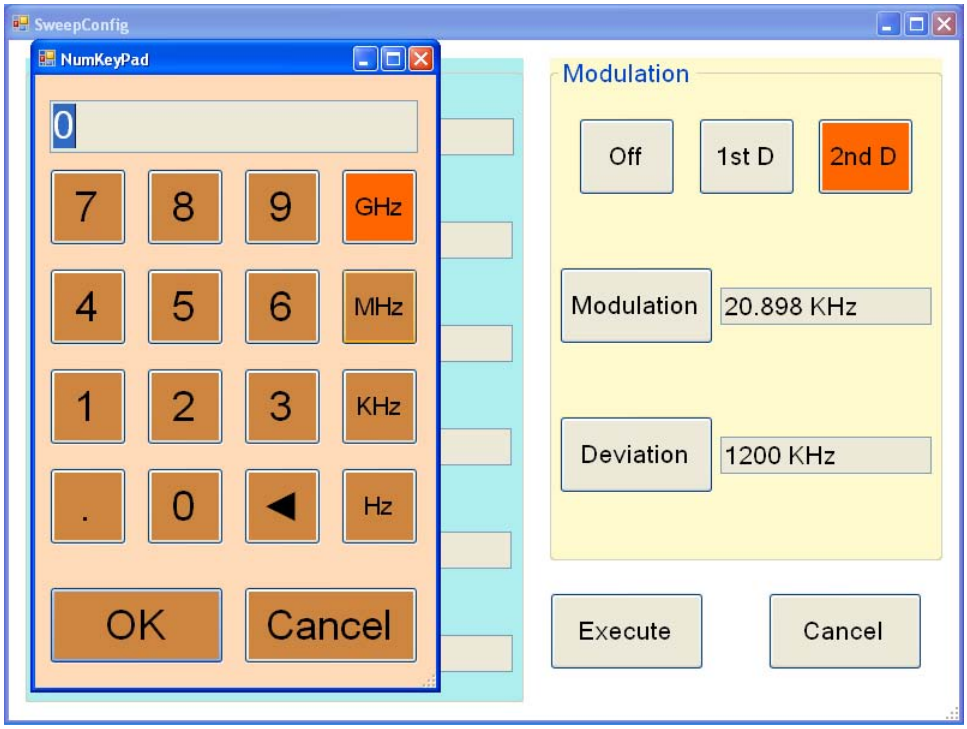

Figure 8.5. Numeric Entry Keypad.

In order to search for a single analyte, the MACS system sweeps multiple frequency segments to confirm the presence of absorption lines at amplitudes and frequencies consistent with the chemical library. For normal operation, the five strongest absorption lines free from other nearby interfering lines are chosen. These frequency segments are then scanned and processed by the SLPA, which is discussed in Section 8.3. The user can monitor the progress of these scans and see the absorption peaks under the SNIPIT tab, which is shown in Figure 8.6.

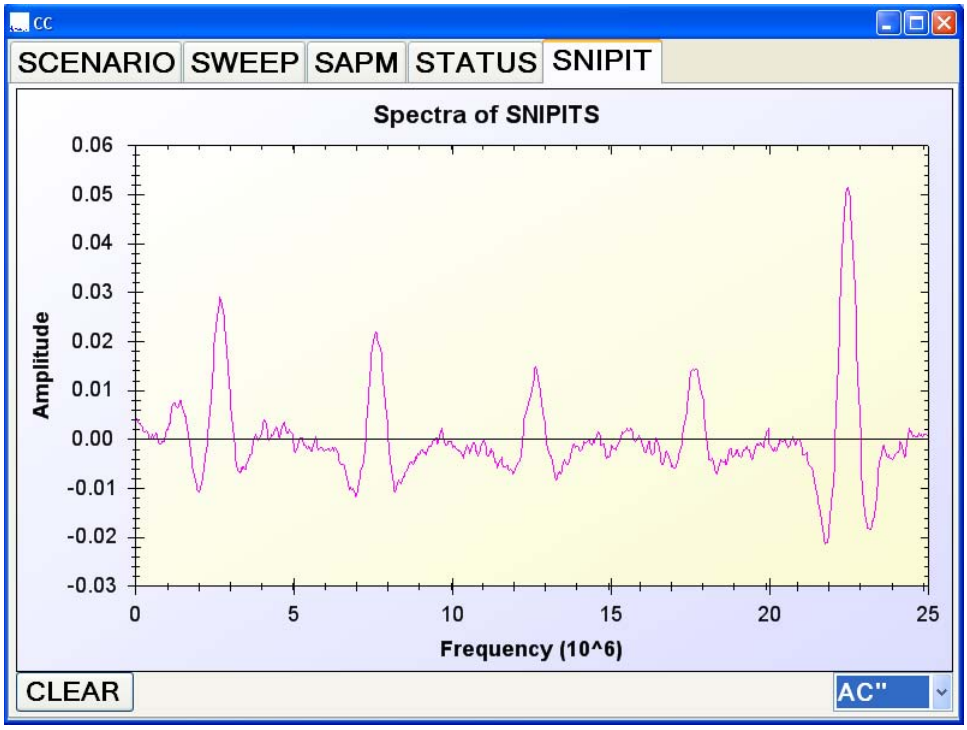

Figure 8.6. SNIPIT Tab

8.2 MACS Scripts

MACS scripts are designed to allow flexible configuration of the MACS unit by an advanced user. A single script can be designed for each MACS mission, and these scripts can then be selected and executed by novice operators. An example of a SAPM control script is given in Table 8.2. This script performs the desorb function which is described in Section 8.1. The script has commands for user feedback, SAPM control, error state detection and error message display, and timer functions. A script can also call other scripts, which allows complex functions to be built with minimal effort. Table 8.3 shows the MainSAPM script, which performs the full cycle of SAPM functions necessary to collect a sample before it can be analyzed.

#desorb.scr	
#SAPM Desorbtion Script	
#This script checks to make sure the cell and SMM module are at proper vacuum	
#It then isolates the SMM module and heats it to 200 C to releast trapped analytes.	
#Hold at 200 C for 40 seconds to fully evolve the sample, and then turn off the heater.	
#The script includes temperature and pressure checks to ensure the SMM is not exposed to	
#high levels of oxygen while at high temperature, as this will oxidize and destroy the sorbent.	
{	
BEGIN,	#Beginning of script
OTHER="DISP Desorption",	# Feedback to User
OTHER="IF (PRES1 .GT. 20) DISPE ERROR: P1 TOO HIGH",	# SMM Cell Area should be purged at this point
OTHER="IF (PRES2 .GT. 10) DISPE ERROR: P2 TOO HIGH EXECUTE SMM PREP",	# Sample Cell should be purged at this point
SAPM="VALV6 OFF",	# Isolate SMM Cell Area
SAPM="VALV5 OFF",	# Isolate SMM Cell Area
OTHER="PRES1 .LT. 1200",	# Make Sure Cell is at Medium Vacuum or better
SAPM="VALV4 ON",	# Continue purging Sample Cell
OTHER="DISP Wait for SMM Temp > 180 C",	# Feedback to User
SAPM="TEMP1 200",	# Set SMM heater target to 200 C
SAPM="TEMP1 ON",	# Heat SMM to 200 C to release analytes
OTHER="TEMP1 .GT. 180"	# Wait until SMM temperature reaches 180 C
OTHER="DISP Hold Temperature 40 seconds",	# Feedback to User
OTHER="WAIT 40000",	# Hold at this temp for 40 seconds
SAPM="TEMP1 OFF",	# Turn off Heater
OTHER="DISP Desorption Done",	# Feedback to User
END,	#End of script
}	

Table 8.2. Desorb.scr

#MainSAPM.scr	
#Calls scripts to perform each stage of SAPM sample collection.	
{	
BEGIN,	#Beginning of script
SCRIPT="OFF.SCR",	#Get to known starting point
SCRIPT="prep.scr",	#Sample Cell and SMM to hard vacuum
SCRIPT="ingest.scr",	#Pull outide air across SMM, trapping analytes
SCRIPT="smm.scr",	#Return SMM to hard vacuum, removing bulk atmosphere
SCRIPT="desorb.scr",	#Heat SMM to 200 C, releasing trapped analytes
SCRIPT="transfer.scr",	#Transfer released analytes to Sample Cell for analysis

END,	#End of script
}	

Table 8.3. MainSAPM.scr

Scenario scripts contain all the necessary information for the MACS system to search for and identify analytes of interest. The key pieces of information the MACS system needs are the frequency segments that should be scanned for each chemical, the sweep parameters, and the libraries to use to estimate the chemical concentration. The concentration estimate is done by the SLPA, which is discussed in Section 8.3. Table 8.4 shows an example scenario script which searches for Acetonitrile (CH_3CN), a widely used solvent.

#Test Sample for CH3CN	
#Repeat 10 times, once every 10 minutes	
{	
SCENARIO(CH3CN Test)	#Scenario name to display to user
BEGIN,	
#Define System Parameters	
SECONDMODE,	#Second Derivative Spectral Data Requested
#Define CH3CN Parameters	
CH3CNLibrary = "CH3CN_2D_Library.macs",	#Define Library data file (CH3CN, 2nd Derivative) to use for analysis
CH3CN_Snippets = { 239094156250,239099156250;	
220706718750,220711718750;	
239117187500,239122187500;	
220744906250,220749906250;	
220740656250,220745656250; }	#Define five frequency segments to scan
#Calibrate the MACS System Baseline	
BASELINESWEEP,	#This Sweep is a Baseline Sweep
SCRIPT="prep.scr",	#Purge the sample cell for baseline sweep.
CH3CNBaseline = CollectSnippets(CH3CN_Snippets),	#Sweep the Intervals provided and store the results in CH3CNBaseline
#Test Environment for CH3CN	
NORMALSWEEP,	#This Sweep is not a Baseline Sweep
:REPEAT,	#Define a Label to jump to.
SCRIPT="MainSAPM.scr",	# Collect a sample using MainSAPM.scr
CH3CNSample = CollectSnippets(CH3CN_Snippets),	#Sweep the Intervals provided and store the results in CH3CNSample
CH3CNConcentration = SLPA(CH3CNSample, CH3CNBaseline, CH3CNLibrary),	#Call the SLPA to estimate CH3CN Concentration
WAIT 600000,	#Wait 10 Minutes (time given in ms)
LOOP REPEAT UNTIL 10,	# Repeat ten times
END,	#End of Scenario
}	

Table 8.4. CH_3CN Scenario Script

The CH_3CN script shows how a complex test process can be easily defined and modified. The script starts by defining the frequency intervals the MACS unit should scan for CH_3CN. Then the system collects a new baseline, only taking data at these frequency intervals of interest, and with the proper modulation mode. Laboratory testing indicates a baseline is reliable for a day or more, so this baseline process does not need to be repeated often. Alternately, if a baseline scan already existed, the script could reference the existing baseline in the "Test Environment" portion of the script. Next the script calls the MainSAPM script, shown in Table 8.3, which collects an air sample and transfers any trapped analytes to the MACS sample cell. The CollectSnippets function then scans the specified frequency intervals and saves the spectral

data. This spectral data, along with the recent baseline and the CH_3CN library are processed by the SLPA to determine the concentration, if any, of CH_3CN in the collected sample.

8.3 Smart Line Processor Algorithm (SLPA)

The SLPA is the main engine of the MACS system software, taking collected spectral data and comparing it to previously collected chemical libraries to determine the concentration of analytes of interest. A simple approach to concentration estimation in a system where only one chemical exists is to just perform a least mean squares (LMS) fit between library data and sample data. The LMS algorithm will come up with a single amplitude constant that will make the two curves match as best as possible. However, in a system where other unknown chemicals are also present in the sample, this approach cannot be applied, particularly when the unknown chemicals are present at concentrations much higher than the chemical of interest. For example, if an unknown chemical had an absorption at a frequency very close to a frequency of the chemical of interest, the LMS would be forced to increase its concentration estimate until it partially canceled out this interfering peak. If the concentration of the unknown chemical was 1000 times stronger than the chemical of interest, it is clear that the LMS estimate would quickly become invalid. These extraneous peaks are referred to as clutter, and overcoming clutter will be the major difficultly in reaching the probability of detection goals of the MACS system.

The SLPA deals with these clutter issues by performing a much more intelligent algorithm which expects, identifies, and removes nearby unknown absorption lines until only the signal of interest remains. This approach is possible because while other chemicals may absorb at frequencies close to those of the chemical of interest, they will never be at exactly the same frequency. These nearby peaks can hide the peak of interest or appear to change the frequency or amplitude of the peak of interest. However, the MACS system has such accurate frequency registration that it can almost always distinguish between these two peaks, and the SLPA algorithm can separate them. In the worst cases, if a nearby peak is so large that it completely obscures the peak of interest, chemicals of interest produce enough absorption lines that this frequency band can safely be discarded, because the probability that enough lines will be obscured so as to prohibit identification is well outside our ROC performance needs. Detailed analysis of the system ROC performance is provided in Section 11.

It is clear that small signals of interest in the proximity of large clutter signals, any algorithm intended to "curve fit" via LMS between the realized spectrum, Q(f), and the library spectrum of substance J, $Q_J(f)$, cannot be relied upon by itself to yield results adequate to meet the MACS performance requirements when the sensor is exposed to real world conditions. This is particularly true when the repertoire of analytes is expanded to realistically cover gases that have numerous small lines that must be observed in order to yield mandatory ROC performance. The presence of clutter lines of virtually any magnitude and of any frequency are conditions that must be "endured" in order for MACS to become a real world system. Such lines can and will destroy ROC performance unless the overall signal processing mitigates them, which is the objective of the SLPA. The SLPA is designed to handle situations where a desired signal line with power S is close to clutter lines of large amplitudes. Since this state can never be predicted, the SLPA must detect potential clutter interferers and then to avoid or mitigate them. The SLPA does this,

and greatly improve the overall signal processing gain beyond other simple techniques. It does utilize LMS techniques, but with corrections and a more complicated method for line removal. This algorithm is based on quantitative measurements in turn that are based on the physics of the spectral lines on a case by case basis.

The spectral library will contain *both* the spectrum $Q_J(f)$ [for species "J"] and the set $\{f(i), A(i)\}_J$ of N_J lines that follow precisely from $Q_J(f)$. These N_J lines have been selected externally and programmed into the script designed to find the chemical of interest. The SLPA will also have library data available for a known concentration of the chemical of interest. $Q_J(f)$ will get parsed into K sub-spectral segments:

$$\{Q_J(f \in [f_{K1}, f_{K2}])\}_K \qquad (1)$$

where 1,2 denote low and high frequency limits to the k^{th} frequency segment. In the event that such an interval contains more than one library line that exceeds an amplitude threshold, then a further parsing will occur so that the SLPA will be evoked for each scenario-specified library spectral line:

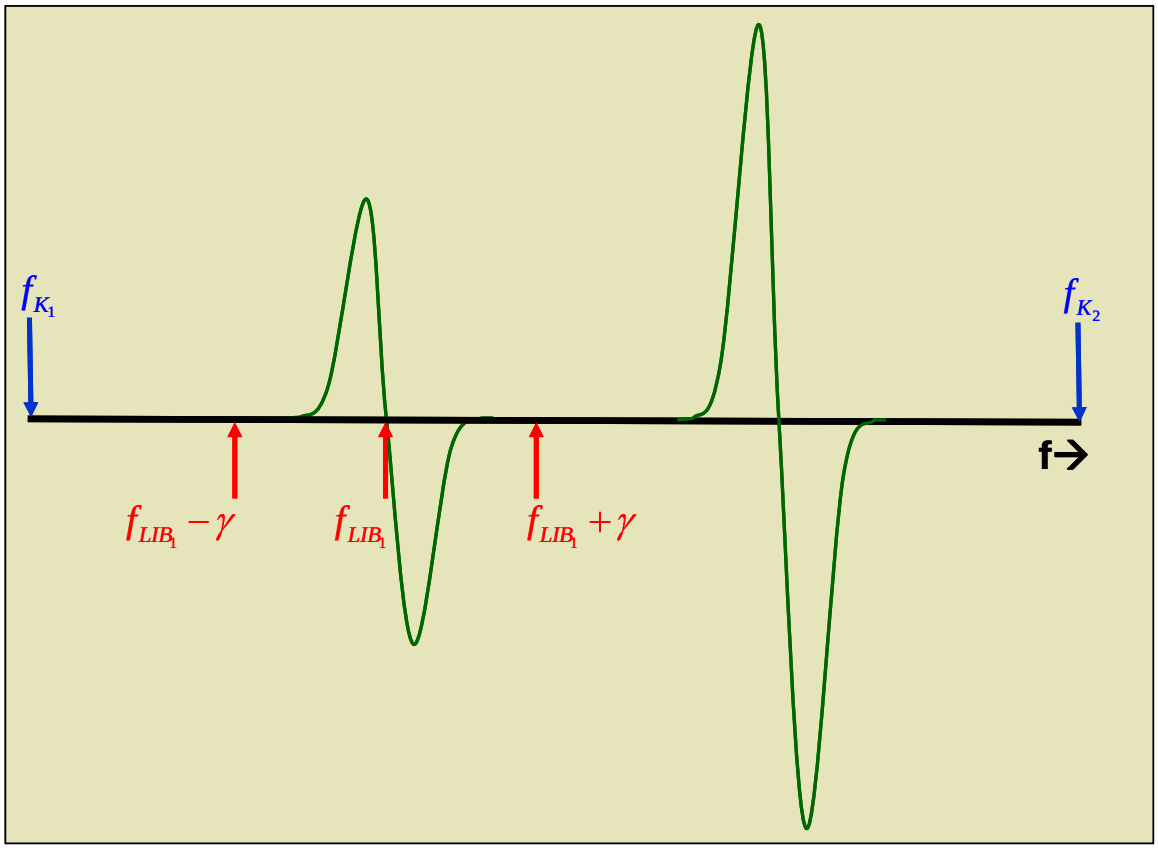

Figure 8.7. Example library snippet Q( )$_K$ defined on [f_{K1}, f_{K2}] (blue) that contains two library lines that are included in the scenario for detection. The "clutter caution" region limits are shown in red for the first of the two lines. Clutter lines beyond the red interval will not disturb the processing of the spectral line and are not to be considered.

$$\{Q_J(f \in [f_{LIB_M} - \gamma, f_{LIB_M} + \gamma])\}_M \qquad (2)$$

where f_{LIB} denotes the library line's frequency, and where γ is a system constant that will be defined and calculated below. An example snippet is shown in Figure 8.7. For purposes of stating the SLPA, the serial evaluation of N library lines as specified by the conditions of the mission scenario is assumed. SLPA assessment of each spectral line will represent a partial solution to the overall assay problem for the given chemical species. The SLPA can operate across multiple species lines and in any desired order. After all N lines are evaluated, there will be a reduction in N (to N_{RED}) due to certain circumstances that preclude accurate rendering of the spectral lines. It is best to consider each line as centered within a region $[f_{LIB_M} - \gamma, f_{LIB_M} + \gamma]$. All clutter beyond this limit will be irrelevant to the computations for this particular line and will be ignored. No library lines will ever be permitted by the scenario generator or even the library data base manager to be employed if they are closer than γ MHz from each other. Time consuming provision for violation of this rule could be considered, but it is unlikely to be necessary.

There are fundamentally two ways to approach the determination of a library fit: determine the spectral parameters (frequency, amplitude, line width) and then define some goodness function to provide quantitative discrepancy overall between these empirical parameters and those of the library, or a statistical curve fit. The latter is the classic LMS determination of the properties with quantification also provided. The SLPA chooses the latter and will provide the fit to the library amplitude within a very carefully controlled frequency interval that adjusts for line pull by residual clutter and also that lies within theoretically possible bounds. As derived below, this is the frequency interval designated $[f_{3L}, f_{3R}]$. The result is that there will be a statistic generated for *each* line. This is a statistical variate the ensemble of which will define the mean value of the LMS-derived best fit multiplier to the library that gives the best estimate of concentration while its variance defines the error in concentration.

The LMS evaluation on the "final assessment interval" $[f_{3L}, f_{3R}]$ defined in the proximity of the library line and utilizing that portion of the library spectrum $Q_J(\ )$ (for species J) with this frequency interval intended to cover better than 99% of the full 1st derivative line shape and with the incoming and preconditioned digital 1st derivative absorption spectrum Q( ) for the same interval. These Qs are for the snippet designated explicitly below by the notation M(J) which is just shorthand for the M^{th} snippet belonging to analyte J from the Snippet_List owned by the ASSAY_PROCESS where these evaluations are to take place.

Noting that there are n frequency points in the interval $[f_{3L}, f_{3R}]$, the LMS derives from the following error in curve fit between the adjusted spectrum snippet (empirical) Q( ) and the library for species J, $Q_J(\ )$:

$$Error = \frac{1}{n}\sum_{i=1}^{n} KQ_J(f_i) - (Q(f_i) - B)^2 \qquad (3)$$

Each empirical and each library snippet has exactly n points corresponding to the master frequency bin structure where f_i corresponds with the first master frequency bin in the snippet

and designated in the Snippet_List as the start frequency. Likewise f_n represents the stopping frequency for the bin. The SLPA is also provided a baseline sweep B, and this is subtracted from the spectral data to remove any systematic frequency or amplitude error. Then the SLPA will make the best fit to the library snippet.

Then $\frac{\partial Error}{\partial K} = 0; \frac{\partial Error}{\partial B} = 0$ are applied and the results for K and B are obtained. We will now show K as related to an index M representing the M^{th} line of the library spectrum for K is

$$K_{M(J)} = \frac{n\sum_{i=1}^{n} Q(f_i)Q_J(f_i) - \sum_{i=1}^{n} Q(f_i)\sum_{i=1}^{n} Q_J(f_i)}{n\sum_{i=1}^{n} Q_J(f_i)^2 - \left(\sum_{i=1}^{n} Q_J(f_i)\right)^2} \quad (4)$$

$$B_{M(J)} = \frac{\sum_{i=1}^{n} Q(f_i) - K_{M(J)}\sum_{i=1}^{n} Q_J(f_i)}{n} \quad (5)$$

The implementer of this software must assure that the divide by zero error does not occur. We will hence ignore the J notation (the species) with the understanding that the computation is strictly for the lines selected for inclusion in the mission-specific assay for species J.

The final adjustment on Q for exportation purposes is:

$$Q_{M(J)}(f_i) = Q_{M(J)}(f_i) - B_{M(J)} \quad (6)$$

From the ASSAY_PROCESS data structure, the total number of snippets N is known. Once the SLPA has completed the sequence of these N lines and evaluated each individual line, $N_{RED} \leq N$ lines will remain. This is because the SLPA may discard some lines if clutter around a particular line is too complex to remove and still provide a reliable amplitude and frequency estimate of the line of interest. This leaves a universe of K variates $\{K_1, K_2, K_3 \ldots N\}$ with some K's set to zero due to exclusion. Only N_{RED} of the Ks are non zero by declaration and the SLPA uses these to compute

$$\overline{K} = \frac{1}{N_{RED}} \sum_{i=0}^{N} \delta_i K_i \quad (7)$$

and

$$\sigma_K = \sqrt{\frac{1}{N_{RED}} \sum_{i=0}^{N} \delta_i \left[K_i - \overline{K}\right]^2} \quad (8)$$

where δ_i is 1 unless the line was declared invalid for which the value is 0. This yields the error term for the overall population:

$$\sigma_{\overline{K}} = \sigma_K / \sqrt{N_{RED}} \qquad (9)$$

The procedure will produce $\overline{K}$ which is directly proportional to the observed concentration relative to that of the (reduced) library species. The library of species J will contain a ppX_J concentration value that directly relates the line amplitudes to the actual concentration; and where $pcon_J$ is provided by the preconcentrator (SAPM) uP to the MACS CC that finalizes its estimate of the concentration at atmosphere relative to what it expects to be present in the sample cell. All approximations for loss due to effects occurring beyond the SAPM are also to be included in this value. The assay result for species J is thus

$$Assay\,Con_J = pcon_J \times ppX_J \times (\overline{K} \pm \sigma_K / \sqrt{N_{RED}}) \qquad (10)$$

where the distribution of means will assuredly be normal and thus statistical inferences can be drawn accordingly. It must be noted that the validity of the measurement process for species J is clearly indicated by the error term. Thus, a very small error term indicates that the measurement process is indeed correctly predicting the assay concentration according to all the data that is available.

The next step is to look at the key properties of 1st derivative spectral lines. Assuming a Gaussian line shape, the literal absorption line and its 1st derivative are:

$$\begin{aligned} P &= P_0 - P_{S\max} e^{+\beta_S (f - f_S)^2} \\ Y_S &= -2P_{S\max}\beta_S (f - f_S) e^{+\beta_S (f - f_S)^2} \end{aligned} \qquad (11)$$

The MAX/MIN of the signal (Y_S) are given at positions:

$$f_{S\max/\min} = f_S \pm 1/\sqrt{2|\beta_S|} \qquad (12)$$

And the absolute 1st derivative signal maximum is:

$$Y_{S\max} = P_{S\max}\sqrt{2|\beta_S|}e^{-0.5} \qquad (13)$$

Or using the half power, half width "line width" W_S:

$$\beta_S = \ln(0.5)/W_S^2 \qquad (14)$$

$$\begin{aligned} Y_{S\max} &= P_{S\max}\sqrt{2\ln(0.5)/W_S^2}\,e^{-0.5} \\ &= 0.71413P_{S\max}/W_S \end{aligned} \qquad (15)$$

Other useful expressions include the frequency separation of the 1st derivative MAX/MIN peaks:

$$\Delta f_S = \sqrt{\frac{2}{|\beta_s|}} = 1.698644 W_S \qquad (16)$$

And thus, the half power, half line width is:

$$W_S = 0.76727 \Delta f_S \qquad (17)$$

The peak absorption power at f_s can then be calculated to be:

$$P_{S\max} = 1.400295 W_S Y_{S\max} = 1.07440 \Delta f_S Y_{S\max} \qquad (18)$$

Thus from the library or other 1st derivative spectrum it is easy to deduce the absorption line amplitude from the frequency splitting of the max/min and the estimated amplitude of those max/min values. It is more likely, however, to use an LMS of the 1st derivative or some more encompassing method. In clutter, however, it is possible that it may be necessary to estimate the line width from the max/min separations. Likewise the amplitude may be best estimated from a measurement of the relative amplitude of the max or min that is furthest from the offending clutter line. It will be less contaminated (distorted) by the clutter.

Using a pressure of 5mT, a temperature of 300K, and a molecular weight of 25 amu, the largest line width encountered by the MACS system is:

W_{max} = 0.63/2 = 0.31 MHz (1/2power, 1/2width) (19)

This maximum line width is then used to determine the SLPA limits for distinguishing two nearby lines, one signal line S, located at f = 0, and one clutter line C, located at f = f_C. As this distance in frequency between S and C is reduced, the error in the frequency and amplitude estimate for S will increase. An error of 0.005 MHz in frequency and 5% in amplitude is considered acceptable. This error will occur at some distance D, which will be smallest at the widest line width. D is calculated using the same integration interval that the SLPA algorithm uses, namely [f_{3L}, f_{3R}] where:

$$f_{3L} = f_{LIB} - 4 * W_{MAX} \quad and \quad f_{3R} = f_{LIB} + 4 * W_{MAX} \qquad (20)$$

Using Equation (9) we have the composite spectrum g(f) for a signal (at f=0) and a single clutter line at f=D), an example of which is shown in Figure 8.8.

$$g(f) = -2P_{S\max}\beta_S f e^{+\beta_S f^2} - 2P_{C\max}\beta_C \left[f - D \right] e^{+\beta_C \left[f - f_C \right]^2} \qquad (21)$$

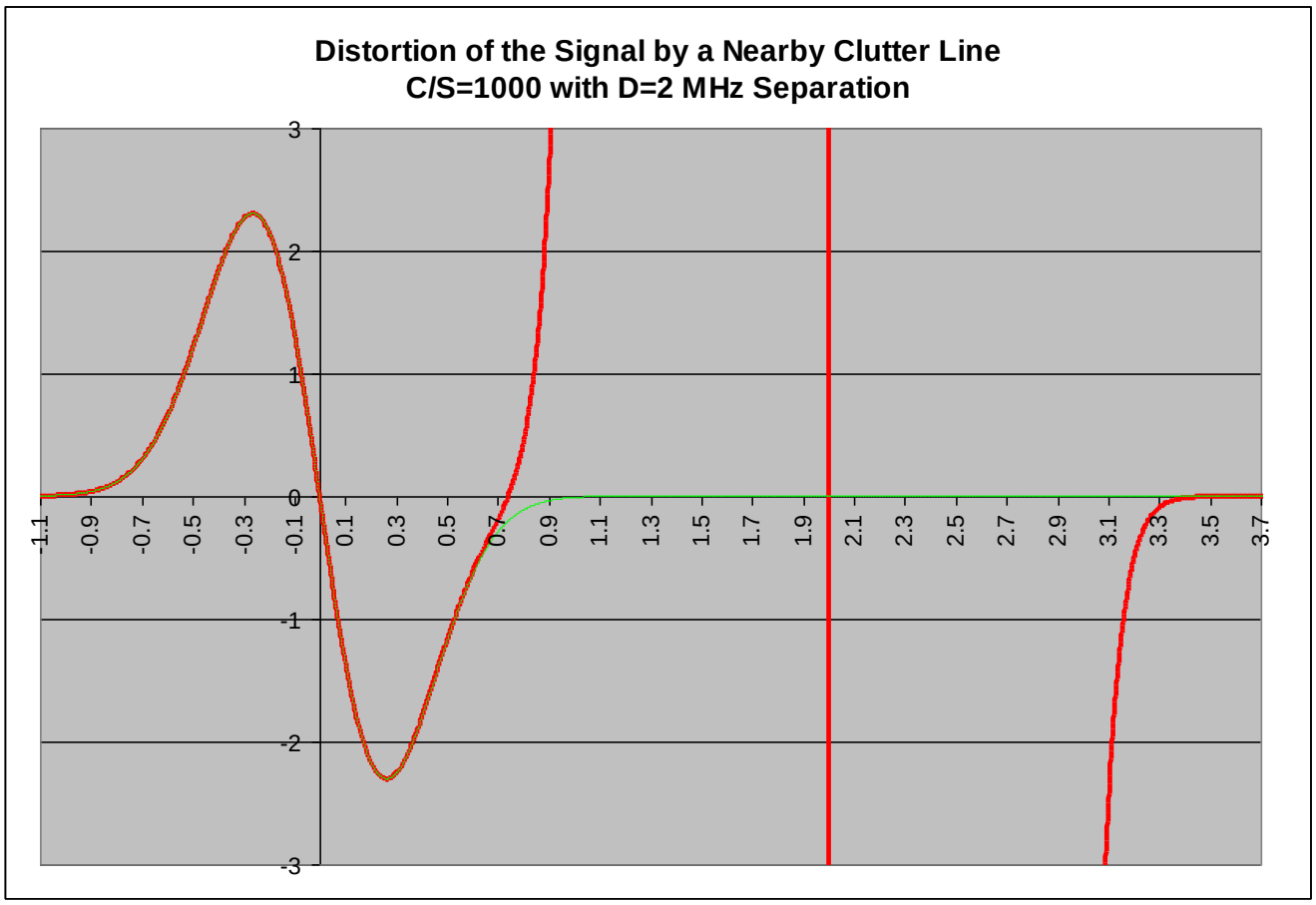

Figure 8.8. Signal distortion by nearby clutter.

The error in the fit to the signal only for the above stated integration interval is given by performing an LMS fit to g(f) on that frequency interval and then comparing the derived LMS fitting parameter to the input (true) signal amplitude. This process has been run for the complete dynamic range of C/S and the results are given in Figure 8.9. From this figure the separation distance γ such that a clutter line of maximum possible amplitude will not introduce an error greater than 5% in amplitude or 0.005MHz in frequency is calculated to be $\log(2^{24})$, assuming the MACS system has 24 bits of dynamic range.

$$\gamma = 2.508 \text{ MHz} \qquad (22)$$

Therefore, any clutter line γ (MHz) away (on either side) from a library peak can be safely ignored. Next, consider D_{MIN} to be the separation distance between two lines that can just be resolved. Figure 8.10, showing D_{MIN}, indicates that for the assumed worst case conditions that the lowest value for D_{MIN} occurs where C/S=1 and this separation ξ is given as:

$$\xi = 0.525 \text{ MHz} \qquad (23)$$

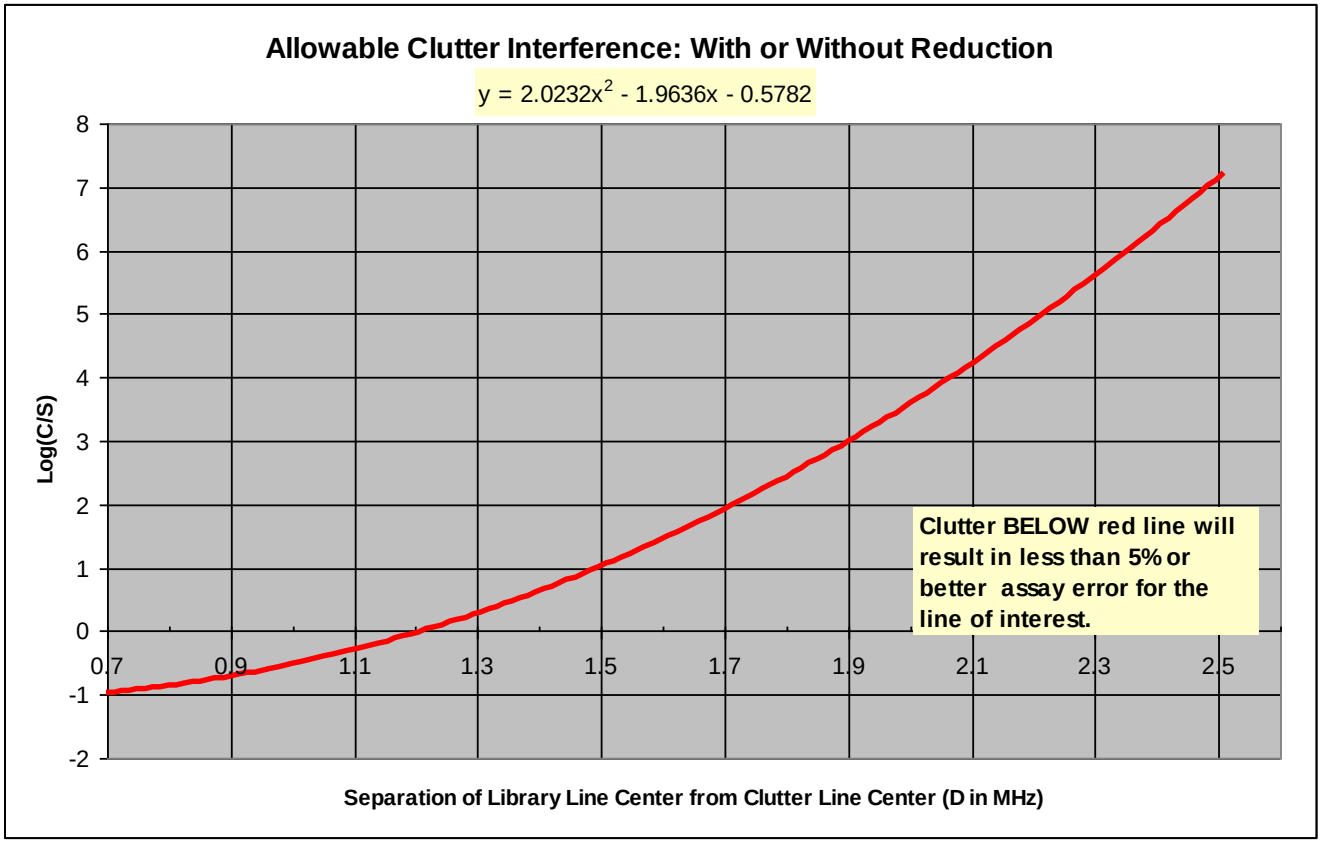

Figure 8.9. Clutter Interference

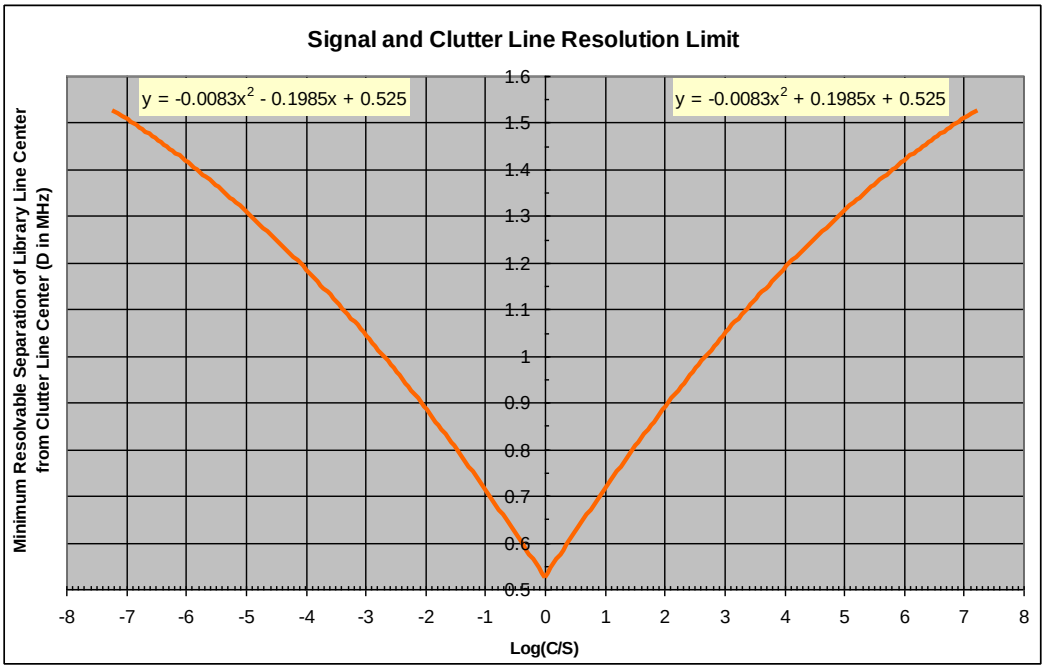

Figure 8.10. Signal and Clutter Line Resolution Limit

These constants will be used to define a set of frequency regions, and the SLPA algorithm will process clutter lines differently depending on which of these regions the clutter line resides. There are four regions used by the SLPA, which are shown in Figure 8.11.

REGION 1: library line central region. Any lines in this region appear as a single irresolvable line that is assumed to be the signal of interest (i.e., the library line centered at f_{LIB}.

$$(f_{1L}=f_{LIB}-\xi,\ f_{1R}=f_{LIB}+\xi) \qquad (24)$$

REGIONS 2L and 2R: Clutter concern "wings" that surround region 1. Here, any clutter lines that are detected must comply with the restrictions of Figure 8.8 or be reduced and then the residue must likewise be contained by the curve listed in Figure 8.9.

$$\text{Region 2L} \cap \text{Region 2R} = [f_{2LL}=f_{LIB}-\gamma,\ f_{2LR}=f_{1L}=f_{LIB}-\xi] \cap [f_{2RL}=f_{1R}=f_{LIB}+\xi,\ f_{2RR}=f_{LIB}+\gamma] \qquad (25)$$

REGION 3: Final evaluation region. After all adjustments are made this is the interval in which the LMS or similar statistical evaluation is made to fit the signal line to the composite spectrum.

$$[f_{3L}=f_{LIB}-4W_{max},\ f_{3R}=f_{LIB}+4W_{max}] \qquad (26)$$

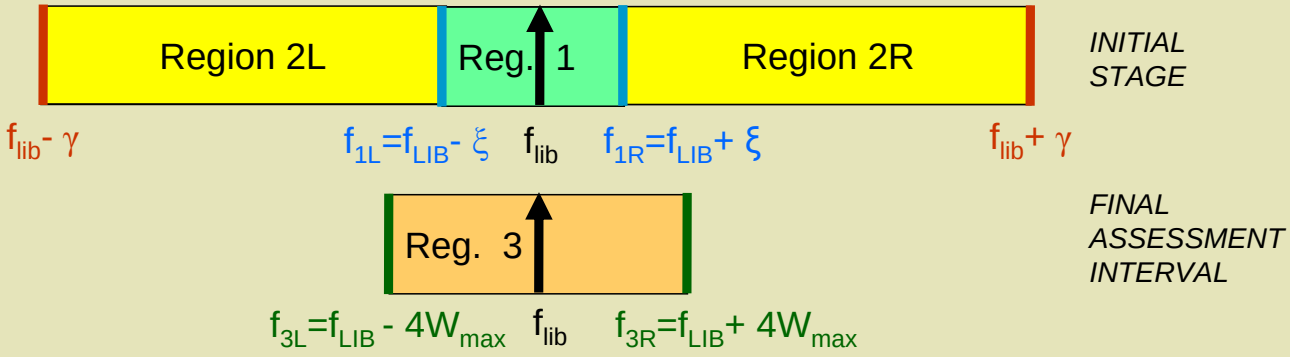

Spectral domains (in frequency) surrounding associated with the library line under test. Clutter in the yellow is detected and reduced—including the "tails" extending into the green region where the signal line (i.e., the library line) may reside. Final integration occurs in the orange region after clutter removal and authorization tests are performed.

Figure 8.11. SLPA Frequency Regions

Clutter Line Removal. The PEAKFINDER will be designated to operate in REGIONS 1, 2L and 2R serially. The routine will determine the presence of a spectral line or lines in each region. It will utilize the resolution uncertainty to attempt to determine:

(1) if there is 1 line in region 2L
(2) if there is 1 line in region 2R
(3) if there are no lines in region 2L
(4) if there are no lines in region 2R
(5) if there are >1 lines in region 2L
(6) if there are >1 lines in region 2R

The explicit algorithm flow will rule out cases (5) and (6) as "TOO COMPLEX". This can be improved in future versions if necessary. In cases (1) and (2) the CLUTTERREMOVAL subroutine will be executed. Another subordinate function of the SLPA will assess the line width of the declared clutter peaks while employing the Gaussian 1st derivative assumption as noted above. This subroutine is called by PEAKFINDER in the event that PEAKFINDER determines a line is present. In the event that there is found to be a clutter line in the appropriate region 2L and/or 2R, then the routine determines:

$$Y_{C_{MAX}} = ave(absloute\ values\ of\ the\ line\ extrema)$$
$$W_{C_{MAX}} = half\ \ power, half\ \ width\ of\ the\ clutter\ line$$
$$f_C = center\ \ frequency\ \ of\ \ the\ clutter\ line$$

It is vital that once the line center is found in region 2L or 2R that the calculations avail of the frequency interval $[f_{2LL}, f_{LIB}]$ for a line in region 2L and $[f_{LIB}, f_{2RR}]$ for a line on region 2R. Thus the curve fitting for the clutter uses not only @L but the left half of region 1; and for a clutter line in region 2R we likewise consider the data from the library frequency to the right edge of 2R. This is done to correct for the Gaussian wings that interfere with the signal within region 1.

Given 0 or 1 clutter lines on each side of the library:

$$Y_C = W_{C_{MAX}} \quad f - f_C \quad e^{+\ln(0.5)/W_{C_{MAX}} \quad f - f_C \quad ^2} \qquad (27)$$

These functions are then subtracted from the composite signal to evaluate the RESIDUAL ERROR and then to determine if the accuracy of the signal of interest is sufficient to include in the assay. Let the spectrum be Q=Q(f). The REDUCED SPECTRUM which will be used in all subsequent computations is:

$$Q_{RED}(f) = Q(f) - Y_{C_L}(f) - Y_{C_R}(f) \qquad (28)$$

For example, if there were no clutter the two Y-terms are zero and the reduced spectrum is identical to the original digital spectrum, Q( ). This subordinate procedure is designated CLUTTERREMOVAL with is input Q( ) and a line frequency and width for each region 2L and 2R.

Residual Errors in Spectral Amplitude Measurement

The errors associated with this reduction are as follows:

1. Residual overall baseline error
2. Spectral noise in this region
3. Presence of smaller lines that may have been subsumed by the clutter line(s)
4. Anomalies in the line shape due to the system implementation
5. Deviation of pure line shape physics from the Gaussian shape model
6. Digitization

Of these, type 3 error is unpredictable and types 4, 5 and 6 are negligible. The error term can be simplified to:

$$E_C \equiv E(f_C) = \sqrt{\text{ResiduaBaselineError}^2 + \text{Noise}^2} \qquad (29)$$

Note E_C can be evaluated anywhere in the effective residual clutter region $[f_{LIB}-\gamma, f_{LIB}+\gamma]$), which is only a few MHz in width. The SLPA function THRESHOLD will set E_c. If the SLPA function PEAKFINDER function determines that there are clutter peaks in regions 2L or 2R above the threshold $P1*E_C$, where P1 is a system parameter, then the CLUTTERREMOVAL function will subtract them. As we remove clutter, the signal spectrum will change and become more accurate. If clutter lines in these regions are complex or very large in amplitude, the residual error after line subtraction may still be too great to expect an accurate amplitude estimate of the line of interest. The SLPA function RESIDUECHECK will analyze the signal level in regions 2L and 2R to determine if this is the case. If this test is passed, the SLPA will perform an LMS fit on region 3 against the corresponding library line. This is done for each library line that is included in the script for the assay scenario. The full SLPA algorithm flow is shown in Figure 8.12.

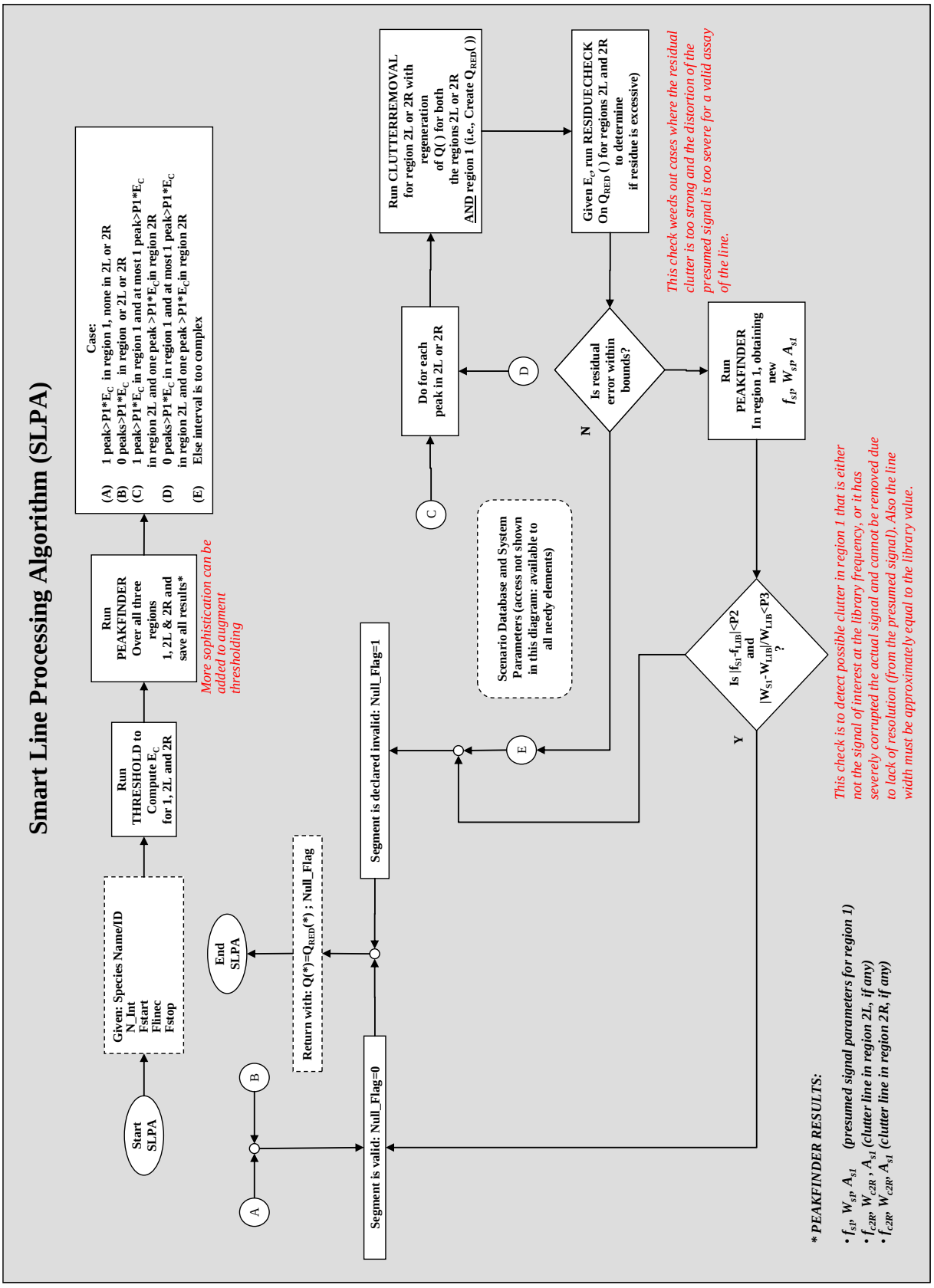

Figure 8.12. The Smart Line Processor Algorithm

8.41 Swap Out System/Surrogate Software

The software that was used for the MET demonstration evolved from that which was written for the science and technology development for MACS. Because this evolution had significant impact on the final surrogate system and its software, we will first outline the evolution of these building blocks and their relation to the hardware of the evolving system.

Building Blocks

1. The development of the TM module did not require a fast sweeping system for testing and optimization. Accordingly, we initially adopted a synchronous - two stepping synthesizer strategy. This used an Agilent E8257D synthesizer (with Ethernet communication) and a Microlamba MLSW-1065 synthesizer (driven by a multifunction board) to provide the required 10.7 MHz off set between the TX and RX frequencies. Data were collected by an Anfatec digital lock-in amplifier, interfaced via a Data Translation multifunction board.

The control software was developed with the '.net' framework using the C# language. This allowed all of the control functions of Labview, but in a format much closer to a final software solution for MACS. This software synchronized all of the hardware devices, provided graphical displays, set relevant system parameters, and saved data to disk.

2. As we approached the need to start to make libraries and experiment with real spectra, in lieu of the FMS and its software, we needed to develop a faster sweep strategy to record spectra over the entire 210 – 270 GHz region. In order to avoid having to sweep synchronously two synthesizers (which we did not have) and to solve the spectral purity problems of the Agilent synthesizer (which were (after multiplication by x24) considerably worse than our spectral line resolution), we:

a. Replaced the narrow 10.7 MHz IF of the MACS's design with a 2.2 – 2.7 GHz IF. This allowed us to use a fixed local oscillator frequency, while sweeping the source in segments of 50 MHz.

b. The FM modulation function of the Agilent synthesizer preserved its good spectral purity and allowed sweeps of 50 MHz for library formation. The same interface was used for each of the hardware components, but the software was modified for this segmented approach.

3. As discussed elsewhere in this report, a 'snippet' strategy was developed. The 'snippet' parameters could be input into the system via either a control panel or a file.

Software for the packaged 1 cu ft system

While the system above was a close electrical surrogate for a MACS, it would not fit into the required 1 cu ft package. This was largely due to the use of the bench top Agilent synthesizer and Anfatec lock-in amplifier; and to a lesser extent due to the use of the OEM Microlambda synthesizer. Additionally, we were still using our lab PC rather than the electrically very similar control computer in MACS.

Accordingly, the system shown in Figure 8.13 was developed to drive the RX and TX multiplier chains. In this system:

1. A smaller, but coarser stepping (0.25 MHz) Microlamba synthesizer in the 8 - 12 GHz region (which when multiplied by x 24 provided a 6 MHz grid) was used as the frequency generator. A portion of its output directly drove the LO chain of the RX.

2. A fast sweeping 400 MHz Analog Devices chip level synthesizer was used to provide a tunable sideband to drive the multiplier chain of the TX. Again, this was done in segments (typically 6 MHz snippets) for the MET demonstration. This board was controlled via a USB port.

3. The YIG filter (which was used to ensure spectral purity among the competing mixer products) was driven by the analog output of the Data Translations interface.

4. The Anfatec lab lock-in amplifier was replaced by its PCI expansion card equivalent. This required the addition of software to replace functionality that was provided by firmware in the lab version of this device.

5. Figure 8.14 figure shows the clickable front panel display that was used to control and monitor the SAPM and to run the sensitivity test. Input choices are entered into the parameter box on the left. In addition, the system can provide real time measurement of parameters such as the cell pressure, sorbent pressure, sorbent temperature, etc. in graphical form.

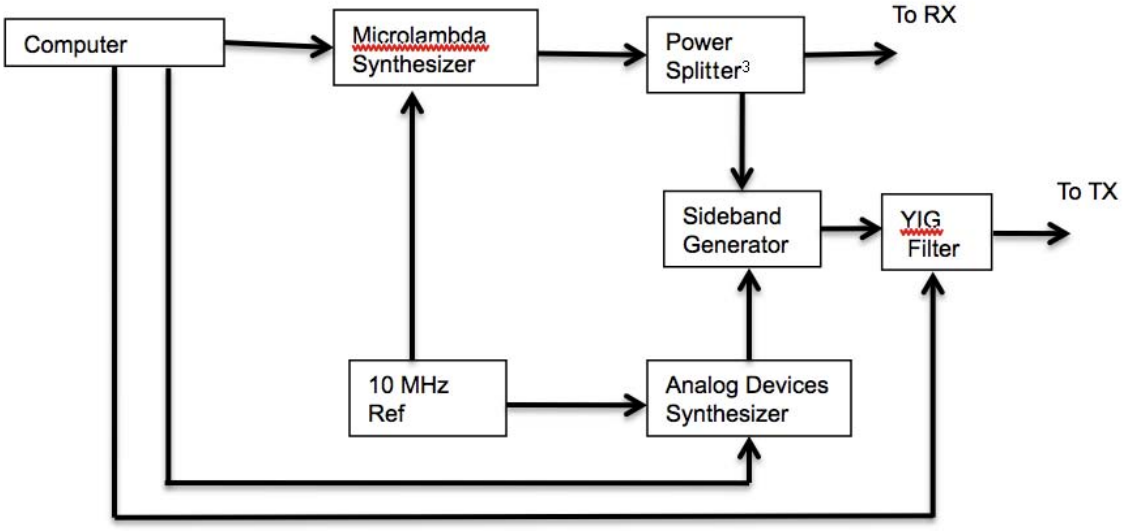

Figure 8.13 Driver used for the GNG tests.

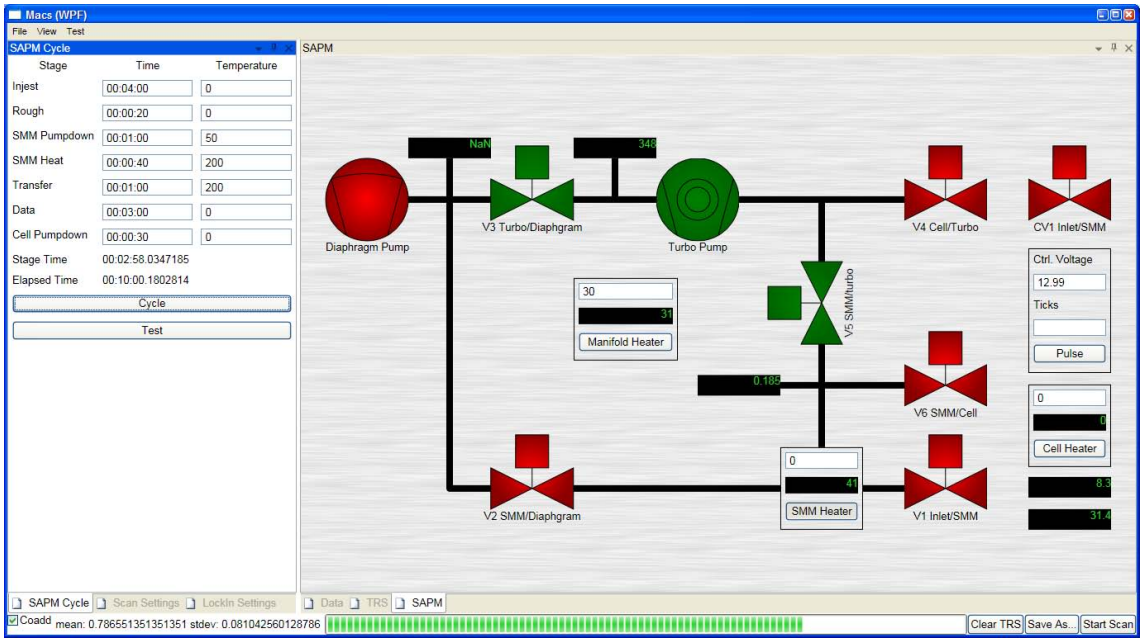

Figure 8.14. SAPM Control Panel

9 Basic System Integration and Packaging

9.1 Architecture of the Packaging for the MACS Phase 1 Systems (1 and 2)

The MACS Phase 1 package architecture was driven primarily by the requirements for the system to fit within one cubic foot. Additionally a modular approach was required to enable the team to integrate the three major subsystems, developed by discrete vendors. For this reason the phase one box was divided into three volume allocations along with physical, mechanical, and electrical interfaces. The overall packaging was done by Smart Transitions utilizing a CAD (computer aided design) package called Alibre® design. Both Battelle Memorial Institute and The Ohio state university utilized Pro-engineer® to model their subsystems and the resultant designs were exported in the "STEP" file format and then imported directly into Alibre design.

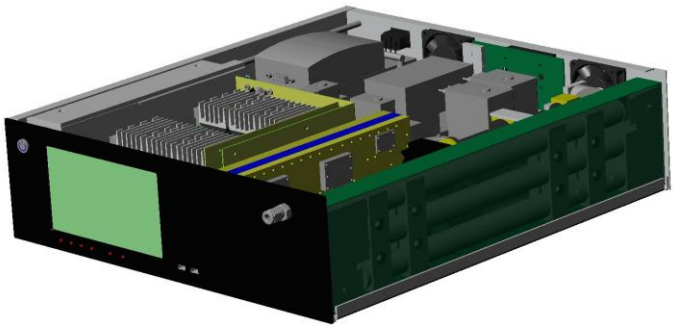

With a majority of the COTS components having their height measurements around 5 inches the team adopted a 3-unit rack height packaging of 5.25 inches yielding approximately 5.16" of usable interior height. In keeping with the rack mount philosophy a width of 17" was selected to fit within the mounting rails. And the finally a depth of 19.36" was selected to utilize the entire 1 cubic foot envelope. This strategy provided for an efficient package allowing for relatively easy access to all the subsystem components with all of the subassemblies mounted in a single plane on the base-plate.

During the packaging process EMI/RFI sensitivities were addressed with the effects of magnetic coupling to the YIG oscillator being the area of greatest concern. Noise coupled to the YIG directly affects the phase/frequency noise spectrum of the Terahertz source reducing system sensitivity and selectivity. The two largest sources of magnetic noise are from the switching power supply used by the entire system and the roughing pump in the vacuum subsystem. These two components were placed in the extreme opposite side of the enclosure from the YIG to provide the best operating environment. Like magnetic coupling mechanical vibration can also cause noise degradation of the YIG. The single largest vibration source is the roughing pump followed by the cooling fans. The roughing pump was mounted on vibration isolators to impede the mechanical vibration coupling into the base plate. The YIG was also mounted on isolators as a further attempt to reduce mechanical induces noise on the THz source. In the end the noise from the roughing pump was too great requiring the pumping and sweeping operation to be exclusive. Moving to phase locked loop control of the YIG in the next generation design will remove this constraint since the source of the noise is well below the loop bandwidth allowing the PLL to track and correct this periodic noise.

9.2 R&D Leading to Phase 2 Improvements (Size, Volume, Cost, Speed, Performance)

9.1 In Phase 2 of the program the overall packaging objectives will be to support an activity demonstration. This will require the MACS system to fit within another system such as a UAV, wheeled vehicle, or shipboard system. In the case of the shipboard system our current rack mounted chassis would suffice, however a UAV or wheeled vehicle application will require additional packaging constraints. For a UAV the MACS payload should have a small cross-sectional area to fit within the equipment bay and the system must be ruggedized to handle the takeoff and landing loads along with vibrations coupled through the airframe. Like the UAV a wheeled vehicle application will require the MACS system to be hardened against vibration and shock.

As mentioned in section 9.1 changing the FMS subsystem from frequency-lock to phase-lock will alleviate the susceptibility of sensitivity degradation due to vibration and EMI/RFI. This single design change will provide the greatest compatibility improvement to varying environments. This is not the end of the story however since the THz components require critical alignments and slight vibrations on this "optical path" could cause amplitude disturbances similar to absorption spectra and therefore reduce sensitivity. We will therefore be required to strengthen and isolate the THz module from external mechanical noise sources. The balance of "hardening" of electronics will be to increase their survivability in harsh environments.

While there will be significant design changes in the second phase of MACS there will not be a significant reduction in overall size, weight, or power consumption. The subsystems that are reduced in size, weight, and power will make room for added capabilities and robustness. A case in point is the sample cell that will be reduced from ~ 100 ml to 10 ml while a second frequency band is added to expand the range of molecules MACS can detect. The net result will be a THz module of about the same volume but with greatly expanded capabilities.

9.3 Design Specifications and Engineering Drawings

9.3 Engineering drawings for the MACS Phase 1 system are all contained within the CAD/CAM domain of the Alibre Design software product and more specifically the "STEP" file formats. Detailed 2-D drawings were made for the sheet metal components on this program but not for machined assemblies. 3-D models were simply exported to the various machine shops resulting in the "finished goods" we desired. Attached in appendix A9.1 are the assembly and fabrication drawings for the MACS Phase 1 chassis.

Fig 9.3.1 MACS Assembly Drawing

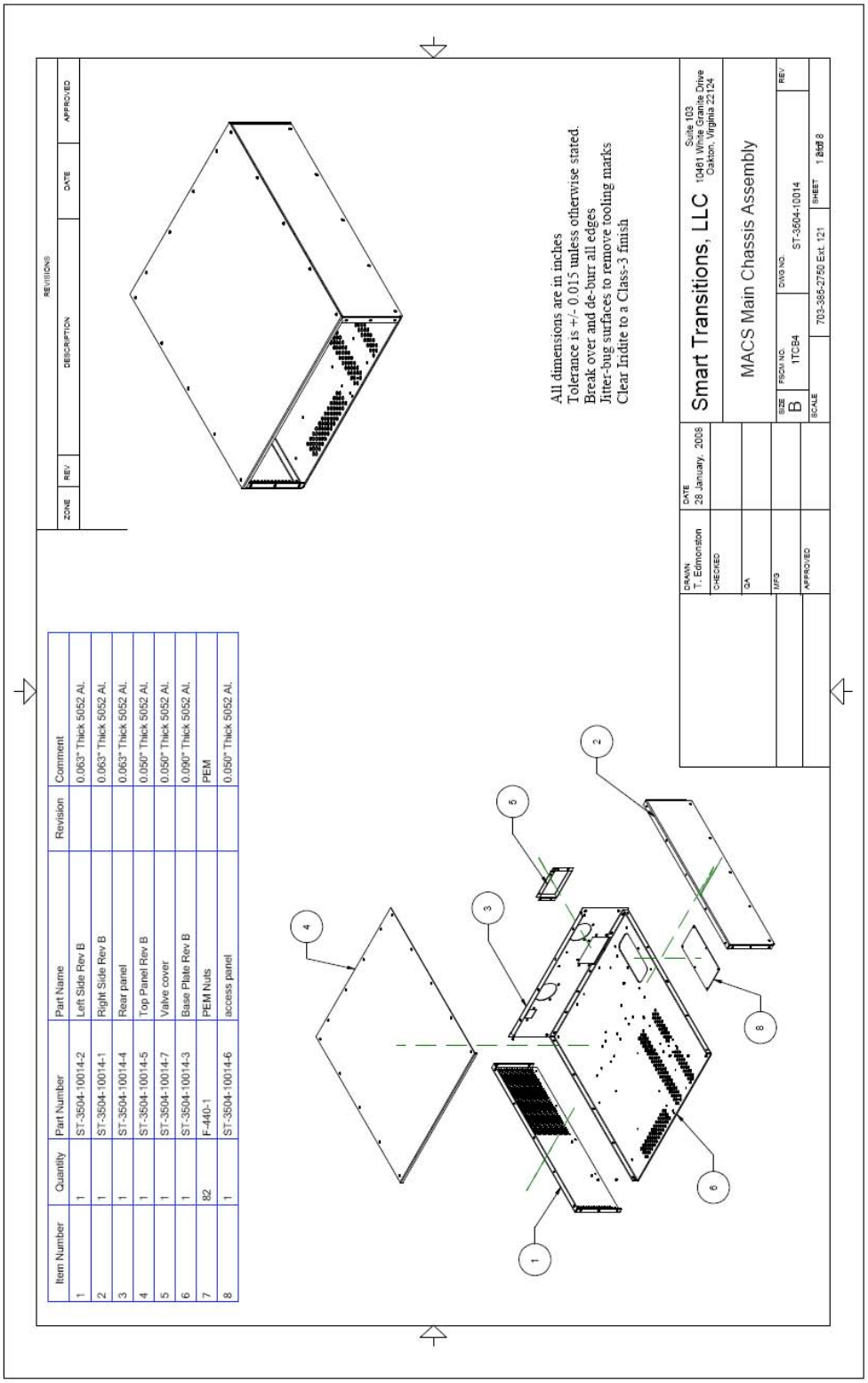

Item Number	Quantity	Part Number	Part Name	Revision	Comment
1	1	ST-3504-10014-2	Left Side Rev B		0.063" Thick 5052 Al.
2	1	ST-3504-10014-1	Right Side Rev B		0.063" Thick 5052 Al.
3	1	ST-3504-10014-4	Rear panel		0.063" Thick 5052 Al.
4	1	ST-3504-10014-5	Top Panel Rev B		0.050" Thick 5052 Al.
5	1	ST-3504-10014-7	Valve cover		0.050" Thick 5052 Al.
6	1	ST-3504-10014-3	Base Plate Rev B		0.090" Thick 5052 Al.
7	82	F-440-1	PEM Nuts		PEM
8	1	ST-3504-10014-6	access panel		0.050" Thick 5052 Al.

Fig 9.3.2 MACS right side panel

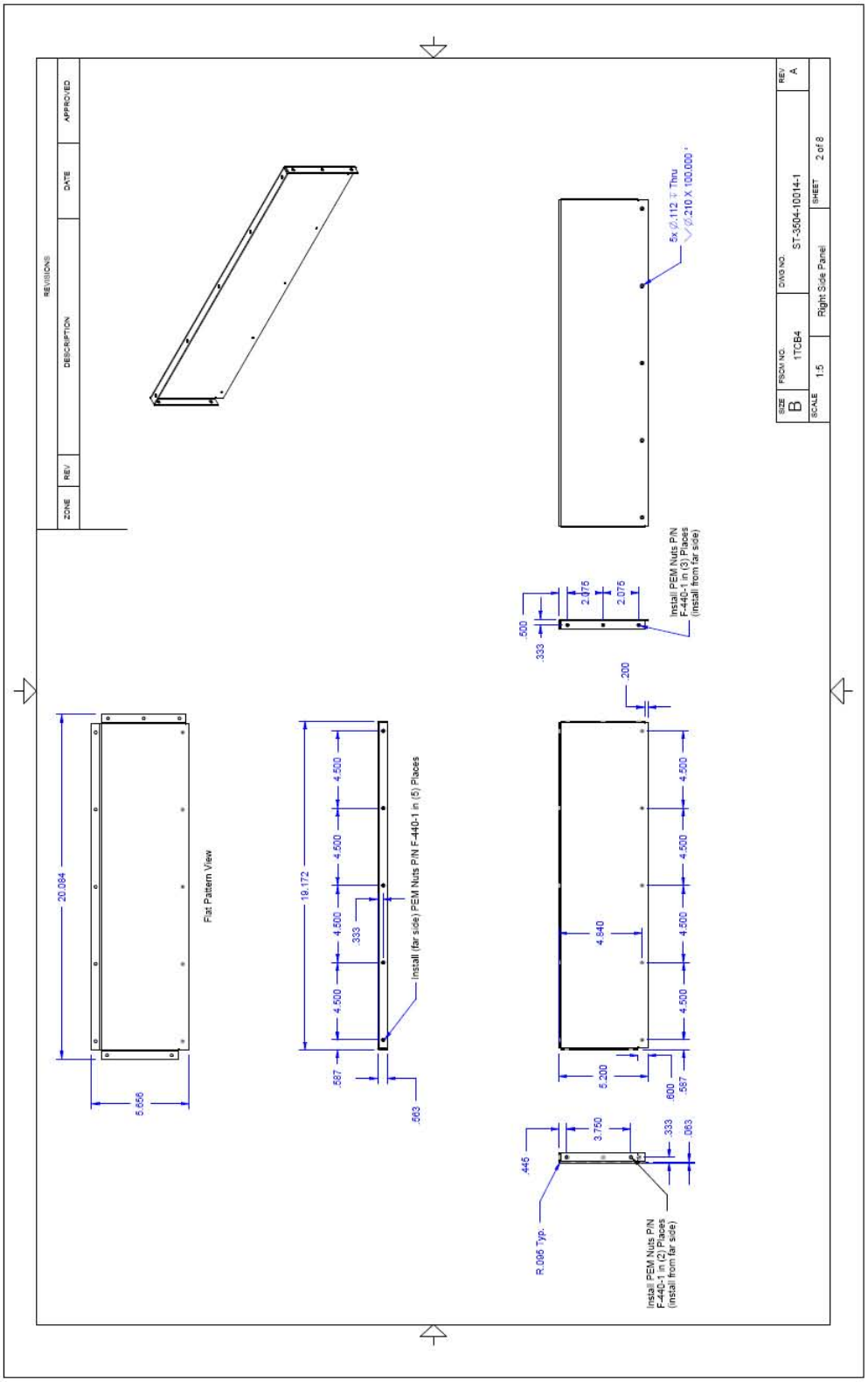

Fig 9.3.3 MACS left side panel

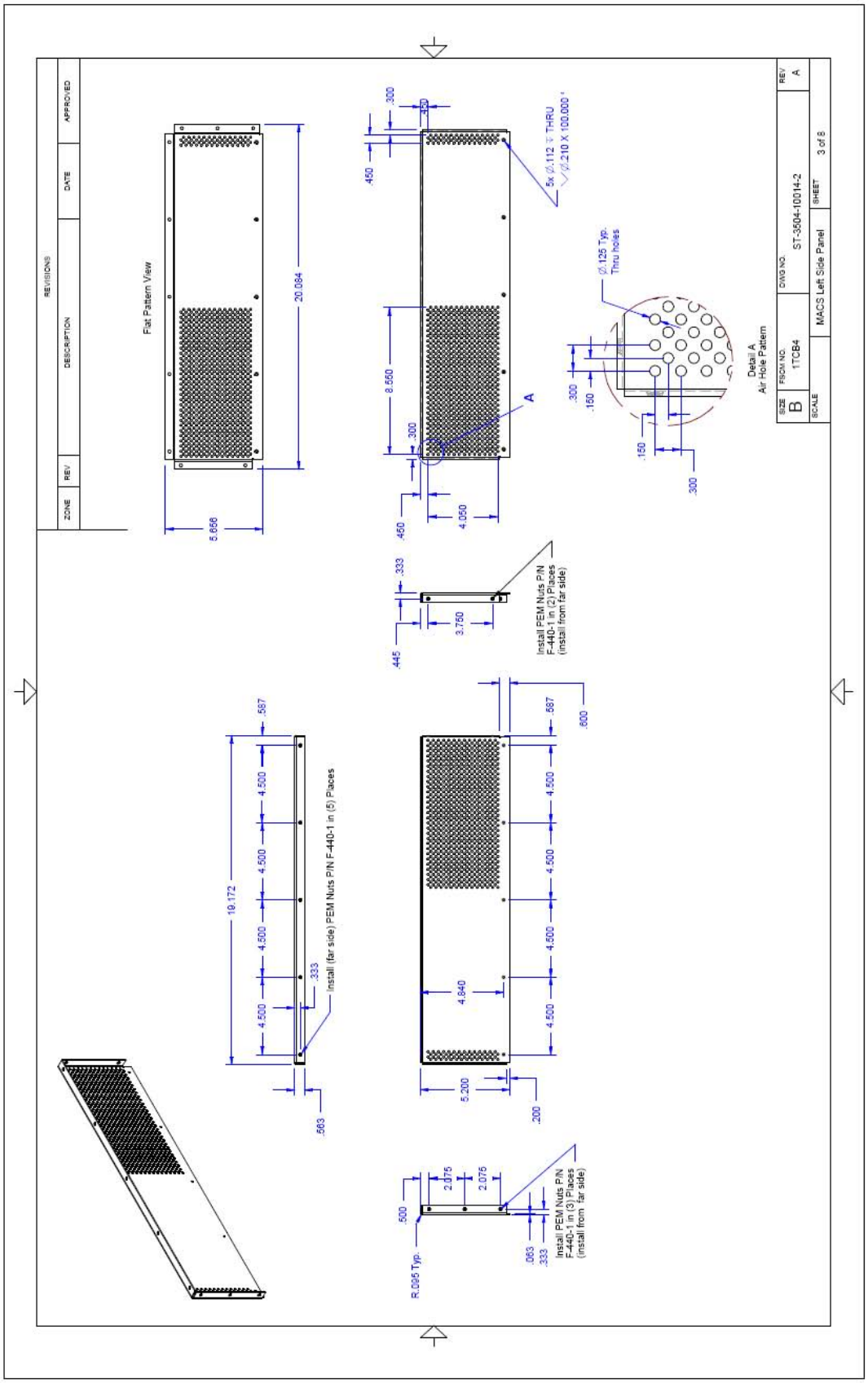

Fig 9.3.4 MACS base plate

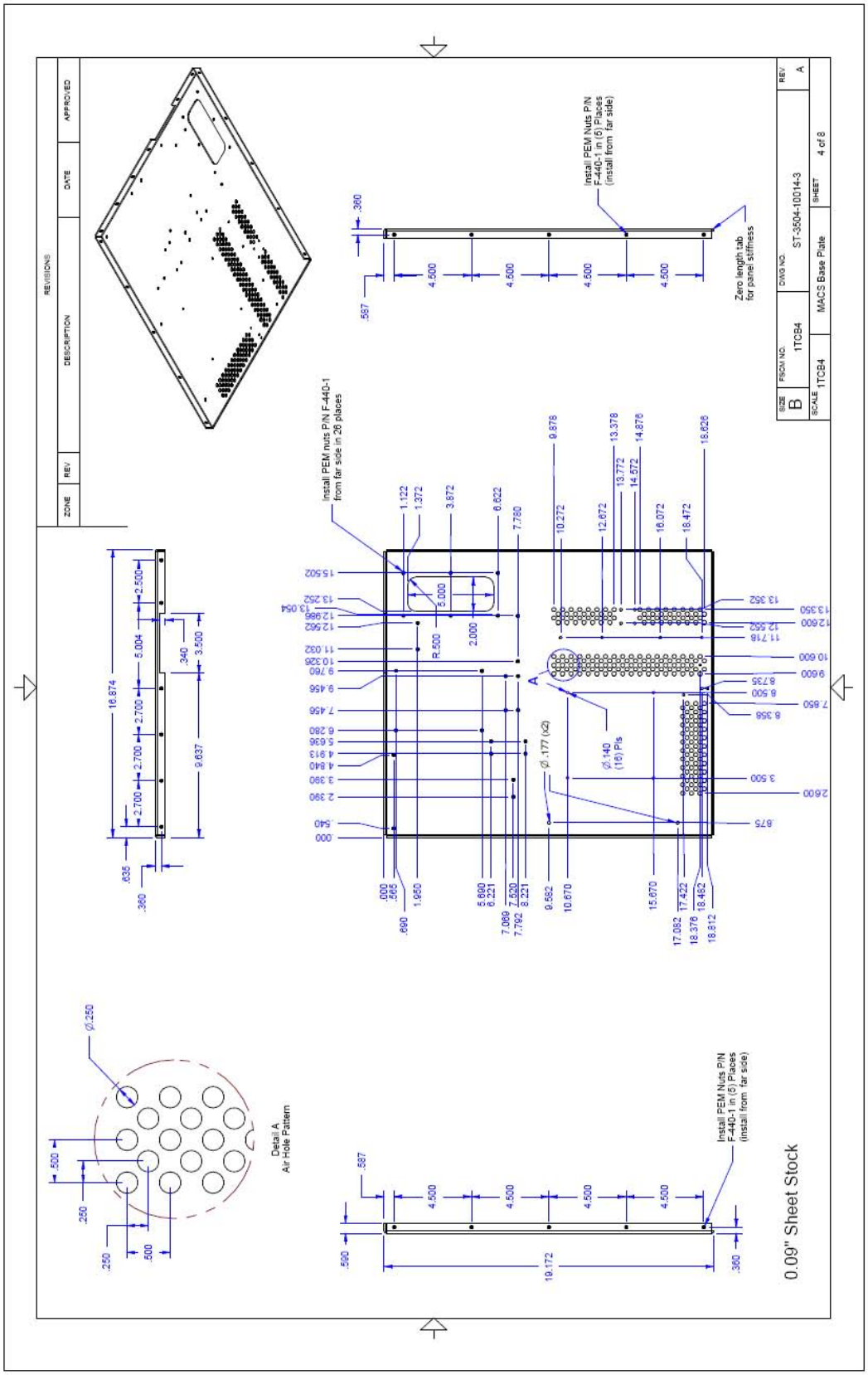

Fig 9.3.5 MACS rear panel

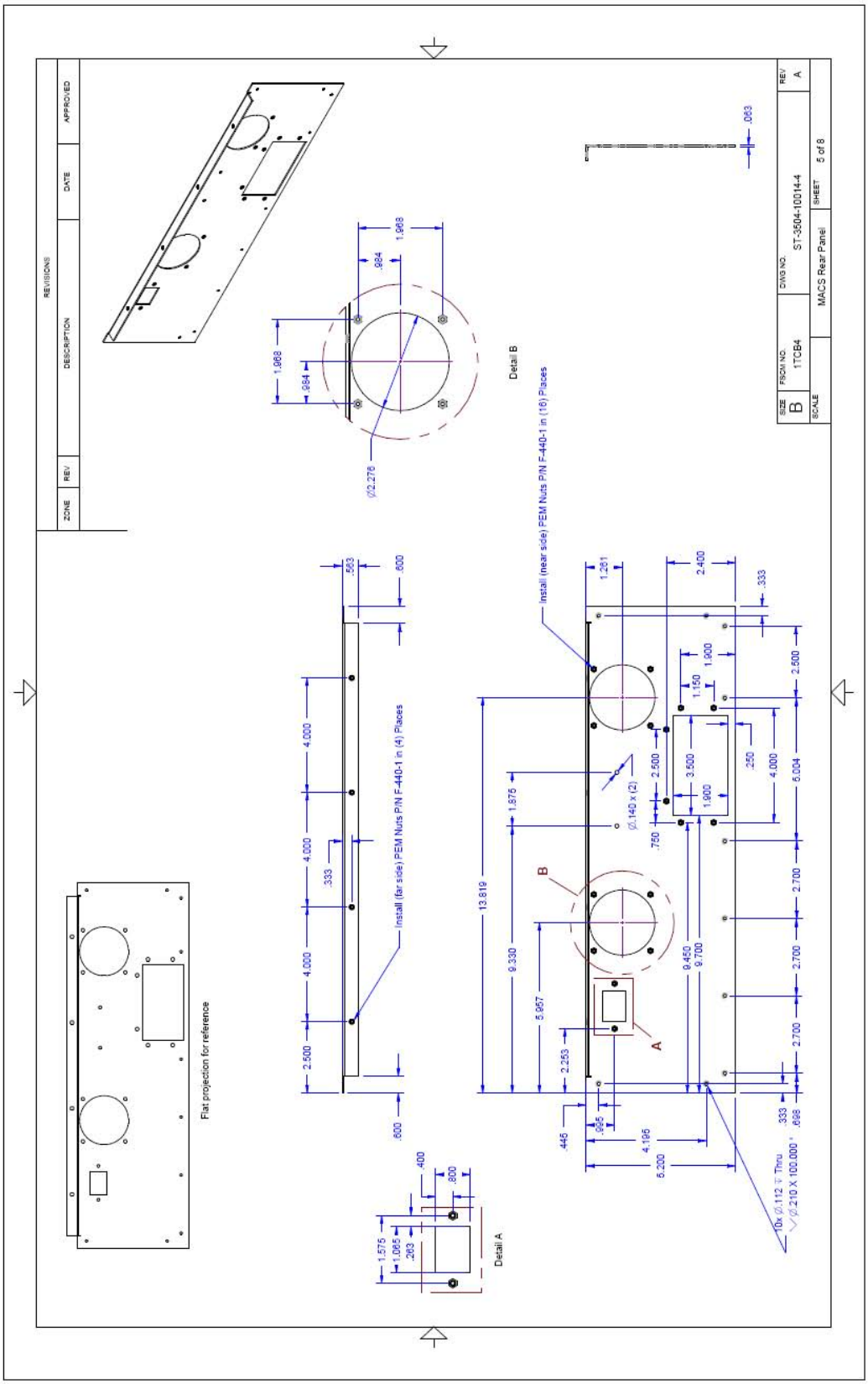

Fig 9.3.6 MACS top panel

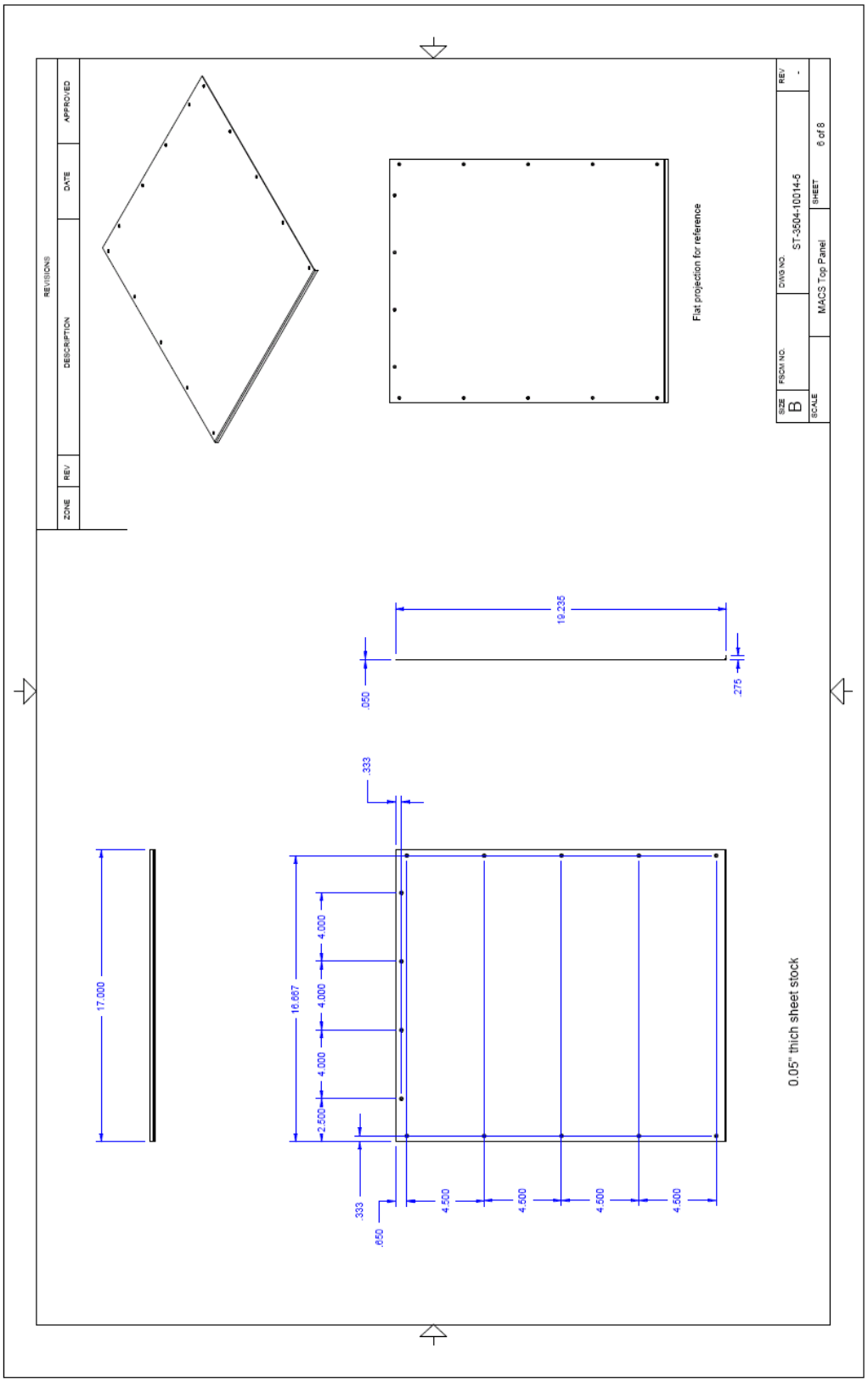

Fig 9.3.7 MACS vacuum connector access cover

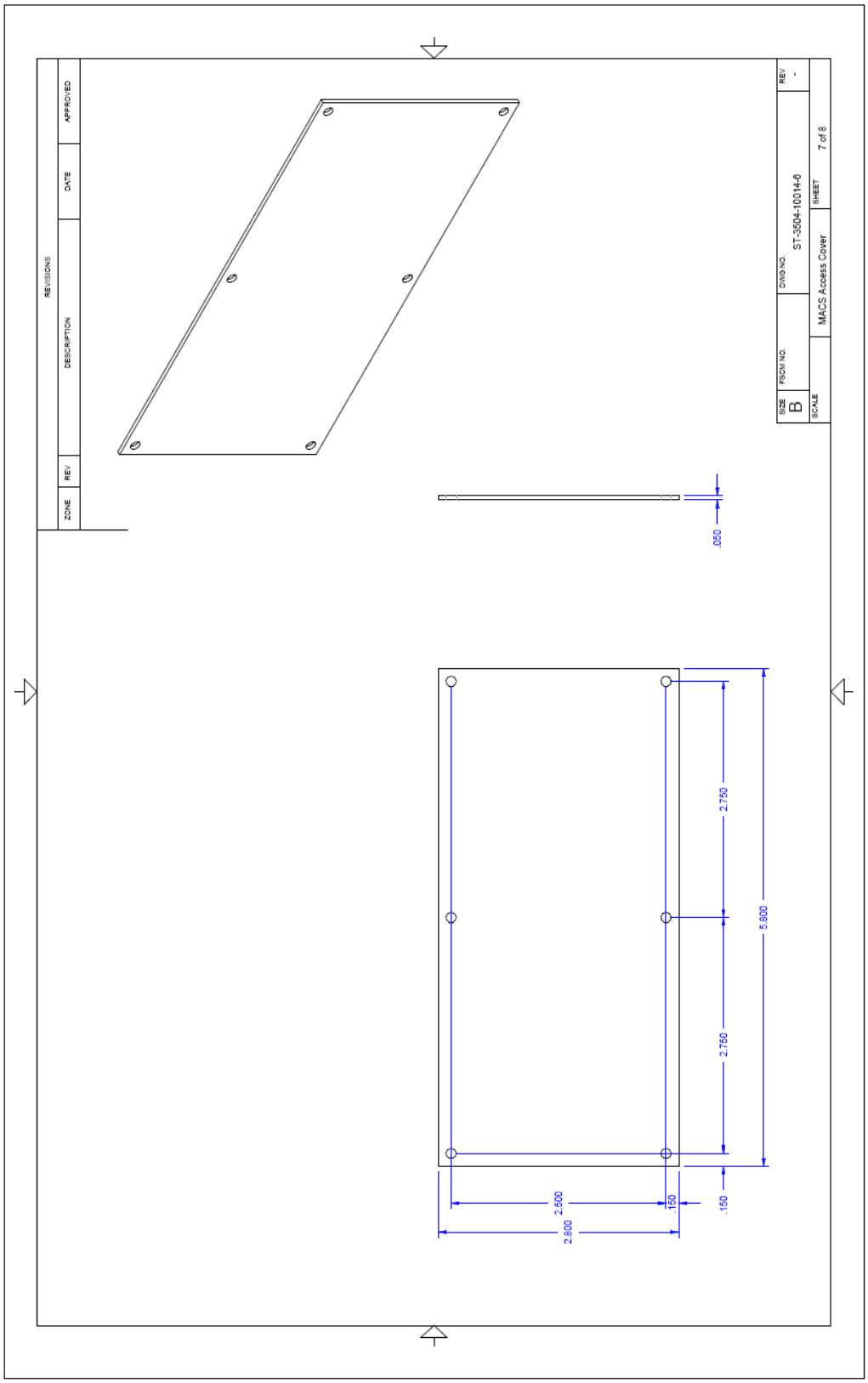

Fig 9.3.8 MACS direct access valve cover

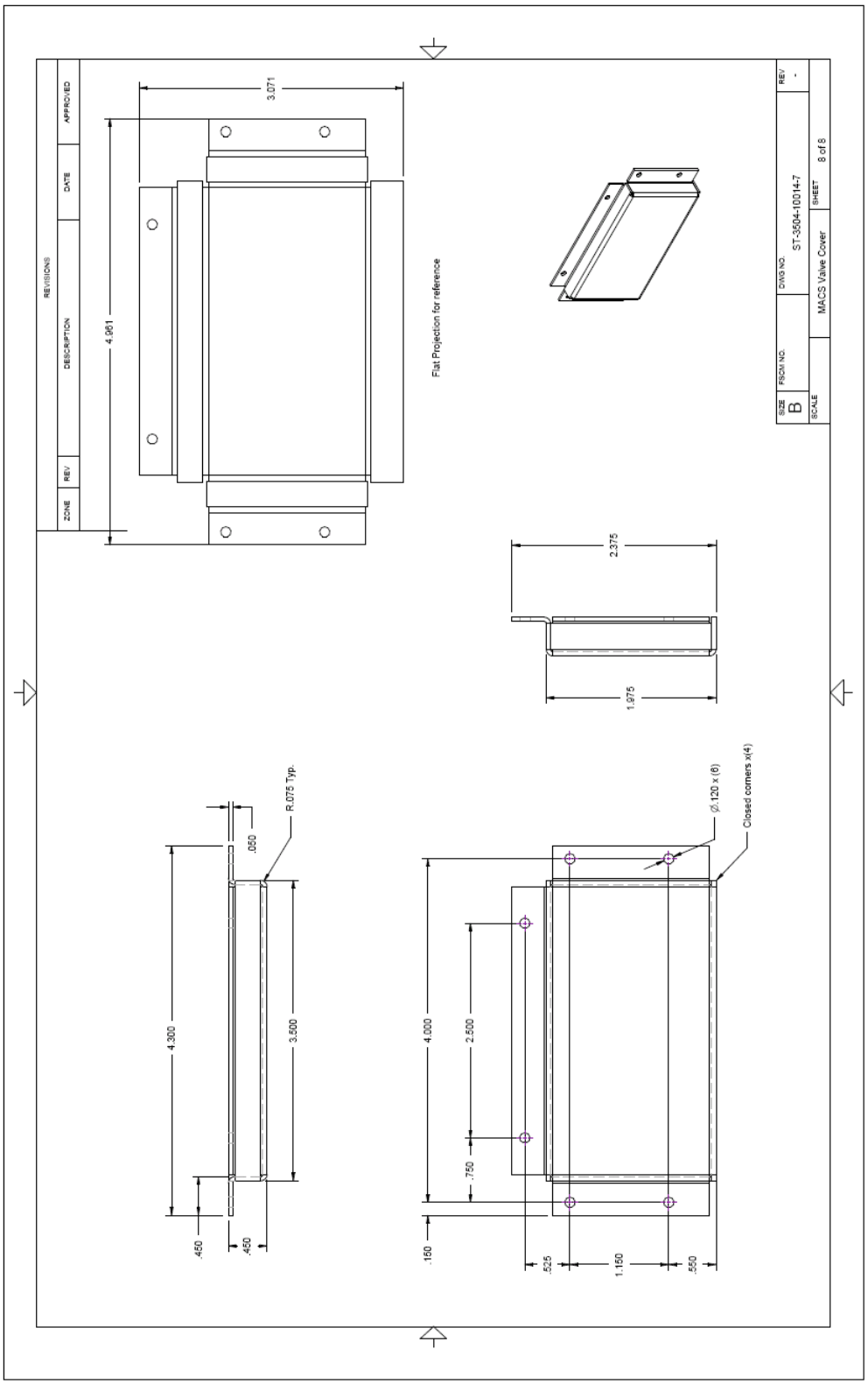

10 Completed Integrated System Calibration and Testing

10.1 Prerequisites to Spectroscopic Measurements (Library, Calibrations, System Parameterization; Various Characterizations)

Evolution and development of required systems: Library development and calibration needed a functional MACS or a close surrogate. The basis of these spectroscopic measurements was originally the MACS Swap Out System (SOS), which evolved into the surrogate system (MACS1). The former was originally intended to provide a system level test bed for development of the SAPM and TM (and their interactions), etc. As the FMS was being developed the SOS was driven a stepping commercial synthesizers (A laboratory Agilent 20 GHz synthesizer and a small Microlambda OEM synthesizer) and the signals present at the output of the RX IF chain were detected by a Herotek diode, followed by a lock in amplifier. Because we needed to do absolute intensity calibrations, the deviation of the Herotek diode from an ideal square law detector was measured. This detector calibration became a part of the intensity measurement software.

Libraries need full sweep: However, this particular synthesizer approach was not suitable for the development of libraries because of its slow scan capabilities. The development of the MACS library required a MACS like system capable of sweeping the entire 210 – 270 GHz band in a reasonable time. The original SOS was not designed to do this. However, as the need to make libraries and to test the broadband response of the TM arrived before the availability of the sweepable FMS, alternatives were developed.

(1) Agilent sweep scheme: In it's native sweep mode, the Agilent synthesizer did not have the required spectral purity for MACS and introduced additional noise into the system. A segmented sweep approach, based on the combined FM/Phase modulation capability of the Agilent synthesizer and an increase of the narrow band 10.7 MHz IF to 500 MHz bandwidth was developed to allow us to sweep the 60 000 GHz in pieces of 200 MHz.

(2) Modulation and signal recovery issues: The original scheme was to make the libraries on the integrated MACS. This would have produced the exact lineshapes associated with the square wave modulation and demodulation of the FMS. However, to make the libraries in a timely fashion we used a sine wave modulation, lock-in detection scheme. We expect that that the lineshapes in these libraries will not be so different from FMS lineshapes as to seriously impact signal recover schemes. However, this is still a TBD.

(3) Absolute intensity calibration: Intensity calibration is an important part of the deconvolution of congested spectra. We had originally planned to make the libraries on the final MACS systems to make sure that the response function of the libraries and the instrument were identical. However, to make the libraries in a timely fashion we developed a scheme that provided absolute calibration (see section 4.5). Although we have not yet been able to compare the libraries/lineshapes made in this fashion with spectra recorded on the FMS, we expect that they will at least be satisfactory for preliminary work. In fact, while this absolute calibration was a more ambitious approach, in the end it worked well.

System development for the GNG: For the preliminary demonstration a system that was functionally equivalent to a final MACS system was used. However, it had two major laboratory units which did not fit into the MACS enclosure and which were not suitable for the GNG (which required a 1 cu ft box): (1) an Agilent frequency synthesizer, and (2) and Anfatec lock in detector, which together were used as a surrogate for the FMS. A lab PC was also used rather than the PC in the MACS chassis as well.

To fit the system into the MACS enclosure, a compact Analog Devices chip level sweeping synthesizer based source (Fig. 10.1) was used to provide the drive for the VDI multiplier chains of the TM and a card level lock-in was inserted into the on-board PC (which was also used to run the system for the these final demonstrations).

In this system a small, course stepping (0.25 MHz) synthesizer was used to directly provide the local oscillator frequency. The sweepable source frequency was produced by mixing this signal with the output of a chip level 400 MHz fast sweeping synthesizer from Analog Devices. A YIG filter was necessary so that the other mixing products that are present in the output of the sideband generator did not grow to problematic levels in the x24 multiplier chain of the TM.

This system preserved the low noise of the small stepping synthesizer system mentioned above, but provided the sweep capability required for these tests. Results from this system are shown in

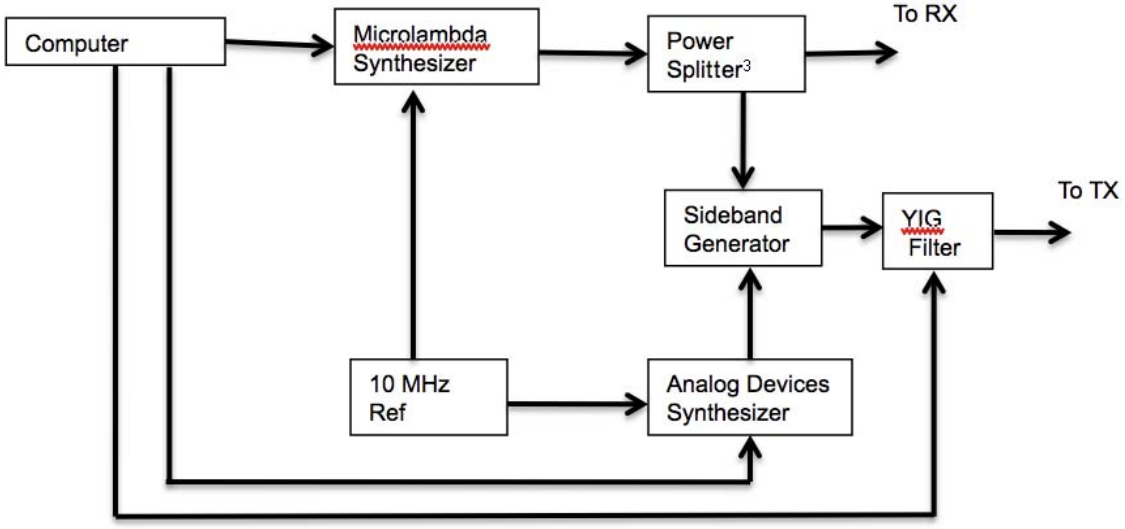

Figure 10.1 Driver used for the GNG tests.

Section 4.5 above.

10.2 Preparations and Test Plans for the MET (MACS Evaluation Team)-Proctored and Facilitated MACS System Level Testing Exercises

Two sets of demonstrations were carried out. The first, a set of preliminary demonstrations, and then the final proctored GNG demonstrations. The former were particularly important to

establish appropriate testing procedures because of reactions among the gases in mixtures before they were introduced into the MACS system and because of decay in trace samples between the time they were prepared and when they were ingested into MACS.

A critical part of both the sensitivity and selectivity tests was the preparation of reliable test samples. The challenge for the mixtures was to develop an understanding of the chemistry that happened after the samples were injected into the mixture bulbs, but before they were ingested by the MACS system. The challenge for the sensitivity tests was the reliable preparation of extremely small concentrations *and* the development of a means to guard against reaction or other wall effects that would remove or reduce the concentrations of the trace samples before they were ingested by MACS. These two challenges had different solutions.

The dilute mixtures: The GNG sensitivity test could best be conducted on a sample whose concentration was ~ 100 ppt. In consultation with the MET, we agreed that part of the solution of this challenge would be to use a known isotopic abundance, in this case deuterium, to account for part of the dilution. While a number of volumetric and storage schemes were explored, in the end we agree to use certified 100 ppm mixtures from a laboratory which routinely prepares these mixtures for the EPA, combined with Mass Flow Controllers to further dilute these mixtures to near 100 ppt. Mass flow controllers are calibrated to provide variable, but known dilutions of the sample mixture in either air or nitrogen. We found this approach to be remarkably reproducible and reliable. Figure 10.2 shows these devices and their control units.

The chemical reactions in the gas mixtures are a fundamental problem. This is because it is possible (and likely) to choose mixtures for tests that can not exist in real atmospheres (if you feed gases that react into the air, they will react, and they will no longer be in the atmosphere!).

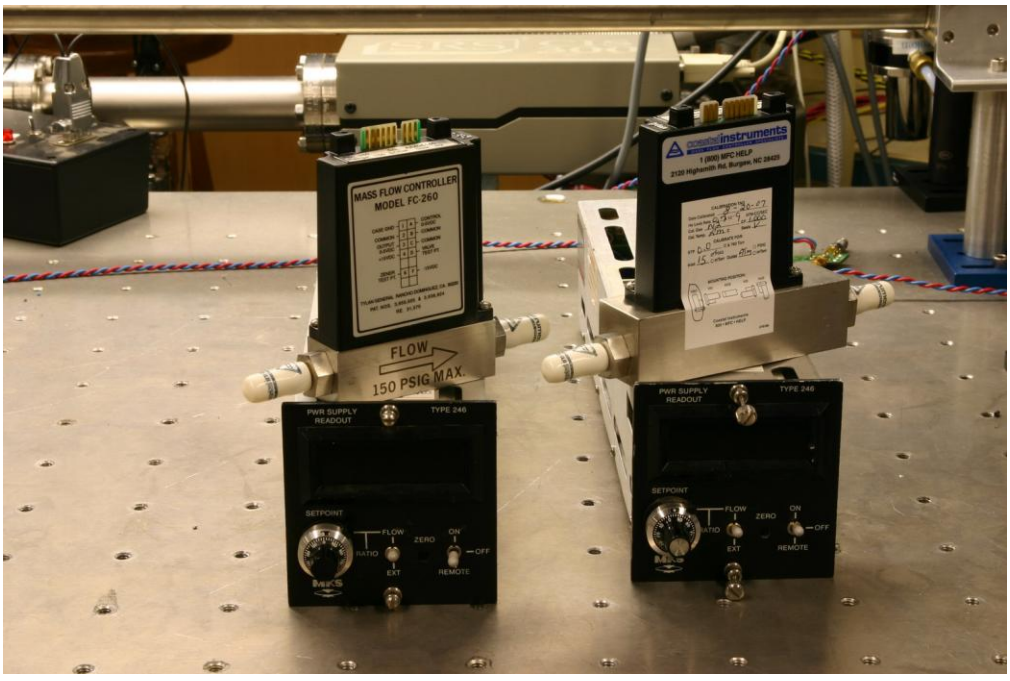

Figure 10.2. Mass Flow controllers used for the preparation of calibrated low concentration mixtures.

However, since MACS is quantitative, it is possible, (with surety) to use MACS to measure what is really in the mixture bulbs, so that it can be compared to what was originally placed in the bulbs. Both the preliminary report (Appendix A) and final report (Appendix B) show these results. This is actually a significantly harder challenge than that posed by the GNG tests because of the much wider variation in concentration and signal strengths encountered.

10.3 Sensitivity Testing and Performance Results

As described in more detail in Appendix B, a 1 sigma sensitivity level of ~ 2 ppt was obtained and the ROC of Fig. 10.3.1 resulted. These results exceed the 100 ppt GNG level by such a large margin that it was not possible to plot the 100 ppt result on this graph.

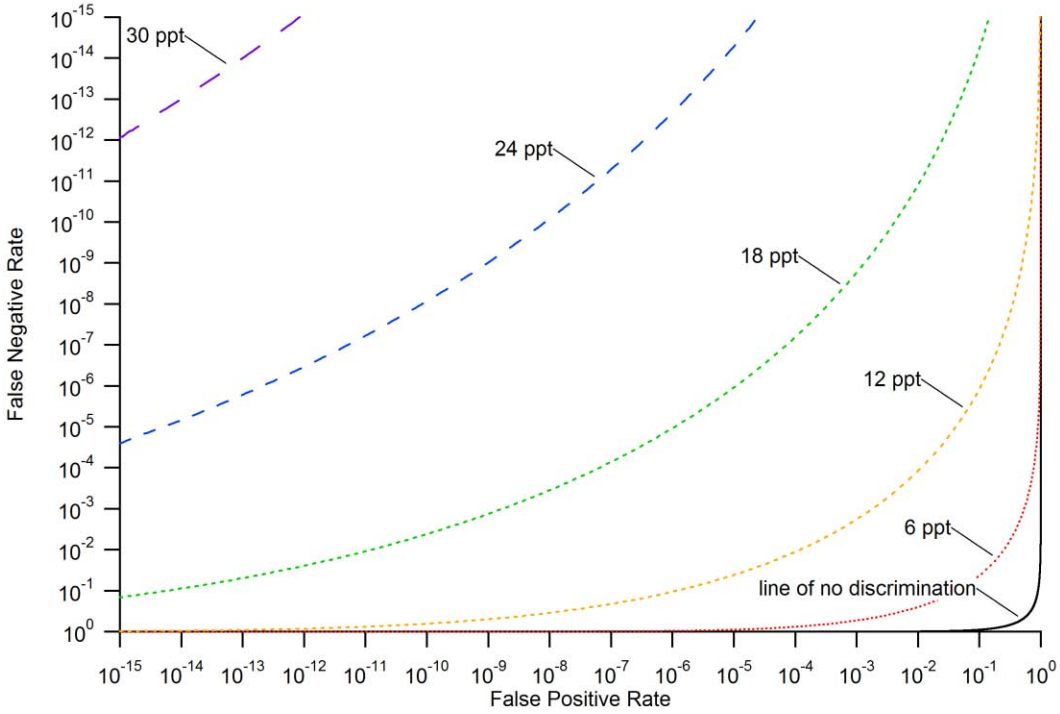

Figure 10.3.1. ROC for sample concentrations less than 100 ppt.

It should be remarked that these results were obtained on a system that was far from optimized. We feel that it will be relatively straightforward to both improve the sensitivity level of these results and to extend them to a considerably wider range of molecules.

10.4 Selectivity Testing and Performance Results

These results are detailed in Appendix B. Figure 10.4.1 shows the results in an informative manner. Currently we adopt the simple procedure of selecting 6 fingerprint lines for each of the 31 gases and then using the frequency agility of MACS to look at a 'snippet' for each fingerprint

line. Although not optimum from a sampling time point of view, we look at all of the snippets for each gas before going on to the next. Since the snippets are displayed in the order they are sampled, this makes the visual inspection of Fig. 10.4.1 straightforward.

In this figure, for each of the gases present, spectral lines appear (in groups of 6) and these are labeled in this figure. (The compressed graphics of this display does not do justice to the sensitivity and spectral information that is in the files). Figure 4.5.2 above shows the snippets for GNG Mixture #1.

In a real sensor, it would be wiser to look at a single snippet first, see if it is present at a predetermined concentration level and then make a decision as to whether to look at other snippets of this gas or to move on to the next gas. This decision will be influenced not only by the presence of absence of the gas at the predetermined level, but also by the suritiy that one

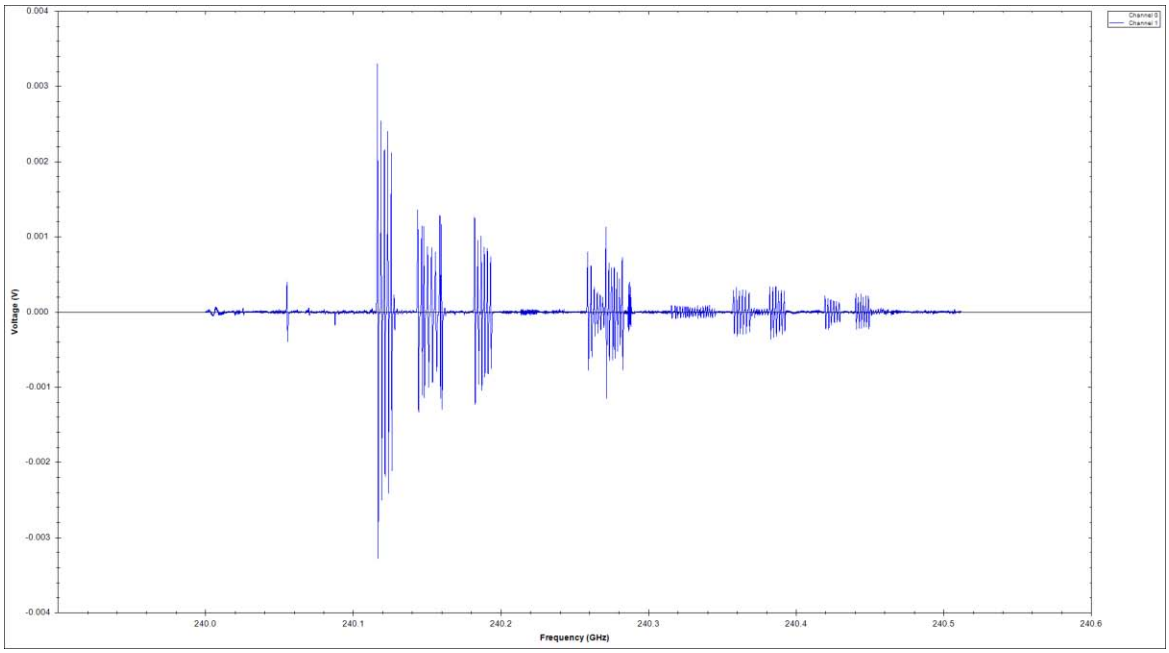

Figure 10.4.1. Snippet display for Mixture #2.

requires of the result (the ROC improves very rapidly as you look at more lines)

10.5 Derived/Calculated Quantities

Sensitivity at 30 ppt:

PFA < 10^{-10}

PFD <10^{-10}

Specificity for 31 gas mixtures *better than*

PFA < 10^{-10}

PFD $<10^{-10}$

11 Summary of Phase 1 Objectives and Results

11.1 Listing of Objectives with Results

Go/No-Go Goals for Phase 1.

SYSTEM: 1 ft3
SENSITIVITY: 100 ppt
SELECTIVITY: 30 species
ASSAY TIME: 10 min
ROC PERFORMANCE2: PD=0.9999; PFA=0.001
SYSTEM SCALING3: computer resources adequate for muiti-missions
USER OUTREACH: establish user community interest
Fulfillment of Phase 1 Goals.

1. The MET was presented a MACS system configuration that is 1 cu ft in volume.

2. The MET observed a test that yielded to spectral lines of deuterated acytonitrile showing 10 lines. The measured reliability of least means squares between these particular lines and those of the previously recorded MACS library for this compound produced results indicating an accurate concentration measurement. The sensitivity test data is shown in APPENDIX 1. The lines are clearly present (see item 5).

3. The MET also participated in a series of mixture tests that covered the 31 gases used in the selectivity demonstration. These results were also satisfactory and are presented in APPENDIX A11.1.

4. The system was operated within the 10 minute assay time limit and observed by the MET.

5. The detection characteristics are calculated in APPENDIX A11.2 and confirm that the MACS 1 unit at 100 ppt can operate with PD and PFA within the bounds prescribed by the conditions.

6. The microcontroller used for MACS is anTMS470 ARM 7 (Evaluation board version – relatively inexpensive); 1MB Flash memory; 60 MHz clock; 64 kB RAM with many features including a direct memory access controller (DMA), twelve communications interfaces, and onboard ADC channels and a 500 GBytes. The memory requirements to store the library (worst-case scenario) of 31 species: 1,920,000 samples (double) per analyte at 8 bytes/sample is approximately 465 Mbytes. That would cover more than 1000 species. The MACS embedded computer language is text script based and consumes negligible space as also do the set of other system parameters and files. For the MACS1 systems, there is no issue with CC-based capacity.

7. Dr. Patten has three letters from USG representatives that meet this condition.

[2] ***Statistical in origin: theoretically estimable only***
[3] ***Set by central computer resource limits (not an issue for Phase 1)***

Conclusion. The objectives are met.

11.2 User Community Outreach and Interest in MACS: MAG (MACS Advisory Group) Report

11.2.1 Background and Objectives of the MAG

The MAG was devised by Smart Transitions (ST) and incorporated into the Phase 1 MACS proposal. The following language from the proposal outlines the function of the envisioned MAG.

From the Executive Summary, objective 2:

> *"Develop a system that is appropriate not only for a Phase I demonstration and for a successful Phase II and beyond into DoD militarization, and also creating a MACS Advisory Group (MAG) to assist post-DARPA transition. To this end we will begin with commercial SMM technology from one of our team members and also include a development program that takes advantage of the basic simplicity of our solid state SMM/THz technology to advance towards more monolithic system modular components that can scale downward in quantity—in size, mass and especially in price."*

And from within the body of the proposal:

> *"Also incorporated into Task 1 will be the formation of the MACS Advisory Group (MAG). The MAG will operate with two levels, one of technical orientation and one of user orientation. The MAG will seek to assist ST and DARPA in aligning the product with the target communities and also in achieving optimum technical capabilities. The MAG will deliver recommendations informally, and periodically, but formally at the end of Phase II."*

The intent of the MAG is not manifest in involvement directly with initial R&D (in particular Phase 1 of the current program). Among its near term objectives, the MAG intends to identify potential users of the MACS technology and to identify system requirements associated with several classes of users. The MAG also seeks to identify transition partners that can work with DARPA to participate in the development of fieldable systems for the identified users.

ST provided leadership for the MAG under the Phase 1 effort. Battelle was subcontracted to assist ST in leading the MAG. The MAG Executive Committee included:

- Keith Reiss (ST), chairman
- Christopher Ball (Battelle), co-chairman
- Joe Maniaci (Strategic Analysis, Inc.), DARPA SETA support
- Laura Vanderberg, consultant
- Frank De Lucia (Ohio State University)
- Tom Edmonston (ST)
- Dev Palmer (ARO), MACS COTR
- Raphael Moon (ECBC)

- Henry Everitt (Army RDEC)

Additional MACS team members provided MAG support on an as-needed basis.

The MAG seeks to optimize technical capabilities in whatever mission areas are best suited to our MACS technology. The applications may ultimately be most relevant will not be manifest in the initial prototype, and various developments beyond Phase 1 will necessarily create expanding capabilities and options, some possibly not yet even envisioned. The MAG was cognizant of the notion that MACS will not be able to do any conceivable detection task. The MAG was also advised to focus *beyond* DARPA, which is sponsoring the initial new technology development. Therefore, it was incumbent upon the MAG to manage expectations for the MACS technology, particularly during its infancy.

11.2.2 MAG Activities

A summary (See Appendix A11.2) of MAG activities includes:

- Locating possible MAG membership
- Invitations and acceptances
- Preparation of MAG Information Packet
- Issuance of MAG Information Packet and personal communications with each member
- MAG data exchange structure development
- Periodic MAG updates via SharePoint
- Periodic MAG feedback solicitations telephone/telecom communications and gathering of or creation of written notes
- Face to face meetings as possible
- Executive membership meetings at least in parallel with the PMRs
- Meetings on firm possibilities and follow up actions/visits and securing of letters of interest or the equivalent--or better as evidence of user interest that will satisfy DARPA Phase 1→2 transition requirements
- Preparation of a near end of Phase 1 performance view packet, possibly with video
- Preparation of a final summary of MAG activities and concomitant suggestions and recommendations.

11.2.3 Outcome of MAG Activities

Numerous potential MACS users and transition partners within the Government (primarily DoD, IC, and other agencies) were contacted by the Executive members of the MAG. These contacts were intended to introduce the technology and to elicit feedback on the types of missions and requirements that each contact brings to the table. Several face-to-face meetings were held to

facilitate information exchanges. A summary of the direct contacts made by the MAG is provided in Appendix 11.2.

One vehicle by which the MAG attempted to compile information from potential users and transition partners was a questionnaire. Appendix 11.2 shows a blank version of this questionnaire along with two responses received by Government contacts.

In the end, the MAG was able to generate strong interest in the MACS technology. In most cases, this interest was expressed verbally and necessitates additional follow-up under Phase 2. In several cases, contacts were able to provide endorsement letters directly to the DARPA PM indicating their interest in the MACS technology and their desire to see the development continue as well as potentially contribute to the development as transition partners. A template of an endorsement letter, developed by the MAG, is presented in Appendix 11.3, along with the three letters received from Government contacts.

Appendix A3.1

SAPM Mechanical Design Details

SAPM Mechanical Component List

Major Equipment	Vendor	Part Number	Quantity
Turbo Pump	Pfeiffer	PM P02 607	1
Diaphragm Pump	Pfeiffer	PK T05 070 B	1
Hi vacuum manifold body mat'l	Mcmaster Carr	8896K74	1
Roughing manifold body mat'l	Mcmaster Carr	89075K461	1
SMM manifold body mat'l	Mcmaster Carr	9083K131	1
Large orifice vacuum valve	CKD Industries	GFVB55-7-O-B2CS-3	4
Small orifice vacuum valve	CKD Industries	GFVB25-2-O-B2CS-3	3
Micropirani OEM sensor kit	MKS	905-0001	6
Proportional vacuum control valve	Pfeiffer	PF I13 931	1
Radial flow vacuum housing mat'l, 2D	Mcmaster Carr	89325K653	1
Kapton manifold heater	Minco	HK5371R136L12A	2
Silicone SMM heater	Minco	HR5579R11.4L12A	4
Kapton heater for radial housing	Minco	HK5576R45.0L12A	2
Kapton heater for radial housing	Minco	HK5161R39.2L12A	2
Small Parts and Materials			
KF16 blank flanges	MDC Vacuum	712000	10
KF16 seal	MKS	100311701	10
KF25 blank flanges	MDC Vacuum	712001	2
KF25 seal	MKS	100312703	2
KF16 bulkhead clamp	MDC Vacuum	716000	2
KF16 band clamp	VWR Scientific	EVC105-12-401	1
Tubing, 1/2" X .035"	Mcmaster Carr	89895K146	1
Tubing, 1/4" X .028"	Mcmaster Carr	89895K124	2
Tubing, 1/4" X .065"	Mcmaster Carr	89895K127	1
Delrin, 12" X 12" X 3/4"	Mcmaster Carr	8575K118	1
Delrin, 3" X 1 1/4" X 12"	Mcmaster Carr	8662K75	1
Delrin, 12" X 12" X 1/4"	Mcmaster Carr	8575K115	1
G-10 Garolite, 12" X 12" X 1/4"	Mcmaster Carr	9910T31	1
Adapter fitting for proportional valve	Pfeiffer	PT 420 912 -T	1
Weldlip vacuum feedthrough	Kurt Lesker	TFT1KY2C151	2
Knurled thumb screw	Mcmaster Carr	91830A204	6
4-40 screws X 7/8"	Mcmaster Carr	92196A114	1
4-40 screws X 7/16"	Mcmaster Carr	92196A109	1
#4 Washers	Mcmaster Carr	96765A110	1
Siltek treatement - 2D housing	Restek		1
Siltek treated 1/4" bulkhead fitting	Restek	22571	2
Siltek treatment - hivac manifold	Restek		1
Siltek treatment - sorbent tube	Restek		2
Siltek treatment - hi-lo manifold	Restek		1
Siltek treatment - filter	Restek		2
Fitting - diaphragm pump	Swagelok	SS-400-1-2RS	2
Filter - inline	Swagelok	SS-4FWS-05	2
Vibration Isolators	Barry Controls	ME-500	4

SAPM Mechanical Drawings

The following mechanical drawings are provided in the remaining pages of this appendix.

- Integrated MACS system, including SAPM
- Integrated SAPM system
- SAPM mock system base plate
- Roughing manifold
- Diaphragm pump valve mounting plate
- Diaphragm pump mounting plate
- Low vacuum tube
- SMM outlet manifold
- SMM outlet valve mounting plate
- High vacuum manifold (3 pages)
- High vacuum manifold mounting plate
- Turbo pump bracket
- Turbo pump outlet tube
- Direct inject port tube

DWG NO	SH 2	REV

REVISION HISTORY

ZONE	REV	DESCRIPTION	DATE	APPROVED

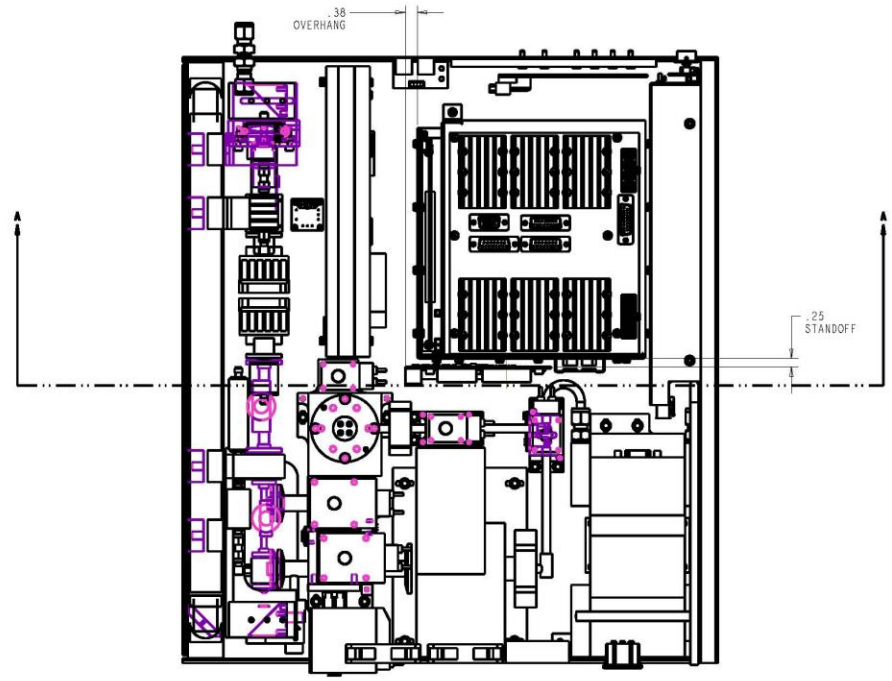

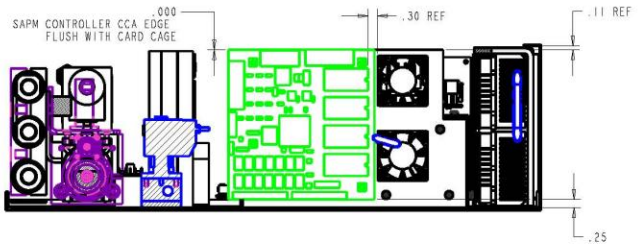

SECTION A-A

CAGE CODE	DWG NO	REV
D 79986		

SCALE 0.600 DO NOT SCALE DRAWING SHEET 2 OF 2

DWG NO	SH	REV
5760SAPM	1	

REVISION HISTORY

ZONE	REV	DESCRIPTION	DATE	APPROVED

NOTES:

1. APPLICABLE STANDARDS/SPECIFICATIONS:
   ASME Y14.5M-1994, DIMENSIONS AND TOLERANCES
   ASME Y14.38, ABBREVIATIONS

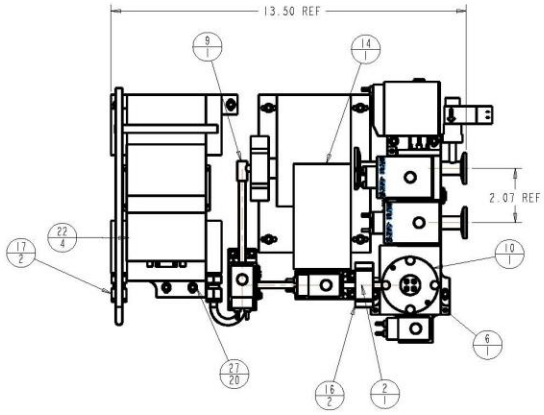

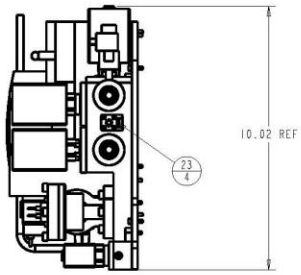

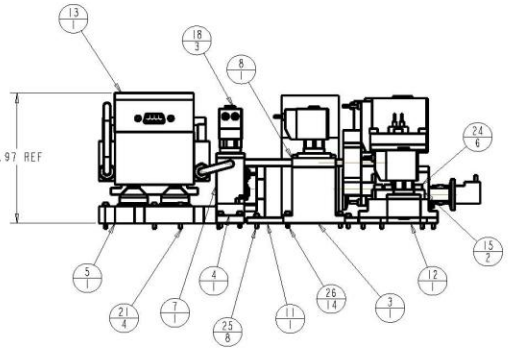

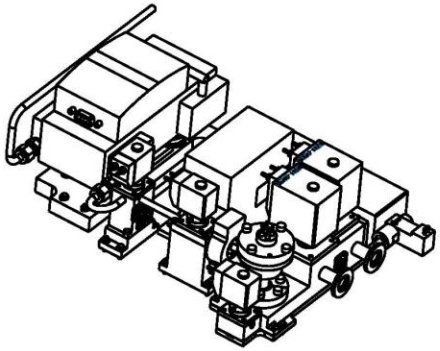

	ITO REQD	FIND NO	PART OR IDENTIFYING NO	CAGE CODE	NOMENCLATURE OR DESCRIPTION	MATERIAL SPECIFICATION
	20	27	96765A110	07BY4	WASHER, #4	18-8 STAINLESS
	14	26	92196A110	79986	SCREW, 4-40	18-8 STAINLESS
	8	25	92196A109	79986	SCREW, 4-40	18-8 STAINLESS
	6	24	92196A271	07BY4	SCREW, 10-32	18-8 STAINLESS
	4	23	MKS 905	23582	SENSOR, VACUUM MICROPIRANI	
	4	22	ME-500	81860	ISOLATOR, VIBRATION	NEOPRENE/ALUMINUM
	4	21	92196A114	79986	SCREW, 4-40	18-8 STAINLESS
	4	20	89885K125	07BY4	TUBE, 1/4" O.D. X .035" WALL	304 SS
	3	19	GVFB55-01	79986	VALVE, SHUTOFF, 7MM ORIFICE	
	3	18	GVFB25-01	79986	VALVE, SHUTOFF, 2MM ORIFICE	
	2	17	SS-4-TA-1	02570	FITTING, 1/4" COMPRESSION TO 1/8" BSP	316 SS
	2	16	EVC105-12-401	0UA56	CLAMP, KF16	304 SS
	2	15	716000	0ALZ2	CLAMP, BULKHEAD KF16	304 SS
	1	14	TPD 011-01	79986	TURBO PUMP	
	1	13	MVP 006-01	79986	DIPHRAGM PUMP	
	1	12	9910T31	07BY4	MOUNT PLATE HIVAC MANIFOLD	G-10 GAROLITE
	1	11	5760TURBBRACK-01	79986	BRACKET, TURBO PUMP	ACETAL
	1	10	5760SMMZD100-10	79986	HOUSING, RADIAL SMM FLOW	304 SS
	1	9	5760SAPMTURBOUT-10	79986	TUBE, TURBO OUTLET	304 SS
	1	8	5760SAPMMANSMM-01	79986	MANIFOLD, SMM OUTLET	304 STAINLESS
	1	7	5760SAPMMANROUGH-01	79986	MANIFOLD, ROUGHING	304 STAINLESS
	1	6	5760SAPMMANHIVAC-10	79986	MANIFOLD, HIGH VAC	304 STAINLESS
	1	5	5760SAPMDIAMNT-01	79986	MOUNT PLATE DIAPHRAGM PUMP	BLACK DELRIN
	1	4	5760SAPMBLOCK2-01	79986	MOUNT BLOCK DIAPHRAGM VALVE	BLACK DELRIN
	1	3	5760SAPMBLOCK1-01	79986	MOUNT BLOCK SMM OUTLET VALVE	BLACK DELRIN
	1	2	712000	0ALZ2	BLANK FLANGE, KF16	304 SS
	1	1	-01	79986	BASE PLATE	SS

PARTS LIST

NEXT ASSY	USED ON
APPLICATION	

UNLESS OTHERWISE SPECIFIED DIMENSIONS ARE IN INCHES
TOLERANCES ARE:
DECIMAL: .XX ±0.01 .XXX ±0.005
FRACTIONAL: ±1/32 ANGULAR: ±0.5°
THIRD ANGLE PROJECTION

CONTRACT NO

	APPROVAL	DATE
DRAWN		27-Aug-07
CHECKED		
ENGINEER		

Battelle
The Business of Innovation
505 King Avenue
Columbus, Ohio 43201-2693
Telephone (614) 424-6424

TITLE
MACS SAPM

SIZE	CAGE CODE	DWG NO	REV
D	79986	5760SAPM	

SCALE 0.500 DO NOT SCALE DRAWING SHEET 1 OF 2

COMPUTER FILE NAME	
DRAWING	SAPM
MODEL	ASSYM SAPM.ASSY

NOTES:

1. APPLICABLE STANDARDS/SPECIFICATIONS:
   ASME Y14.5M-1994, DIMENSIONS AND TOLERANCES
   ASME Y14.38, ABBREVIATIONS
2. REMOVE ALL BURRS AND SHARP EDGES R.02 OR .02 X 45 CHAMFER MAX.
3. UNLESS OTHERWISE SPECIFIED SURFACE ROUGHNESS 63

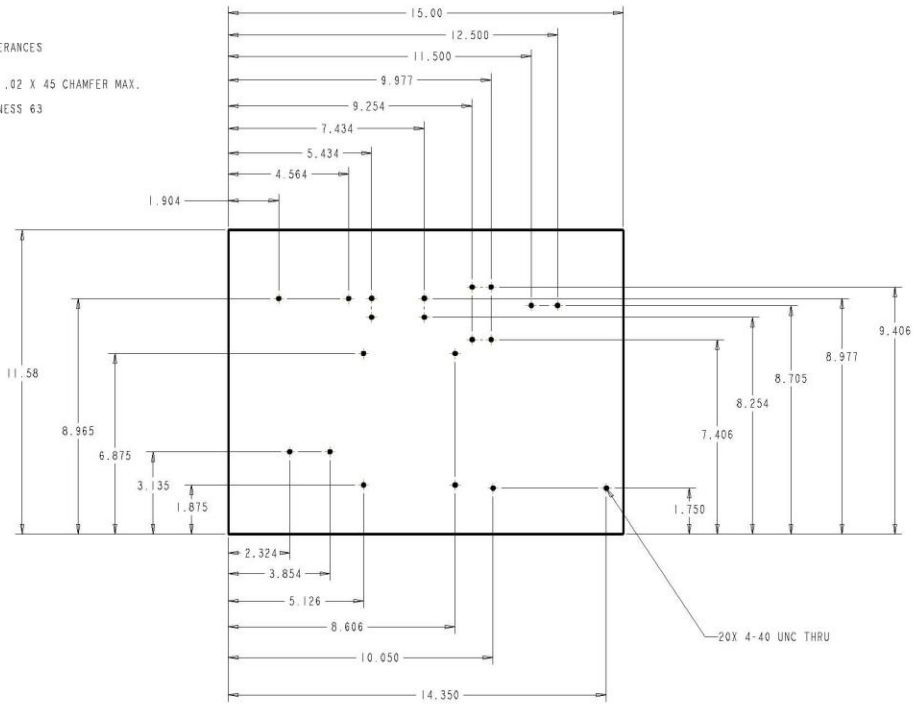

DWG NO	SH	REV
	1	

REVISION HISTORY

ZONE	REV	DESCRIPTION	DATE	APPROVED

PARTS LIST

QTY REQD	ITEM NO	FIND NO	PART OR IDENTIFYING NO	CAGE CODE	NOMENCLATURE OR DESCRIPTION	MATERIAL SPECIFICATION
1		1			PLATE, BASE	ALUMINUM

UNLESS OTHERWISE SPECIFIED DIMENSIONS ARE IN INCHES
TOLERANCES ARE:
DECIMAL: .XX ±0.01 .XXX ±0.005
FRACTIONAL: ±1/32 ANGULAR: ±0.5°
THIRD ANGLE PROJECTION

NEXT ASSY | USED ON
APPLICATION

CONTRACT NO

	APPROVAL	DATE
DRAWN		11-Jan-08
CHECKED		
ENGINEER		

Battelle
The Business of Innovation
505 King Avenue
Columbus, Ohio 43201-2693
Telephone (614) 424-6424

TITLE
BASE PLATE
SAPM MOCK SYSTEM

SIZE	CAGE CODE	DWG NO	REV
D	79986		

SCALE 0.500 | DO NOnot SCALE DRAWING | SHEET 1 OF 1

COMPUTER FILE NAME
DRAWING | SAPM_MOCK_DELIVERABLE
MODEL | ASSM SAPM_MOCK_DELIVERABLE

NOTES:

1. APPLICABLE STANDARDS/SPECIFICATIONS:
   ASME Y14.5M-1994, DIMENSIONS AND TOLERANCES
   ASME Y14.38, ABBREVIATIONS
2. REMOVE ALL BURRS AND SHARP EDGES R.02 OR .02 X 45 CHAMFER MAX.
3. UNLESS OTHERWISE SPECIFIED SURFACE ROUGHNESS 63
4. MATERIAL: 304 STAINLESS STEEL

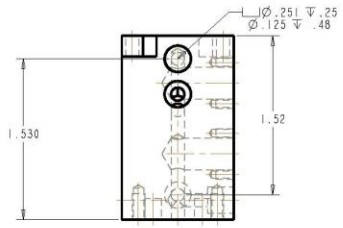

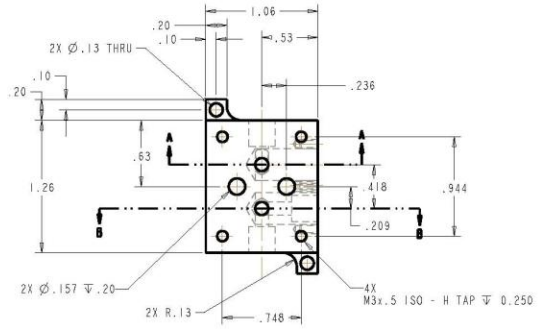

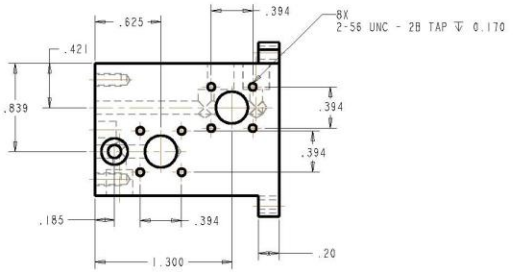

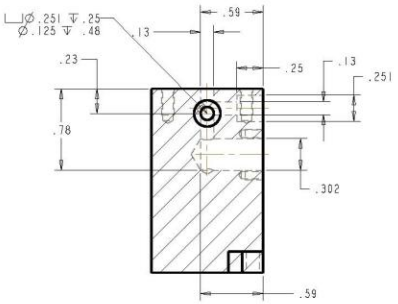

SECTION B-B

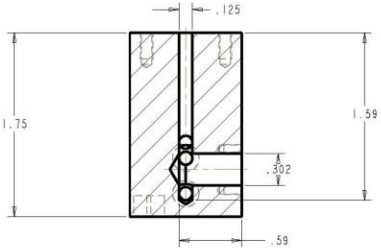

SECTION A-A

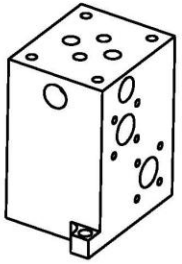

QTY. REQD	PART OR IDENTIFYING NO	CAGE CODE	NOMENCLATURE OR DESCRIPTION	MATERIAL SPECIFICATION
	-01	79986	MANIFOLD, ROUGHING	SEE NOTE 4

PARTS LIST

ZONE	REV	DESCRIPTION	DATE	APPROVED

REVISION HISTORY

DWG NO | SH 1 | REV

UNLESS OTHERWISE SPECIFIED DIMENSIONS ARE IN INCHES
TOLERANCES ARE:
DECIMAL: .XX ±0.01 .XXX ±0.005
FRACTIONAL: ±1/32 ANGULAR: ±0.5°
THIRD ANGLE PROJECTION

NEXT ASSY | USED ON
APPLICATION

CONTRACT NO

	APPROVAL	DATE
DRAWN		20-Sep-07
CHECKED		
ENGINEER		

Battelle
The Business of Innovation
505 King Avenue
Columbus, Ohio 43201-2693
Telephone (614) 424-6424

TITLE
MANIFOLD, ROUGHING

SIZE D | CAGE CODE 79986 | DWG NO | REV
SCALE 2.000 | CALC. WT. | SHEET 1 OF 2

COMPUTER FILE NAME
DRAWING SAPM_DIAPHRAGM_MANIFOLD
MODEL PART: SAPM DIAPHRAGM_MANIFOLD

DWG NO	SH	REV
5760SAPMBLOCK2	1	

REVISION HISTORY

ZONE	REV	DESCRIPTION	DATE	APPROVED

NOTES:

1. APPLICABLE STANDARDS/SPECIFICATIONS:
   ASME Y14.5M-1994, DIMENSIONS AND TOLERANCES
   ASME Y14.38, ABBREVIATIONS
2. REMOVE ALL BURRS AND SHARP EDGES R.02 OR .02 X 45 CHAMFER MAX.
3. UNLESS OTHERWISE SPECIFIED SURFACE ROUGHNESS 63

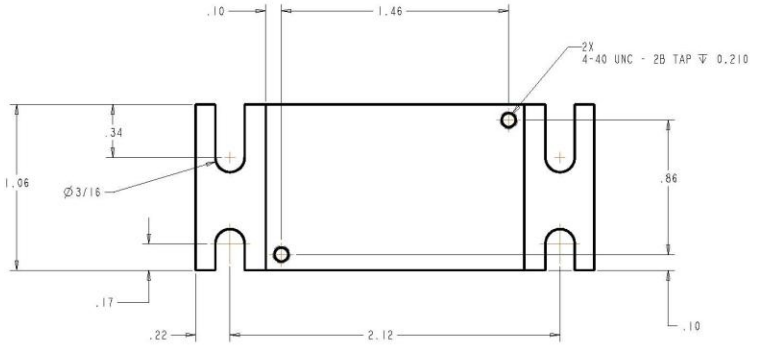

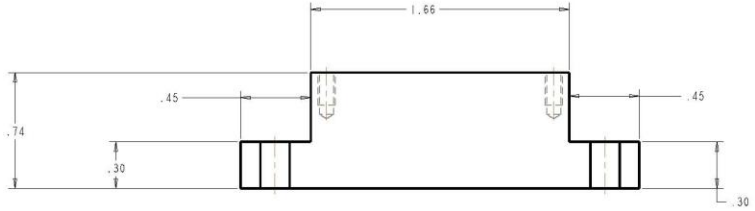

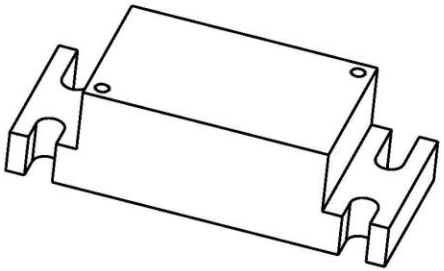

QTY. REQD	PART OR IDENTIFYING NO	CAGE CODE	NOMENCLATURE OR DESCRIPTION	MATERIAL SPECIFICATION
	5760SAPMBLOCK2-01	79986	MOUNT BLOCK DIAPHRAGM VALVE	BLACK DELRIN

PARTS LIST

UNLESS OTHERWISE SPECIFIED DIMENSIONS ARE IN INCHES
TOLERANCES ARE:
DECIMAL: .XX ±0.01 .XXX ±0.005
FRACTIONAL: ±1/32 ANGULAR: ±0.5°
THIRD ANGLE PROJECTION

NEXT ASSY | USED ON
APPLICATION

CONTRACT NO

	APPROVAL	DATE
DRAWN		27-Dec-07
CHECKED		
ENGINEER		

Battelle
The Business of Innovation
505 King Avenue
Columbus, Ohio 43201-2693
Telephone (614) 424-6424

TITLE
MOUNT BLOCK
DIAPHRAGM VALVE

SIZE	FSCM NO	DWG NO	REV
D	79986	5760SAPMBLOCK2	

SCALE 3.000 WT. SHEET 1 OF 1

COMPUTER FILE NAME: SAPM_PDASTAL_DIAPHRAGM.MAS
DRAWING: SAPM_PDASTAL_DIAPHRAGM.MAS
MODEL: PART SAPM_PDASTAL_DIAPHRAGM.MAS

NOTES:

1. APPLICABLE STANDARDS/SPECIFICATIONS:
   ASME Y14.5M-1994, DIMENSIONS AND TOLERANCES
   ASME Y14.38, ABBREVIATIONS
2. REMOVE ALL BURRS AND SHARP EDGES R.02 OR .02 X 45 CHAMFER MAX.
3. UNLESS OTHERWISE SPECIFIED SURFACE ROUGHNESS 63
4. MATERIAL: BLACK DELRIN

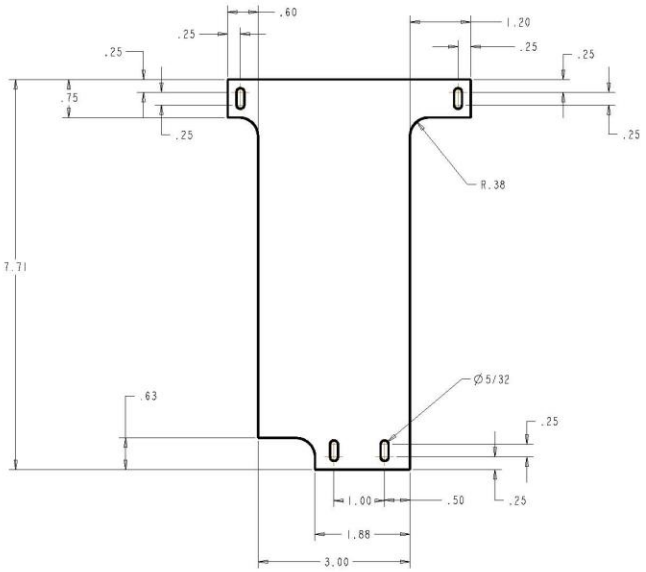

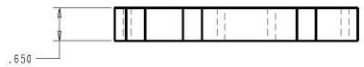

DWG NO | SH 1 | REV

REVISION HISTORY

ZONE	REV	DESCRIPTION	DATE	APPROVED

PARTS LIST

QTY. REQD	PART OR IDENTIFYING NO	CAGE CODE	NOMENCLATURE OR DESCRIPTION	MATERIAL SPECIFICATION
	-01	79986	MOUNT PLATE DIAPHRAGM PUMP	SEE NOTE 4

NEXT ASSY | USED ON
APPLICATION

UNLESS OTHERWISE SPECIFIED DIMENSIONS ARE IN INCHES
TOLERANCES ARE:
DECIMAL: .XX ±0.01 .XXX ±0.005
FRACTIONAL: ±1/32 ANGULAR: ±0.5°
THIRD ANGLE PROJECTION

CONTRACT NO

APPROVAL	DATE
DRAWN	31-Dec-07
CHECKED	
ENGINEER	

Battelle
The Business of Innovation
505 King Avenue
Columbus, Ohio 43201-2693
Telephone (614) 424-6424

TITLE
MOUNT PLATE DIAPHRAGM PUMP

SIZE D | CAGE CODE 79986 | DWG NO | REV
SCALE 1.000 | CALC. WT. | SHEET 1 OF 1

COMPUTER FILE NAME
DRAWING SAPM_V1B_ISO_PLATE
MODEL PART SAPM_V1B_ISO_PLATE

DWG NO	SH	REV
89895K125	1	

REVISION HISTORY

ZONE	REV	DESCRIPTION	DATE	APPROVED

NOTES:

1. APPLICABLE STANDARDS/SPECIFICATIONS:
   ASME Y14.5M-1994, DIMENSIONS AND TOLERANCES
   ASME Y14.38, ABBREVIATIONS
2. REMOVE ALL BURRS AND SHARP EDGES R.02 OR .02 X 45 CHAMFER MAX.
3. UNLESS OTHERWISE SPECIFIED SURFACE ROUGHNESS 63

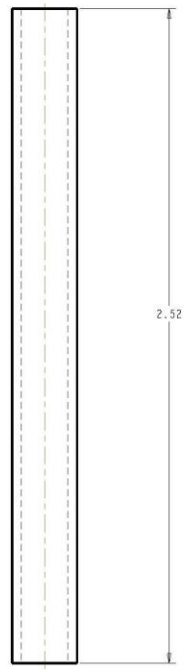

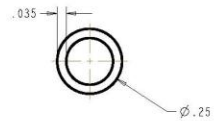

PARTS LIST

QTY. REQD	PART OR IDENTIFYING NO	CAGE CODE	NOMENCLATURE OR DESCRIPTION	MATERIAL SPECIFICATION
	89895K125	07BY4	TUBE, SAPM LOVAC	SEE NOTE 4

NEXT ASSY | USED ON
APPLICATION

UNLESS OTHERWISE SPECIFIED
DIMENSIONS ARE IN INCHES
TOLERANCES ARE:
DECIMAL: .XX ±0.01 .XXX ±0.005
FRACTIONAL: ±1/32 ANGULAR: ±0.5°
THIRD ANGLE PROJECTION

CONTRACT NO

APPROVAL	DATE
DRAWN	09-Jan-08
CHECKED	
ENGINEER	

Battelle
The Business of Innovation
505 King Avenue
Columbus, Ohio 43201-2693
Telephone (614) 424-6424

TITLE
TUBE, SAPM LOVAC

SIZE/CAGE CODE: D 79986 | DWG NO: 89895K125 | REV
SCALE: 5.000 | CALC. WT. | SHEET 1 OF 1

COMPUTER FILE NAME: SAPM_TUBE_LOVAC_MAINFOLD
DRAWING MODEL: PART_SAPM_TUBE_04_STRAIGHT_6

DWG NO	SH	REV
	1	

REVISION HISTORY

ZONE	REV	DESCRIPTION	DATE	APPROVED

NOTES:

1. APPLICABLE STANDARDS/SPECIFICATIONS:
   ASME Y14.5M-1994, DIMENSIONS AND TOLERANCES
   ASME Y14.38, ABBREVIATIONS
2. REMOVE ALL BURRS AND SHARP EDGES R.02 OR .02 X 45 CHAMFER MAX.
3. UNLESS OTHERWISE SPECIFIED SURFACE ROUGHNESS 63
4. FUSION WELD - VERY LITTLE FILLER AND HEAT
   DRILL THRU FLANGE FOR 1/4" O.D. TUBE
   POSITION TUBE END FLUSH WITH FLANGE FACE AS SHOWN

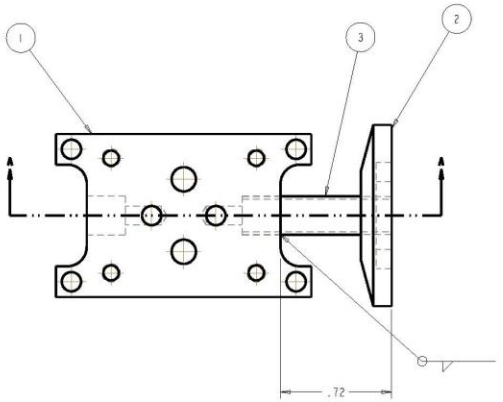

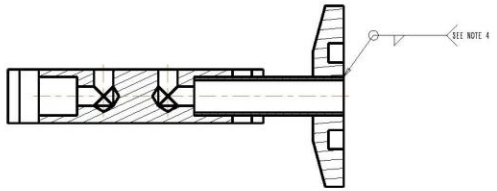

SECTION A-A

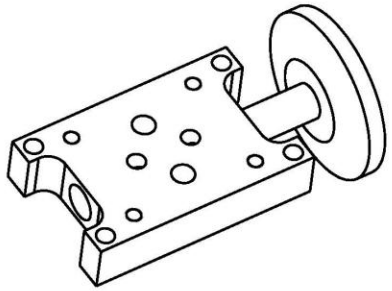

QTY REQD	FIND NO	PART OR IDENTIFYING NO	CAGE CODE	NOMENCLATURE OR DESCRIPTION	MATERIAL SPECIFICATION
1	3	89885K125	07BY4	TUBE, 1/4" O.D. X .035" WALL	304 SS
1	2	712000	DALZ2	BLANK FLANGE, KF16	304 SS
1	1	-01	79986	MANIFOLD, SMM OUTLET	304 STAINLESS

PARTS LIST

UNLESS OTHERWISE SPECIFIED DIMENSIONS ARE IN INCHES
TOLERANCES ARE:
DECIMAL: .XX ±0.01 .XXX ±0.005
FRACTIONAL: ±1/32 ANGULAR: ±0.5°
THIRD ANGLE PROJECTION

NEXT ASSY | USED ON
APPLICATION

CONTRACT NO

	APPROVAL	DATE
DRAWN		09-Jan-08
CHECKED		
ENGINEER		

Battelle
The Business of Innovation
505 King Avenue
Columbus, Ohio 43201-2693
Telephone (614) 424-6424

TITLE
MANIFOLD, SMM OUTLET ASSY

SIZE	CAGE CODE	DWG NO	REV
D	79986		

SCALE 3.000 | DO NOT SCALE DRAWING | SHEET 1 OF 1

COMPUTER FILE NAME: SAPM_DIAPHRAGM_MANIFOLD_ASSY
DRAWING: ASSEM SAPM_DIAPHRAGM_MANIFOLD_ASSY
MODEL:

NOTES:

1. APPLICABLE STANDARDS/SPECIFICATIONS:
   ASME Y14.5M-1994, DIMENSIONS AND TOLERANCES
   ASME Y14.38, ABBREVIATIONS
2. REMOVE ALL BURRS AND SHARP EDGES R.02 OR .02 X 45 CHAMFER MAX.
3. UNLESS OTHERWISE SPECIFIED SURFACE ROUGHNESS 63

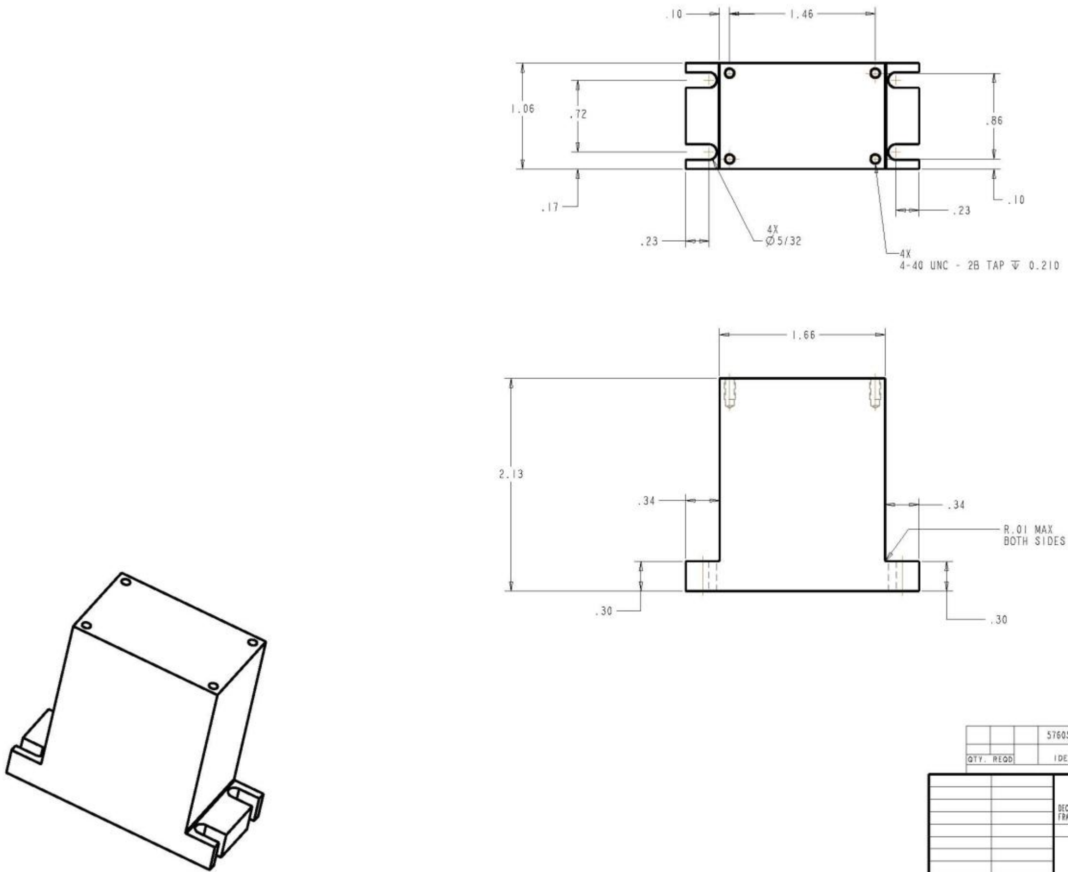

DWG NO 5760SAPMBLOCK1	SH 1	REV

REVISION HISTORY

ZONE	REV	DESCRIPTION	DATE	APPROVED

PARTS LIST

QTY. REQD	PART OR IDENTIFYING NO	CAGE CODE	NOMENCLATURE OR DESCRIPTION	MATERIAL SPECIFICATION
	5760SAPMBLOCK1-01	79986	MOUNT BLOCK SMM OUTLET VALVE	BLACK DELRIN

NEXT ASSY	USED ON
APPLICATION	

UNLESS OTHERWISE SPECIFIED
DIMENSIONS ARE IN INCHES
TOLERANCES ARE:
DECIMAL: .XX ±0.01 .XXX ±0.005
FRACTIONAL: ±1/32 ANGULAR: ±0.5°

THIRD ANGLE PROJECTION

CONTRACT NO	
APPROVAL	DATE
DRAWN	27-Dec-07
CHECKED	
ENGINEER	

Battelle
The Business of Innovation
505 King Avenue
Columbus, Ohio 43201-2693
Telephone (614) 424-6424

TITLE
MOUNT BLOCK SMM OUTLET VALVE

SIZE	CAGE CODE	DWG NO	REV
D	79986	5760SAPMBLOCK1	

SCALE 2.000 CALC. WT. SHEET 1 OF 1

COMPUTER FILE NAME
DRAWING SAPM_PEDASTAL_DIAPHRAGM_MANI_2
MODEL PART SAPM_PEDASTAL_DIAPHRAGM_MANI_2

NOTES:

1. APPLICABLE STANDARDS/SPECIFICATIONS:
   ASME Y14.5M-1994, DIMENSIONS AND TOLERANCES
   ASME Y14.38, ABBREVIATIONS
2. REMOVE ALL BURRS AND SHARP EDGES R.02 OR .02 X 45 CHAMFER MAX.
3. UNLESS OTHERWISE SPECIFIED SURFACE ROUGHNESS 63
4. MATERIAL: 304 STAINLESS STEEL

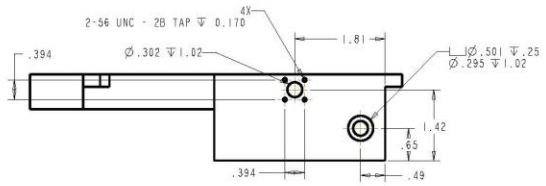

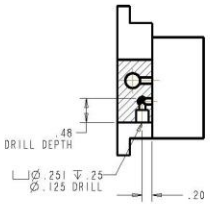

SECTION B-B

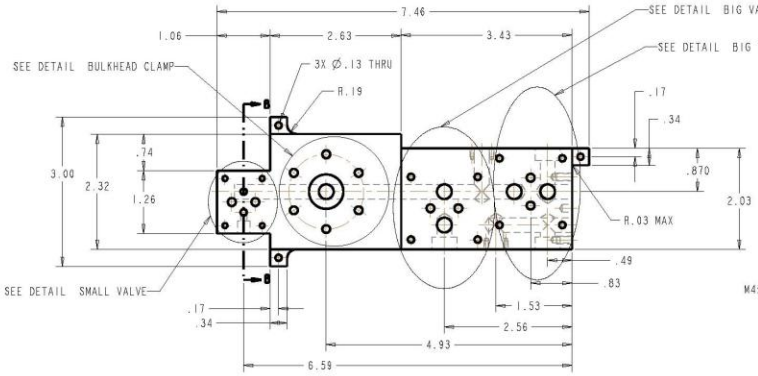

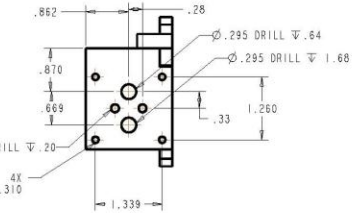

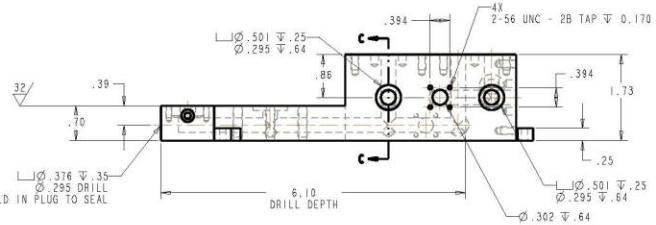

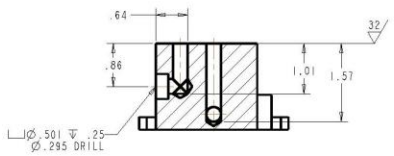

SECTION C-C

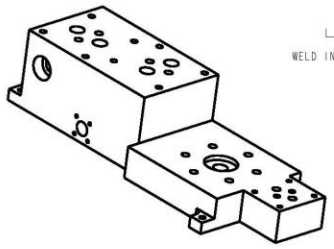

QTY. REQD	PART OR IDENTIFYING NO	CAGE CODE	NOMENCLATURE OR DESCRIPTION	MATERIAL SPECIFICATION
	5760SAPMHIVACMAN-01	79986	MANIFOLD, HIGH VACUUM	SEE NOTE 4

PARTS LIST

ZONE	REV	REVISION HISTORY DESCRIPTION	DATE	APPROVED

DWG NO 5760SAPMHIVACMAN SH 1 REV

UNLESS OTHERWISE SPECIFIED DIMENSIONS ARE IN INCHES
TOLERANCES ARE:
DECIMAL: .XX ±0.01 .XXX ±0.005
FRACTIONAL: ±1/32 ANGULAR: ±0.5°
THIRD ANGLE PROJECTION

NEXT ASSY | USED ON
APPLICATION

CONTRACT NO

	APPROVAL	DATE
DRAWN		18-Sep-07
CHECKED		
ENGINEER		

Battelle
The Business of Innovation
505 King Avenue
Columbus, Ohio 43201-2693
Telephone (614) 424-6424

TITLE
MANIFOLD, HIGH VACUUM

SIZE | CAGE CODE | DWG NO | REV
D | 79986 | 5760SAPMHIVACMAN |

SCALE 1.000 | CALC. WT. | SHEET 1 OF 3

COMPUTER FILE BASE
DRAWING | SAPM_MANIFOLD_COMBINED
MODEL | PART SAPM_MANIFOLD_COMBINED

DWG NO	SH	REV
799865760SAPMHIVACMAN	2	

REVISION HISTORY

ZONE	REV	DESCRIPTION	DATE	APPROVED

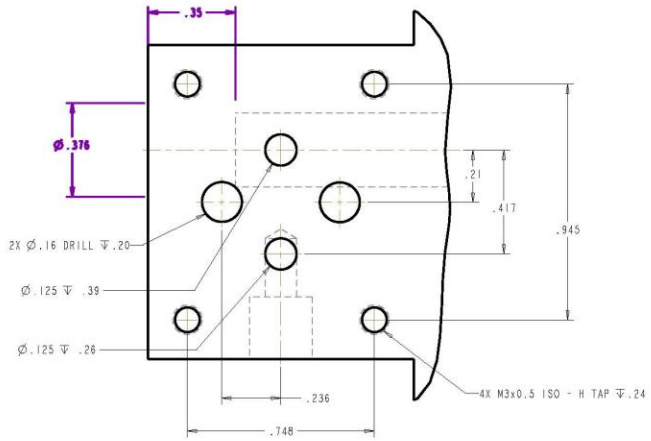

DETAIL SMALL VALVE
SCALE 5.000

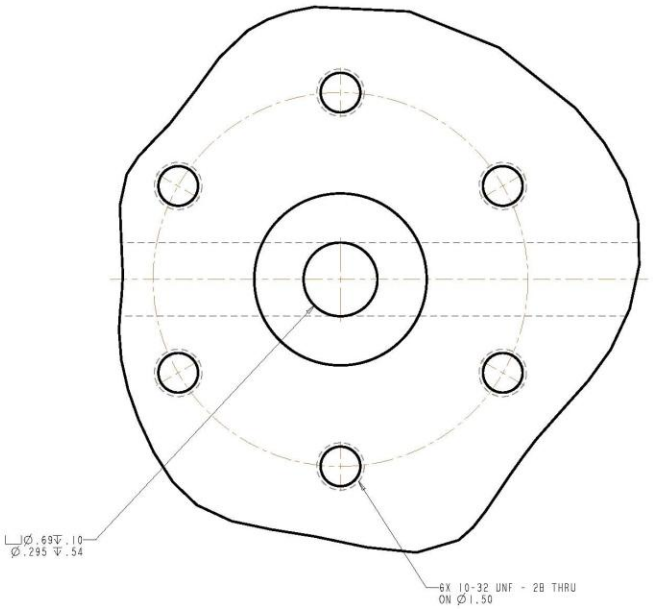

DETAIL BULKHEAD CLAMP
SCALE 5.000

SIZE/CAGE CODE	DWG NO	REV
D	799865760SAPMHIVACMAN	
SCALE 1.000	DO NOT SCALE DRAWING	SHEET 2 OF 3

DWG NO	SH	REV
3760SAPMHIVACMAN	2	

REVISION HISTORY

ZONE	REV	DESCRIPTION	DATE	APPROVED

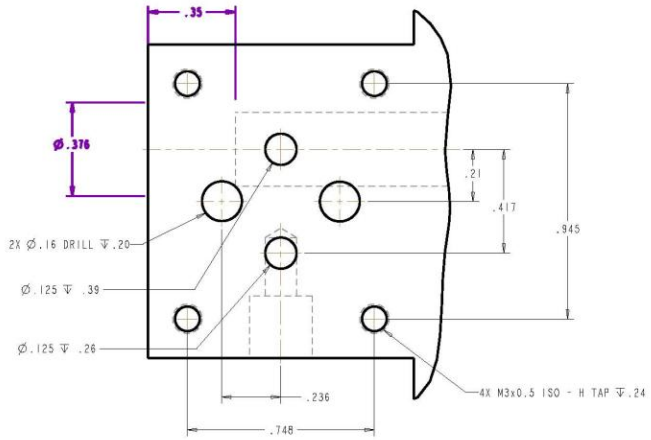

DETAIL SMALL VALVE
SCALE 5.000

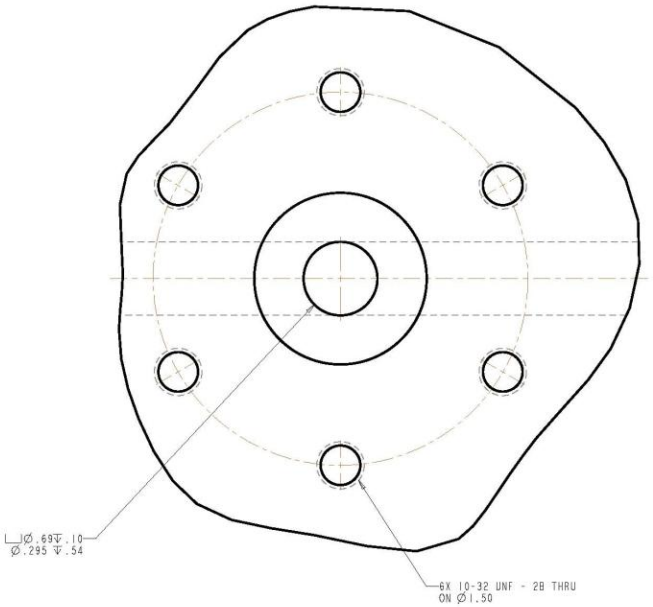

DETAIL BULKHEAD CLAMP
SCALE 5.000

DRAWING SIZE	DWG NO	REV
D	799865760SAPMHIVACMAN	
SCALE 1.000	DO NOT SCALE DRAWING	SHEET 2 OF 3

DWG NO	SH	REV
3760SAPMHIVACMAN	3	

REVISION HISTORY

ZONE	REV	DESCRIPTION	DATE	APPROVED

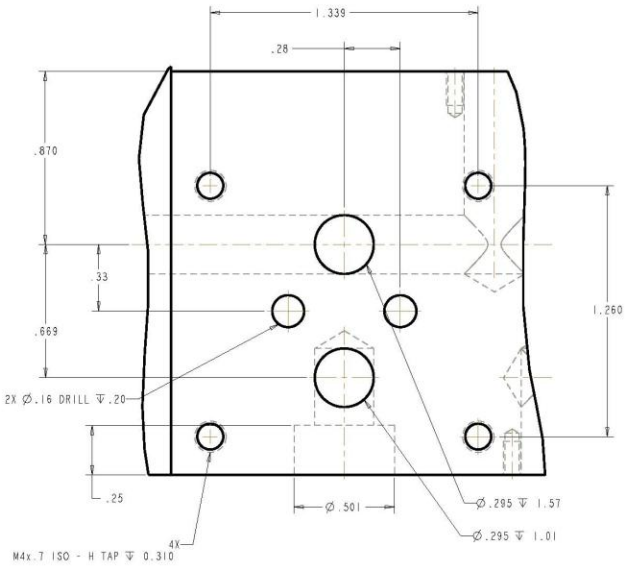

DETAIL BIG VALVE TRANSFER
SCALE 4.000

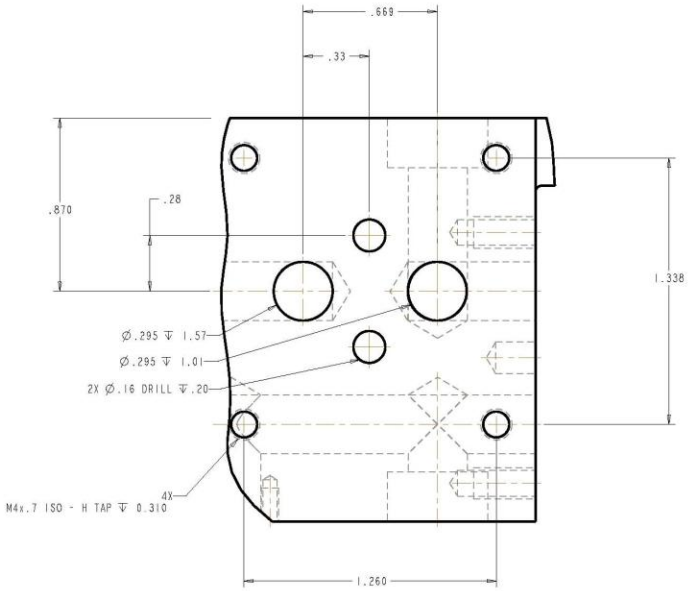

DETAIL BIG VALVE SMM TURBO
SCALE 4.000

SIZE	CAGE CODE	DWG NO	REV
D	799865760SAPMHIVACMAN		

SCALE 1.000 DO NOT SCALE DRAWING SHEET 3 OF 3

DWG NO	SH	REV
9910T31	1	

REVISION HISTORY

ZONE	REV	DESCRIPTION	DATE	APPROVED

NOTES:

1. APPLICABLE STANDARDS/SPECIFICATIONS:
   ASME Y14.5M-1994, DIMENSIONS AND TOLERANCES
   ASME Y14.38, ABBREVIATIONS
2. REMOVE ALL BURRS AND SHARP EDGES R.02 OR .02 X 45 CHAMFER MAX.
3. UNLESS OTHERWISE SPECIFIED SURFACE ROUGHNESS 63
4. MATERIAL: G-10 GAROLITE

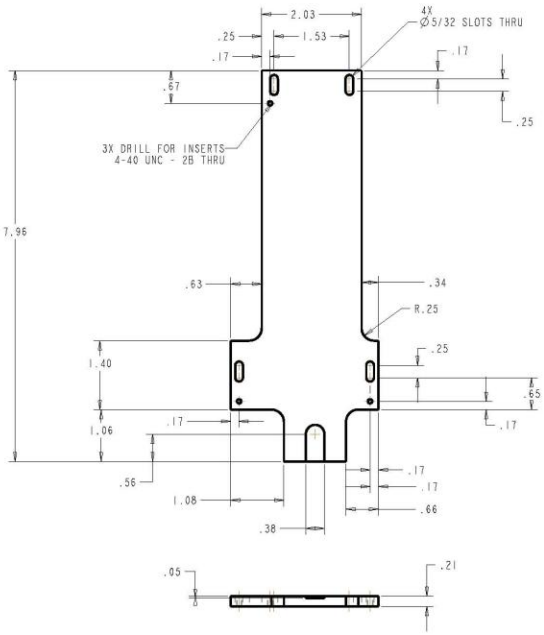

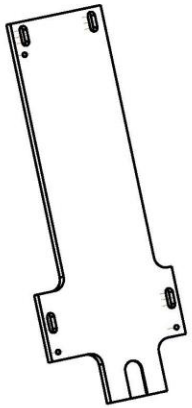

QTY. REQD	PART OR IDENTIFYING NO	CAGE CODE	NOMENCLATURE OR DESCRIPTION	MATERIAL SPECIFICATION
	9910T31	07BY4	MOUNT PLATE HIVAC MANIFOLD	G-10 GAROLITE

PARTS LIST

NEXT ASSY	USED ON
APPLICATION	

UNLESS OTHERWISE SPECIFIED DIMENSIONS ARE IN INCHES
TOLERANCES ARE:
DECIMAL: .XX ±0.01 .XXX ±0.005
FRACTIONAL: ±1/32 ANGULAR: ±0.5°
THIRD ANGLE PROJECTION

CONTRACT NO

	APPROVAL	DATE
DRAWN		09-Jan-08
CHECKED		
ENGINEER		

Battelle
The Business of Innovation
505 King Avenue
Columbus, Ohio 43201-2693
Telephone (614) 424-6424

TITLE
MOUNT PLATE HIVAC MANIFOLD

SIZE	CAGE CODE	DWG NO	REV
D	79986	9910T31	

SCALE 1.000 CALC. WT. SHEET 1 OF 1

COMPUTER FILE NAME: SAPM_PEDESTAL_MANIFOLD_COMBINED
DRAWING MODEL: PART SAPM_PEDESTAL_MANIFOLD_COMBINED

DWG NO	SH	REV
5760TURBBRACK	1	

REVISION HISTORY

ZONE	REV	DESCRIPTION	DATE	APPROVED

NOTES:

1. APPLICABLE STANDARDS/SPECIFICATIONS:
   ASME Y14.5M-1994, DIMENSIONS AND TOLERANCES
   ASME Y14.38, ABBREVIATIONS
2. REMOVE ALL BURRS AND SHARP EDGES R.02 OR .02 X 45 CHAMFER MAX.
3. UNLESS OTHERWISE SPECIFIED SURFACE ROUGHNESS 63
4. MATERIAL: BLACK DELRIN

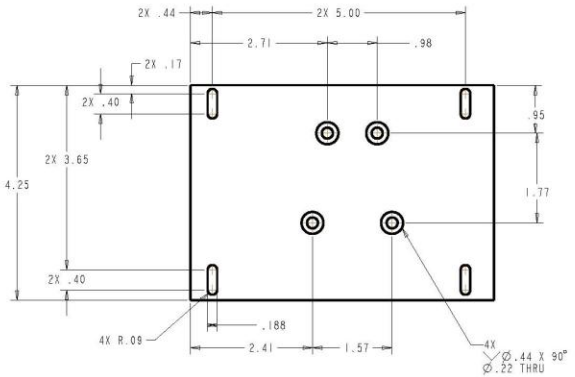

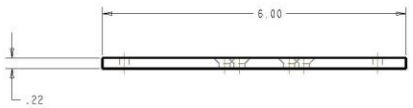

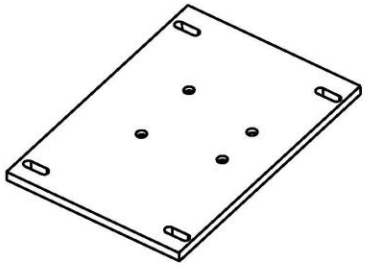

QTY. REQD	PART OR IDENTIFYING NO	CAGE CODE	NOMENCLATURE OR DESCRIPTION	MATERIAL SPECIFICATION
	5760TURBBRACK-01	79986	BRACKET, TURBO PUMP	SEE NOTE 4

PARTS LIST

UNLESS OTHERWISE SPECIFIED DIMENSIONS ARE IN INCHES
TOLERANCES ARE:
DECIMAL: .XX ±0.01 .XXX ±0.005
FRACTIONAL: ±1/32 ANGULAR: ±0.5°
THIRD ANGLE PROJECTION

CONTRACT NO

APPROVAL	DATE
DRAWN	14-Dec-07
CHECKED	
ENGINEER	

NEXT ASSY | USED ON
APPLICATION

Battelle
The Business of Innovation
505 King Avenue
Columbus, Ohio 43201-2693
Telephone (614) 424-6424

TITLE
BRACKET, TURBO PUMP

SIZE	CAGE CODE	DWG NO	REV
D	79986	5760TURBBRACK	

SCALE 1.000 CALC. WT. SHEET 1 OF 1

COMPUTER FILE NAME: S&PM_PEDASTAL_TURBO_PUMP
DRAWING: S&PM_PEDASTAL_TURBO_PUMP
MODEL: PART S&PM_PEDASTAL_TURBO_PUMP

DWG NO	SH	REV
799865760SAPMTURBOOUT	1	

REVISION HISTORY

ZONE	REV	DESCRIPTION	DATE	APPROVED

NOTES:

1. APPLICABLE STANDARDS/SPECIFICATIONS:
   ASME Y14.5M-1994, DIMENSIONS AND TOLERANCES
   ASME Y14.38, ABBREVIATIONS
2. REMOVE ALL BURRS AND SHARP EDGES R.02 OR .02 X 45 CHAMFER MAX.
3. UNLESS OTHERWISE SPECIFIED SURFACE ROUGHNESS 63
4. DRILL THRU SIDEWALL FOR 1/4" O.D. TUBE
   MAINTAIN .18" MINIMUM FLOW DIAMETER AFTER WELD
5. FUSION WELD - VERY LITTLE FILLER AND HEAT:
   DRILL THRU KF16 FLANGE FOR 1/4" O.D. TUBE
   POSITION TUBE END FLUSH WITH FLANGE FACE AS SHOWN

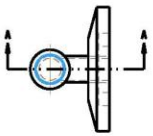

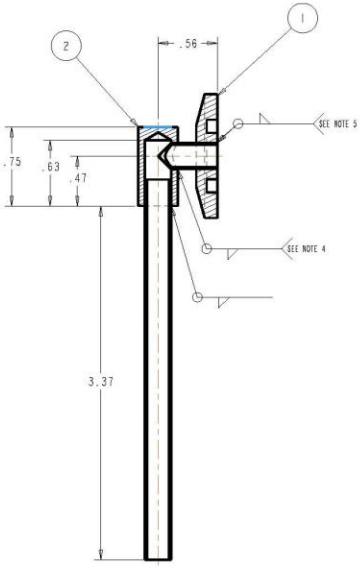

SECTION A-A

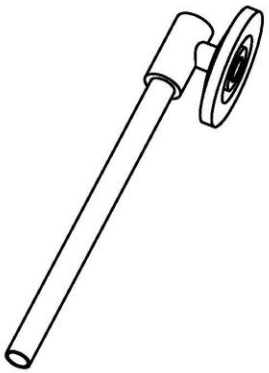

QTY REQD	FIND NO	PART OR IDENTIFYING NO	CAGE CODE	NOMENCLATURE OR DESCRIPTION	MATERIAL SPECIFICATION
2	3	89885K125	07BY4	TUBE, 1/4" O.D. X .035" WALL	304 SS
1	2	89535K23	07BY4	ROD, 3/8" DIA	304 SS
1	1	712000	0ALZ2	BLANK FLANGE, KF16	304 SS

PARTS LIST

UNLESS OTHERWISE SPECIFIED DIMENSIONS ARE IN INCHES
TOLERANCES ARE:
DECIMAL: .XX ±0.01 .XXX ±0.005
FRACTIONAL: ±1/32 ANGULAR: ±0.5°
THIRD ANGLE PROJECTION

NEXT ASSY | USED ON
APPLICATION

CONTRACT NO

APPROVAL	DATE
DRAWN	09-Jan-08
CHECKED	
ENGINEER	

Battelle
The Business of Innovation
505 King Avenue
Columbus, Ohio 43201-2693
Telephone (614) 424-6424

TITLE
TUBE, TURBO OUTLET

SIZE	CAGE CODE	DWG NO	REV
D	799865760SAPMTURBOOUT		

SCALE 2.000 DO NOT SCALE DRAWING SHEET 1 OF 1

COMPUTER FILE NAME	
DRAWING	SAPM_TUBE_TURBO_OUTLET
MODEL	ASSEM SAPM_TUBE_TURBO_OUTLET

DWG NO	SH	REV
5760SAPMDIRINJ	1	01

REVISION HISTORY

ZONE	REV	DESCRIPTION	DATE	APPROVED
	01	LENGTHEN 1/2" TUBE BY 0.3"	2/28/2008	RWD

NOTES:

1. APPLICABLE STANDARDS/SPECIFICATIONS:
   ASME Y14.5M-1994, DIMENSIONS AND TOLERANCES
   ASME Y14.38, ABBREVIATIONS
2. REMOVE ALL BURRS AND SHARP EDGES R.02 OR .02 X 45 CHAMFER MAX.
3. UNLESS OTHERWISE SPECIFIED SURFACE ROUGHNESS 63
4. MODIFY ADAPTER FITTING:
   A. MACHINE OFF KF10 FLANGE TO Ø .75"
   B. MAKE WELD PLUG FOR FLANGE SEAT APPROX. Ø.49 X .10
   C. DRILL THRU PLUG FOR 1/4" TUBE AND FUSION WELD INSIDE
   D. FUSION WELD PLUG INTO FITTING
5. WELD 1/4" TUBE WITH FITTING INTO SIDEWALL:
   A. DRILL THRU SIDEWALL OF 1/2" O.D. TO FIT 1/4" O.D.
   B. TIGHTEN FITTING (WITH O-RING) FULLY ON VALVE
   C. ROTATE 1/4" TUBE UNTIL VALVE IS 90° AS SHOWN
   D. .18" MINIMUM FLOW DIAMETER AFTER WELD

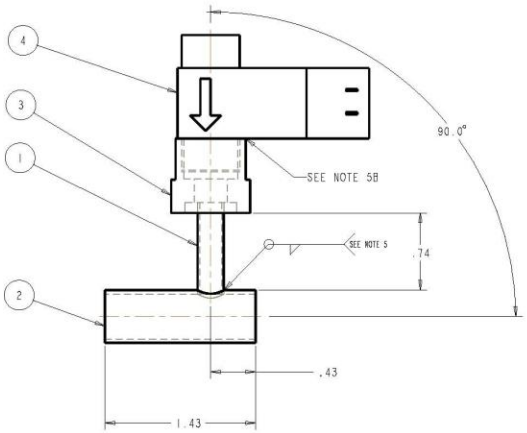

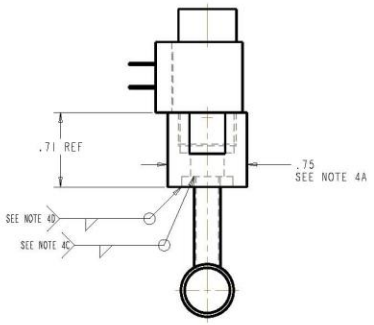

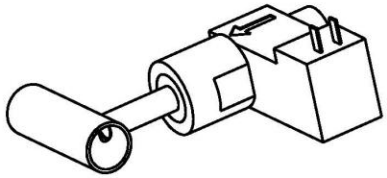

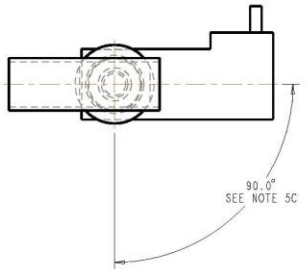

QTY REQD	FIND NO	PART OR IDENTIFYING NO	CAGE CODE	NOMENCLATURE OR DESCRIPTION	MATERIAL SPECIFICATION
1	4	RME005	1B0F1	VALVE, 0-24V PROPORTIONAL	SS BODY
1	3	PT420912-T	1B0F1	FITTING, MODIFIED M14X1 ADAPTER	STAINLESS
1	2	89895K737	07BY4	TUBE, 1/2" OD X .035 WALL	304 SS
1	1	89895K125	07BY4	TUBE, 1/4" OD X .035 WALL	304 SS

PARTS LIST

UNLESS OTHERWISE SPECIFIED DIMENSIONS ARE IN INCHES
TOLERANCES ARE:
DECIMAL: .XX ±0.01 .XXX ±0.005
FRACTIONAL: ±1/32 ANGULAR: ±0.5°
THIRD ANGLE PROJECTION

NEXT ASSY | USED ON
APPLICATION

CONTRACT NO

APPROVAL	DATE
DRAWN	03-Jan-08
CHECKED	
ENGINEER	

Battelle
The Business of Innovation
505 King Avenue
Columbus, Ohio 43201-2693
Telephone (614) 424-6424

TITLE
TUBE, DIRECT INJECT PORT

SIZE	CAGE CODE	DWG NO	REV
D	79986	5760SAPMDIRINJ	01

SCALE 2.000 DO NOT SCALE DRAWING SHEET 1 OF 1

COMPUTER FILE NAME	
DRAWING	S&PM_TUBE_DIRECT_INJECT_ASSY
MODEL	ASSEM S&PM_TUBE_DIRECT_INJECT_ASSY

Appendix A3.2

SAPM Electronic Design Details
SAPM CCA Parts List

REF. #	Part Type	Footprint	Package	Value	Quantity	Available fron
Resistors						
R1	WSL2010R3000FEA	RC2010	TAPE	0.3	1	Digikey
R2, R11, R36, R41, R56-57	ERJ-6GEY0R00V	RC0805	TAPE	0	6	Digikey
R3-4, R8-10, R18-19, R25-27, R48	ERJ-6GEYJ112	RC0805	TAPE	1.1K	11	Digikey
R5-6, R13-15, R23-24. R31-33	ERJ-6GEYJ244V	RC0805	TAPE	240K	10	Digikey
R7, R28-30, R34-35, R37-39, R42-43, R45-47, R50-53, R59, R61	ERJ-6GEYJ103V	RC0805	TAPE	10K	20	Digikey
R12	ERJ-6GEYJ303V	RC0805	TAPE	30K	1	Digikey
R16-17, R49	ERJ-6GEYJ104V	RC0805	TAPE	100K	3	Digikey
R20-22	ERJ-6GEYJ222V	RC0805	TAPE	2.2K	3	Digikey
R40	ERJ-6GEYJ362V	RC0805	TAPE	3.6K	1	Digikey
R44	ERJ-6GEYJ106V	RC0805	TAPE	10M	1	Digikey
R54	ERJ-6GEYJ204V	RC0805	TAPE	200K	1	Digikey
R55	ERJ-6GEYJ101V	RC0805	TAPE	100	1	Digikey
R58, R60	ERJ-6GEYJ393V	RC0805	TAPE	39.0K	2	Digikey
R62	ERJ-L1DKF10CU	RC2010	TAPE	0.1	1	Digikey
R63	ERJ-P14J103U	RC1210	TAPE	10K	1	Digikey
Capacitors						
C1-2, C15 C3-4, C11-14, C16, C18, C22, C24-29, C34-40, C43-C52, C56-C63, C65, C67, C70-71, C74-81	ECJ-4YF1H106Z	CC1210	Tape	10uF	3	Digikey
	ECJ-2FB1H104K	CC0805	Tape	0.1uF	52	Digikey
C5-6	ECJ-2VB2A471K	CC0805	Tape	470pF	2	Digikey
C17, C20	T495X476K035ATE300	CC7343	Loose	47uF, tant	2	Newark
C19	293D335X9050C2TE3	CC6032	Tape	3.3uF, tant	1	Mouser
C21, C23, C31-33, C41-42, C53-55	ECJ-2YB1H683K	CC0805	Tape	0.068uF	10	Digikey
C30	ECJ-2VC1H121J	CC0805	Tape	120pF	1	Digikey
C64	ECJ-2VB1H103K	CC0805	Tape	10nF	1	Digikey
C66	ECJ-2YB1E224K	CC0805	Tape	0.22uF	1	Digikey
C68-69	LMK325BJ107MM-T	CC1210	Tape	100uF	2	Digikey
C72-73	ECJ-2VC1H220J	CC0805	Tape	22pF	2	Digikey
Inductors						
L1	SPD127-473M	Surface mount	TAPE		1	Allied
L2	SPD127R-224M	Surface mount	TAPE		1	Allied
Chips						
U1, U3-6, U12-13, U15-17	LTC1050CS8	8 SOIC	TUBE		10	Digikey
U2, U10-11	LT1025	8 SOIC	TUBE		3	Nu Horizons
U7	MC33063ADG	8 SOIC	LOOSE		1	Mouser
U8-9	DRV104PWPRG4	14 HTSSOP	TAPE		2	AVNET
U14, U23	MCP4822	8 SOIC	TUBE		2	Digikey
U18	MC9S12XDP512CAG	144 LQFP	LOOSE		1	Newark
U19-U21	MAX232ACWE+	16 SOIC	TUBE		3	Digikey
U20	NC7SZ157	SC-70-6	TAPE		1	Digikey
U22	MAX809LEUR	SOT-23-3	TAPE		1	Digikey
U24-U30, U32-38	BTS428L2INCT	TO-252-2 (DPAK)	TAPE		14	Digikey
U31	LM358DR	8 SOIC	TAPE		1	Digikey
U39	INA138NA	SOT-23-5	TAPE		1	Digikey
U40	L2720	16-PowerDIP	TUBE		1	Digikey
Q1	2N7002LT1G	SOT23	TAPE		1	Digikey
D1-3	SML-211UTT86	0805	TAPE		3	Digikey
D4	1N5819HW-7-F	SOD-123	TAPE		1	Digikey
D5-D19	SS36	DO-214AB	TAPE		15	Digikey
Y1	HC49US4.000MABJ-UB	HC49/US	LOOSE		1	Digikey
F1	015401.5DRT	Surface mount	TAPE		1	Digikey
Connectors						
J1	2-5748003-0	Tyco Electronics 9 dsub	Loose		1	Digkey
J2	747299-8	15-pin Receptacle straight	Loose		1	Digkey
J3	5747872-8	15-pin Plug straight	Loose		1	Digkey
J5	B6B-PH-K-S	6-pin JST connector	Loose		1	Digkey
J4	M80-4101042	10-pin Harwin connector	Loose		1	Newark
J6-7	M80-5003442	34-pin Harwin connector	Loose		2	Newark

SAPM Electronic Support Drawings

The following drawings are provided in the remaining pages of this appendix.

- PWB controller board
- SAPM CCA mount

NOTES:

1. APPLICABLE STANDARDS AND SPECIFICATIONS:
   A. BSR/ASME Y14.100 D. ASME Y14.24 H. IPC-2221
   B. ASME Y14.35 E. IPC-6011 I. IPC-2222
   C. BSR/ASME Y14.34 G. IPC-6012 J. ANSI/IPC J-STD-001
2. REFERENCE SCHEMATIC DRAWING NUMBER 57602002 FOR ELECTRICAL CONNECTIVITY.
3. THIS BOARD IS TYPE 3C, PERFORMANCE CLASS 2 (DEDICATED SERVICE), PRODUCIBILITY LEVEL C, AS DEFINED IN ACCORDANCE WITH IPC-2220 AND IPC-6010 SERIES STANDARDS.
4. MATERIAL TO BE FR4 L21 METAL CLAD LAMINATES AND PREPREG IN ACCORDANCE WITH THE IPC-4100 SERIES DOCUMENTS. FABRICATE THE BOARDS USING THE FOIL WEIGHTS SHOWN BELOW AND BALANCED DISTRIBUTION OF DIELECTRIC MATERIALS, UNLESS OTHERWISE INDICATED. A MINIMUM OF 2 LAYERS OF GLASS FABRIC SHALL BE USED BETWEEN ALL CONDUCTIVE LAYERS AND THE MINIMUM DIELECTRIC THICKNESS SHALL MEET THE HIGH POT TESTING REQUIREMENTS TO WITH STAND 500 VOLTS FOR 30 SECONDS. SEE THE STACK-UP DIAGRAM FOR NOMINAL DIMENSIONS AND TOLERANCES.
5. OVERALL BOARD THICKNESS SHALL BE 0.062 ±10%.
6. MINIMUM CONDUCTOR WIDTH SHALL BE 0.008, AND MINIMUM SPACING BETWEEN CONDUCTORS SHALL BE 0.007.
7. MINIMUM HOLE WALL AND CONDUCTOR PLATING TO BE 0.001[25?m] THICK IN ACCORDANCE WITH IPC-6010 SERIES SPECIFICATIONS FOR CLASS 3 REQUIREMENTS FOR COPPER PLATING.
8. ALL HOLE SIZES APPLY AFTER PLATING.
9. UNLESS OTHERWISE SPECIFIED ALL PLATED HOLE SIZES SHALL HOLD A TOLERANCE OF ±0.003, ALL NON-PLATED HOLE SIZES SHALL HOLD A TOLERANCE OF ±0.005.
10. ANNULAR RING TO BE 0.002 MINIMUM. BREAK OUT OF DRILLED HOLES IS UNACCEPTABLE.
11. APPLY SOLDER MASK OVER BARE COPPER (SMOBC) PER IPC-SM-840 CLASS H. COLOR TO BE GREEN
12. PADS AND EXPOSED COPPER AREAS TO BE FINISH COATED USING TIN-LEAD HASL.
    A.) FINISH PLATING WITH THE EXCEPTION OF DIG TO CONFORM TO IPC-6010 SERIES CLASS 3
    SPECIFICATIONS.
    B.) WHEN IMMERSION SILVER FINISH IS SPECIFIED, iAg PLATING IS TO CONFORM TO IPC-4553
    REQUIREMENTS FOR THIN PLATING.
13. APPLY LEGEND USING NON-CONDUCTIVE PERMANENT ORGANIC INK. COLOR TO BE WHITE.
14. MAXIMUM WORKING VOLTAGE SHALL BE 48VDC.
15. ☒ BARE BOARDS SHALL BE 100% ELECTRICALLY TESTED USING THE SUPPLIED IPC-D-356 NET LIST.
    ☐ BARE BOARD TESTING REQUIREMENT WAIVED.
16. ☒ MANUFACTURERS LOGO, DATE CODE AND UL LOGO MAY BE ADDED TO THIS BOARD AT THE FABRICATORS DISCRETION AS EITHER LEGEND OR COPPER FEATURE.
    ☐ MANUFACTURERS LOGO, DATE CODE AND UL LOGO MAY NOT BE ADDED TO THIS BOARD.
17. ☒ NO THIEVING MAY BE ADDED TO THIS DESIGN, FABRICATOR SHALL USE ONLY AREAS OUTSIDE OF THE BOARD EDGE ROUTING TO BALANCE COPPER DENSITY.
    ☐ THIEVING MAY BE ADDED IN THE INDICATED AREA TO COMPENSATE FOR LOWER DENSITY AREAS IN THIS DESIGN. THIEVING MUST MEET THE FOLLOWING SPACING REQUIREMENTS:
    A.) NO EXPOSED THIEVING IN AREAS WITH REMOVED SOLDER MASK OR INTERNAL COPPER PLANE.
    B.) THIEVING SHALL MAINTAIN A MINIMUM CLEARANCE OF 0.100 FROM ALL COPPER BOARD FEATURES.
    C.) THIEVING SHALL MAINTAIN A MINIMUM CLEARANCE OF 0.250 FROM ALL BOARD EDGES, NON-PLATED MOUNTING HOLES, AND FIDUCIALS.
18. VIAS TO BE MASK RELIEVED TO DRILL SIZE.
19. RECEIVING INSPECTION TO CONFORM TO IPC-A-600 CLASS 2.
20. ☐ THIS BOARD SHALL BE SINGULATED PRIOR TO DELIVERY.
    ☒ THIS BOARD SHALL BE DELIVERED IN PANELIZED ARRAYS IN ACCORDANCE WITH DRAWING NUMBER 57602003.

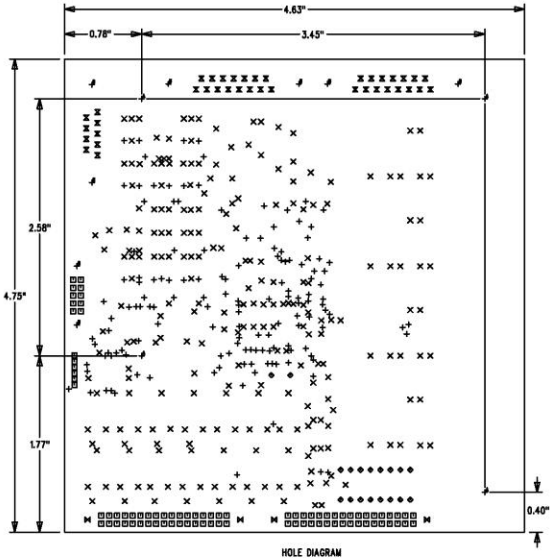

HOLE DIAGRAM

SIZE	QTY	SYM	PLTD
15	142	+	PLTD
20	241	X	PLTD
30	84	□	PLTD
35	18	◇	PLTD
45	39	⧖	PLTD
90	4	⋈	PLTD
125	4	A	PLTD
125	8	B	NPLTD

LAYER STACK UP

PRIMARY SIDE — LAYER 1
LAYER 2
LAYER 3
LAYER 4
LAYER 5
SECONDARY SIDE — LAYER 6

Title	CONTROLLER BOARD		
Project	MACS	Designer	JAMc
Part No	57602001	Rev.	NC
File Name	57602001NC.PCB	Date	08.01.02

LAYER DESCRIPTION	FILE NAME	FILE TYPE	BASE Cu WT Oz	MINIMUM TRACE/SPACE
PRIMARY SIDE	2001ART1.PHO	RS-274X	1	8/7
LAYER 2	2001ART2.PHO	RS-274X	1	10/10
LAYER 3	2001ART_3PHO	RS-274X	1	10/7
LAYER 4	2001ART4.PHO	RS-274X	1	10/7
LAYER 5	2001ART5.PHO	RS-274X	1	10/10
SECONDARY SIDE	2001ART6.PHO	RS-274X	1	8/7
PRIMARY SOLDER MASK	2001SMT1.PHO	RS-274X		
SECONDARY SOLDER MASK	2001SMB6.PHO	RS-274X		
PRIMARY SILK SCREEN	2001SST1.PHO	RS-274X		
SECONDARY SILK SCREEN	2001SSB6.PHO	RS-274X		
PRIMARY PASTE STENCIL	2001PST1.PHO	RS-274X		
SECONDARY PASTE STENCIL	2001PST6.PHO	RS-274X		
NC DRILL FILE	2001DRL1.DRL	EXCELLON		
TOOL TABLE	2001DRL1.TBL	ASCII TEXT		
ARRAY DRAWING	57602003NEW.PDF	ADOBE PDF		
READ ME FILE	README.TXT	ASCII TEXT		

REVISIONS

ZONE	REV	DESCRIPTION	DATE	APPROVED

PARTS LIST

Battelle
The Business of Innovation

PRINTED WIRING BOARD, CONTROLLER, MACS

D | 79986 | 57602001

SHEET 1 OF

DWG NO. 57602001 REV. 1

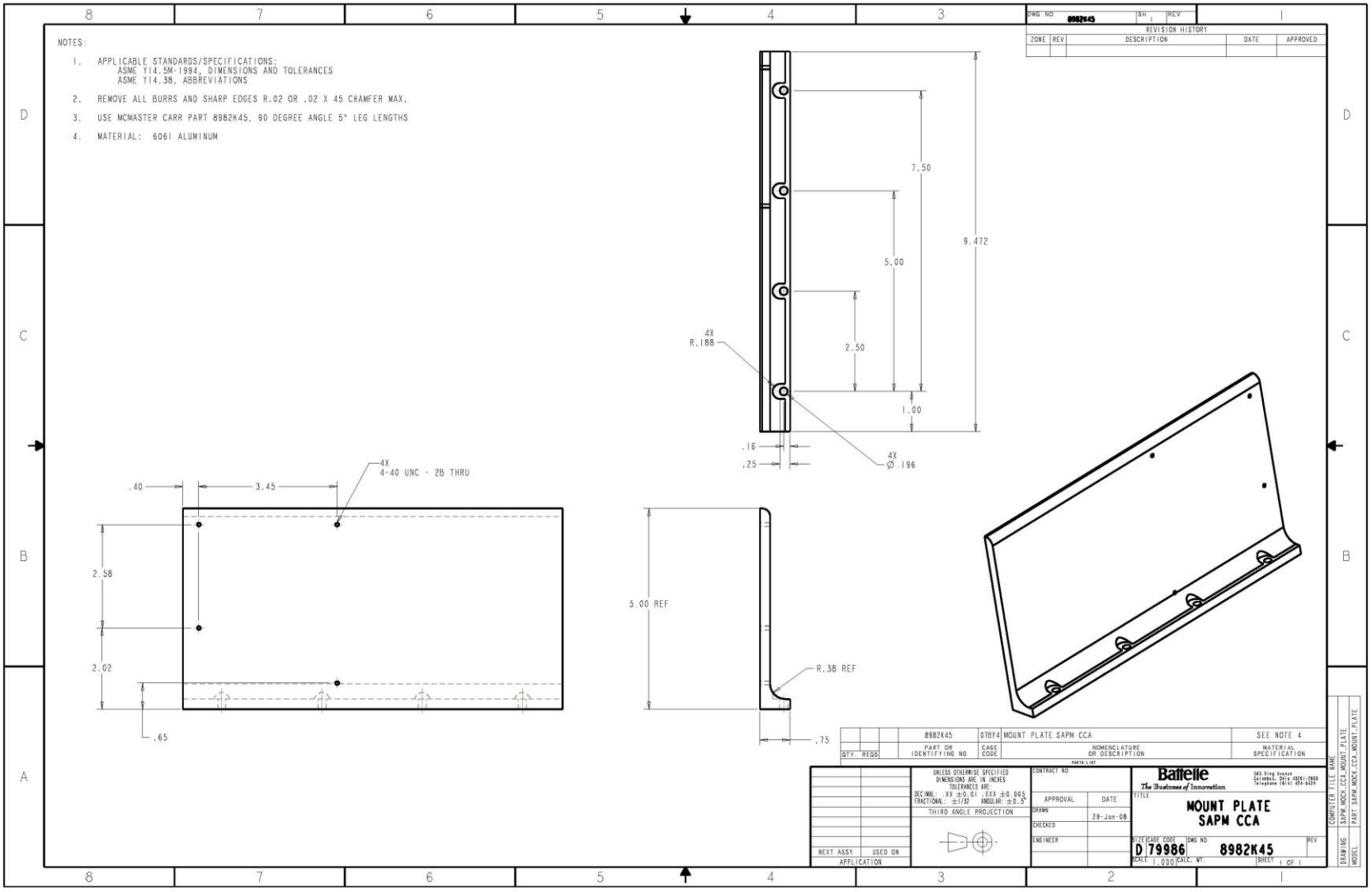
NOTES:
1. APPLICABLE STANDARDS/SPECIFICATIONS:
ASME Y14.5M-1994, DIMENSIONS AND TOLERANCES
ASME Y14.38, ABBREVIATIONS
2. REMOVE ALL BURRS AND SHARP EDGES R.02 OR .02 X 45 CHAMFER MAX.
3. USE MCMASTER CARR PART 8982K45, 90 DEGREE ANGLE 5" LEG LENGTHS
4. MATERIAL: 6061 ALUMINUM
REVISION HISTORY
ZONE REV DESCRIPTION DATE APPROVED
7.50
9.472
5.00
2.50
1.00
4X R.188
.16
.25
4X Ø.196
.40
3.45
4X 4-40 UNC - 2B THRU
2.58
2.02
.65
5.00 REF
R.38 REF
.75
8982K45 0TBY4 MOUNT PLATE SAPM CCA SEE NOTE 4
QTY. REQD PART OR IDENTIFYING NO CAGE CODE NOMENCLATURE OR DESCRIPTION MATERIAL SPECIFICATION
UNLESS OTHERWISE SPECIFIED DIMENSIONS ARE IN INCHES TOLERANCES ARE: DECIMAL: .XX ±0.01 .XXX ±0.005 FRACTIONAL: ±1/32 ANGULAR: ±0.5°
THIRD ANGLE PROJECTION
APPROVAL DATE
DRAWN 29-Jan-08
CHECKED
ENGINEER
Battelle The Business of Innovation
505 King Avenue Columbus, Ohio 43201-2693 Telephone (614) 424-5429
TITLE
MOUNT PLATE SAPM CCA
SIZE/CAGE CODE D 79986 DWG NO 8982K45 REV
SCALE 1.000 CALC. WT. SHEET 1 OF 1
NEXT ASSY USED ON APPLICATION
COMPUTER FILE NAME: SAPM_MOCK_CCA_MOUNT_PLATE
DRAWING PART: SAPM_MOCK_CCA_MOUNT_PLATE
MODEL

Appendix A3.3

Serial Control Interface Document

Serial Communications Interface Overview

The CCA serial interface is setup to allow the central computer to control the SAPM module through a serial port.

Physical Connections

The Central Computer will have communications access to the SAPM CCA through a standard DB-9 connector.

Communications Format

All communications will be done using RS232 with a plain text ASCII interface, and may be accessed through any terminal program, such as HyperTerminal.

Baud Rate: 9600
Data Bits: 8
Parity: None
Stop Bits: 1
Flow Control: None

SAPM CCA Command Set

Query and Command Syntax

The command structure will be as follows:
<command> <parameter><NULL>

The structure required for a query is:
<query> ?<NULL>

Response Syntax

The query and command response will done with through an acknowledge or error command response. This will be done with the ASCII characters ‘ACK’ or ‘NAK,’ respectively indicating a successful command or an error within XXmS of receiving query or command.

Query and Command Set

System Status - SSTAT

The system status query returns the following parameters of the system with a <CR> after each: temperatures, pressure, valve position, pump status, and if there are any faults in the system.

Query: SSTAT ?<NULL>
Query Response:
ACK

TEMP1 <value>
PRES1 <value>
PRES2 <value>
PRES3 <value>
PRES4 <value>
VALV1 <open/close>
……..

Sorbent Heater Temperature 3D configuration – TEMP1

The TEMP1 command sets the maximum temperature of the 3D sorbent heater. The query returns the temperature setting and the current temperature of the heater. All temperature values will be in degrees Celsius (°C).

Query: TEMP1 ?<NULL>
Query Response:
ACK
TEMP1 <value>
.

Command: TEMP1 <parameter> <NULL>
Command Response: ACK<CR>

Manifold Heater Temperature – TEMP2

The TEMP2 command can be used to set, and check the temperature of the manifold heater as well as turn it on.

Query: TEMP2 ?<CR>
Query Response:
ACK
TEMP2 <value>
.

Command: TEMP2 <parameter> <CR>
Command Response: ACK<CR>

Cell Heater Temperature – TEMP3

The TEMP3 command sets and checks the temperature of the cell. Once the desired temperature is set the cell can then be turned on.

Query: TEMP3 ?<CR>
Query Response:
ACK
TEMP3 <value>

TEMP4 <value>
TEMP5 <value>
.

Command: TEMP3 <parameter> <CR>
Command Response: ACK<CR>

Pressure data – PRES

Each of the pressure commands returns the current pressure reading of the respective MicroPirani. PRES returns all of the gauges pressures at once. Pressure values are returned in scientific notation, and the units are Torr.

Query: PRES ?<CR>
Query Response: ACK<CR>
PRES1 <value>
PRES2 <value>
PRES3 <value>
PRES4 <value>

Micropiranis – MKS1, MKS2, MKS3, MKS4

Direct communication to the four Micropiranis attached to the system is possible using this command.

Query: MKS1 PR1?<CR>
Query Response: ACK <CR> <response from Pirani>

Command: MKS1 ATM!7.60E+2 <CR>
Command Response: ACK<CR> <response from Pirani>

Temperature data- TEMP

TEMP returns all of the system heaters current temperatures. All temperature values will be in degrees Celsius (°C).

Query: TEMP ?<CR>
Query Response: ACK<CR>
TEMP1 <valve>
TEMP2 <value>
TEMP3 <value>

Control Valve – CVV2, CVP2

The CVV, CVP commands allow the user to slowly leak air into the SAPM system and the cell for a specified amount of time. The CVV command sets the desired voltage level for bleed in. The CVP command toggles the valve on and off.

Pulse Control Valve – PULSE

The PULSE commands opens and closes the control valve for the length of time specified in the parameter. Note: The parameter increments the time open by 10µsecs.

Command: PULSE <parameter> <CR>
Command Response: ACK<CR>

Valves – VALV1, VALV2, VALV3, VALV4, VALV5, VALV6

See command set table.

Pumps- tPUMP, dPUMP

tPUMP returns the status of the turbo pump: ON, OFF, STDBY, ERR. dPUMP returns the status of the diaphragm pump: ON, OFF, ERR.

Command Set Summary

Command	Parameter	Description
SSTAT	?	Returns the status of the system.
PRES	?	Returns the pressure at all points in the system.
MKS1	PR1?/ATM!7.60E+2/TEM	Passes commands directly to the micropirani
MKS2		
MKS3		
MKS4		
TEMP	?	Returns all the systems heaters current temperatures.
TEMP1	0-250/ON/OFF/?	Returns temperature of all system heaters.
TEMP2	0-30/ON/OFF/?	Returns the temperature of the Manifold heater.
TEMP3	25-60/ON/OFF/?	Returns the temperature of the Cell heater.
CVV2	0-24V	Presets the voltage to be applied to the control valve.
CVP2	ON/OFF	Turns on the power to the control valve.

Command	Parameter	Description
PULSE	0-1000	Turns on control valve for a specific length of time.
VALV1	ON/OFF	Returns status of Inlet/SMM valve, OPEN (on) /CLOSE (close).
VALV2	ON/OFF	Returns status of SMM/Diaphragm valve, OPEN (on) /CLOSE (off).
VALV3	ON/OFF	Returns the status of Turbo/Diaphragm valve, OPEN (on) /CLOSE (off).
VALV4	ON/OFF	Returns the status of the Cell/Turbo valve, OPEN (on) /CLOSE (off).
VALV5	ON/OFF	Returns the status of the SMM/Turbo valve, OPEN (on) /CLOSE (off).
VALV6	ON/OFF	Returns the status of the SMM/Cell valve, OPEN (on) /CLOSE (off).
tPUMP	ON/OFF	Returns the status of the turbo pump, ON/OFF/STDBY/ERR.
dPUMP	ON/OFF	Returns the status of the diaphragm pump, ON/OFF/ERR.

Appendix A3.4

CCA Specification Document

SCOPE

Identification

This specification provides performance requirements for the SAPM CCA, a module in the Mission Adaptable Chemical Sensor (MACS) system.

System Overview

The Sample Acquisition and Processing Module (SAPM), is responsible for sample collection and transfer to THz Spectrometer for spectral interrogation. The SAPM will collect air samples and separate targeted analytes over a collection cycle. To separate the analyte from atmospheric constituents, the analyte is first absorbed onto sorbent. The SAPM then evacuates atmospheric gases through a two-stage pump system. The sorbent is then heated to release the analyte, which is then transferred through the SAPM into the THz Spectrometer. The SAPM module is also responsible for heating the THz cell.

CCA Requirements

The SAPM system consists of mechanical and electrical components that each have different power and communications aspects, which will be addressed by the CCA. This section is a brief summary of the major components that shall be controlled by the CCA, as well as a description of what the CCA shall accomplish with each.

Sensors

Micropirani 905

The Micropirani 905 sensor kit will be replacing the Micropirani 925C sensor in the deliverable system. It has the benefit of being more compact than its predecessor, reducing space, gas volume, and leakage. Its typical measuring accuracy is ±5% of the reading at 10^{-3} to 100 Torr. The 905 will communicate with the CCA through a RS232 connection in ASCII format. The 905 supports 2400, 4800, 9600, and 19200 baud rates. The RS232 data format is 8 data bits, no parity, and one stop bit. Post processing on the data will be done at the CCA level to account for the temperature drift of the pressure reading. Further tests of the gauge's sensitivity to temperature will be performed to generate an accurate pressure vs. temperature curve for the sensor. In addition to communication, the CCA will also control power to the 905 through screw terminals, located on the evaluation board of the sensor. The 905 has an operating power range of 9 to 30V @ 50 to 18mA .

722A Baratron

The MKS type 722A Baratron will be added onto the THz for a consistently reliable pressure measurement. The CCA of the deliverable system will provide power to the 722A baratron, 24V @ 10mA. The 722A signal output will be from 0 – 5 VDC and converted to digital signalby the

CCA. The CCA will then output the corresponding pressure in Torrs of the received 722A output signal.

TSI Flowmeter

The CCA of the deliverable system will support the TSI flowmeter though it is not expected to be incorporated. The flowmeter requires 7.5 VDC ± 20%, with 300mA maximum. It can be powered through its 8 pin mini-DIN connector or an external power jack. Possible measurement options of the flowmeter that will be utilized are flowrate, temperature (flowrate must be >1 Std L/min), pressure, and volume. The flowmeter will use RS232 for serial communication with a set baud rate of 38400, 8 data bits, no parity, and one stop bit. The command set for the flowmeter is set up to allow the programmer to choose the data format for each command: ASCII, binary, and ASCII followed by CR and LF.

Thermocouples

K-type thermocouples will be located in order to monitor each of the heaters in the system and the four Micropirani 905s. The K-type thermocouples provide a large temperature range of: -200°C to 1200°C. Signal conditioning will be required prior to the analog to digital converter that will be used to convert the generated voltage to digital. Additionally, cold junction compensation will be performed in the CCA.

Pumps

Diaphragm Pump (Pfeiffer MVP006-4)

The CCA will only need to control the power to the diaphragm pump. The diaphragm pump requires 24V ± 10% @0.9A. When operating alone the diaphragm pump can be switched on and off at any time. However, when operating in conjunction with the turbo pump, the diaphragm pump should not be turned off while the turbo pump is running. This will need to be enforced through software.

Turbo Pump (Pfeiffer TPD 011)

The CCA will control power to the turbo pump. The turbo pump requires 24V ± 5% @0.9A. The CCA will also control the optional Standby feature on the turbo pump. The standby feature adjusts the rotation of the pump to 66% of its nominal rotation speed, allowing the system to save power. Safety measures will be implemented in software for safe start up and shut down of the pump.

Valve and Heaters

Control Valve (Pfeiffer RME 005)

The control valve opens and closes as a function of voltage, allowing the operator to bleed air into the system. The CCA will be required to manipulate the system voltage to open the valve to the desired degree. The control valve comes with a gas flow vs. control voltage curve. This curve will be implemented to allow the user to have range of gas flow values to select from, which will then be converted by the CCA to the corresponding voltage. The control valves operating in the following voltage range: 7 to 24VDC @ 0.32 to 0.12A.

Manifold Valves (CKD GFVB55 & CKD GFVB25)

These valves require 24VDC @0.34, and 0.17A. The CCA will allow the user to select either manual or automatic control of the valves.

Heaters

The CCA will be used to control various heaters throughout the system. These heaters will be required to heat the manifold, critical tubing, cell, and the sorbent. The manifold, tubing, and cell heaters will be created to design by MINCO. Instead of controlling all the heaters using proportional or relay controllers, most of the heaters will receive a *pulse-width modulated voltage signal;* to decrease the waste of power to heat that would be dissipated with proportional control. The system will be designed to support both a 3D heater (sorbent tube heater) and a 2D heater. The 3D heater will be controlled through a *pulse-width modulated voltage signal*. The 2D heater however, will be controlled through a variable voltage source that will allow for greater control of its maximum temperature.

Stepper Motor

R208 Microstepping Driver

The stepper motor on the THz cell will be controlled by the CCA through the use of RMS Technologies' R208 Microstepping Driver. The CCA will provide 24V @ 2A, as well as 5V @ 10mA for the R208. The CCA will provide control signals to the microstepping driver, this includes: an enable/disable signal, a direction of rotation signal, and a clock signal. The default settings of the R208 will be: disable, counterclockwise rotation, and a digital output for the clock signal.

CCA

General

The CCA will be provided 24VDC ±**5**% @12A, and most components will operate at 24VDC to reduce power losses due to conversion. Components needing voltages other than 24VDC are the proportional control valve which requires 0–24VDC, the 2D heater which requires 0-24V, and the TSI flow meter which requires 7.5VDC. Digital I/Os will be used to control the manifold valves, inline valves, and pumps. Analog to digital converter inputs will be used to monitor the temperature, voltage, pressure (722A), and current at critical points within the system. Communications with the Central Computer will be through a RS232 serial connection and will use plain text ASCII communications. RS232 connections will also be used to conduct all communications internally to the SAPM, specifically to program and receive data from the Micropirani 905 transducer, and the TSI flowmeter, for communication with main CC, and debugging. In addition, a trigger in and trigger out will be included into the SAPM CCA to allow for easy future integration of timing elements. The flow diagram below shows the basic outline for the needed input and outputs capabilities of the CCA.

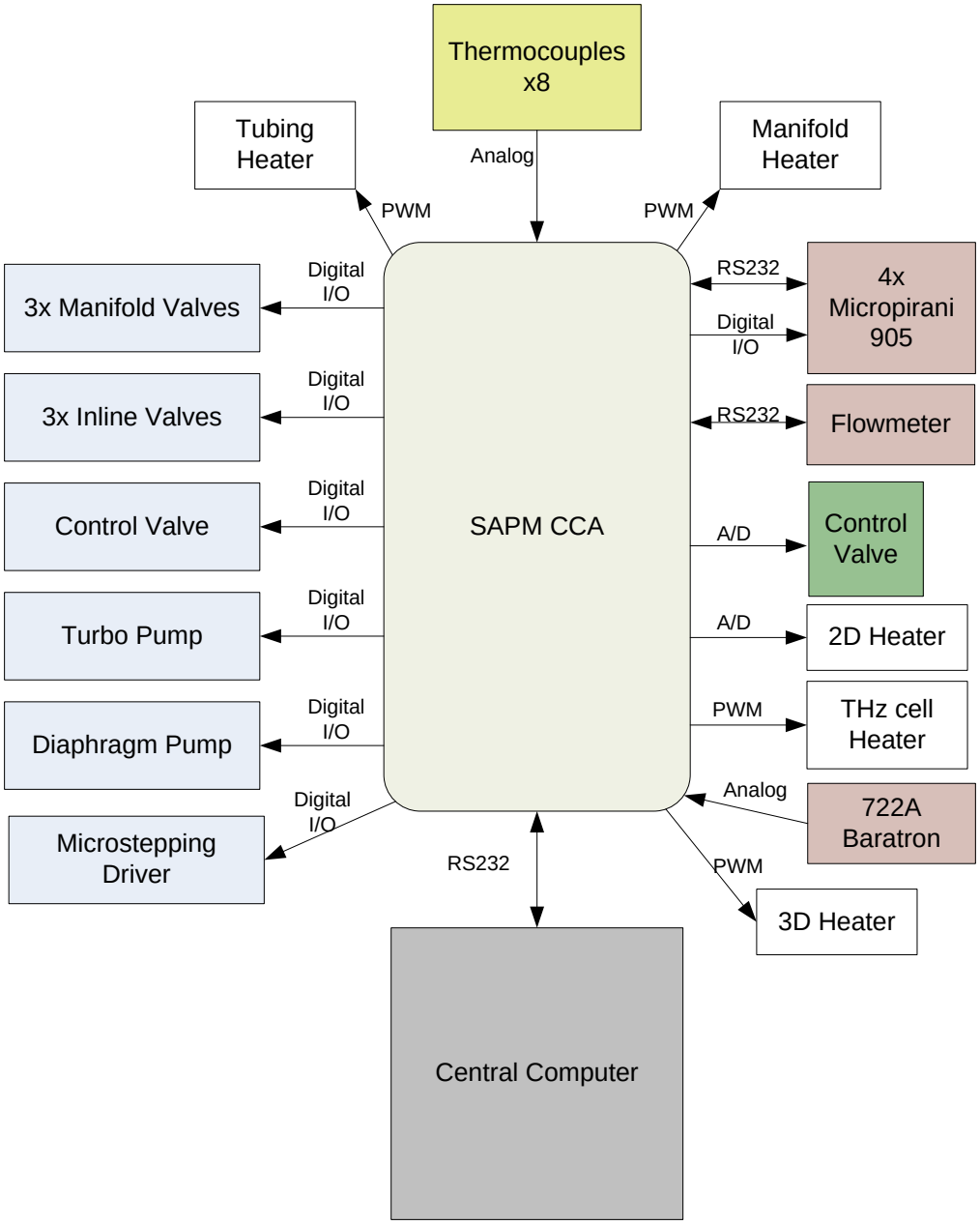

Figure 3-1: CCA Block Diagram

CCA Microcontroller

The SAPM CCA will use a Freescale Semiconductor MC9S12XDP512, 16-bit microcontroller.

General Characteristics

16-Bit CPU12X
Supply voltage 3.15V to 5.5V
512K Byte Flash
20K Byte RAM
4K EEPROM

XGATE peripheral co-processor
12MHz Bus frequency
Temperature -40°C to 125°C

Peripherals

6 SCI modules
3 SPI modules
8 channel x 8-bit or 4 channel x 16-bit PWM
24 channel ATD
119 I/O ports
4 channel Periodic Interrupt Timer (PIT)
Eight 16-bit channels Enhanced Capture Timer (ECT)

CCA Connections

Connection to the Central Computer

CCA Power Connector

Connector Name	Designation	Manufacturer	Part Number 90°	Number of Positions
SAPM Power	J3	Amphenol	FCE17-A15PE-240	15
PIN	**SIGNAL**	**DESCRIPTION**		
J3-1	24V	Power supplied from CC		
J3-2	24V	Power supplied from CC		
J3-3	24V	Power supplied from CC		
J3-4	24V	Power supplied from CC		
J3-5	24V	Power supplied from CC		
J3-6	24V	Power supplied from CC		
J3-7	24V	Power supplied from CC		
J3-8	24V	Power supplied from CC		
J3-9	GND	Ground supplied from CC		
J3-10	GND	Ground supplied from CC		
J3-11	GND	Ground supplied from CC		
J3-12	GND	Ground supplied from CC		
J3-13	GND	Ground supplied from CC		
J3-14	GND	Ground supplied from CC		
J3-15	GND	Ground supplied from CC		

CCA Control Connector

Connector Name	Designation	Manufacturer	Part Number Straight	Number of Positions
CCA Control	J4	HARWIN	M80-4101042	10
PIN	**SIGNAL**	**DESCRIPTION**		
J4-1	TRIGGER OUT	CCA Trigger out to CC		
J4-2	TRIGGER IN	CCA Trigger in to CC		
J4-3	CC_TXD	CCA RS232 transmit pin		
J4-4	CC_RXD	CCA RS232 receive pin		
J4-5	COM	CCA RS232 signal ground pin		
J4-6	NC			
J4-7	NC			
J4-8	NC			
J4-9	NC			
J4-10	NC			

Connection from CCA to SAPM System Components

Debug Connector

Table 4.2.1-2: Debug Connector

Connector Name	Designation	Manufacturer	Part Number Straight	Number of Positions
Debug Connector	J5	JST	B6B-PH-K-S	6
PIN	**SIGNAL**	**DESCRIPTION**		
J5-1	DEBUG_SEL	CCA - Microprocessor Debug Mode Select pin		
J5-2	DEBUG_TXD	CCA - Microprocessor Debug RS232 TXD pin		
J5-3	DEBUG_RXD	CCA - Microprocessor Debug RS232 RXD pin		
J5-4	DEBUG_COM	CCA - Microprocessor Debug RS232 digital ground pin		
J5-5	BKGD	CCA - Microprocessor Background Debug pin		
J5-6	RESET	CCA - Microprocessor Reset pin		

Pumps Power Connector

Connector Name	Designation	Manufacturer	Part Number Straight	Number of Positions
Pump Power Connector	J6	HARWIN	M80-5003442	34
PIN	**SIGNAL**	**DESCRIPTION**		
J6-1	A1	CCA – Extra Analog output		
J6-2	A2	CCA – Extra Analog output		
J6-3	NC	Not Connected		
J6-4	IOC1	CCA – Extra I/O		
J6-5	IOC2	CCA – Extra I/O		
J6-6	IOC3	CCA – Extra I/O		
J6-7	NC	Not Connected		
J6-8	NC	Not Connected		
J6-9	NC	Not Connected		
J6-10	NC	Not Connected		
J6-11	NC	Not Connected		
J6-12	NC	Not Connected		
J6-13	COM_TXD	CCA – Extra RS232 transmit		
J6-14	COM_RXD	CCA – Extra RS232 receive		
J6-15	COM_GND	CCA – Extra RS232 GND		
J6-16	NC	Not Connected		
J6-17	NC	Not Connected CCA – Extra Analog output		
J6-18	NC	Not Connected		
J6-19	V1_PWR	CCA - 24V to V1 valve		
J6-20	V1_GND	CCA - GND to V1 valve		
J6-21	P1_PWR	CCA – 24V to Diaphragm pump		
J6-22	P1_GND	CCA – GND to Diaphragm pump		
J6-23	V2_PWR	CCA - 24V to V2 valve		
J6-24	V2_GND	CCA - GND to V2 valve		
J6-25	P2_STDBY	CCA – 24V to Turbo pump standby pin		
J6-26	NC	Not Connected		
J6-27	H1_PWR	CCA - 24V tube heater		
J6-28	H1_GND	CCA - GND to tube heater		
J6-29	P2_PWR	CCA - 24V to Turbo pump		
J6-30	P2_GND	CCA – GND to Turbo pump		
J6-31	NC	Not Connected		
J6-32	NC	Not Connected		
J6-33	NC	Not Connected		
J6-34	NC	Not Connected		

Manifold Power Connector

Connector Name	Designation	Manufacturer	Part Number Straight	Number of Positions
Manifold Power Connector	J7	HARWIN	M80-5003442	34
PIN	**SIGNAL**	**DESCRIPTION**		
J7-1	M_E/D	CCA – Microstep motor enable/disable		
J7-2	M_DIR	CCA – Microstep motor direction choice		
J7-3	M_CLK	CCA – Clock to Microstep motor		
J7-4	NC	Not Connected		
J7-5	NC	Not Connected		
J7-6	R208_GND	CCA GND to Microstepper		
J7-7	R208_5V	CCA 5V to Microstepper		
J7-8	R208_24V	CCA 24V to Microstepper		
J7-9	NC	Not Connected		
J7-10	NC	Not Connected		
J7-11	B_H	Baratron analog input high		
J7-12	B_L	Baratron analog input low		
J7-13	NC	Not Connected		
J7-14	NC	Not Connected		
J7-15	CV1_PWR	CCA Variable voltage to Control Valve 1		
J7-16	CV1_GND	CCA GND to Control Valve 1		
J7-17	CV2_PWR	CCA Variable voltage to Control Valve 2		
J7-18	CV2_GND	CCA GND to Control Valve 2		
J7-19	2D_PWR	CCA – variable voltage to 2D heater		
J7-20	2D_GND	CCA – GND to 2D heater		
J7-21	B_PWR	CCA 24V to Baratron		
J7-22	B_GND	CCA GND to Baratron		
J7-23	V6_PWR	CCA 24V to V6		
J7-24	V6_GND	CCA GND to V6		
J7-25	H2_PWR	CCA 24V to Manifold heater		
J7-26	H2_GND	CCA GND to Manifold heater		
J7-27	V5_PWR	CCA 24V to V5		
J7-28	V5_GND	CCA GND to V5		
J7-29	V4_PWR	CCA 24V to V4		
J7-30	V4_GND	CCA GND to V4		
J7-31	V3_PWR	CCA 24V to V3		
J7-32	V3_GND	CCA GND to V3		
J7-33	H4_PWR	CCA 24V to 3D heater		
J7-34	H4_GND	CCA GND to 3D heater		

Thermocouple Connectors

Table 4.2.2-1: Therm1 Connector

Connector Name	Designation	Manufacturer	Part Number 90°	Number of Positions
Therm1	J1	Harting	09-64-122-7210	9
PIN	**SIGNAL**	**DESCRIPTION**		
J1-1	TC8-Y	Thermocouple 8 - Chromel		
J1-2	TC8-R	Thermocouple 8 - Alumel		
J1-3	TC9-Y	Thermocouple 9 - Chromel		
J1-4	TC9-R	Thermocouple 9 - Alumel		
J1-5	TC10-Y	Thermocouple 10 - Chromel		
J1-6	TC10-R	Thermocouple 10 - Alumel		
J1-7	H3_PWR	Cell Heater Power		
J1-8	H3_GND	Cell Heater Ground		
J1-9	NC	Not Connected		

Table 4.2.3-2: Therm1 Connector

Connector Name	Designation	Manufacturer	Part Number Straight	Number of Positions
Therm2	J2	Amphenol	FCE17A15PA-410	15
PIN	**SIGNAL**	**DESCRIPTION**		
J2-1	TC1-Y	Thermocouple 1 – Chromel		
J2-2	TC1-R	Thermocouple 1 - Alumel		
J2-3	TC2-Y	Thermocouple 2 – Chromel		
J2-4	TC2-R	Thermocouple 2 - Alumel		
J2-5	TC3-Y	Thermocouple 3 - Chromel		
J2-6	TC3-R	Thermocouple 3 - Alumel		
J2-7	TC4-Y	Thermocouple 4 – Chromel		
J2-8	TC4-R	Thermocouple 4 - Alumel		
J2-9	TC5-Y	Thermocouple 5 – Chromel		
J2-10	TC5-R	Thermocouple 5 – Alumel		
J2-11	TC6-Y	Thermocouple 6 – Chromel		
J2-12	TC6-R	Thermocouple 6 – Alumel		
J2-13	TC7-Y	Thermocouple 7 – Chromel		
J2-14	TC7-R	Thermocouple – Alumel		
J2-15	NC	Not Connected		

Power

The SAPM system peak and continuous power consumptions are shown in
Table 5-1 The CCA will use the supplied 24VDC ±5% @ 12A, to meet the peak and continuous power demands of the system. The peak power demonstrates the effect of transient current on the system through the opening and closing of valves.

Table 5-1: SAPM Power Consumption

Component	Quantity	Voltage		Current		Total Component Power	
		Max	Min	Peak	Cont.	Peak	Cont.
RME 005	1	24	1	0.32	0.12	7.68	2.88
GFVB55	3	24		0.52	0.34	37.44	24.48
GFVB25	3	24		1.26	0.17	90.72	12.24
Pfeiffer MVP 006-4	1	24		1.76	0.74	42.24	17.76
Pfeiffer TPD011	1	24		1.8	0.74	43.2	17.76
MINCO Heater, sorbent	1	24		3	2.11	72	50.64
Flowmeter	1	9	6	0.3		2.7	1.8
905 Micropirani	4	24	10	0.018		1.728	1.728
722A Baratron	1	24	13	0.01		0.24	0.24
Heater Rope, Cell	1	24		1.5	1.15	36	27.6
Minco heater, manifold	1	24		7.5	0.18	180	4.32
CCA Board	1	24		1.14		27.36	27.36
R208 Microstepping Driver	1	24		2		48	48
				Total System Power		589.308	236.808

Bake-out Mode

The CCA will have a Bake-Out Mode, which will purge the SAPM module of sticky or low volatility analytes. This mode will bring the SAPM module down to a vacuum of XX Torr while heating it at 40-50°C for XX hours.

Environmental

TBD

Appendix A3.5

SMM Mechanical Drawings

The following drawings are provided in the remaining pages of this appendix.

- 3D sorbent tube
- 2D sorbent disk housing (4 pages)

NOTES:

1. APPLICABLE STANDARDS/SPECIFICATIONS:
   ASME Y14.5M-1994, DIMENSIONS AND TOLERANCES
   ASME Y14.38, ABBREVIATIONS
2. REMOVE ALL BURRS AND SHARP EDGES R.02 OR .02 X 45 CHAMFER MAX.
3. UNLESS OTHERWISE SPECIFIED SURFACE ROUGHNESS 63
4. FUSION WELD - DRILL FLANGE FOR TIGHT RADIAL CLEARANCE WTH TUBE O.D.
   POSITION TUBE END FLUSH WITH FLANGE FACE
   JOIN WITH VERY LITTLE FILLER AND HEAT

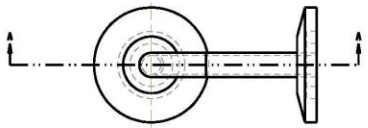

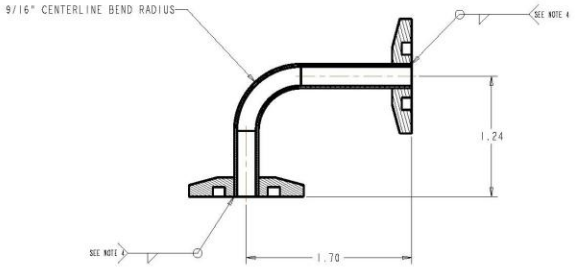

SECTION A-A

REVISION HISTORY

ZONE	REV	DESCRIPTION	DATE	APPROVED

PARTS LIST

QTY REQD	-10	FIND NO	PART OR IDENTIFYING NO	CAGE CODE	NOMENCLATURE OR DESCRIPTION	MATERIAL SPECIFICATION
2	2		112000	0AL22	BLANK FLANGE, KF16	304 SS
1	1		89885K124	07BY4	TUBE, 1/4 X .028 WALL	304 SS

UNLESS OTHERWISE SPECIFIED DIMENSIONS ARE IN INCHES
TOLERANCES ARE:
DECIMAL: XX ±0.01 .XXX ±0.005
FRACTIONAL: ±1/32 ANGULAR: ±0.5°
THIRD ANGLE PROJECTION

NEXT ASSY | USED ON
APPLICATION

CONTRACT NO

APPROVAL	DATE
DRAWN	26-Dec-07
CHECKED	
ENGINEER	

Battelle
The Business of Innovation
505 King Avenue
Columbus, Ohio 43201-2693
Telephone (614) 424-6424

TITLE
TUBE, SORBENT

SIZE | CAGE CODE | DWG NO | REV
D | 79986 |

SCALE 2.000 DO NOT SCALE DRAWING | SHEET 1 OF 1

COMPUTER FILE NAME:
DRAWING | SAPM TUBE 24.SORB.TUBE
MODEL | ASSEM SAPM TUBE 24.SORB.TUBE

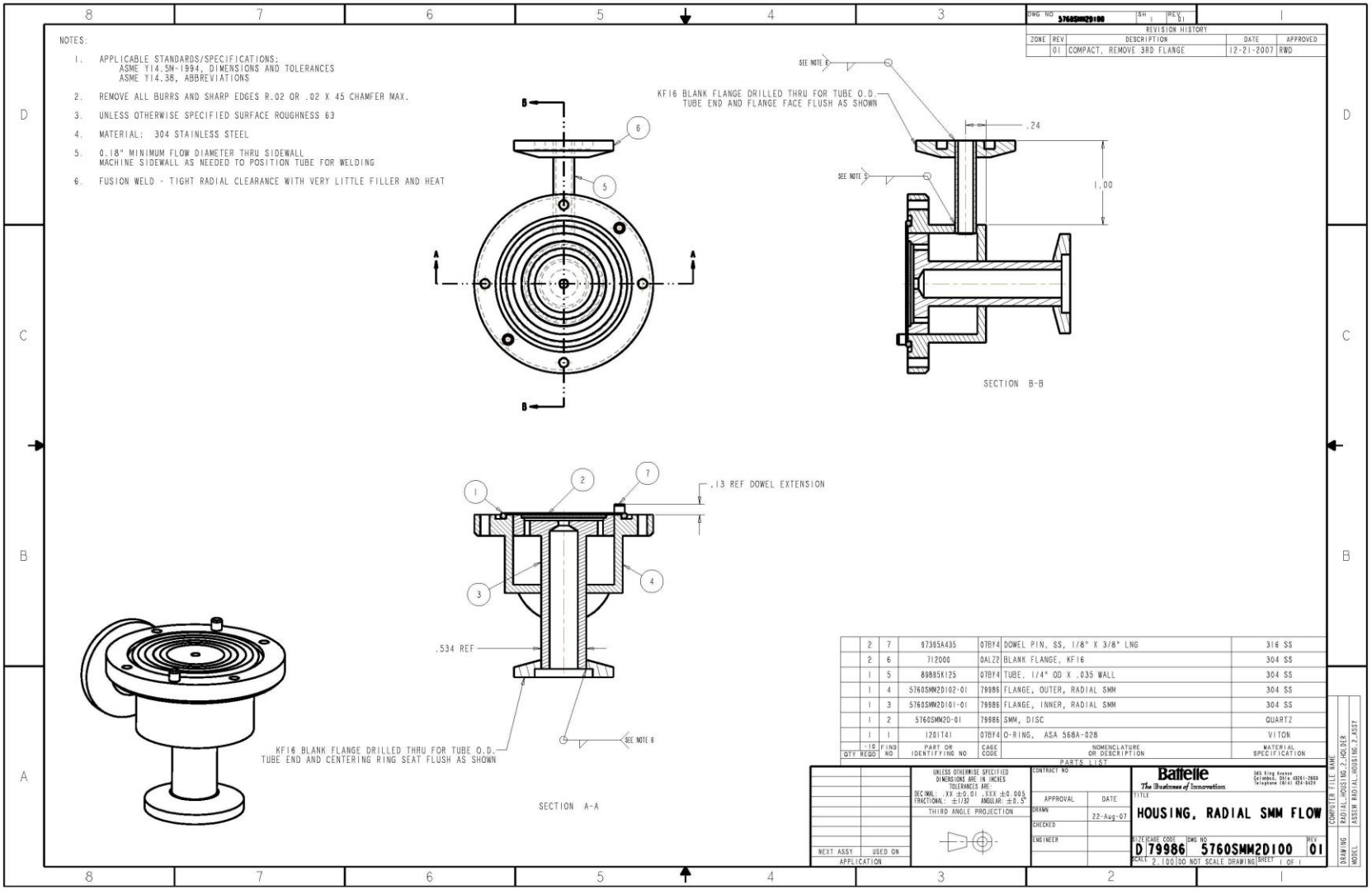
DWG NO 5760SMM2D100 SH 1 REV 01
REVISION HISTORY
ZONE REV DESCRIPTION DATE APPROVED
01 COMPACT, REMOVE 3RD FLANGE 12-21-2007 RWD
NOTES:
1. APPLICABLE STANDARDS/SPECIFICATIONS: ASME Y14.5M-1994, DIMENSIONS AND TOLERANCES ASME Y14.38, ABBREVIATIONS
2. REMOVE ALL BURRS AND SHARP EDGES R.02 OR .02 X 45 CHAMFER MAX.
3. UNLESS OTHERWISE SPECIFIED SURFACE ROUGHNESS 63
4. MATERIAL: 304 STAINLESS STEEL
5. 0.18" MINIMUM FLOW DIAMETER THRU SIDEWALL MACHINE SIDEWALL AS NEEDED TO POSITION TUBE FOR WELDING
6. FUSION WELD - TIGHT RADIAL CLEARANCE WITH VERY LITTLE FILLER AND HEAT
KF16 BLANK FLANGE DRILLED THRU FOR TUBE O.D. TUBE END AND FLANGE FACE FLUSH AS SHOWN
SEE NOTE 5
.24
1.00
SECTION B-B
.13 REF DOWEL EXTENSION
.534 REF
KF16 BLANK FLANGE DRILLED THRU FOR TUBE O.D. TUBE END AND CENTERING RING SEAT FLUSH AS SHOWN
SEE NOTE 6
SECTION A-A
PARTS LIST
QTY REQD ITEM NO PART OR IDENTIFYING NO CAGE CODE NOMENCLATURE OR DESCRIPTION MATERIAL SPECIFICATION
2 7 97395A435 07BY4 DOWEL PIN, SS, 1/8" X 3/8" LNG 316 SS
2 6 712000 0ALZ2 BLANK FLANGE, KF16 304 SS
1 5 89895K125 07BY4 TUBE, 1/4" OD X .035 WALL 304 SS
1 4 5760SMM2D102-01 79986 FLANGE, OUTER, RADIAL SMM 304 SS
1 3 5760SMM2D101-01 79986 FLANGE, INNER, RADIAL SMM 304 SS
1 2 5760SMM2D-01 79986 SMM, DISC QUARTZ
1 1 12011T41 07BY4 O-RING, ASA 568A-028 VITON
UNLESS OTHERWISE SPECIFIED DIMENSIONS ARE IN INCHES TOLERANCES ARE: DECIMAL .XX ±0.01 .XXX ±0.005 FRACTIONAL ±1/32 ANGULAR ±0.5°
THIRD ANGLE PROJECTION
NEXT ASSY USED ON APPLICATION
CONTRACT NO
APPROVAL DATE
DRAWN 22-Aug-07
CHECKED
ENGINEER
Battelle The Business of Innovations
505 King Avenue Columbus, Ohio 43201-2693 Telephone (614) 424-6424
TITLE
HOUSING, RADIAL SMM FLOW
SIZE D CAGE CODE 79986 DWG NO 5760SMM2D100 REV 01
SCALE 2.100 DO NOT SCALE DRAWING SHEET 1 OF 1
COMPUTER FILE NAME
DRAWING RADIAL_HOUSING_2_HOUSER
MODEL ASSEM RADIAL_HOUSING_2_ASSY

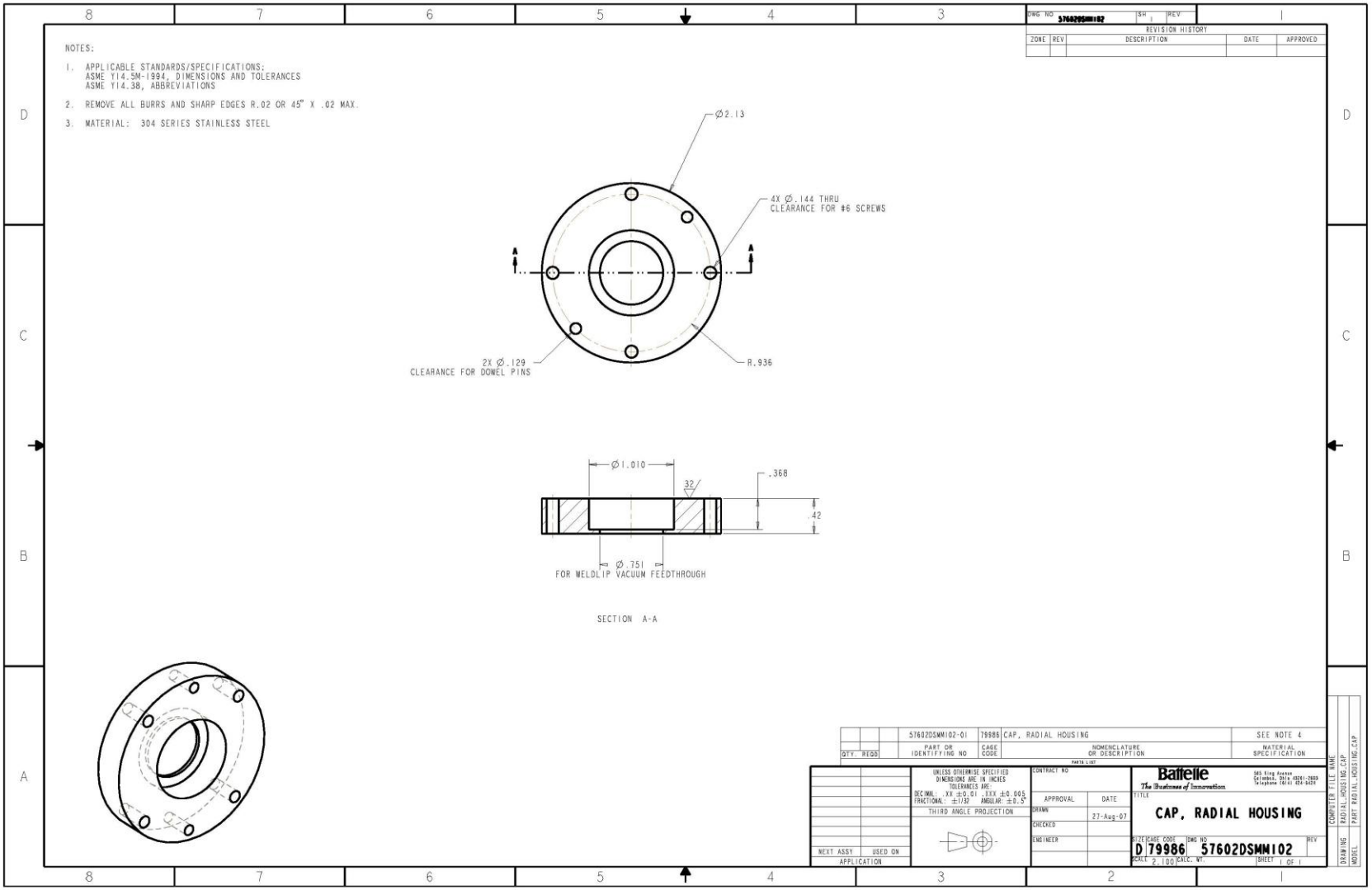
DWG NO 57602DSMM102 SH 1 REV
REVISION HISTORY
ZONE REV DESCRIPTION DATE APPROVED
NOTES:
1. APPLICABLE STANDARDS/SPECIFICATIONS:
ASME Y14.5M-1994, DIMENSIONS AND TOLERANCES
ASME Y14.38, ABBREVIATIONS
2. REMOVE ALL BURRS AND SHARP EDGES R.02 OR 45° X .02 MAX.
3. MATERIAL: 304 SERIES STAINLESS STEEL
Ø2.13
4X Ø.144 THRU
CLEARANCE FOR #6 SCREWS
2X Ø.129
CLEARANCE FOR DOWEL PINS
R.936
Ø1.010
32
.368
.42
Ø.751
FOR WELDLIP VACUUM FEEDTHROUGH
SECTION A-A
57602DSMM102-01 79986 CAP, RADIAL HOUSING SEE NOTE 4
QTY. REQD PART OR IDENTIFYING NO CAGE CODE NOMENCLATURE OR DESCRIPTION MATERIAL SPECIFICATION
PARTS LIST
UNLESS OTHERWISE SPECIFIED DIMENSIONS ARE IN INCHES
TOLERANCES ARE:
DECIMAL .XX ±0.01 .XXX ±0.005
FRACTIONAL ±1/32 ANGULAR ±0.5°
THIRD ANGLE PROJECTION
NEXT ASSY USED ON
APPLICATION
CONTRACT NO
APPROVAL DATE
DRAWN 27-Aug-07
CHECKED
ENGINEER
Battelle
The Business of Innovation
505 King Avenue
Columbus, Ohio 43201-2693
Telephone (614) 424-6424
TITLE
CAP, RADIAL HOUSING
SIZE D CAGE CODE 79986 DWG NO 57602DSMM102 REV
SCALE 2.100 CALC. WT SHEET 1 OF 1
COMPUTER FILE NAME
DRAWING RADIAL_HOUSING_CAP
MODEL PART RADIAL_HOUSING_CAP

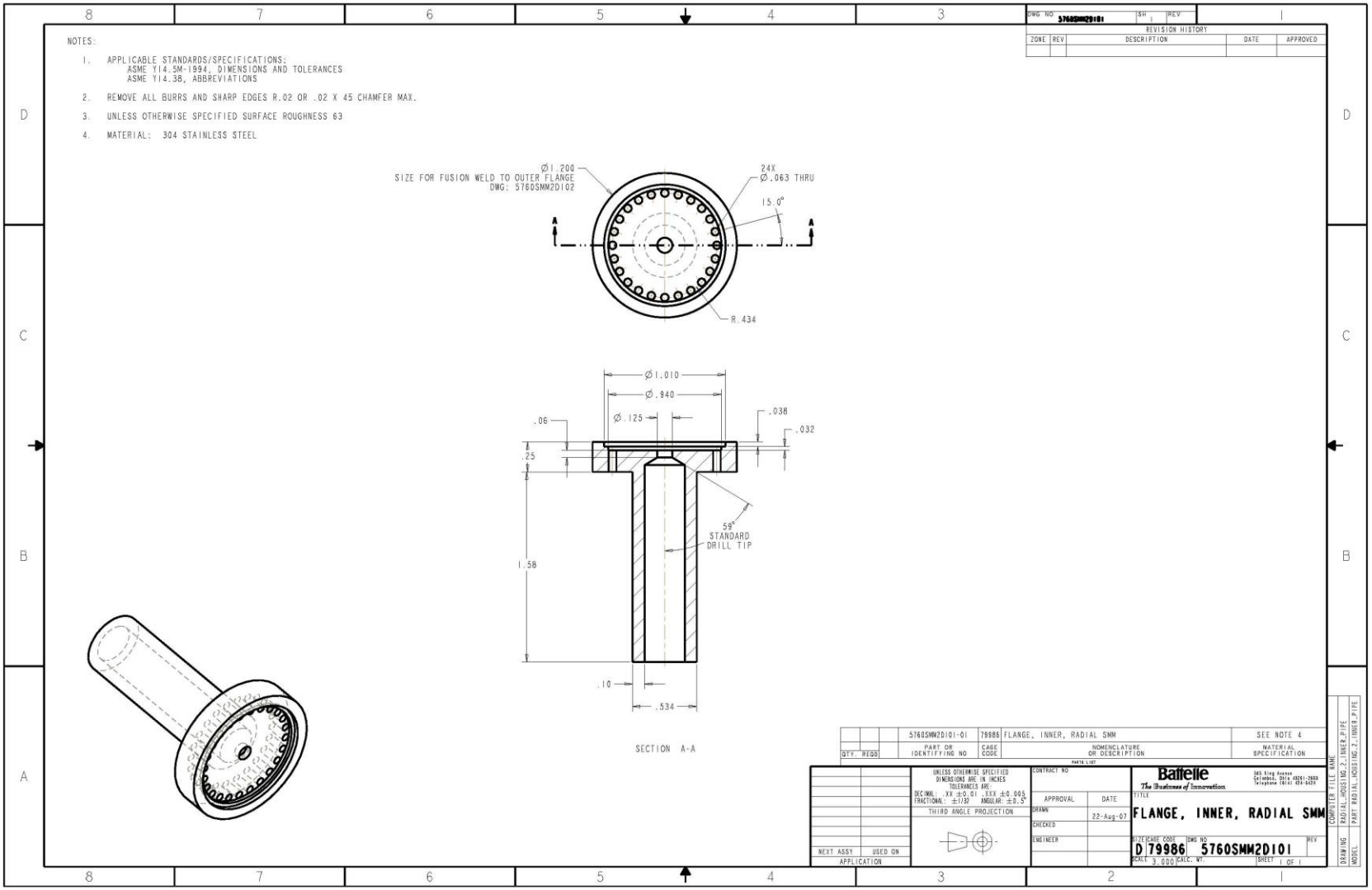
NOTES:
1. APPLICABLE STANDARDS/SPECIFICATIONS:
ASME Y14.5M-1994, DIMENSIONS AND TOLERANCES
ASME Y14.38, ABBREVIATIONS
2. REMOVE ALL BURRS AND SHARP EDGES R.02 OR .02 X 45 CHAMFER MAX.
3. UNLESS OTHERWISE SPECIFIED SURFACE ROUGHNESS 63
4. MATERIAL: 304 STAINLESS STEEL
Ø1.200
SIZE FOR FUSION WELD TO OUTER FLANGE
DWG: 5760SMM2D102
24X
Ø.063 THRU
15.0°
R.434
Ø1.010
Ø.940
Ø.125
.06
.038
.032
.25
59°
STANDARD
DRILL TIP
1.58
.10
.534
SECTION A-A
REVISION HISTORY
ZONE
REV
DESCRIPTION
DATE
APPROVED
5760SMM2D101-01
79986
FLANGE, INNER, RADIAL SMM
SEE NOTE 4
QTY. REQD
PART OR IDENTIFYING NO
CAGE CODE
NOMENCLATURE OR DESCRIPTION
MATERIAL SPECIFICATION
UNLESS OTHERWISE SPECIFIED DIMENSIONS ARE IN INCHES
TOLERANCES ARE:
DECIMAL .XX ±0.01 .XXX ±0.005
FRACTIONAL ±1/32 ANGULAR ±0.5°
THIRD ANGLE PROJECTION
CONTRACT NO
APPROVAL
DATE
DRAWN
22-Aug-07
CHECKED
ENGINEER
Battelle
The Business of Innovation
505 King Avenue
Columbus, Ohio 43201-2693
Telephone (614) 424-6424
TITLE
FLANGE, INNER, RADIAL SMM
SIZE
D
CAGE CODE
79986
DWG NO
5760SMM2D101
REV
SCALE 3.000
CALC. WT.
SHEET 1 OF 1
NEXT ASSY
USED ON
APPLICATION
COMPUTER FILE NAME
DRAWING
RADIAL_HOUSING 2_INNER_PIPE
MODEL
PART RADIAL_HOUSING 2_INNER_PIPE

NOTES:

1. APPLICABLE STANDARDS/SPECIFICATIONS:
   ASME Y14.5M-1994, DIMENSIONS AND TOLERANCES
   ASME Y14.38, ABBREVIATIONS
2. REMOVE ALL BURRS AND SHARP EDGES R.02 OR .02 X 45 CHAMFER MAX.
3. UNLESS OTHERWISE SPECIFIED SURFACE ROUGHNESS 63
4. MATERIAL: 304 STAINLESS STEEL

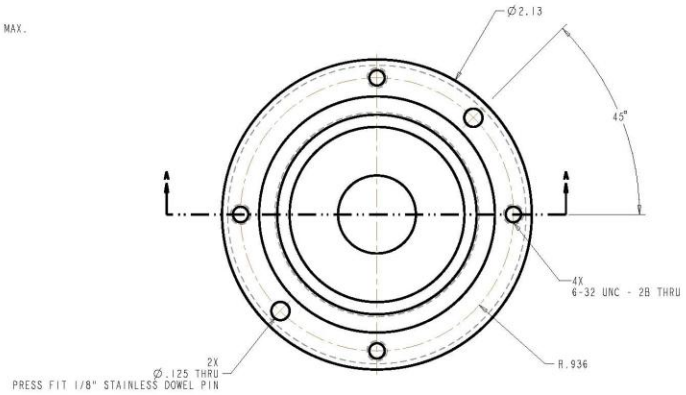

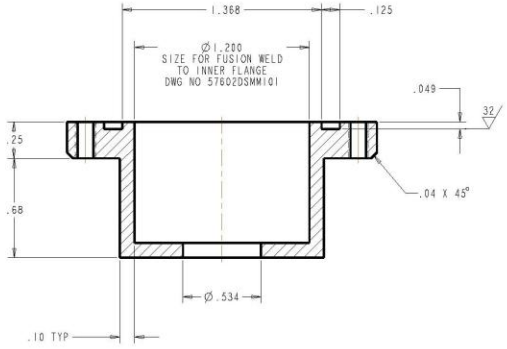

SECTION A-A

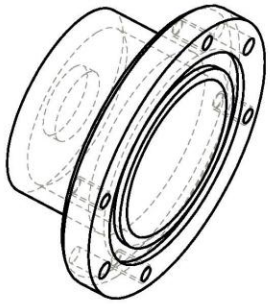

QTY. REQD	PART OR IDENTIFYING NO	CAGE CODE	NOMENCLATURE OR DESCRIPTION	MATERIAL SPECIFICATION
	5760SMM2D102-01	79986	FLANGE, OUTER, RADIAL SMM	SEE NOTE 4

PARTS LIST

ZONE	REV	DESCRIPTION	DATE	APPROVED

REVISION HISTORY

DWG NO 5760SMM2D102 SH 1 REV

UNLESS OTHERWISE SPECIFIED DIMENSIONS ARE IN INCHES
TOLERANCES ARE:
DECIMAL .XX ±0.01 .XXX ±0.005
FRACTIONAL ±1/32 ANGULAR ±0.5°
THIRD ANGLE PROJECTION

CONTRACT NO

APPROVAL	DATE
DRAWN	22-Aug-07
CHECKED	
ENGINEER	

NEXT ASSY USED ON
APPLICATION

Battelle
The Business of Innovation
505 King Avenue
Columbus, Ohio 43201-2693
Telephone (614) 424-6424

TITLE
FLANGE, OUTER, RADIAL SMM

SIZE D | CAGE CODE 79986 | DWG NO 5760SMM2D102 | REV
SCALE 3.000 | CALC. WT | SHEET 1 OF 1

COMPUTER FILE NAME:
DRAWING RADIAL_HOUSING_2_OUTER_P.IPT
MODEL PART RADIAL_HOUSING_2_OUTER_P.IPT

Appendix A 3.6

Sorbent Testing Analysis Results

Sorption/Desorption Efficiencies (Percent Recoveries) for Different Sorbent Target Analyte Combinations

Data are blank-corrected for native contributions from the background. For each analyte, air blank and sorbent tube blank were analyzed prior to the sample analyte. The air blank was a conditioned sorbent tube that had not sampled a air with out the target analyte present while the sorbent tube blank was the same sorbent tube except it had process ~10 L of blank air.

Compound	Pump Out Temperature (C)	Percent Recovery												
		Carboxen-569	Carboxen-1000	Carboxen-1001	Carboxen-1002	Carboxen-1003	Carboxen-1016	Carboxen-1018	Carbosieve-SIII	Carbosieve-G	Carbotrap C	Carbotrap F	GasPro PLOT	Alumin GS PLOT
Acetone	25		93						213					
	50		99						232					
	100		68						225					
Acetonitrile	25		79				0		99	58	0	0	0	0
	50		89				0		NA	NA	0	0		
	100		53				NA		86	NA	0	0		
Acrylonitrile	25	63	91					93	40					
	50	69	91					88	65					
	100	58	71					64	70					
Bromomethane	25													
	50													
	100													
Chloroacetone	25		46						0					
	50		42						0					
	100		44						0					
Chlorobenzene	25		57											
	50		93											
	100		76											
Chlorodibromethane	25		55											
	50		55											
	100		49											
Chloroform	25		118						49					
	50		122						41					
	100		100						29					
Cyanogen Chloride	25													
	50													
	100													
Dichlorobenzene,	25		13											

Compound	Pump Out Temperature (C)	Percent Recovery												
		Carboxen-569	Carboxen-1000	Carboxen-1001	Carboxen-1002	Carboxen-1003	Carboxen-1016	Carboxen-1018	Carbosieve-SIII	Carbosieve-G	Carbotrap C	Carbotrap F	GasPro PLOT	Alumin GS PLOT
1,2-	50		15											
	100		20											
Dichloroethylene, cis-1,2-	25		109											
	50		110											
	100		107											
Dichloroethylene, trans-1,2-	25		104											
	50		69											
	100		54											
1,1-Dichloroethene	25		102											
	50		102											
	100		97											
Dimethyl Phosphite	25		5						0					
	50		4						0					
	100		2						NA					
Di-N-butylphthalate	25		0.1											
	50		3.7											
	100		0											
Dimethylmethyl phosphonate	25		47											
	50		40											
	100		67											
1,4-Dioxane	25		139											
	50		146											
	100		142											
Ethanol	25		28						83					
	50		18						75					
	100		0						72					
Ethyl ether	25		136						65					
	50		130						93					
	100		135						NA					
Formaldehyde	25													
	50													
	100													
2-Hexanone	25		48											
	50		50											
	100		49											
Hydrogen Sulfide	25													
	50													
	100													
Methanol	25		0						0					
	50		0						0					

Compound	Pump Out Temperature (C)	Percent Recovery												
		Carboxen-569	Carboxen-1000	Carboxen-1001	Carboxen-1002	Carboxen-1003	Carboxen-1016	Carboxen-1018	Carbosieve-SIII	Carbosieve-G	Carbotrap C	Carbotrap F	GasPro PLOT	Alumin GS PLOT
	100		0						0					
Methylene Chloride	25	65	109					118	88	73				
	50	63	101					116	86	110				
	100	52	99					115	82	103				
Methyl Ethyl Ketone	25		85											
	50		84											
	100		67											
Methyl isoButyl Ketone	25		75											
	50		87											
	100		86											
Methyl isocyanate	25		0						16					
	50		0						12					
	100		0						0					
Methyl methacrylate	25		107											
	50		128											
	100		116											
Methyl t-Butyl ether	25		84											
	50		83											
	100		68											
NALED	25		0											
	50		0											
	100		0											
Nitrobenzene	25		5.5						0.2					
	50		5.3						0.1					
	100		6.8						0.1					
Styrene	25		16											
	50		18											
	100		20											
Tetrachloroethene	25		84						5					
	50		91						12					
	100		110						18					

Compound	Pump Out Temperature (C)	Percent Recovery												
		Carboxen-569	Carboxen-1000	Carboxen-1001	Carboxen-1002	Carboxen-1003	Carboxen-1016	Carboxen-1018	Carbosieve-SIII	Carbosieve-G	Carbotrap C	Carbotrap F	GasPro PLOT	Alumin GS PLOT
Toluene	25		61											
	50		50											
	100		43											
1,2,4-Trichlorobenzene	25		0.8											
	50		1.1											
	100		1.4											
1,1,1-Trichloroethane	25		92						0.5					
	50		108						0.6					
	100		106						0.3					
2,2,4-Trimethylpentane	25		58											
	50		64											
	100		85											
Trimethylphosphate	25		11											
	50		12											
	100		12											
Vinyl Chloride	25													
	50													
	100													
p-Xylene	25		25											
	50		39											
	100		51											

Appendix A5.1
FMS Commands

Command	Value	Function
FREQ.START=	210e9 – 270e9	Assign Sweep Start Frequency Returns FREQ.START=<Start Frequency>
FREQ.START?	--	Query Current Start Frequency Returns FREQ.START=<Start Frequency>
FREQ.STOP=	210e9 – 270e9	Assign Sweep Stop Frequency Returns FREQ.START=<End Frequency>
FREQ.STOP?	--	Query Current Stop Frequency Returns FREQ.START=<End Frequency>
FREQ.SLOPE=	20.4e6 – 1.306e9	Assign Sweep Slope. Slope is rounded to closest valid value. Valid values are 2^N * (20.4e6), N = 1,2,4,8,16,32,64 Returns FREQ.SLOPE=<Slope>
FREQ.SLOPE?	--	Query Current Sweep Slope Returns FREQ.SLOPE=<Slope>
FREQ.MODULATION.MODE=	0 – 2	Sets Modulation Mode. 0 = No modulation 1 = First Derivative Modulation 2 = Second Derivative Modulation Returns FREQ.MODUALTION.MODE=<mode>
FREQ.MODULATION.MODE?	--	Query Current Modulation Mode Returns FREQ.MODUALTION.MODE=<mode>
FREQ.MODULATION.FREQUENCY=	500 – 100e3	Assign Modulation Rate in Hz Returns FREQ.MODUALTION.FREQUENCY=<rate>
FREQ.MODULATION.FREQUENCY?	--	Query Current Modulation Rate Returns FREQ.MODUALTION.FREQUENCY=<rate>
FREQ.MODULATION.AMPLITUDE=	0 – 9.6e6	Assign Modulation Depth in Hz Returns FREQ.MODULATION.AMPLITUDE=<depth>
FREQ.MODULATION.AMPLITUDE?	--	Query Current Modulation Depth Returns FREQ.MODULATION.AMPLITUDE=<depth>
FREQ?	--	Query All Current FREQ settings. Identical to issuing all query commands listed above.
SWEEP.REPEAT=	-1, 1 – 65535	Set Number of Times a sweep should repeat. -1 = Repeat until SWEEP.STOP command issued. 1 – 65535 = Execute a total of 1 - 65535 times. Returns SWEEP.REPEAT=<Number>
SWEEP.START	--	Begin Execution of Programmed Sweep Returns SWEEP.START=1 if successful, SWEEP.START=0 if sweep is invalid or another sweep in progress.
SWEEP.STOP	--	Stop Current Sweep Execution. Returns SWEEP.STOP=1
FPGA.DATA.START	--	Begin Programming FPGA Image Returns FPGA.DATA.START=1 Accepts a binary image for the FPGA from this point forward. Exit this mode by sending an end of line <CR>
FPGA.DATA.DONE?	--	Returns FPGA.DATA.DONE=0 if FPGA not programmed Returns FPGA.DATA.DONE=1 if FPGA is programmed.

Appendix A5.2

Advanced FMS Design and Test

A5.2.1 Introduction:

As stated in the MACS Phase I report submitted in July 2008: The Frequency Management System (FMS) is one of the key technologies of the MACS system. The main objectives of the FMS are:

- Provide LO and RF signals to the THz module, which are then multiplied up in frequency by 24 and used for the spectroscopy
- Provide precise frequency knowledge of the current THz output frequency to the MACS system for both frequency output control (in order to perform the spectroscopy we need precise frequency knowledge to within 100 kHz at 300 GHz system operation) and in the data recovery
- Perform frequency sweeps across bands of interest – different chemical species exhibit different absorption characteristics versus frequency; The MACS system selects key frequency bands where these differences are most pronounced.
- Perform data processing on the received power spectrum input from the THz module, including all filtering, averaging, derivatives, and data formatting.

A5.2.2 Requirements Update:

In Phase I of the MACS program, rotational spectroscopy was performed in the frequency band 210-270 GHz. The FMS produced a "base" frequency in the range of 8.75-11.25GHz which was multiplied up by a factor of 24 in the THz module to produce the 210-270GHz signals used to excite the samples to be analyzed.

Additional information can be obtained by expanding the frequency range in which the spectroscopy is being performed. One frequency range of interest is the 540-660GHz range. This requires a base frequency of 11.25-13.75GHz and an additional 2x multiplier stage in the THz module for a total multiplication factor of 48. The FMS requirements have been expanded to include producing this frequency range.

A5.2.3 Architecture Update:

The primary system concerns (apart from the functionality listed above) were size, power, and then ability to lock to a given frequency quickly and to perform sweeps.

As discussed in section 5, the initial architecture for the MACS FMS would be overly complex to handle the new system requirements without severely compromising the system concerns mentioned above. Thus we have modified the FMS RF architecture, which may increase parts

cost, but will reduce size, power, and system complexity, as well as produce a more accurate "base" frequency, one that will be more immune to temperature changes, system noise (magnetic fields), and mechanical stress such as vibration. A further shortcoming of the first architecture was the variation of the output power over the frequency band; we aim to address this issue as well with the new architecture.

A preliminary block diagram of the new transmit architecture is shown below.

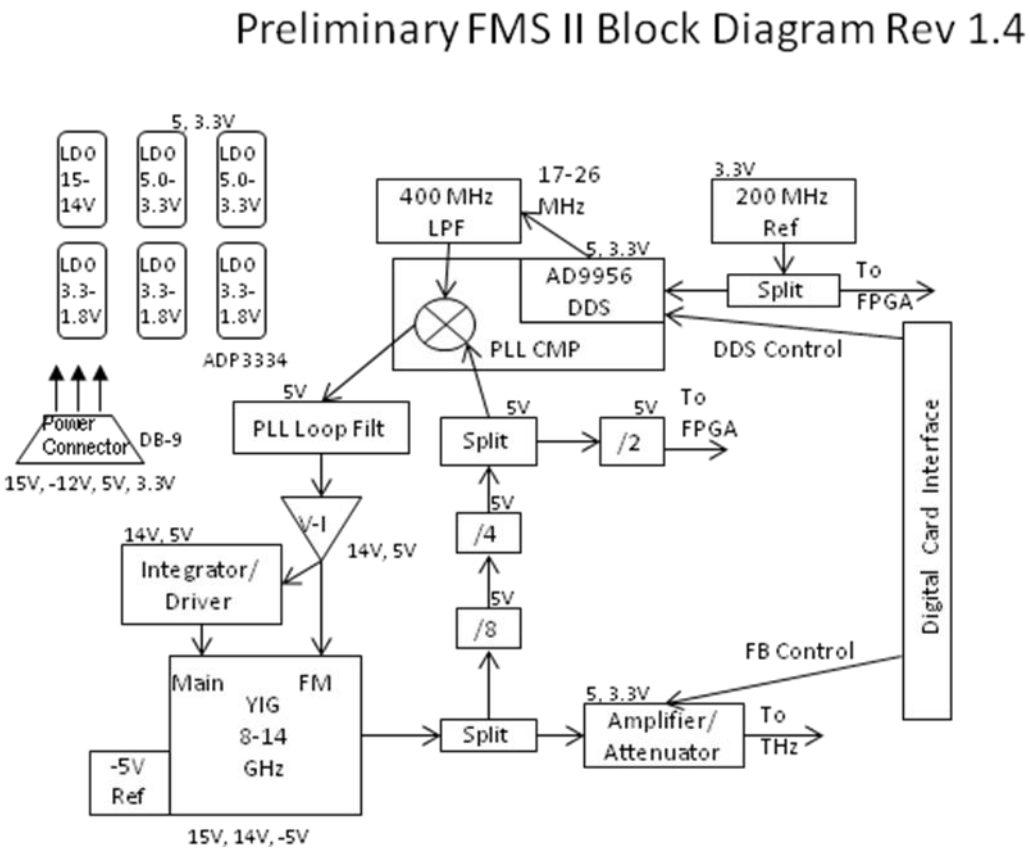

A5.2.3.1 Permanent Magnet YIG:

One of the improvements we have been investigating is the use of a permanent magnet YIG-tuned oscillator. In a YIG-tuned oscillator, current running through a tuning coil produces a magnetic field which controls the rate of oscillation. More current running through the tuning coil produces a larger magnetic field and increases the rate of oscillation. A permanent magnet YIG-tuned oscillator, however, has a permanent magnetic field setting a baseline oscillation frequency. This reduces the amount of current needed to drive the YIG and achieves substantial power savings over a standard YIG.

To illustrate the potential power savings of this change to the system, the currently selected MicroLambda YIG oscillator specifies a current-to-frequency sensitivity of 18MHz/mA, and a coil resistance of 8 ohms. To achieve an output frequency of 13.75GHz, the input current to the tuning coil would be 13.75GHz/18MHz/mA = ~764mA, consuming 4.7 watts of power. The lowest power solution is a permanent magnet YIG with a base frequency at 11.25GHz, the center

of the required 8.75GHz to 13.75GHz range. To affect an output frequency change of 2.5GHz, the input current to the tuning coil needs to be 2.5GHz/18MHz/mA = ~139mA, consuming 0.15 watts of power. This is a 30x power reduction, and removing this thermal load also greatly reduces the heat dissipation requirements for the FMS module.

In our initial research, MicroLambda Corporation informed us that a permanent magnet YIG with more than +/- 2GHz of tuning would be difficult to achieve. An alternative vendor, OmniYIG Corporation, has offered to produce a permanent magnet YIG with the magnetic field set to the lowest system frequency (8.75GHz) with a 5GHz tuning option, but this is sub-optimal in terms of power savings. We plan to continue our investigation for other vendors and consult further on this matter with MicroLambda to see if there are other YIG specifications that can be relaxed in order to produce a +/- 2.5GHz tuning range.

A5.2.3.2 Change from Frequency Locked Loop to Phase Locked Loop:

A major architecture change is in the frequency generation scheme. As proposed by Dr. Richard Eden in section 5.3 of the July 2008 report, we are moving from a frequency-locked loop (FLL) system to a phase-locked loop (PLL) system. In this phase-locked loop system, the YIG output is divided down (by 32 in our current design) to compare with a reference oscillator whose frequency is known; the difference in phases of the two signals produces an error voltage that is used to correct the YIG output frequency. The advantages are that the PLL gives nearly instant (tens of ns) feedback and frequency knowledge whereas the FLL gave a delayed feedback and only averaged information (over 1.53ms for MACS I), thus it was less accurate in its frequency knowledge.

Dr. Richard Eden in section 5.3 of the July 2008 report further discusses the use and benefits of direct digital synthesis (DDS) technology. The DDS chip takes as its input a stable reference oscillator (one with low frequency drift and low phase noise) and produces different frequency outputs based on its internal accumulator settings. The DDS output is used as the reference frequency for the PLL. Because the DDS output frequency can be changed quickly (through a software change of the accumulator setting), we can perform quick and accurate frequency sweeps. Under software control, the DDS chip can ramp up the PLL reference frequency, causing the YIG output frequency to ramp as well. The DDS chip can also perform the frequency modulation required to analyze the 1^{st} and 2^{nd} derivatives of the power spectrum.

A5.2.3.3 Simplification of the FMS Architecture and Ease of Testability:

The original FMS architecture had an RF PCB and a digital PCB. We chose this architecture primarily to isolate the RF signals from the digital card noise. With this architecture, it was very difficult to test either card's functionality by itself, because the FLL feedback counters were on the digital card. Additionally, the microprocessor was on the digital card and digital control signals were driven onto the RF PCB. The new FMS architecture shifts away from a RF/digital PCB model to a transmit/receive PCB model. In the new architecture, there will likely be 3 boards: Two transmit (TX) PCBs, one to generate the RF output, one to generate the LO output, and one receive (RX) PCB. By having two nearly identical transmit PCBs (the only difference being different output frequencies), the test and debug effort is effectively cut in half. Furthermore, because the PLL is located on the TX PCB, the RX PCB is not needed to test and debug the transmit PCB. There will be some digital logic on the TX PCBs; however, the advantages of this model make it worth the change, and we will work to isolate the RF and digital portions on each PCB. Lastly, separating the RF and LO modules into two cards should eliminate a lot of the crosstalk we observed between the two transmit chains on the Phase I RF card, resulting in cleaner (less noisy) RF and LO output signals.

A5.2.4 Bench Top System Tests and results:

We first created a bench-top system to test out the new TX architecture. The main system components were the ADF4108 PLL evaluation board, the AD9910 DDS evaluation board, a custom loop filter prototype board, and a prototype YIG control/driver module. A picture of the system is shown here for reference.

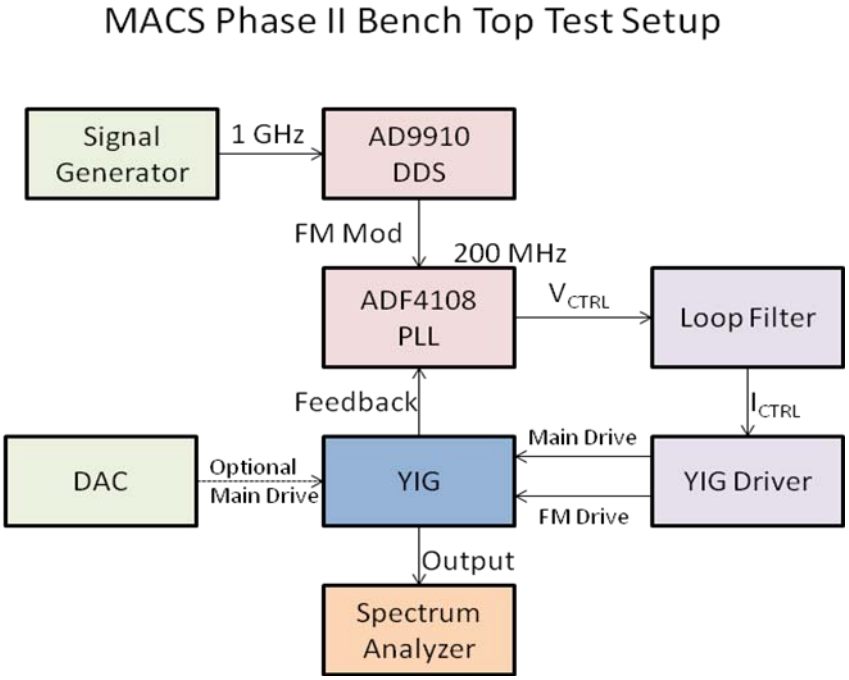

When we first set up the bench top system, to simplify the test, we drove the YIG main coil with a precision DAC and used the PLL to control the YIG FM driver and phase lock the YIG to a signal generator output. The YIG output spectrum was as follows (centered @ 7.2 GHz):

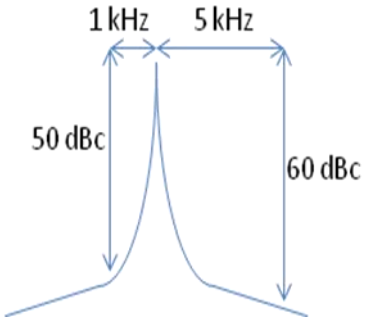

A5.2.4.1 Loop Filter Design Considerations

One of the key FMS requirements is the ability to perform frequency modulation while ramping. The frequency modulation provides the receiver with the ability to analyze the 1st and 2nd derivative of the input power spectrum as well as the power spectrum itself. The DDS chip has eight profiles that can be pre-programmed for different modes of operation. These profiles save a complete set of DDS register settings, including the output frequency of the DDS. Three digital inputs to the DDS select which profile is currently active, and the DDS is capable of switching between profiles in just a few clock cycles. In order to implement 1st derivative frequency modulation with a variable modulation depth and modulation rate, two profile settings are used. The two profiles are set to two different output frequencies equidistant from the desired output frequency. The digital controller on the TX module then toggles between these two profiles at the desired modulation rate. To allow the DDS to continuously modulate while ramping across a frequency band of interest, the digital controller uses an additional pair of profiles. Profiles 0 and 1 are programmed for the current desired output frequency, and while toggling between these two profiles, profiles 4 and 5 are programmed to the next desired output frequencies. The digital controller then switches to profiles 4 and 5 at the appropriate time, and reprograms profiles 0 and 1. This process repeats until the DDS has ramped across the entire band of interest. For 2nd derivative modulation, four profiles are needed for each center output frequency. The same scheme described above is used, only all 8 profiles are required. Most PLL systems have a loop filter after the phase detector, to smooth out the correction signal sent from the phase detector to the oscillator. Without a loop filter, phase detector output voltage spikes would cause wide instantaneous variations of the output frequency and possibly cause the loop to break lock. The loop filter (low pass) integrates the spikes and provides the YIG with an averaged correction voltage. A general rule of thumb is to have the loop filter cutoff (3dB) frequency be at least 10x less than the PLL phase detector frequency. In our system, the planned phase detector frequency is ~20MHz, so with this guideline in mind, a loop filter with a cutoff frequency of 2MHz or less would be suitable for the application.

Our system has an additional consideration, because the YIG FM coil has a 3dB bandwidth of 2MHz, according to the datasheet (Dr. Eden experimentally verified the bandwidth as 1.5MHz during Phase I of the MACS program). The loop filter bandwidth should be less than this frequency as well; otherwise, the FM coil could not respond quickly enough to the correction

voltage. This would lead to a condition where the YIG frequency would not change fast enough for the phase detector to notice, and the phase detector would repeatedly put out a correction voltage, which would eventually overdrive the YIG output past the reference frequency. The YIG output frequency would eventually oscillate as the phase detector overcorrects in both directions.

In terms of performing the FM modulation, we have an opposing design guideline. A larger loop filter bandwidth allows for a higher maximum modulation rate. For a given square wave modulation frequency, the loop filter bandwidth should be at least 5 times this frequency, to allow the first three harmonics of the square wave to pass through. However, the loop filter cannot have an arbitrarily wide bandwidth, because it must average the PLL CMP high frequency error correction voltage/current spikes which drive the YIG, as stated above. The modulation rate of 40 kHz used in MACS phase I was found to be suitable for derivative analysis. For this modulation rate, a loop bandwidth of at least 200 kHz is necessary. An additional design consideration is the filter topography, the primary choice being between an active (using an operational amplifier) filter or a passive filter (passive components only). On MACS Phase I, we initially chose an active filter design, but during the test phase, found that the filter did not perform as we expected, so we settled on a passive filter design. Active filters also tend to generate more system noise.

The simplest passive filter design is a capacitor to ground followed by a resistor and capacitor to ground. Using an Analog Devices PLL simulation program, and independently verified in SPICE, we designed a simple passive loop filter into out PLL, as shown below.

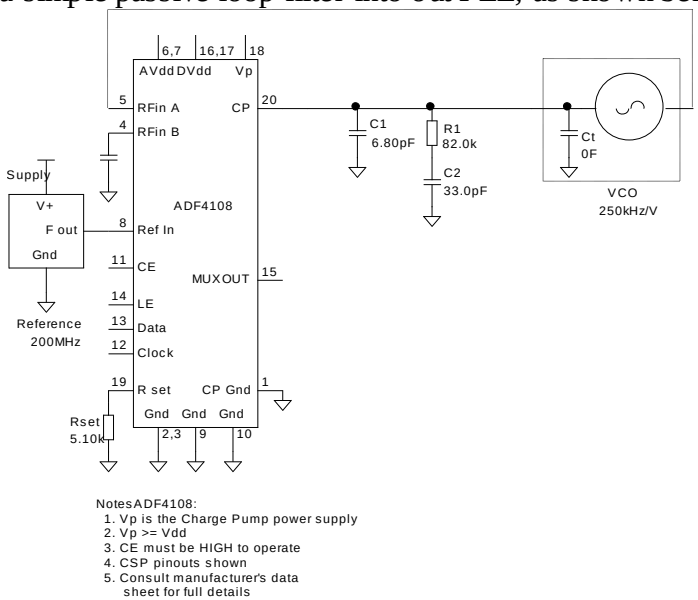

The filter consists of the 6.8pF capacitor to ground followed by the 82k ohm resistor and the 33pF capacitor to ground. The bandwidth of this filter was analyzed by software to be 232 kHz, meeting all the design considerations, allowing for 40 kHz modulation and also averaging the PLL CMP output spikes.

We contemplated choosing a lower value than 6.8pF for the first capacitor, in order to increase the loop bandwidth somewhat, however, we believed that stray PCB capacitance would begin to dominate the calculation and wanted to create a circuit we could predict and analyze.

A5.2.4.2 Frequency Modulation

After first getting the YIG phase locked, we then modulated the signal generator output +/- 630 Hz. Because our YIG divide ratio in the demo system was 36, this produced an output modulation of approximately +/-22 kHz. The results are shown here:

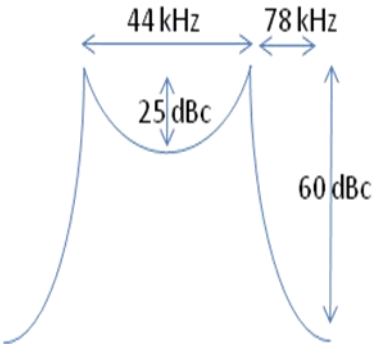

A5.2.4.3 DDS Performance and OCXO Options

Moving closer to the full bench top system, we next replaced the signal generator output with the DDS output. We performed an assessment of the DDS phase noise compared to the signal generator phase noise. (Obviously, it could not be any better, but we wanted to see how much worse it might be). The results are shown here.

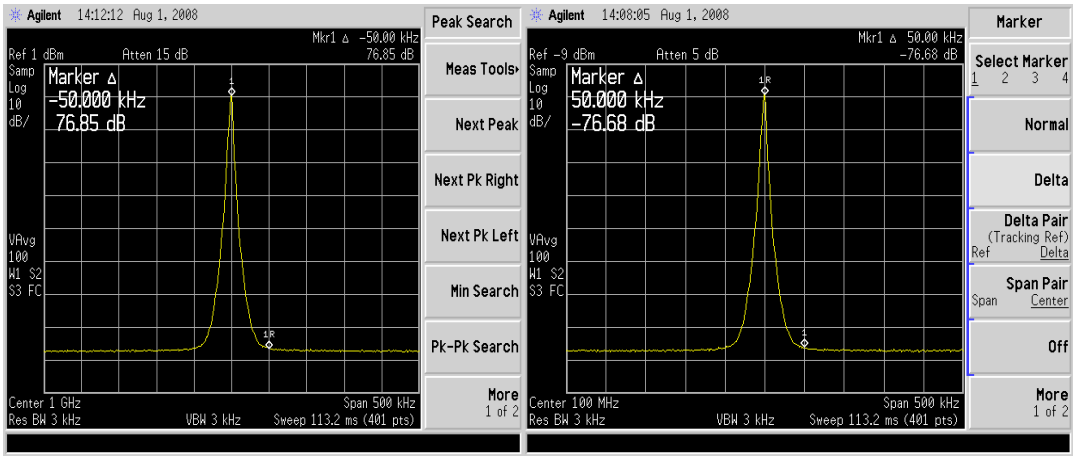

The plot on the left is the 1GHz signal generator output, and the plot on the right is the 100MHz DDS output when the DDS input is the 1GHz signal generator. From these (nearly identical) plots, we concluded that the DDS chip likely is performance limited by the input signal generator, given that the AD9910 datasheet specifies the output residual phase noise @ -140dBc, and the Spurious Free Dynamic Range (SFDR) @ -91dBc for the 100 MHz output frequency. At the time this plot was taken, we did not have a better generator to test the theory.

We have investigated the use of a precision, low phase noise reference oscillator to use for the DDS input. One alternative under consideration was the Wenzel Associates Agate I oscillator, which produces a 1GHz signal with 200ppb (parts per billion) accuracy. Despite having the maximum input reference frequency that the AD9910 DDS chip can handle, the size is 2.5" x 5", and requires a lot of power for the internal frequency multipliers and amplifiers. We have more recently investigated (and are leaning towards) a precision OCXO from Valpey Fisher Corporation. The VFOV400 Series oscillators have SSB phase noise of -90dBc/Hz @1Hz, and -125dBc/Hz @10Hz, in addition to 50ppb stability, a 3.3V power supply option (the Wenzel part needed 15V), and a footprint less than 1 in^2. A disadvantage of the VFO series is that the maximum frequency is 250 MHz, which would lead to a less smooth DDS output than would an output signal sampled at 1GHz. Since the phase noise specifications of the VCO exceed the capabilities of the AD9910 DDS chip, the DDS performance would be limited only by the DDS chip itself, not by the reference oscillator (as in our experiment). We did not purchase an OCXO for the test setup because our decision has not been finalized.

We were then able to insert the DDS chip into the system. The signal generator produced a 1 GHz reference clock for the DDS chip, and the DDS chip (first in RAM and then by toggling between discrete frequency settings) produced the FM modulation. The results are shown here:

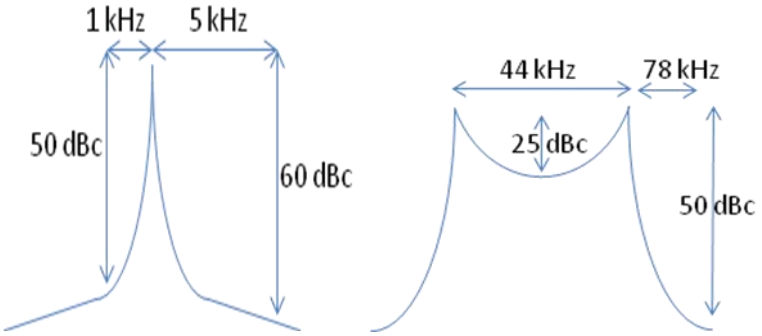

Basically, the DDS continued to perform no worse than the signal generator in the non-modulated plot. However, in the modulated plot, there appeared to be more system noise. We were initially unsure why this was happening.

We then tested to see how fast we could frequency modulate, and we found that we could only modulate up to 45 kHz, which was contrary to our loop filter SPICE simulation. We concluded that there was too much stray capacitance in the bench top system setup to get the full filter bandwidth and that the loop filter cutoff frequency was causing the noisy modulation plots. Reducing stray capacitance became one of the motivations to move toward a prototype PCB.

A5.2.4.4 Self-locking YIG control and other YIG driver improvements:

The last feature we implemented on the bench top system was the self-locking YIG control mechanism using the main coil in addition to the FM coil. We successfully disconnected the YIG main coil driver from the DAC and connected it to the filtered PLL phase comparator V_{tune} output. This last modification resulted in our bench-top system matching the block diagram given earlier.

One of the benefits of the self locking YIG control mechanism over the phase I architecture is that the integrating cap no longer needs to be polypropylene (ultra-low leakage). To elaborate, the MACS I main coil driver needed a current drive precision in the nA range, because of the 18MHz/mA current-to-frequency characteristic of the main coil. Small variations in the main coil current could produce large variations in the output frequency. In the new proposed FMS architecture, the YIG is being coarsely locked through the main coil, and finely locked through the FM coil, which has a 400 kHz/mA current to frequency transfer characteristic. Thus, tiny variations in current aren't going to adversely affect the YIG output frequency nearly as much in the new architecture.

Additionally, for MACS I, we needed a very slow integration rate for frequency sweeps, which led to a very high resistor value in the integrator circuit. In this new architecture, we are using the main coil not for sweeps but to quickly achieve coarse lock of the YIG frequency. (As explained above, the DDS chip will be responsible for sweeping the YIG output frequency.) This requirement suggests we use a much faster integration ramp rate than the MACS Phase I architecture. Because the integration rate is proportional to the inverse of the integration resistance value ($V_{out} = -1/RC * \int V_{in}\, dt$), we can reduce the large (specialty 400 Megaohm through hole) resistor to a smaller, surface mount component. We selected a value of 220 kilohms to move between frequency bands quickly without losing PLL lock. To verify a reasonable ramp rate, we calculated the change in frequency over a 1 second ramp. With a 2.2uF capacitor, a 220 kilohm resistor, a 2.5V V_{tune} input voltage, a 10 ohm main coil resistance, and a 18 MHz/mA current to frequency sensitivity of the main coil, we can hop (1/.484) * 2.5V * 1/10(ohms) * 18GHz/A = ~9.3 GHz in one second. That means it will take just over ½ a second to jump from 8.75 GHz to 13.75 GHz.

A5.2.5 DDS Chip Selection:

The reader may have noticed a discrepancy between the system block diagram on page 2 of this appendix and the bench top test block diagram on page 4. Specifically, the system block diagram shows the DDS module as AD9956, while the bench top setup shows DDS module AD9910. In our initial development, we targeted the AD9910 DDS module for use in MACS; however, we have more recently decided upon using the AD9956 module.

The AD9910 DDS module may actually be the superior DDS component. The AD9910 chip runs at 1GHz, compared to 400MHz for the AD9956. The AD9910 also has many other programmable frequency output modes. Our initial plan was to use the AD9910 DDS module along with the Wenzel 1GHz reference oscillator, running the ADF4108 PLL reference oscillator as fast as possible (up to 100MHz) to achieve the most accurate YIG output. However, analysis of our system needs revealed that we did not need all this capability, and so we looked to simplify the architecture and reduce cost, size, and power consumed.

The AD9956 DDS module includes both a PLL and a DDS frequency generator in a single chip. This allows us to remove the ADF4108 PLL chip from our system; saving cost, board space, and simplifying the design. Producing an output frequency around 20MHz is not compromised greatly by the lower frequency DDS. Additionally, as mentioned previously, the Valpey Fisher VFO400 series OCXO running at 250MHz was smaller, cheaper, and had a tighter tolerance

specification, making it a better input reference to the AD9956. Together, these two components can frequency lock, ramp, and modulate the YIG output frequency.

Using the system block diagram on page 2 as a reference, we can provide more specific information on the anticipated system operation. The YIG output will be between 8.75 and 13.75 GHz. Because the AD9956 PLL section requires RF inputs to the PLL to be below 655 MHz, we need to divide the YIG output by a factor of 32, making the PLL RF input in the range of 273.4375 – 429.6875MHz. The PLL inputs have a maximum divide of 16 to the phase detector. Selecting this divide value of 16, the phase detector will have an operating frequency of ~17MHz to ~26.8MHz. The DDS output becomes the reference input to the phase detector and with an input frequency of 250MHz (from the OCXO), and a 48 bit DDS accumulator, the frequency tuning resolution on the DDS output is 8.88×10^{-7} Hz. Of course, the frequency multiplier from the PLL to the YIG is 32 x 16 = 512, but this still gives us 455 microHertz resolution on the YIG output frequency! While we will not likely achieve this best case scenario, we believe that we can know the YIG output frequency to within 1Hz. As a point of comparison, we were able to have ~600Hz resolution on the YIG frequency output in the Phase I FLL configuration, using an integration period of 1.53ms.

The AD9956 datasheet gives a simplified application diagram that describes its usage in our system. In our system, the YIG is equivalent to the VCO from the diagram

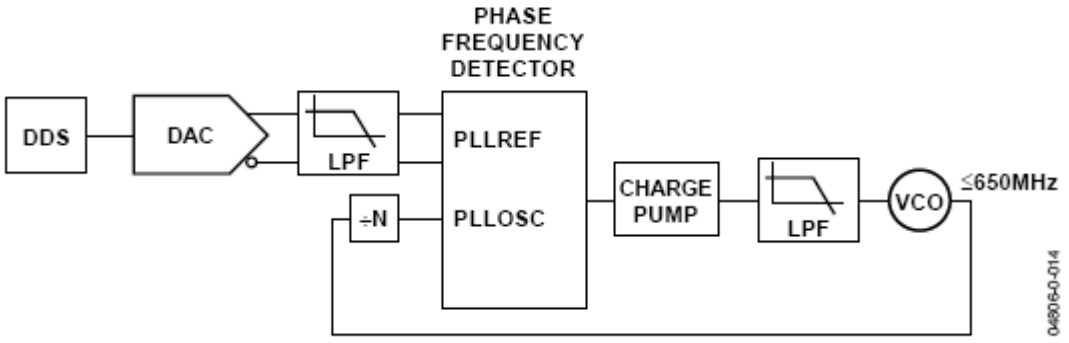

A5.2.6 Additional TX System Considerations, Changes, and Enhancements:

A5.2.6.1 Maintaining constant TX output power:

One area of concern is maintaining a constant output power to the THz module. The MACS phase 1 RF card exhibited a varying output power response over its frequency range. Thus, different amounts of energy were being used to excite the chemical samples at different frequencies. This caused differing receiver power levels in different frequency bands. This made it complicated to accurately compare chemical signatures across a wide frequency band.

In analyzing and reviewing our Phase I architecture (shown below for reference), we concluded that the numerous circuit elements and RF strip line traces in the RF/LO output path made it very difficult to produce a constant output power. Multiple amplifiers, attenuators, mixers, and band pass filters made for a complex architecture, where even a single component malfunction was difficult to isolate and debug. Additionally, the numerous strip-line 50 ohm traces all needed to

be specified to a certain distance so as not to set up standing waves on the traces, and the traces had to be properly trimmed in width at the pins of all the components to maintain the 50 ohm impedance. Slight miscalculations could easily prove harmful. Lastly, the YIG oscillator was running at 11-13.5 MHz, and mixed down to 8.75-11.25 MHz. These high frequency RF traces ran all over the PCB and were subject to trace losses resulting in a significant power loss on the Phase I system TX output power.

Dual Band RF Module rev 2.2

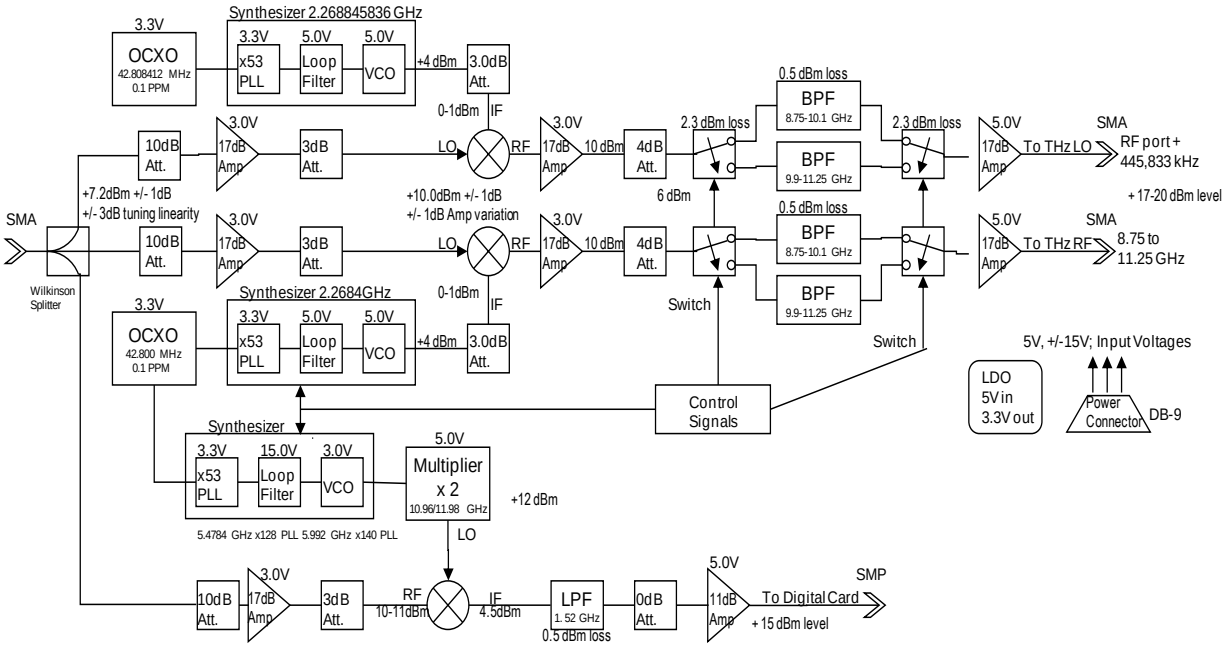

In the new architecture, our hope is that by having only 1 attenuator and 1 amplifier in the transmit path from the YIG to the THz module, we can minimize the variations in output power. The only high speed traces on the PCB are from the YIG to the THz module and in the feedback path from the YIG to the PLL, and the frequency of the signals decreases through each divider stage. The prototype PCB described in the next section has been designed with a variable gain amplifier in order to experiment with an output power control mechanism. The VGA can correct for power differences across the frequency regime, and be run in saturation, which lowers the signal to noise ratio of the RF/LO output without over-amplifying the signal.

A5.2.6.2 A worthwhile cost tradeoff:

One of the costs of using the new architecture is the need for 2 YIG-tuned oscillators, one for each of the RF/LO transmit chains. YIG-tuned oscillators are expensive components, with a price of $2000-$3000. We decided to incur this additional parts cost in order to simplify the design and remove the mixer/filter architecture of phase I. In addition to the variable output power issue discussed above, we believe the old architecture was causing some noise issues in the phase I RF board, due to unwanted mixer products and possible coupling between the many PCB traces routing these high frequency signals. Furthermore, the removal of the band pass filters (we no longer have undesired mixer products in the new architecture) does save approximately $1200 and significant PCB space. Lastly, the old architecture would not have adapted well to producing RF and LO signals from 8.75-13.75 GHz, instead of only 8.75-11.25

GHz. We would have likely needed additional filters for the higher frequency bands, and would have needed to give great design concern and consideration to the additional mixer scenarios.

A5.2.6.3 Expanding ST internal capabilities:

For the first two iterations of the FMS, the PCB layout was contracted to a layout and prototype manufacturing firm outside Smart Transitions. While that decision allowed ST to focus on other complexities of the Phase I design, it cost money and took time to produce the finished PCBs. Now, with a proven design in hand, ST has invested resources in learning RF PCB layout techniques and producing the PCB of the next-generation FMS in house. This decision will provide ST with more flexibility to change and improve designs on short notice, as well as increase organizational capabilities.

Two specific areas where this flexibility will make a difference are: 1) Tweaking the layout/routing/placement to achieve a constant transmit output power, given the difficulties described in section A5.2.6.1, and 2) Eliminating/accounting for the effects of stray capacitance on the PCB, specifically in the PLL loop filter, as described in section A5.2.4.1. Optimizing the performance in these areas is often a trial and error process; by having control over the full design in house, we can quickly and efficiently conduct multiple trials within the program time frame. (On MACS I we only had time for 2 PCB iterations.)

A5.2.7 Design and preliminary test of the prototype PCB:

After successfully testing the bench top system, we next turned towards generating a prototype PCB. As stated previously, the main intentions of the prototype development were 1) to begin to miniaturize the bench top test setup and move closer to a realistic and viable Phase II transmit PCB, 2) expand ST's capabilities to perform high speed RF design and layout, and 3) provide ST with the control and flexibility over the development process.

A5.2.7.1 Architecture and block diagram:

The PCB and system block diagram is shown below. The diagram closely resembles the system block diagram on page 2 of this appendix.

As we can see from the block diagram, the prototype board was designed to interface both with the AD9910 and AD9956 DDS chips. In the AD9956 configuration, we only need the single demo board, while in the AD9910 configuration, we need both the AD9910 demo board and the ADF4108 PLL demo board. Although at the time of design we were leaning towards the AD9956 DDS chip, we had still tested the bench top system with the AD9910 and ADF4108, so we decided to keep the ability to use those components for the sake of having a smooth migration from the bench top system to the PCB, and for this reason, most of our initial testing with the PCB still used the AD9910 and ADF4108 components.

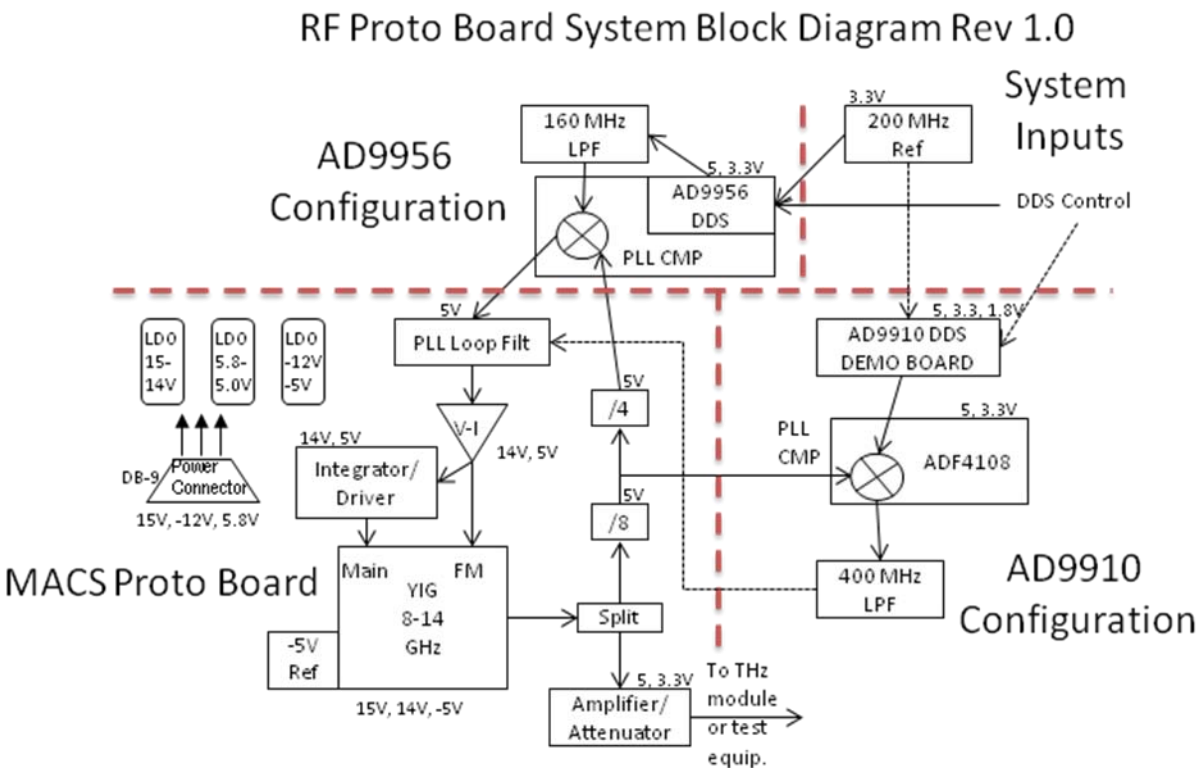

A5.2.7.2 Schematic Diagram:

The schematic diagram is shown on the next page. We immediately see 4 subsections of the board (clockwise starting from the upper right):

1) Power Input and Filtering. The TX PCB will require 3 input voltages, +15V, -12V, and +5.8V. The power inputs come in through a DB-9 connector. A linear dropout regulator (LDO) is used to produce a clean 14V supply needed for the YIG internal amplifier circuit, and another LDO is used to produce a clean +5V from the +5.8V supply. Power supply filtering is a critical portion of the design, so as to eliminate noise on the GHz system signals. The -5V is generated from a 5V reference generator (using the 5.8V supply as its input) and inverted using an op-amp circuit which requires the -12V; only 20mA of -5V is needed by the PCB, so an LDO is not necessary in this case.
2) YIG Main Coil and FM Drivers. The YIG driver circuit is based on the MACS Phase I design. We replaced the polypropylene low leakage capacitor and 400 Megaohm resistor with a 2.2uF ceramic through-hole capacitor and a 220 kilohm surface mount resistor. The PLL V_{tune} output goes through the passive loop filter and is split at the input of a low noise OPA2228 op amp. One path goes the FM coil driver and filter, which has a pulldown resistor R17 of 200 ohms setting the maximum FM driver current to 5V/200 ohms = 40mA, which is equivalent to 40mA * 400kHz/mA = 16MHz of FM coil pulling capability, which is sufficient for the application. (5V is the maximum V_{tune} output.) The other path goes to a voltage follower, and then to the integrator circuit (R20, C56, U18).

The baseline voltage for the YIG is set to be 2.5V by R19, R24, and C58 (assuming the jumper ties R19 to ground). 2.5V is the center of the V_{tune} range, and when the PLL is locked, the tuning voltage will hold at midscale, giving the circuit maximum tuning flexibility. Additionally, the 2.5V is a small enough input voltage to keep the YIG off (and conserving power) until the PLL is configured by the system. Switch U17 is a carryover from Phase I which allows us to reset the YIG main coil voltage; we do not believe we will need this switch in the final design, but we left it in for safety. The rest of the driver circuit, including the FET and the diode, has been copied from the successful phase I implementation.

3) YIG amplifier and ADF4108 prescaler. This is the high frequency portion of the PCB. The YIG output waveform comes into the card via SMA and is immediately routed to a splitter. Both splitter outputs are attenuated to make the signal level compatible with the downstream ICs. One signal path is to a +12dB variable gain amplifier (VGA). As discussed in section A5.2.6.1, the VGA sends the signal into saturation (+16dBm) and can correct unanticipated changes in output power to produce a constant output power. The +16dBm output power level is a bit lower than the diode chain specification, +17 to +20dBm, of the THz module; one purpose of this prototype board is to see if +16dBm would work in the MACS system. We could have inserted higher power amplifiers (and yet may do so), but the variable gain setting was an attractive option for prototype development.

   The second signal path is to a divide by 8 IC. This component (U3) brings the YIG feedback frequency into a range which the ADF4108 PLL chip can handle. Specifically, the lower frequency bound is 8.75GHz/8 = 1.09375GHz, and the upper bound is 13.75GHz/8 = 1.71875GHz. An additional attenuator and amplifier stage is necessary to make the signal level fall within the -5dBm to +5dBm range of the ADF4108, as well as the signal level range of the divide by 4 IC, described in the next section.

   Many of the high frequency components require DC blocking capacitors on the inputs and outputs. Values were chosen to make the impedance at operating frequencies less than 5ohms, or 1/10 of the 50 ohm trace impedance, but it is possible for the capacitors to impact the actual RF signal levels, and this needs to be accounted for and tested.

4) AD9956 Prescaler. In order to bring the YIG feedback frequency below 655MHz (the maximum input frequency the PLL of the AD9956 can handle), we need an additional divide by 4 on the output of the divide by 8 module. Again there is an amplifier/attenuator pair to create the desired AD9956 signal level of +3dBm.

   In this section of the schematic are also three 50 ohm traces. These traces are ST's attempt to characterize and gain insight into the power losses in the PCB traces at high >10GHz frequencies that we believe occurred on the Phase RF PCB. One of the traces is straight, one is curved, and the third is also curved with a capacitor in the signal path. The plan is to input a high frequency signal of known power and measure the output power levels while performing a frequency sweep.

A list of key components is shown here:

YIG PLL REV1a Parts List		
Reference Designator	**Manufacturer**	**Part Number**
Q1	Fairchild Semiconductor	MMBT2222A
Q2	International Rectifier	IRLML6401GPBF
U1	IMS	IPS2290-50R0J
U2, U4, U6, U9	IMS	IA3-0805S
U3	Hittite Microwave Corp.	HMC494LP3
U7	Hittite Microwave Corp.	HMC463LP5
U8	Hittite Microwave Corp.	HMC363S8G
U10, U21	Hittite Microwave Corp.	HMC374
U11	Analog Devices	ADP3334ARZ
U12	Analog Devices	ADR445BRZ
U13	Analog Devices	AD8599ARZ
U14	Linear Technology Corp.	LTC1763CDE
U15	MicroLambda	MLXM-0618
U16, U18	Texas Instruments	OPA2228UA
U17	Analog Devices	ADG417BRZ
U19	Analog Devices	ADR441BRZ
U20	ST Microelectronics	STP40NF03L

All parts (with the exception of the YIG) are readily available and easily procurable.

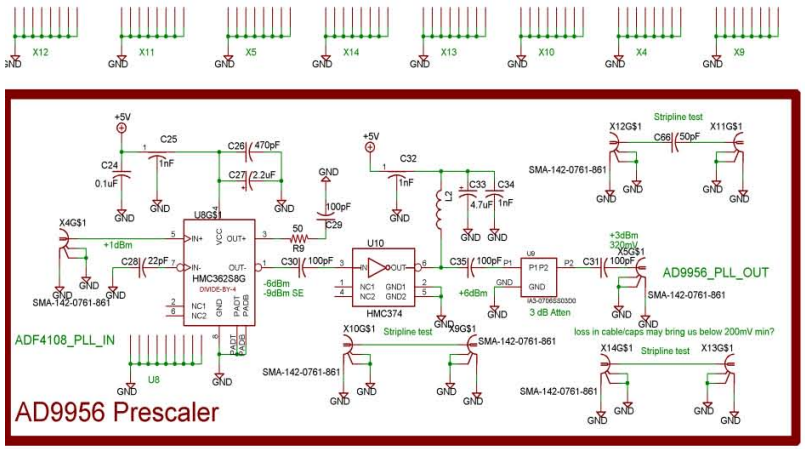
AD9956 Prescaler
ADF4108_PLL_IN
AD9956_PLL_OUT
HMC362S8G
HMC374
3 dB Atten
-6dBm
-9dBm SE
+6dBm
+3dBm
320mV
Stripline test
SMA-142-0761-861
loss in cable/caps may bring us below 200mV min?

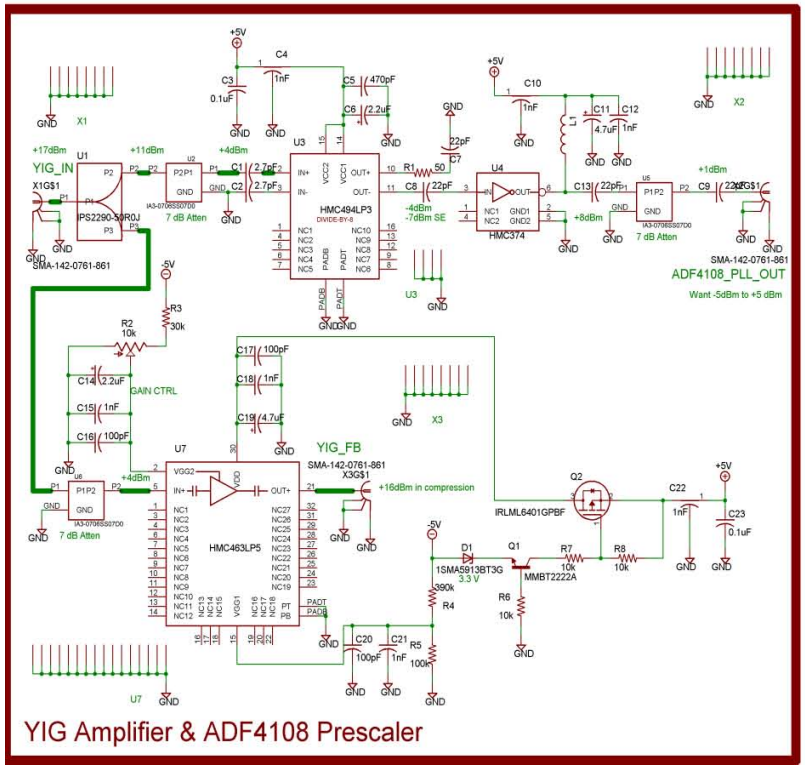
YIG Amplifier & ADF4108 Prescaler
YIG_IN
ADF4108_PLL_OUT
Want -5dBm to +5 dBm
HMC494LP3
HMC374
HMC463LP5
7 dB Atten
GAIN CTRL
YIG_FB
+16dBm in compression
IRLML6401GPBF
MMBT2222A
1SMA5913BT3G
3.3 V
SMA-142-0761-861

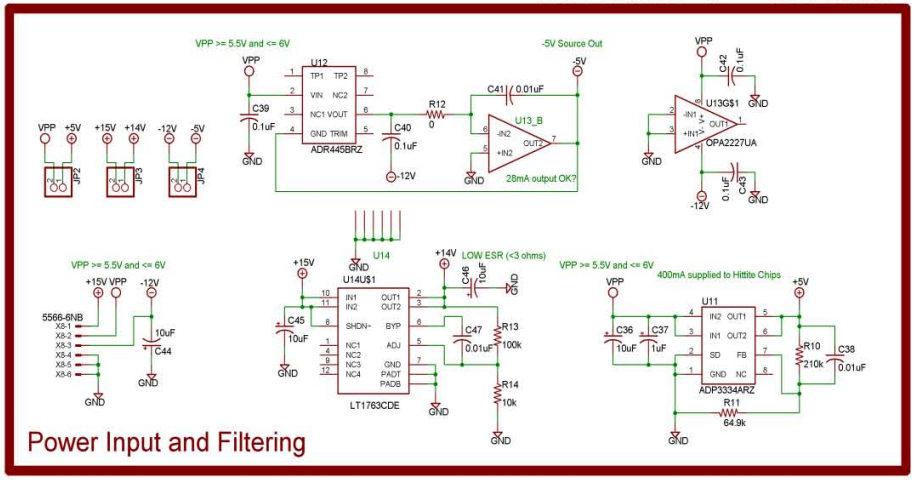
Power Input and Filtering
VPP >= 5.5V and <= 6V
-5V Source Out
ADR445BRZ
28mA output OK?
OPA2227UA
LT1763CDE
LOW ESR (<3 ohms)
ADP3334ARZ
400mA supplied to Hittite Chips

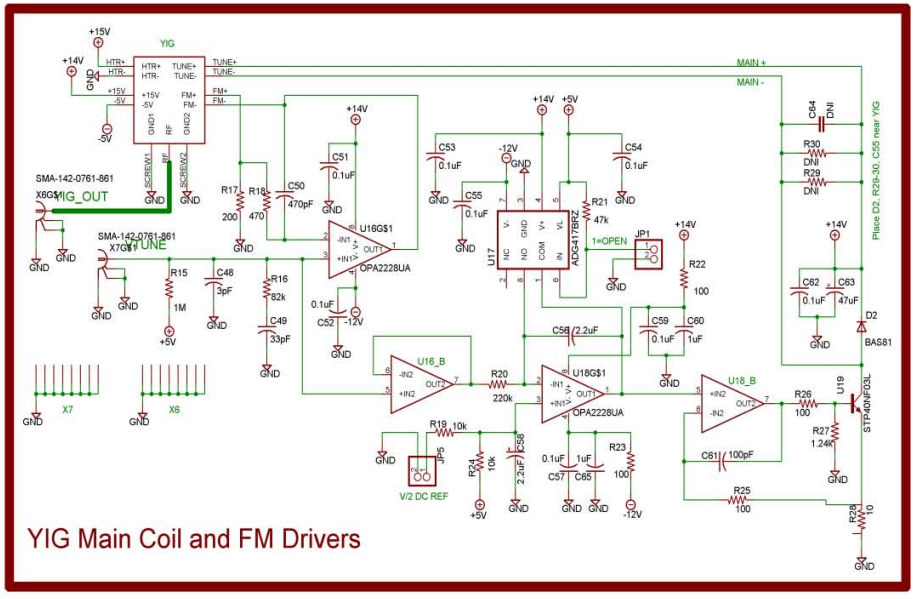
YIG Main Coil and FM Drivers
YIG
MAIN +
MAIN -
YIG_OUT
TUNE
OPA2228UA
ADG417BRZ
1=OPEN
V/2 DC REF
Place D2, R29-30, C55 near YIG

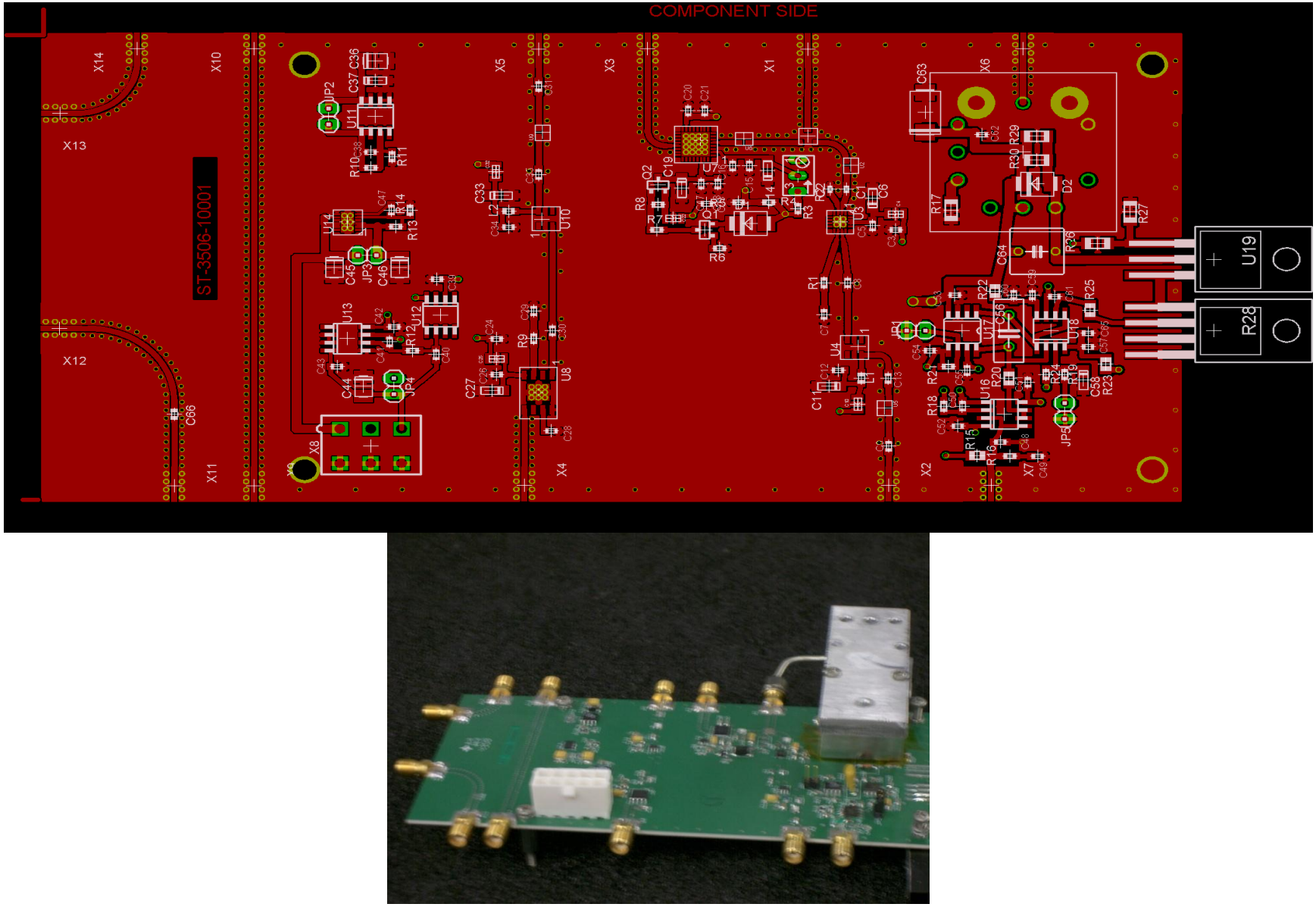
COMPONENT SIDE
ST-3506-10001

A5.2.7.3 Layout and Initial Build:

Pictures of the PCB layout and completed prototype PCB are shown above. The PCB size is approximately 3"x5", and a lot of the space is blank or consumed by test traces, which validates the projected reduction in size, even when the DDS chip and associated circuitry is added to the final TX PCB.

While performing the layout, we researched RF PCB routing guidelines. We used this information to calculate the trace width and separation distance from the ground planes. The model we used was the grounded coplanar waveguide model. A basic tutorial on this model can be found at http://www.microwaves101.com/encyclopedia/coplanarwaveguide.cfm. This board was produced on Rogers 4350 material, with a dielectric constant of $\varepsilon = 3.36$. A discussion of the recommended curvature of RF signal traces can be found at http://www.absoluteastronomy.com/topics/Microstrip, the basic conclusion being the radius should be 3 times the trace width (in our case 32 mils), for a radius of at least 96 mils.

All RF PCB trace lengths were calculated to $3/8\lambda$ to reduce the possibility of setting up a standing wave on the PCB trace at lengths of $\lambda/4$, $\lambda/2$, and λ. The frequency assumed was 11.25GHz, the center frequency of the system.

Ground plane stitching was provided at a maximum distance of $\lambda/20$ for the various high frequency signals, and 1/4" stitching was provided on the edge of the PCB, to minimize EMI radiation.

One can see from the populated PCB that the YIG is directly soldered into the PCB, unlike MACS phase I, where the YIG was mounted separately and connected to the driver circuit with cables. This will simplify the overall architecture and reduce stray capacitance on the YIG interface signals. For this prototype build, we used a spare MicroLambda YIG from the Phase I development. Once we have a permanent magnet YIG selected, we will incorporate that into our system. Also, the YIG will be mounted on the underside of the PCB and likely heat-sinked to the main chassis. Here the YIG is mounted on top of the PCB.

A5.2.7.4 Prototype Test Results:

Initial tests of the PCB have validated our ability to successfully frequency lock the YIG using the ADF4108 PLL. A plot of the locked signal is shown here.

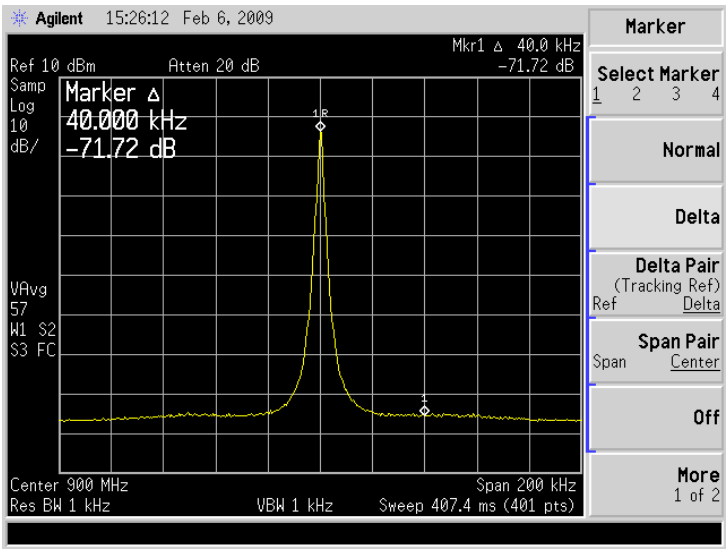

Here, the YIG is locked at 7.2 GHz, and we can see the phase noise (~-72dBc @40kHz) of the signal. We expect that this performance is only a baseline, and will improve once a more stable reference oscillator is used. In this example, the 200MHz output from our signal generator was directly used as the frequency reference for the ADF4108.

Additional tests have validated our ability to frequency lock the YIG using the AD9956 chip. In one setup, we had a YIG output frequency of 9.6 GHz.

A5.2.7.5 Debugging the prototype PCB:

One of the key challenges we faced in getting the board to frequency lock was a design omission on the divide by 4 and divide by 8 Hittite chips. Because we are running these chips single ended, and they are differential circuits, when there is no valid input on these signals, the other differential input appears to be picking up noise and amplifying it, oscillating wildly at the output pins, and making the PLL think there was a valid high frequency signal when there was not. After consulting an applications guide from Hittite, we inserted pull down resistors to ground (using values recommended in the guide) in parallel with the blocking capacitors on the unused differential inputs, and the noise was eliminated at the expense of a slightly smaller input power range of these parts.

A second obstacle was encountered on the HMC463LP5 VGA chip. The VGA is set by a voltage present on one of the chips input pins. For our design, we included a 15 kilohm resistor and a 5 kilohm potentiometer connected to this VGA pin, and hoped to tune the output power level by adjusting the voltage on this pin. While the final version plans include a DAC output controlling the VGA, we thought the potentiometer would be sufficient for our purposes. Unfortunately, the amplifier tuning pin has two relatively low value (6.5 kilohm and 1.5 kilohm) resistors biasing the pin more effectively than our 15 kilohm resistor and 5 kilohm potentiometer. In future revisions of the PCB, we calculated that we will need bias resistors in the hundreds of ohms to override the automatic bias on the gain pin.

A third obstacle were persistent 300 kHz (and multiples) spurs we observed approximately -18dBc from the divided by 8 YIG feedback signal to the PLL. We discovered that the op amp

which was generating the -5V power rail was ringing due to the capacitance on the op amp output. Once we removed C40, the spurs disappeared.

A5.2.7.6 Key points of remaining validation:

We are still in the process of validating the entire board's functionality, examining the PCB's ability to handle 14 GHz signals using the test traces, verifying a flat transmit power spectrum, and validating the circuit with the AD9956 DDS chip. We have no data on these design goals at this time.

The next key point of debug is to understand and eliminate the power losses being experienced at higher system frequencies. The ADF4108 PLL chip has a test port where the RF input signal can be measured. In our system, the PLL RF input comes from the divided by 8 YIG output. Because the divider and amplifier are specified to produce a constant power output, we would expect this ADF4108 test port to exhibit a constant output power across the range of frequencies. Instead, for our setup, the higher the YIG output frequency, the more power losses the signals exhibited. Above 11.2 GHz (essentially our proposed mid-band), we could no longer frequency lock the YIG, because the feedback signals were not reaching the PLL. The graph below is one illustration of the issue.

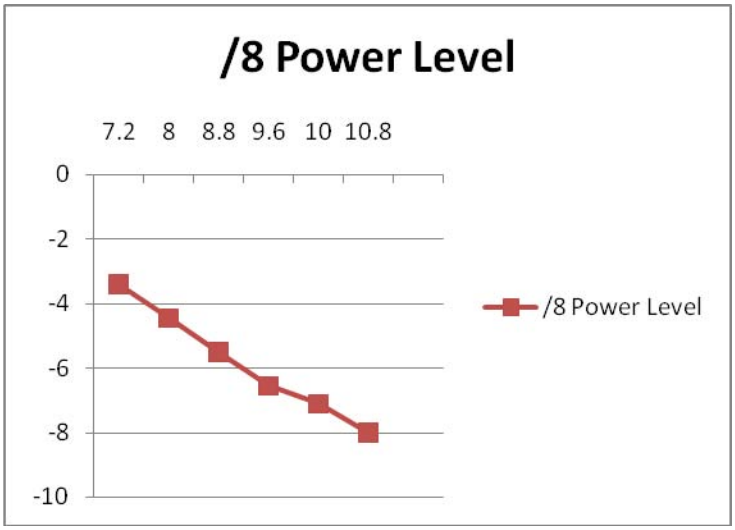

A5.2.7.7 Next Steps:

The next planned integration step is to combine all components (by adding the PLL circuitry) onto a single PCB. This single PCB will additionally reflect any changes and improvements we'd need to make to the current prototype design, based on the results of our validation testing.

A5.2.8 Additional System Level Considerations, Changes, and Enhancements:

A5.2.8.1 Changes to the receiver architecture:

While we have spent the majority of our research efforts improving on the transmit subsystem architecture, we have contemplated changes in the receiver architecture as well. The first big change is necessitated by the addition of the 540-660GHz band. Instead of a single transmit/receive path to/from the THz cell, there will be two paths for the x24 and x48 chains. On the receiver side, we will need to multiplex between the 210-270 and 540-660GHz channels. We still plan to keep the heterodyne architecture, where the RF and LO frequencies are "mixed down" to produce an IF frequency in the digital logic range. However, we have proposed some changes. The two most significant changes are (1) the incorporation of a crystal filter in the receiver path to limit IF interference, and (2) A change in the receiver IF frequency.

The use of a crystal filter allows for more flexibility in the IF frequency. Normally, the higher the IF frequency, the larger the pass band in the IF filter. With a crystal filter, a larger pass band can be avoided to some extent, eliminating noise and spurs from the input power spectrum. Our investigation into commercially available crystal filters revealed the most common filter frequencies are 10.7MHz, 21.4MHz, 45MHz, and 70MHz; however, custom filters have been built up to the 200-250MHz range as well. Increasing the IF frequency reduces the 1/f receiver noise that we may have had at 10.7MHz in the MACS Phase I system. Additionally, it will allow for the RF and LO output frequencies to be farther apart. Part of the rationale for moving the RF and LO frequencies farther apart was to reduce the crosstalk between the RF and LO transmit chains; however, as described in section A5.2.3.3, the separation of the RF and LO generation onto separate cards should achieve this goal.

We have not yet selected a new IF frequency, but a likely scenario and calculation is given here. Suppose we choose 70MHz for the IF frequency. Then, for the 210-270GHz frequency range, we would need the RF and LO signals to be 70/24 = 2.916666 MHz apart. For the 540-660GHz frequency range, the RF and LO signals would need to be 70/48 = 1.458333 MHz apart. With a 1Hz YIG output frequency resolution provided by the DDS, we can easily set the RF and LO output frequencies to achieve a precise IF value.

A5.2.8.2 Changes to the Power System Architecture:

In our phase 1 system, our FMS input voltages consisted of +24V, +15V, +12V, -12V, +5V, and +3.3V. We have investigated eliminating the +24V and +12V supplies. The +24V actually became unnecessary in Phase I when we replaced the OmniYIG YIG with the MicroLambda component. The MicroLambda YIG oscillator can accept down to +15V for its heater, whereas the OmniYIG oscillator needed +24V for its heater. Additionally, after analysis of the FMS, we have determined that any component which used +12V can also use +15V. Eliminating these two voltages from the FMS will simplify the overall FMS architecture, and removing the power supply filters on the receiver module will decrease board space and routing complexity as well. While the full MACS system will still need the +24V supply for the SAPM module, the +12V can be safely eliminated from the full system. This will reduce the power dissipated from the main AC supply and either reduce the size of the Vicor system power supply module or allow us to use the Vicor to generate an additional system voltage of our choice (TBD, maybe +5.8V).

A5.2.8.3 Changes to the MACS communications fabric:

The current MACS design uses serial (RS-232) and parallel busses for internal communications, and has limited external communications options. We have explored using Ethernet cables to replace the parallel bus for transmitting FMS receiver data to the central computer. The FPGA software comes with standard IP cores for an Ethernet controller, to handle the receiver data communications between the FMS receiver card and the central computer. Additionally, we could use an Ethernet port to connect each deployed MACS to an intranet or the internet and establish a method of remote control/monitoring for numerous MACS units arrayed in a sensor network, as shown in the picture below.

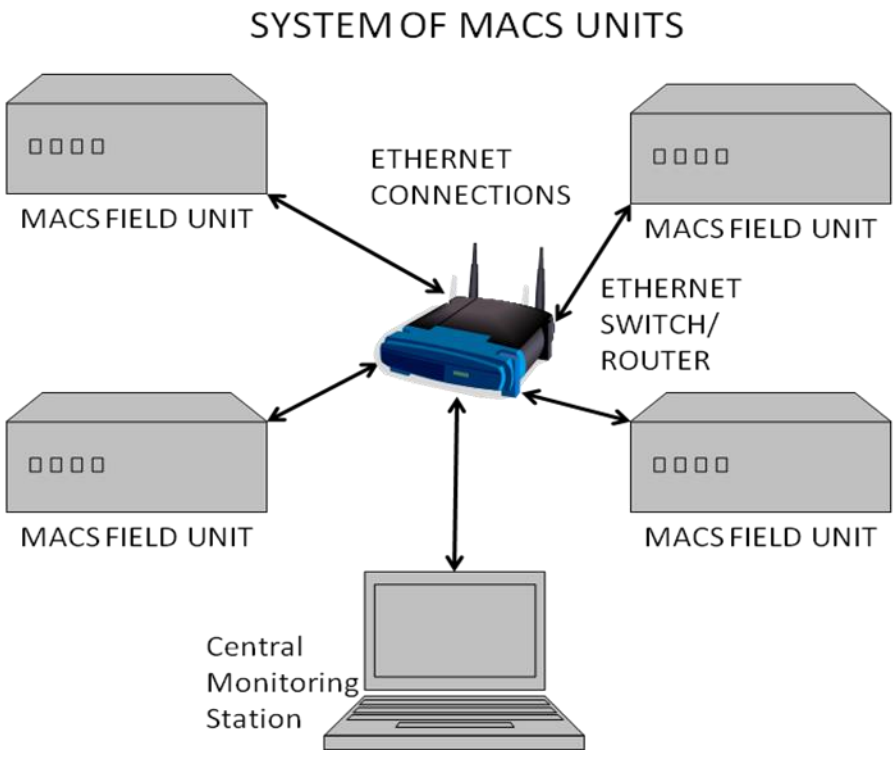

A5.2.8.4 FPGA Change:

The increase in input clock frequencies and the usage of new Ethernet IP cores in the FPGA may necessitate a change in the FPGA to a faster and perhaps larger FPGA. Specifically, from the system block diagram on page 2, we see that the FPGA is expecting clock input signals of up to 13.75GHz/64 = ~215MHz. While the Spartan 3E component is specified to be able to handle clock signals up to 300MHz, we may want to provide ourselves with more margin on this parameter. This is still under investigation.

A5.2.9 CH_3CN contamination findings on the MACS unit:

A5.2.9.1 Background:

At the conclusion of MACS Phase I, we observed two phenomenon/points of weakness with the system integrated as a whole: 1) The THz module frequency multiplier was easily susceptible to electrical shock, evidenced by the two replacement modules we needed to procure for continued proper operation, and 2) Our attempts to purge gas samples from the SAPM were unsuccessful, as the unit detected a residue of CH_3CN for weeks after exposure to a CH_3CN sample. We set out to investigate this at the beginning of our phase II work.

A5.2.9.2 Investigation and isolation of the contamination:

We received a 3rd THz frequency multiplier module and replaced the damaged unit in the ST MACS unit I. At the same time, we also installed a bypass SMM (SAPM Mission Module). The SMM is a right angle tube with quick flanges welded on either end (just like the real SMM but without sorbent material or heater). This allowed us to test if the CH_3CN contamination/residue spectrum lines would go away when the real SMM was removed. Indeed, with the bypass tube installed the residue lines did in fact go away. Because the SMM contains the sorbent material, we concluded that this was the location/source of the contamination.

Using the bypass SMM, we then connected the bottle containing our sample of CH_3CN into the MACS system and were able to introduce enough of a sample to give us very large spectral lines. Once this was done, we removed the CH_3CN source and continuously cycled the SAPM, searching for CH_3CN spectral lines. After about 5 minutes the system had leaked enough to raise the pressure within the sample cell to about 10 m-torr above minimum pressure and there were still no traces of the CH_3CN. This proved that the problem was only within the SMM, and that we did not have a condensation problem in the sample cell or an issue with the 0.5 micron filter. This helped further convince us the issue is only related to the sorbent.

A5.2.9.3 Possible system modifications:

We removed the buffer SMM and replaced it with the defective SMM, connecting it on one end to the MACS input and capping off the other end from the outside world using various KF adaptors and fittings. Although we were unable to run a standard sample analysis script (because the SMM was capped off), we utilized the manual system commands to manipulate the SAPM analyze the SMM. This required us to first pull a medium vacuum on the SMM and then prepare the cell for transfer. We next ran the "CH_3CN with no SAPM" script to look for contamination. As the gas escaped from the sorbent material in the SMM and entered the sample cell, we noticed and increase in the pressure in the cell. We were able to see faint lines of CH_3CN.

Next we connected a lab power supply to the SMM heater terminals so we could elevate the temperature to about 150 C and release whatever gas was trapped in the sorbent. (This is standard procedure for releasing chemicals from a sorbent.) As the temperature increased in the sorbent tube, more CH_3CN was released, and the spectral lines became larger and more noticeable.

By cycling the SAPM we were able to see the lines reduce in amplitude as we ran subsequent tests but they never went away completely. We postulated that we had not desorbed the material fully. With the lab thermometer connected to the tube we increased the voltage slowly until the temperature reached 200 C (the required voltage was ~ 17.5 and the current ~ 0.5A). The contamination lines initially increased to about 3 times the size of the 150 C experiment. When we cycled the SAPM and heater with the elevated temperatures the contamination almost completely went away (but not quite completely). Encouraged by this result, we increased the temperature to 220 C which is ~ 18.4 volts and we finally baked off all the contamination.

Once again we carefully manipulated the SAPM through manual control, pulling air across the sorbent bed, capping off the input to simulate what happens within a normal cycle when the SMM is installed in the box and the temperature controller is performing to specification. The residue disappeared completely.

A5.2.9.4 Conclusions and next steps:

We believe the original heater never got all of the sorbent material to 200 C due to its small coverage area even though we could see local temperatures at 200 C. When we switched over to nichrome wire (around the SMM) in phase I, we produced uniform heating but the temperature controller had a limit of 12 volts which kept the temperatures below 150 C. Both of these conditions would cause some or all of the sorbent material to hold on to a portion of the CH_3CN and then release a little during the next cycle. When the temperature was driven uniformly above 220 C the residual gas was driven off eliminating the problem. The solution is to return he voltage limit back to 24 volts and set the temperature to 220 C. We predict we will get acceptable performance from the SMM section of the SAPM.

Appendix A6.1 CC Hardware

Motherboard: Commell LV-677

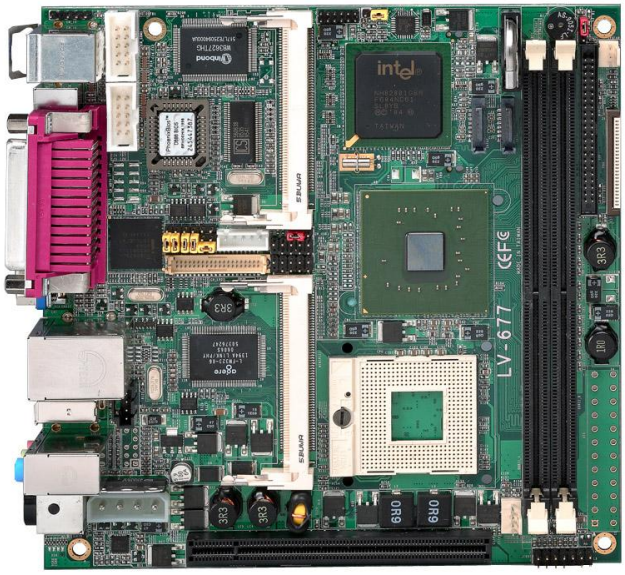

- **Support Intel Core Duo processor**
- **Onboard VGA, one Intel Gigabit LAN**
- **6x USB2.0, 2 X Mini-PCI,**
- **18-bit dual channel LVDS interface**
- **Realtek ALC880 HD Audio, serial ATA**
- **Form Factor** Mini-ITX express motherboard
- **CPU** Support Intel Core Duo/Core solo Processor
- Package type: Micro-FCPGA478
- Front side bus: 533/667MHz
- **Memory** Two DDRII 533/667MHz DIMM up to 3GB with dual channel Interleaved mode
- **Chipset** Intel 945GM &ICH7M
- **Real Time Clock** Chipset integrated RTC with onboard lithium battery
- **Watchdog Timer** Generates a system reset with internal timer for 1min/s ~ 255min/s
- **Power Management** ACPI 1.0 compliant, supports power saving mode
- **PCI Enhanced IDE** One 44-pin UltraATA33 IDE interface supports up to 2 ATAPI devices
- **Serial ATA Interface** 2 x serial ATA interface with 150MB/s transfer rate
- **VGA Interface** Intel integrated extreme GMA950 Technology
- **Video Memory** Up to 224MB shared with system memory
- **LVDS interface** Onboard 18-bit dual channel LVDS connector
- **Audio Interface** Intel integrated ICH7M with Realtek ALC880 HD Audio
- **LAN Interface** Intel 82537L Gigabit LAN
- **Solid State Disk** IDE supports 44-Pin DiskOnModule with +5V power supply
- One Compact Flash Type II
- **GPIO interface** Onboard programmable 8-bit Digital I/O interface
- **Extended Interface** One PCI Express slot support x1 & x16 add on Card
- Two Mini PCI socket to support Mini PCI Type III
- **Internal I/O Ports** RS232 port, RS232/422/485, slim FDD port, GPIO port, CDIN connector, 4x USB ports, IrDA connector, 44-pin IDE, LVDS, Audio connector
- **External I/O Ports** RJ45 LAN port, DB15 VGA port, PS/2 Keyboard/Mouse Port, 2x USB2.0 ports, IEEE1394 port , SPDIF connector, Parallel Port, Audio Line-out, Line-in and MIC-in ports
- **Power Requirement** Standard 24-pin ATX power supply (20-pin compatible)
- **Dimension** 170mm x 170mm
- **Temperature** Operating within 0~60 centigrade

Processor, Memory and Storage

- 2 GHz Intel Core 2 Duo Mobile (Merom) T7200, 667 MHz FSB
- 2 x 1 GB DDR2 667 MHz RAM
- 750GB 3.5" SATA Hard Drive

Digital IO Module

National Instruments PCIe-6536

- 32 Bit Parallel Bus
- 25 MHz maximum clock rate
- 100 MB/s maximum throughput
- Selectable voltage levels of 2.5 and 3.3 V (5V compatible)
- Synchronous and asynchronous (handshaking) timing modes
- Software Support
    - Windows and Linux Drivers
    - C, C#, LabView Support

Touchscreen Display

XENARC 700 TSV

- 7” Diagonal 800 x 480 Display
- 5 wire resistive touchscreen with USB interface
- LCD Brightness: 500 cd/m²
- Contrast Ratio: 400:1
- Viewing Angle: 140° Horizontal, 100° Vertical
- Operating Voltage Range: DC 11V ~ 24V
- Power Consumption: <8W
- Operating Temperature: 23°F ~ 158°F
- Storage Temperature: -22°F ~ 185°F
- Dimension (in): 7.75W x 4.75H x 1.38D
- Weight (lb): 1.28

Appendix A11.1

Results and Discussion of the Sensitivity and Specificity Tests

This document (and its appendices, which provide additional detail) describes the results of the tests on the samples provided by Dr. Everitt of the MET. The evaluation team prepared the samples, watched over the MACS during analyses, timed the processes, etc. The details of this are contained in their own report.

Results in the format provided by the MET are contained in Appendix C.

I. Final results of the sensitivity test

We chose to monitor 10 lines (for redundancy) of deuterated acetonitrile. Figure **1** shows a picture of these 10 lines for a mixture of 89 ppt, provided by mass flow controllers.

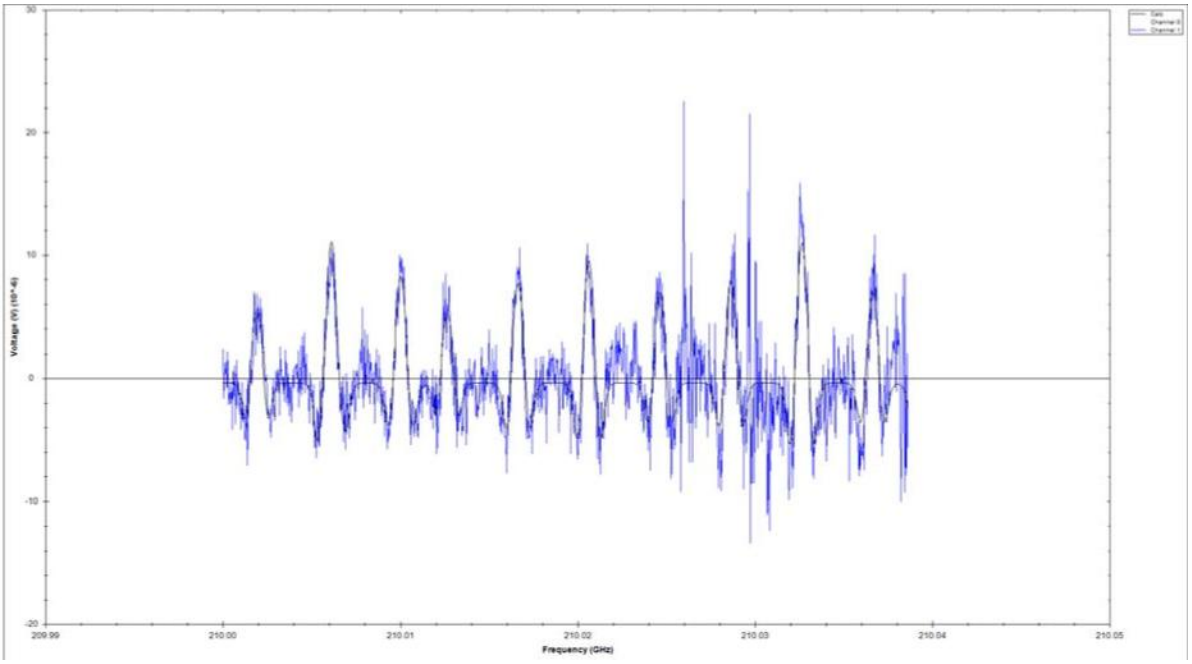

Figure 1. Spectra of 10 lines of sample for an 89 ppt sample dilution from mass flow controllers. Integration time per bin is 105 ms.

A. **Numerical analysis:** A straightforward LSQ fit to a intensity calibrated synthetic spectrum provided a concentration of 47.4 ± 0.9 for our sensitivity run in arbitrary units. When the sample is calibrated via the mass flow controlers, we obtain 89 ± 1.9 ppt. Blanks (a full data collection run with the same sample capture for the SAPM, except that the dilute sample flow was removed from the Mass Flow Controllers) were run. These runs returned results that were consistent with zero, to within the calculated uncertainty.

From these results, it is possible to plot the ROC shown in Fig. **2.** Because of the large number of independent channels in the spectral signature, the resultant ROC is very favorable. As a result, if the ROC were plotted in the usual fashion, to within the graphical presentation the curve would simply run along the axes of the plot. To make deviation from the ideal observable, we have used logarithmic axes and plotted concentrations far smaller than the 100 ppt of the

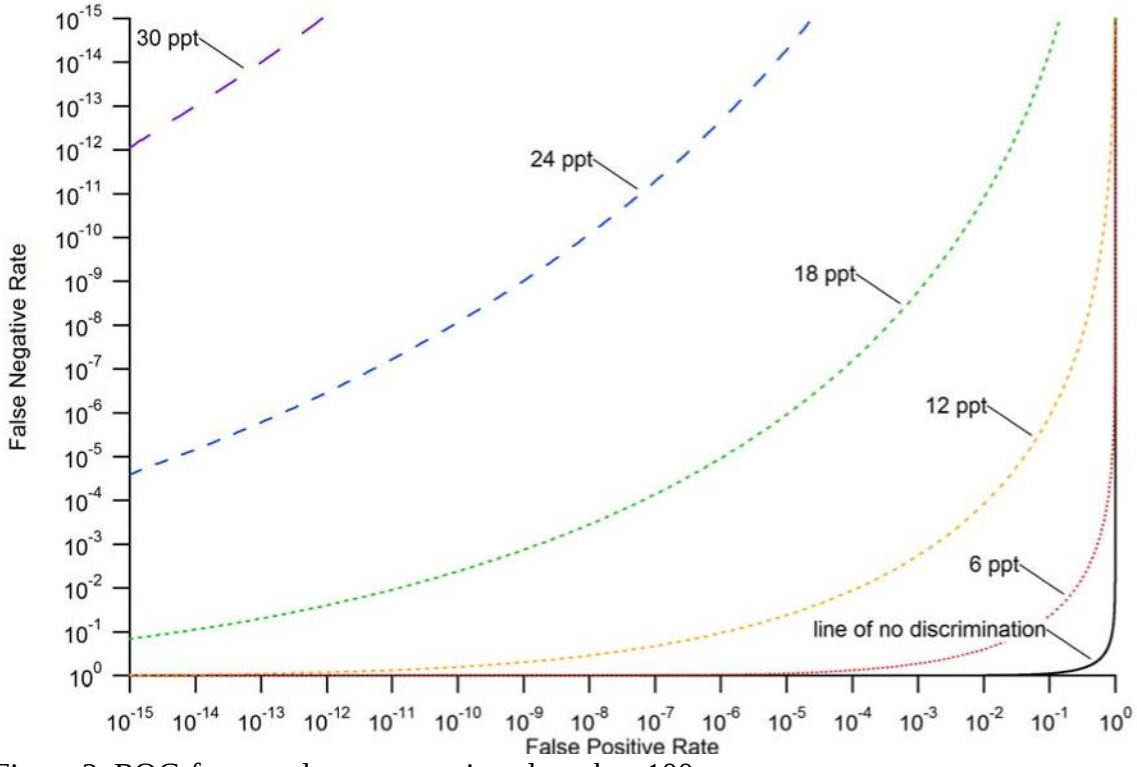

Figure 2. ROC for sample concentrations less than 100 ppt.

GNG requirements.

B. **Alternative, simple analysis:** Because believing statistics can be an overly aggressive means of establishing system sensitivity in an environment in which there could be systematic error, we offer here an alternative 'back-of-the envelope' approach based on a visual inspection of the data shown in Fig. **1.** The signal to rms noise of these lines is ~10. But in each line there are many bins (we could increase the apparent S/N in the figure by integrating over adjacent bins). If we say that 10% of the 1000 bins have significant spectral strength (100 bins for round

numbers), integrating over these for detection increases this S/N from 10 to 100. This rough calculation is consistent with the numerical analysis above.

II. Final results of the specificity tests

For these tests, the gas mixtures were ingested into the system and the spectrometer interrogated each of six frequencies for the spectral signature associated with the 31 gases - a total of ~1 80 'snippets'. This was done for 3 separate mixtures. Mixture 1 is described Table **1** and Mixtures 2 and 3 in Appendix **B.** The figure below Table 1 shows the snippets that are associated with Mixture 1. During the analyses, the spectral lines associated with each snippet appear in real time as the spectrometer samples each snippet. Appendix **C** contains this information in the MET

Unknown 1; 1 mtorr 9 mtorr air
6/23/08 15:12

Code	Name	LSQ	ERR	FoM	Result 1	Result 2	6/23 : 6/12
104	Hydrogen Cyanide (HCN)	0.000285	0.000012	24.1			
103	Cyanogen Chloride (ClCN)	0.000005	0.000009	0.6			
21	Cyanogen Bromide (BrCN)	0.000001	0.000012	0.1			
24	Acetonitrile (CH_3CN)	0.082716	0.000135	610.8	0.0827	0.0827	1.36
19	Carbonyl Sulfide (OCS)	0.000000	0.000048	0.0			
22	Methyl Fluoride (CH_3F)	0.037487	0.000110	341.7	0.0375	0.0375	1.39
25	Methyl Chloride (CH_3Cl)	-0.000180	0.000066	2.7			
9	Acrylonitrile (C_2H_3CN)	0.084564	0.000185	456.2	0.0846	0.0846	1.28
12	Sulfur Dioxide (SO_2)	0.073111	0.000207	353.9	0.0731	0.0731	1.35
15	Dichloromethane (CH_2Cl_2)	0.000125	0.000099	1.3			
29	Methyl Iodide (CH_3I)	0.141031	0.000346	407.9	0.1410	0.1410	1.09
26	Methyl Bromide (CH_3Br)	0.104535	0.000254	412.2	0.1045	0.1045	1.24
8	Difluoromethane (CH_2F_2)	0.000076	0.000152	0.5			
49	Ethylene Oxide (C_2H_4O)	-0.000147	0.000169	0.9			
52	Trifluoromethane (CHF_3)	0.095300	0.000305	312.2	0.0953	0.0953	1.37
34	Acrolein (C_3H_4O)	0.070891	0.000230	307.6	0.0709	0.0709	1.21
63	Propionitrile (C_2H_5CN)	0.084551	0.000222	381.5	0.0846	0.0846	1.41
106	Pyridine (C_5H_5N)	-0.000025	0.000144	0.2			
13	1,1 Difluoroethene (CH_2CF_2)	0.070820	0.000311	227.4	0.0708	0.0708	1.28
58	Vinyl Fluoride (C_2H_3F)	0.052326	0.000266	196.8	0.0523	0.0523	1.31
11	Vinyl Chloride (C_2H_3Cl)	-0.000357	0.000269	1.3			
35	Oxetane (C_3H_6O)	-0.000244	0.000314	0.8			
54	1,1,1 Trifluoroethane ($C_2H_3F_3$)	0.000066	0.000214	0.3			
23	Propyne (C_3H_4)	0.000396	0.000341	1.2			
62	Carbonyl Fluoride (COF_2)	0.003010	0.000489	6.2			
36	Thietane ($(CH_2)_3S$)	-0.000284	0.000495	0.6			
6	Methyl mercaptan (CH_3SH)	-0.000324	0.000604	0.5			
31	Methyl isocyanate (CH_3NCO)	-0.000361	0.000531	0.7			
2	Methanol (CH_3OH)	0.000034	0.000466	0.1			
57	Thionyl fluoride (F_2SO)	-0.000974	0.000586	1.7			
48	Vinyl bromide (CH_2CHBr)	0.083776	0.000593	141.3	0.0838	0.0838	1.19
101	1,2 dichloroethane ($C_2H_4Cl_2$)	0.090298	0.000896	100.7	0.0903	0.0903	1.52
					1.0714	1.0714	

Table 1. Results for the analysis of a 1 mTorr sample of unknown mixture #1. See text for comments on gases 104 and 62.

report format.

As we will show below, MACS is highly specific (>>0.9999) for the identification of the gases introduced into the mixture *if* there is no reaction among the gases in the mixture. However, as we will show in some detail, reactions do occur.

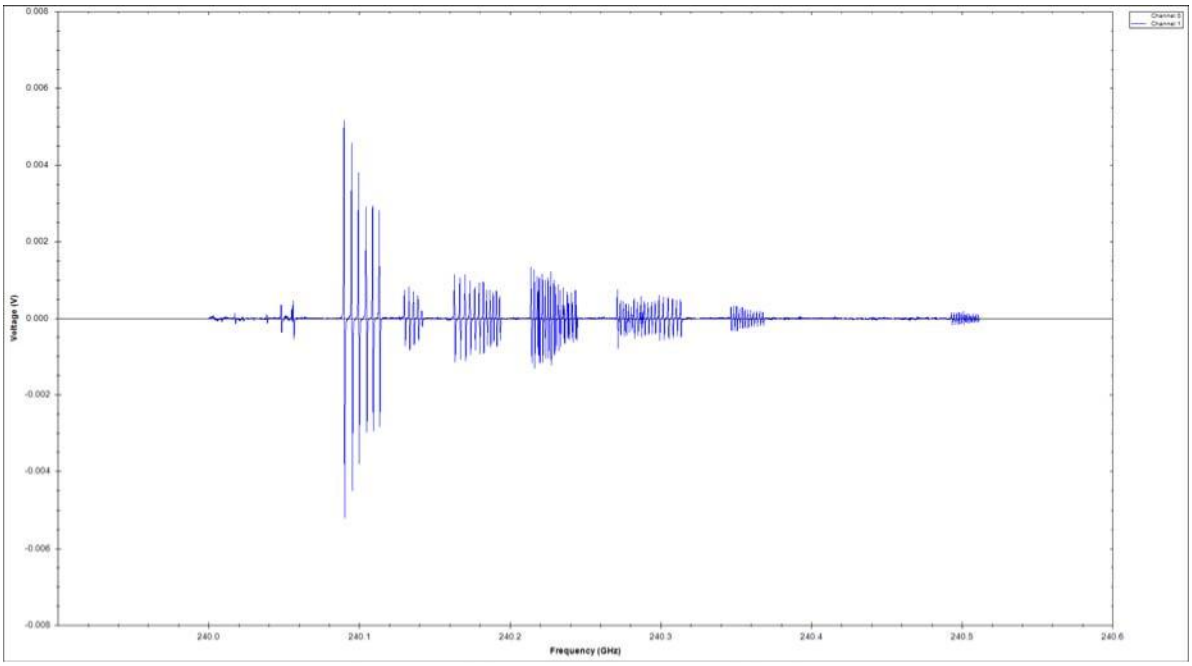

Snippets from Mixture 1.

A. Analysis: Since these results are quantitative, we should look at the LSQ column (in units of mTorr – note that making this column be in absolute pressure is a relatively recent software addition). If all of the gases had been filled at the same partial pressure, undergone no chemical reactions, and no wall absorbance in the fill system or bulbs, then all of the gases present in the mixture would have the same concentration and the other gases in the library would have concentrations statistically consistent with zero.

For Unknown 1, we note that there is a cluster of values around 0.06 mTorr in the LSQ column and that the partial pressures add to 1.07 mTorr. - very close to the nominal gas pressure introduced into MACS for this analysis. The columns labeled 'Result 1' and 'Result 2' contain concentration values only if they meet the criteria which we established in an effort to make clearer our analysis of the bulb chemistry. For 'Result 2', the single criterion is that the value for the partial pressure is greater than 0.015 mTorr. This is an attempt to select only those gases whose concentrations are roughly appropriate for a gas that was placed in the bulb and for which modest chemical or wall reactions have occurred. These are labeled as 'yes' on the MET form in Appendix **C**. 'Result 1' is a column with the criteria that the concentration be above 0.0015 mTorr and the Figure of Merit (FoM) be greater than 10 (The FoM is related to the uncertainty in the calculated concentration, but is a complex function because we must allow for the fact that in addition to system noise, we do not have perfect intensity calibration for the strong spectral lines). This lower threshold is set to still provide

strong confidence that the sample was in the mixture bulb, but to include smaller concentrations that were also in the mixture bulb – either because chemistry reduced a concentration from its initial fill partial pressure or because the species was a byproduct of a reaction. For Mixture #1, these two different criteria provide the same list. However, for Unknown Mixtures 2 and 3, there was considerable bulb chemistry and the two columns are not the same.

Additionally, on the far right there is a column (6/23:6/12) that provides the ratio of the 'Results' columns for two runs that were separated by 11 days June 23 and June 12 (the June 12 Table is not reproduced here, but is similar to the June 23 data shown in Table 1). This is to provide the MET with some measure of the long-term stability of the samples. This ratio is quite close to 1.3 (a number determined by the details of the amount of gas sampled), as is the sum of the partial pressures. A closer inspection shows that CH_3I has decreased by about 20% during these 11 days – a result consistent with the lesser stability of iodine compounds. The second point here is that the system very accurately assesses the absolute concentrations – limited primarily by the gas fill and chemistry.

In addition to the runs at 1 mTorr, we did runs at a higher pressure, ~10 mTorr. This was to provide additional information about mixture bulb chemistry and to show that some of the smaller concentrations reported here came from the mixture bulbs rather than outgassing of our system. Although we do not reproduce these tables here, for each of the gases we report observing, their signals increased appropriately (the ~10 mTorr runs are not as quantitative as the 1 mTorr runs) - showing that the observed gas originated in the mixture bulb.

The HCN is interesting. In both of the 1 mTorr and 10 mTorr runs on 6/12/08 it is absent both in the statistical analysis and in a visual inspection of the spectra. However, 11 days later it is clearly present in the '10' mTorr sample and marginally present in the 1 mTorr sample. However, we see that its concentration is about 200 times smaller than for 'full fill' gases. We view this as clear evidence that HCN was a product of the reactions in the bulb over the 11 day period. On the MET form, we have listed this as 'trace'. However, in Table 1 we have left its entry blank because it did not meet our criteria.

The other gas that merits special mention is F_2CO. If one inspects the spectra for the more sensitive '10' mTorr runs, it is clearly present on both 6/12/08 and 6/23/08. The 1 mTorr runs are consistent with this, but less certain. From the quantitative analysis, we conclude that it was present in about the same concentration on both dates, but in a concentration that was down by a large margin from a standard fill. We speculate that this was either due to air being present in the reservoir bulb used to make the mixture or that air was later introduced into the mixture. Of course, these results are also consistent with F_2CO not being one of the original fill gases, but rather being due to a reaction that quickly went to completion, thus preserving the same small concentration over the 11 day period. For the MET form, we have listed this as 'trace', but again we do not include it in Table 1 because it did not meet our criteria.

Specificity:

If we were to run the same samples many times, the results would be the same to within the noise of the system. Spectral line frequencies do not change - they are set by quantum mechanics, and

the clock in our system provides orders of magnitude overkill on the spectrometer frequencies. While it would be possible to invoke strategies similar to that used above in the sensitivity test to provide a ROC for the specificity test, since the signals are stronger here and since whatever clutter problems there are will never change, we would get even a better ROC than shown in Fig. 2.

B. Analysis of synthetic mixtures.

One means of overcoming the sample reactivity issues - thus overcoming the ambiguity of the sample mixtures - is to make a synthetic mixture via computational techniques. Accordingly, the libraries prepared on the system were provided to the MET. The MET subsequently selected gases and concentrations and made mixtures in software. These should be representative of what would be observed by the system if there were no chemical reactions.

Although we do not know what the MET did, we encouraged them to modify the libraries provided by us before preparing the mixtures to account for the fact that our system and its libraries will not have perfect absolute intensity calibration. As we have noted, this intensity information is an extremely powerful analysis tool. Again, we suggested that they consider modulating the overall library intensity on a scale that is broad in comparison to the linewidth (< 1 MHz) and narrow in comparison to the spectral interval of the spectrometer (60000 MHz).

Although the spectra of the 'mixtures' provided to us by the MET included the full 60 000 MHz bandwidth of the system, we elected to consider only the spectra within the much narrower windows which we would have sampled had we been using the MACS spectrometer. This allows us to provide the information in the same format as used for the display of the results from the real mixtures.

There are two sets of synthetic spectra: The ones from the mixtures provided to us recently, and the earlier mixtures that were provided to us as a part of the early demonstration. The results from these analyses have been entered into the MET forms in Appendix C. Here we provide additional commentary. The first three mixtures: A, B, and C are from the most recent MET mixtures. The last four Mixtures: 325a, 325b, 403, and 407 are from the earlier preliminary demonstration.

Sample2008_06_05_A.txt

Code	Name	LSQ	LSQ err	FoM	Result
104	Hydrogen Cyanide (HCN)	1.001604	0.001886	531.1	1.0016
103	Cyanogen Chloride (ClCN)	0.999708	0.001497	667.7	0.9997
21	Cyanogen Bromide (BrCN)	1.000429	0.001626	615.3	1.0004
24	Acetonitrile (CH_3CN)	1.010134	0.001666	606.3	1.0101
19	Carbonyl Sulfide (OCS)	0.993791	0.002406	413.0	0.9938
22	Methyl Fluoride (CH_3F)	1.000127	0.002340	427.4	1.0001
25	Methyl Chloride (CH_3Cl)	1.006531	0.002044	492.4	1.0065
9	Acrylonitrile (C_2H_3CN)	1.005205	0.002006	501.1	1.0052
12	Sulfur Dioxide (SO_2)	1.012727	0.002464	411.0	1.0127
15	Dichloromethane (CH_2Cl_2)	0.998912	0.002022	494.0	0.9989
29	Methyl Iodide (CH_3I)	1.000772	0.002299	435.3	1.0008
26	Methyl Bromide (CH_3Br)	0.999694	0.002136	468.0	0.9997
8	Difluoromethane (CH_2F_2)	1.001115	0.002507	399.4	1.0011
49	Ethylene Oxide (C_2H_4O)	1.010089	0.002564	394.0	1.0101
52	Trifluoromethane (CHF_3)	0.994390	0.002442	407.3	0.9944
34	Acrolein (C_3H_4O)	1.010964	0.002337	432.7	1.0110
63	Propionitrile (C_2H_5CN)	1.013344	0.002158	469.5	1.0133
106	Pyridine (C_5H_5N)	1.005505	0.001586	634.1	1.0055
13	1,1 Difluoroethene (CH_2CF_2)	1.007539	0.002706	372.3	1.0075
58	Vinyl Fluoride (C_2H_3F)	1.003076	0.002578	389.1	1.0031
11	Vinyl Chloride (C_2H_3Cl)	0.997825	0.002470	404.0	0.9978
35	Oxetane (C_3H_6O)	1.014750	0.002622	387.0	1.0148
54	1,1,1 Trifluoroethane ($C_2H_3F_3$)	0.995145	0.001757	566.4	0.9951
23	Propyne (C_3H_4)	1.012516	0.002680	377.8	1.0125
62	Carbonyl Fluoride (COF_2)	0.993736	0.002920	340.3	0.9937
36	Thietane ($(CH_2)_3S$)	1.004098	0.002812	357.1	1.0041
6	Methyl mercaptan (CH_3SH)	0.980649	0.002856	343.3	0.9806
31	Methyl isocyanate (CH_3NCO)	1.016514	0.002776	366.2	1.0165
2	Methanol (CH_3OH)	1.049101	0.002706	387.7	1.0491
57	Thionyl fluoride (F_2SO)	0.971181	0.002881	337.1	0.9712
48	Vinyl bromide (CH_2CHBr)	0.999291	0.002789	358.2	0.9993
101	1,2 dichloroethane ($C_2H_4Cl_2$)	1.024067	0.003187	321.3	1.0241
					32.1345

Sample Mixture A

For Sample Mixture A, we conclude from the Result column, that all gases were present in this mixture in equal quantity. We presume that the small variation around 1.0 comes from the suggested intensity modulation.

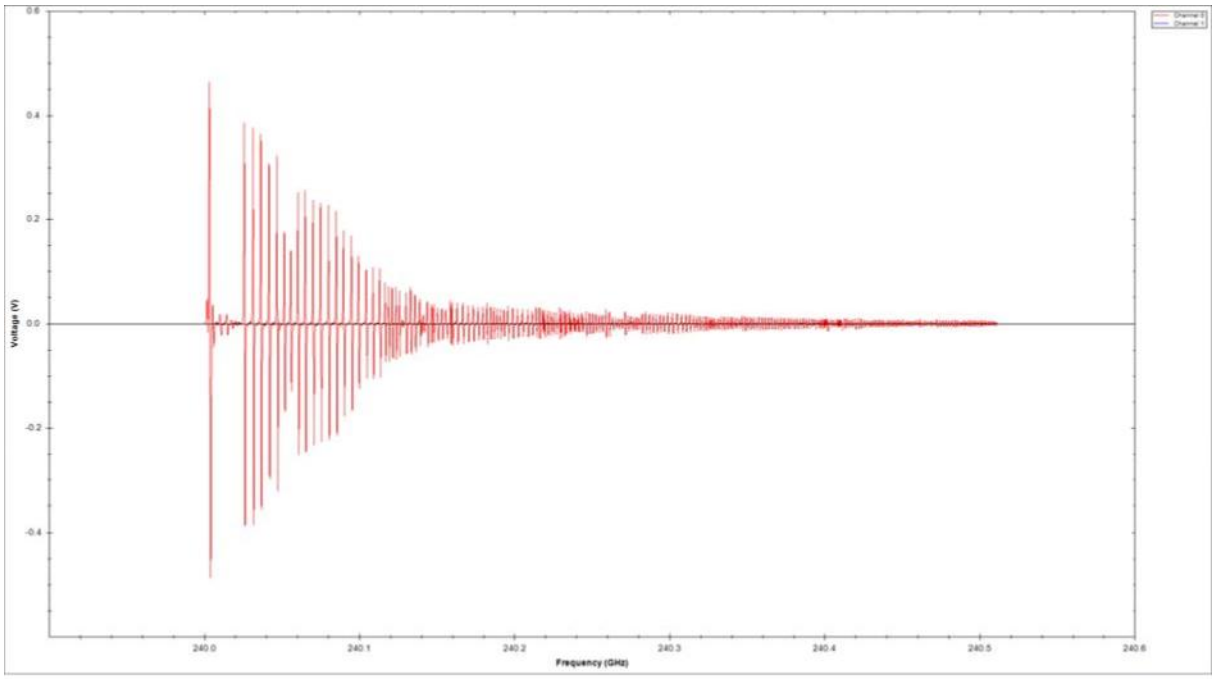

Spectral Data for Sample #A

Sample2008_06_05_B.txt

Code	Name	LSQ	LSQ err	FoM	Result
104	Hydrogen Cyanide (HCN)	1.002670	0.001891	530.3	1.0027
103	Cyanogen Chloride (ClCN)	1.000694	0.001493	670.3	1.0007
21	Cyanogen Bromide (BrCN)	1.000883	0.001625	616.1	1.0009
24	Acetonitrile (CH_3CN)	0.003247	0.000015	216.7	0.0032
19	Carbonyl Sulfide (OCS)	0.000545	0.000032	16.8	
22	Methyl Fluoride (CH_3F)	1.000006	0.002354	424.9	1.0000
25	Methyl Chloride (CH_3Cl)	0.004968	0.000047	104.6	0.0050
9	Acrylonitrile (C_2H_3CN)	1.005986	0.001820	552.9	1.0060
12	Sulfur Dioxide (SO_2)	0.005668	0.000069	82.3	0.0057
15	Dichloromethane (CH_2Cl_2)	0.000492	0.000072	6.8	
29	Methyl Iodide (CH_3I)	0.003078	0.000103	29.9	
26	Methyl Bromide (CH_3Br)	0.001357	0.000081	16.7	
8	Difluoromethane (CH_2F_2)	-0.001300	0.000096	13.6	
49	Ethylene Oxide (C_2H_4O)	1.004948	0.002464	407.8	1.0049
52	Trifluoromethane (CHF_3)	-0.002403	0.000166	14.5	
34	Acrolein (C_3H_4O)	0.002878	0.000123	23.4	
63	Propionitrile (C_2H_5CN)	0.003694	0.000107	34.4	
106	Pyridine (C_5H_5N)	1.007742	0.001512	666.3	1.0077
13	1,1 Difluoroethene (CH_2CF_2)	0.004884	0.000169	28.9	
58	Vinyl Fluoride (C_2H_3F)	0.994527	0.002410	412.7	0.9945
11	Vinyl Chloride (C_2H_3Cl)	1.003384	0.002466	406.9	1.0034
35	Oxetane (C_3H_6O)	0.003672	0.000299	12.3	
54	1,1,1 Trifluoroethane ($C_2H_3F_3$)	0.989033	0.001697	582.7	0.9890
23	Propyne (C_3H_4)	1.002802	0.002649	378.6	1.0028
62	Carbonyl Fluoride (COF_2)	-0.001199	0.000327	3.7	
36	Thietane ($(CH_2)_3S$)	-0.004284	0.000348	12.3	
6	Methyl mercaptan (CH_3SH)	-0.015386	0.000511	30.1	
31	Methyl isocyanate (CH_3NCO)	1.003372	0.002227	450.6	1.0034
2	Methanol (CH_3OH)	0.039452	0.000347	113.5	0.0395
57	Thionyl fluoride (F_2SO)	1.014731	0.002957	343.2	1.0147
48	Vinyl bromide (CH_2CHBr)	-0.000888	0.000358	2.5	
101	1,2 dichloroethane ($C_2H_4Cl_2$)	1.011802	0.002838	356.5	1.0118
					14.0959

Sample Mixture B

In this mixture we have 14 clear hits, all of which have concentrations near 1. In addition we have four others: 24, 25, 12, and 2 that we list for completeness. Inspection of the spectrum shows that 24 is indeed present (and is labeled as 'T' in the MET forms in Appendix C), but that 25, 12, and 2, with lower figures of merit are not. Although it is speculation, we believe that the small amount of gas 24 that is present is a result of small (and probably individually difficult to observe) contaminations of gas 24 in the library spectra of several of the gases that were included in the mixture. When added together these become observable because of the randomness of the noise in the 14 library gases.

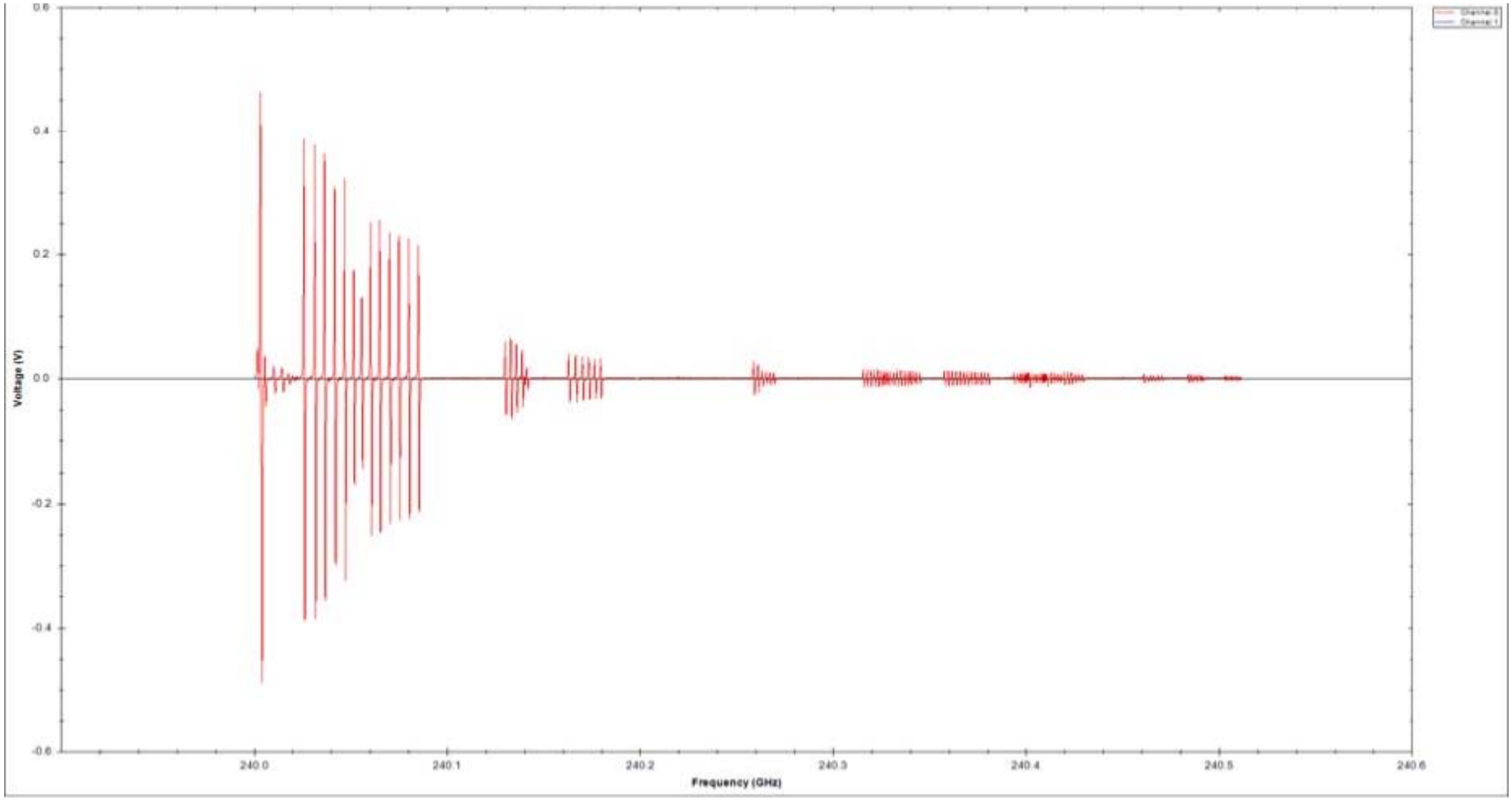

Spectral data for sample mixture B

Sample2008_06_05_C.txt

Code	Name	LSQ	LSQ err	FoM	Result
104	Hydrogen Cyanide (HCN)	-0.000010	0.000005	1.9	
103	Cyanogen Chloride (ClCN)	0.000097	0.000004	25.1	
21	Cyanogen Bromide (BrCN)	-0.000075	0.000005	15.4	
24	Acetonitrile (CH_3CN)	0.001259	0.000009	147.1	0.0013
19	Carbonyl Sulfide (OCS)	0.005472	0.000025	217.6	0.0055
22	Methyl Fluoride (CH_3F)	0.050227	0.000123	409.6	0.0502
25	Methyl Chloride (CH_3Cl)	0.000240	0.000028	8.7	
9	Acrylonitrile (C_2H_3CN)	0.000170	0.000030	5.7	
12	Sulfur Dioxide (SO_2)	-0.000713	0.000041	17.4	
15	Dichloromethane (CH_2Cl_2)	0.000060	0.000041	1.5	
29	Methyl Iodide (CH_3I)	0.201021	0.000458	439.1	0.2010
26	Methyl Bromide (CH_3Br)	-0.001482	0.000047	31.7	
8	Difluoromethane (CH_2F_2)	0.701364	0.001750	400.8	0.7014
49	Ethylene Oxide (C_2H_4O)	0.002725	0.000101	26.9	
52	Trifluoromethane (CHF_3)	-0.000895	0.000079	11.4	
34	Acrolein (C_3H_4O)	0.000913	0.000068	13.4	
63	Propionitrile (C_2H_5CN)	-0.001081	0.000061	17.8	
106	Pyridine (C_5H_5N)	0.000851	0.000059	14.3	
13	1,1 Difluoroethene (CH_2CF_2)	-0.000498	0.000097	5.1	
58	Vinyl Fluoride (C_2H_3F)	0.001023	0.000094	10.9	
11	Vinyl Chloride (C_2H_3Cl)	-0.002339	0.000111	21.1	
35	Oxetane (C_3H_6O)	0.608817	0.001241	490.4	0.6088
54	1,1,1 Trifluoroethane ($C_2H_3F_3$)	0.000416	0.000086	4.8	
23	Propyne (C_3H_4)	-0.000638	0.000134	4.8	
62	Carbonyl Fluoride (COF_2)	0.000180	0.000189	1.0	
36	Thietane ($(CH_2)_3S$)	0.000702	0.000208	3.4	
6	Methyl mercaptan (CH_3SH)	-0.000220	0.000262	0.8	
31	Methyl isocyanate (CH_3NCO)	0.006362	0.000236	27.0	
2	Methanol (CH_3OH)	0.000613	0.000192	3.2	
57	Thionyl fluoride (F_2SO)	-0.006669	0.000228	29.2	
48	Vinyl bromide (CH_2CHBr)	0.497116	0.001238	401.4	0.4971
101	1,2 dichloroethane ($C_2H_4Cl_2$)	1.012690	0.002023	500.5	1.0127
					3.0780

Sample Mixture C

Mixture C is a more interesting mixture, with a much wider variety of concentrations. 101, 48, 35, 8, 29, 22, and 19 are clearly in the mix with concentrations that vary from 1.01 down to 0.055. Gas 24 is also clearly in the spectroscopic signature as well, but we are suspicious that this is due to the library contamination discussed in mixture B, rather than it being introduced in a concentration of 0.0013. Again, we label it at 'T' in Appendix C.

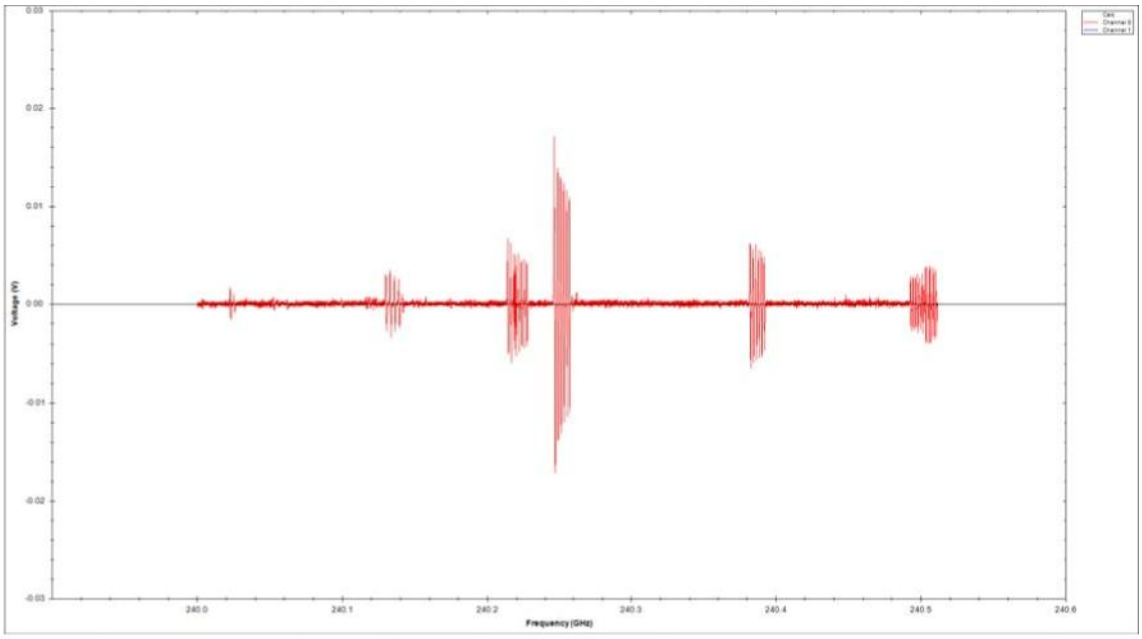

Spectra from sample mixture C

Sample0325a

Code	Name	LSQ	LSQ err	FoM	Result
104	Hydrogen Cyanide (HCN)	1.019273	0.001913	532.8	1.0193
103	Cyanogen Chloride (ClCN)	0.996759	0.001496	666.2	0.9968
21	Cyanogen Bromide (BrCN)	1.000432	0.001625	615.5	1.0004
24	Acetonitrile (CH_3CN)	1.023779	0.001680	609.3	1.0238
19	Carbonyl Sulfide (OCS)	0.994932	0.002405	413.6	0.9949
22	Methyl Fluoride (CH_3F)	1.002626	0.002352	426.4	1.0026
25	Methyl Chloride (CH_3Cl)	1.003058	0.002039	492.0	1.0031
9	Acrylonitrile (C_2H_3CN)	0.995763	0.001986	501.5	0.9958
12	Sulfur Dioxide (SO_2)	1.017737	0.002434	418.2	1.0177
15	Dichloromethane (CH_2Cl_2)	1.000694	0.002021	495.2	1.0007
29	Methyl Iodide (CH_3I)	0.999957	0.002298	435.1	1.0000
26	Methyl Bromide (CH_3Br)	1.000342	0.002136	468.4	1.0003
8	Difluoromethane (CH_2F_2)	1.000212	0.002503	399.6	1.0002
49	Ethylene Oxide (C_2H_4O)	1.005311	0.002557	393.1	1.0053
52	Trifluoromethane (CHF_3)	0.992120	0.002427	408.8	0.9921
34	Acrolein (C_3H_4O)	1.023526	0.002233	458.4	1.0235
63	Propionitrile (C_2H_5CN)	1.014319	0.002013	504.0	1.0143
106	Pyridine (C_5H_5N)	1.009963	0.001580	639.2	1.0100
13	1,1 Difluoroethene (CH_2CF_2)	1.002462	0.002691	372.5	1.0025
58	Vinyl Fluoride (C_2H_3F)	1.001073	0.002577	388.5	1.0011
11	Vinyl Chloride (C_2H_3Cl)	0.999181	0.002453	407.4	0.9992
35	Oxetane (C_3H_6O)	1.015023	0.002645	383.8	1.0150
54	1,1,1 Trifluoroethane ($C_2H_3F_3$)	0.995287	0.001760	565.6	0.9953
23	Propyne (C_3H_4)	1.010906	0.002664	379.4	1.0109
62	Carbonyl Fluoride (COF_2)	-0.009907	0.000384	25.8	
36	Thietane ($(CH_2)_3S$)	-0.000192	0.000524	0.4	
6	Methyl mercaptan (CH_3SH)	-0.021281	0.000613	34.7	
31	Methyl isocyanate (CH_3NCO)	-0.000371	0.000526	0.7	
2	Methanol (CH_3OH)	0.019002	0.000450	42.2	
57	Thionyl fluoride (F_2SO)	-0.018569	0.000482	38.5	
48	Vinyl bromide (CH_2CHBr)	0.002327	0.000442	5.3	
101	1,2 dichloroethane ($C_2H_4Cl_2$)	0.028003	0.000832	33.7	
					24.1247

Mixture 325a

This is one of the early demonstration mixtures. Clearly the first 24 gases are present and none of the last 8.

104	Hydrogen Cyanide (HCN)	0.991670	0.001852	535.6	0.9917
103	Cyanogen Chloride (ClCN)	0.992684	0.001483	669.2	0.9927
21	Cyanogen Bromide (BrCN)	0.999744	0.001625	615.4	0.9997
24	Acetonitrile (CH_3CN)	0.980916	0.001621	605.0	0.9809
19	Carbonyl Sulfide (OCS)	1.002069	0.002418	414.4	1.0021
22	Methyl Fluoride (CH_3F)	0.999775	0.002344	426.6	0.9998
25	Methyl Chloride (CH_3Cl)	0.999731	0.002032	492.1	0.9997
9	Acrylonitrile (C_2H_3CN)	0.938512	0.001862	504.1	0.9385
12	Sulfur Dioxide (SO_2)	0.957560	0.002347	407.9	0.9576
15	Dichloromethane (CH_2Cl_2)	0.980461	0.001977	496.0	0.9805
29	Methyl Iodide (CH_3I)	0.997639	0.002289	435.9	0.9976
26	Methyl Bromide (CH_3Br)	1.000799	0.002134	468.9	1.0008
8	Difluoromethane (CH_2F_2)	0.999305	0.002497	400.2	0.9993
49	Ethylene Oxide (C_2H_4O)	1.001525	0.002540	394.4	1.0015
52	Trifluoromethane (CHF_3)	0.999803	0.002437	410.2	0.9998
34	Acrolein (C_3H_4O)	0.809554	0.002014	402.0	0.8096
63	Propionitrile (C_2H_5CN)	0.859128	0.001788	480.4	0.8591
106	Pyridine (C_5H_5N)	1.004116	0.001557	645.0	1.0041
13	1,1 Difluoroethene (CH_2CF_2)	0.996402	0.002672	372.8	0.9964
58	Vinyl Fluoride (C_2H_3F)	0.998715	0.002560	390.2	0.9987
11	Vinyl Chloride (C_2H_3Cl)	0.951176	0.002393	397.4	0.9512
35	Oxetane (C_3H_6O)	1.005122	0.002599	386.7	1.0051
54	1,1,1 Trifluoroethane ($C_2H_3F_3$)	0.994816	0.001749	568.8	0.9948
23	Propyne (C_3H_4)	0.996972	0.002617	381.0	0.9970
62	Carbonyl Fluoride (COF_2)	-0.003067	0.000170	18.1	
36	Thietane ($(CH_2)_3S$)	0.006496	0.000224	29.1	
6	Methyl mercaptan (CH_3SH)	0.000015	0.000216	0.1	
31	Methyl isocyanate (CH_3NCO)	-0.000744	0.000223	3.3	
2	Methanol (CH_3OH)	0.001985	0.000180	11.0	
57	Thionyl fluoride (F_2SO)	0.004839	0.000213	22.7	
48	Vinyl bromide (CH_2CHBr)	0.000142	0.000183	0.8	
101	1,2 dichloroethane ($C_2H_4Cl_2$)	-0.013304	0.000309	43.1	
					23.4582

Mixture 325 b

This is one of the early demonstration mixtures. The first 24 are in the mixture. All but two of these have concentrations very close to one, with the difference attributable to the aforementioned intensity modulation. 34 and 63, however, have concentrations that are smaller by 15% and 20%, respectively. While it is possible that this is due to intensity modulation, it seems more likely to be due to a small, but real concentration variation.

Code	Name	LSQ	LSQ err	FoM	Result
104	Hydrogen Cyanide (HCN)	0.000405	0.000005	82.5	
103	Cyanogen Chloride (ClCN)	1.093686	0.001631	670.4	1.0937
21	Cyanogen Bromide (BrCN)	-0.000026	0.000005	5.5	
24	Acetonitrile (CH_3CN)	0.006157	0.000014	453.7	0.0062
19	Carbonyl Sulfide (OCS)	-0.000591	0.000021	27.9	
22	Methyl Fluoride (CH_3F)	0.000121	0.000022	5.4	
25	Methyl Chloride (CH_3Cl)	0.000634	0.000027	23.9	
9	Acrylonitrile (C_2H_3CN)	0.002465	0.000031	80.7	
12	Sulfur Dioxide (SO_2)	0.000546	0.000044	12.4	
15	Dichloromethane (CH_2Cl_2)	-0.000093	0.000042	2.2	
29	Methyl Iodide (CH_3I)	-0.000165	0.000060	2.7	
26	Methyl Bromide (CH_3Br)	-0.000061	0.000050	1.2	
8	Difluoromethane (CH_2F_2)	0.000696	0.000061	11.4	
49	Ethylene Oxide (C_2H_4O)	0.504135	0.001226	411.1	0.5041
52	Trifluoromethane (CHF_3)	-0.001298	0.000087	14.9	
34	Acrolein (C_3H_4O)	1.011987	0.001712	591.2	1.0120
63	Propionitrile (C_2H_5CN)	0.003466	0.000066	52.8	
106	Pyridine (C_5H_5N)	-0.000224	0.000063	3.5	
13	1,1 Difluoroethene (CH_2CF_2)	-0.000829	0.000100	8.3	
58	Vinyl Fluoride (C_2H_3F)	0.000401	0.000108	3.7	
11	Vinyl Chloride (C_2H_3Cl)	0.000101	0.000117	0.9	
35	Oxetane (C_3H_6O)	0.002375	0.000154	15.4	
54	1,1,1 Trifluoroethane ($C_2H_3F_3$)	0.198227	0.000364	544.1	0.1982
23	Propyne (C_3H_4)	0.002681	0.000134	19.9	
62	Carbonyl Fluoride (COF_2)	0.000417	0.000198	2.1	
36	Thietane ($(CH_2)_3S$)	0.002971	0.000218	13.6	
6	Methyl mercaptan (CH_3SH)	-0.003495	0.000286	12.2	
31	Methyl isocyanate (CH_3NCO)	-0.002491	0.000258	9.7	
2	Methanol (CH_3OH)	0.004112	0.000227	18.1	
57	Thionyl fluoride (F_2SO)	0.003805	0.000232	16.4	
48	Vinyl bromide (CH_2CHBr)	0.003557	0.000232	15.4	
101	1,2 dichloroethane ($C_2H_4Cl_2$)	0.009728	0.000402	24.2	
					2.8142

Mixture 403b

This is one of the early demonstration mixtures. This mixture has 4 clear components and a trace of gas 24. While this gas is clearly present as a trace spectroscopically, again we believe that it is due to a library contamination rather than its addition in such a small concentration to the mixture.

104	Hydrogen Cyanide (HCN)	0.013374	0.000041	324.7	0.0134
103	Cyanogen Chloride (ClCN)	0.996905	0.001493	667.9	0.9969
21	Cyanogen Bromide (BrCN)	0.000078	0.000009	8.6	
24	Acetonitrile (CH_3CN)	0.014759	0.000028	522.8	0.0148
19	Carbonyl Sulfide (OCS)	0.995406	0.002409	413.2	0.9954
22	Methyl Fluoride (CH_3F)	-0.000188	0.000032	5.9	
25	Methyl Chloride (CH_3Cl)	0.000876	0.000048	18.4	
9	Acrylonitrile (C_2H_3CN)	0.999225	0.001708	585.1	0.9992
12	Sulfur Dioxide (SO_2)	0.000838	0.000065	12.9	
15	Dichloromethane (CH_2Cl_2)	-0.001387	0.000067	20.6	
29	Methyl Iodide (CH_3I)	1.002280	0.002297	436.4	1.0023
26	Methyl Bromide (CH_3Br)	0.001822	0.000077	23.7	
8	Difluoromethane (CH_2F_2)	0.001496	0.000090	16.7	
49	Ethylene Oxide (C_2H_4O)	0.002738	0.000103	26.7	
52	Trifluoromethane (CHF_3)	-0.002995	0.000152	19.7	
34	Acrolein (C_3H_4O)	1.014582	0.002001	507.1	1.0146
63	Propionitrile (C_2H_5CN)	1.026946	0.001808	568.1	1.0269
106	Pyridine (C_5H_5N)	1.022137	0.001381	740.0	1.0221
13	1,1 Difluoroethene (CH_2CF_2)	1.001333	0.002674	374.5	1.0013
58	Vinyl Fluoride (C_2H_3F)	0.002734	0.000160	17.1	
11	Vinyl Chloride (C_2H_3Cl)	1.007487	0.002293	439.3	1.0075
35	Oxetane (C_3H_6O)	1.015003	0.002413	420.7	1.0150
54	1,1,1 Trifluoroethane ($C_2H_3F_3$)	1.000202	0.001755	570.0	1.0002
23	Propyne (C_3H_4)	1.012021	0.002664	379.9	1.0120
62	Carbonyl Fluoride (COF_2)	-0.004328	0.000290	14.9	
36	Thietane ($(CH_2)_3S$)	0.002403	0.000399	6.0	
6	Methyl mercaptan (CH_3SH)	-0.002809	0.000460	6.1	
31	Methyl isocyanate (CH_3NCO)	0.001712	0.000392	4.4	
2	Methanol (CH_3OH)	0.017522	0.000335	52.3	
57	Thionyl fluoride (F_2SO)	-0.009652	0.000358	26.9	
48	Vinyl bromide (CH_2CHBr)	-0.005573	0.000354	15.7	
101	1,2 dichloroethane ($C_2H_4Cl_2$)	0.033254	0.000621	53.6	
					12.1217

Mixture 407

This is one of the early demonstration mixtures. Again, there are clearly 12 gases present, plus two traces gases (104 and 24) that are spectroscopically observable. We believe that these two trace gases are due to library contamination rather than their inclusion as trace species in the mixtures.

Appendix A. The Demonstrations and Tests - Systems and Procedures

All of the results contained in the main body of the report and the following Appendix which contains the results for the several additional mixtures were done using the system as described below and were done on samples prepared under the supervision of the MET team. The gases included in these mixtures were (and are) unknown to the MACS team.

In addition, a number of demonstrations and tests on other mixtures and with precursor systems were also carried out. While we focus on the final supervised tests, we provide information from several additional tests and demonstration that will provide richer information to the MET.

1. Systems: The systems that were used included the final 1 cu ft MACS system as well as precursors. As we will describe, these systems are functionally equivalent, except for the size and packaging, and provide very similar capability. This is because all systems used the same Terahertz Module and SAPM, the differences are in well defined electronic components. The earlier versions were used to provide baselines and feedback both to us and the MET as to how to deal with the sample challenges which are describe in this document.

a. The early demonstration made use of

i. a large external synthesizer and a smaller external synthesizer to provide the drives for the transmit and receive chains of the TM, respectively.

ii. A laboratory lock-in amplifier for signal recovery.

iii. An external PC rather than the PC in the MACS box

b. The tests and demonstrations made immediately after the final samples were prepared on and about June 12, 2008.

i. Replaced the large synthesizers with a compact source module, which would fit into the 1 cu. ft. box. However, just before the mixtures were made, the driver (a 1" x 1" PC board) in a MicroLamda YIG filter died and we used an external driver for this YIG. The manufacturer rapidly provided a replacement board and the filter was repaired. While this had no impact on the performance of the system, the driver would not have fit into the 1 cu ft chassis.

ii. The laboratory lock-in of 'a' was replaced with a functionally equivalent board, resident in the computer.

iii. We were still doing some software development, using software tools in place on our lab computer. This lab computer was used to run the system rather than the computer that was within the 1 cu ft box. The digital card that replaced the lock-in was also resident in this computer. Since the two computers are functionally very similar (and MACS does not stress either of them), this had no impact on the operational characteristics of the system.

c. The final demonstrations reported here were run on a system that was contained within the 1 cu ft MACS chassis. With the replacement of the YIG driver board, the driver module fit into its place in the MACS chassis. Operation (and the lock-in board) was transferred to the on board computer. We ordinarily operate this system from an external monitor so that observers can monitor the operation of the system. This provided MET observers real time access to the

internal operation of the system, thus augmenting and providing validation to the more compact statistical output.

2. Operational modes: In the spirit of 'Mission Adaptable' the software provides a number of user selected options. These include a choice of operational modes, ranging from 'one button and report' to modes with considerable operator involvement. The former are more typical of what users might choose, while the latter are used for system diagnostics and optimization. Additionally, operator chosen parameters can be input into the system in a convenient format. Examples of these might include length of time for sample collection, choice of species to be monitored, etc.

i. The sensitivity demonstrations

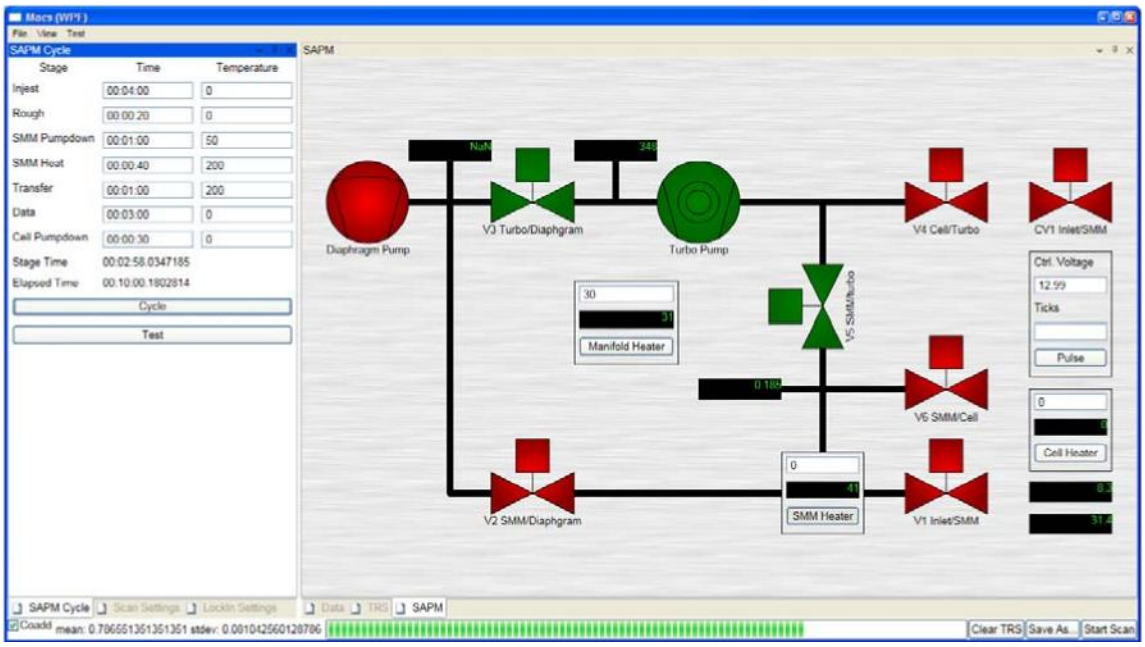

Figure A. 1 SAPM Control Panel

Figure A. 1 shows the clickable input screen used to run the SAPM/THz combination. Input choices are entered into the parameter box on the left. In addition, the system can provide real time measurement of parameters such as the cell pressure, sorbent pressure, sorbent temperature, etc. in graphical form. Figure 1 in the main section is an example of its spectral output. Statistical concentrations are also obtainable numerically.

ii. The specificity demonstrations

Throughout this document are displayed both numerical output that is obtainable from the system as well as the spectral snippets. The spectral snippets are displayed in real time so that the progress of the analysis as the spectrometer interrogates the different spectral signatures can be observed.

Appendix B. Samples and results from the analyses of Unknowns 2 and 3.

For the evaluation of this project, a number of samples were prepared by Dr. Everitt and his associates on the behalf of the MET. They fell into two general categories: (1) mixtures for specificity tests, and (2) dilute samples for sensitivity test. Both of these are challenging and additional details will be provided by Dr. Everitt and the MET. For completeness, we will also describe them here.

(1) The dilute samples

a. The GNG criteria require the preparation of a sample diluted to 100 ppt. This is extremely challenging, from the point of view of preparing the dilution, insuring that the dilution does not change because of wall effects in the storage container or chemistry, and having a volume and pressure of sample that presents a constant 1 atmospheric pressure for MACS to ingest. The MET decided that this difficulty could be reduced by using the well-known abundance of an isotopic species, deuterium, as a part of the dilution to 100 ppt.

b. The first approach that was adopted is common in EPA circles, the use of Tedlar bags. This allowed mixtures to be made remotely (typically in Huntsville) and transported to OSU, but at a cost of sample deterioration with time. The second was the use of a 100 ppm certified mixture and calibrated gas mass flow meters to further reduce the sample pressure to 0.2 ppm. With the deuterium ratio molecular ratio (and taking account of the three identical hydrogen nuclei) being 0.000 149 x 3, yielding a sample of 89 ppt.

c. MACS showed that the concentration in these bags declined with time. The first bags that were mixed in Huntsville for the early demonstration, showed no detectable sample (after a period of ~ 6 wks). MACS determined that the second set of bags filled in Huntsville contained 58 ppt after ~ 7 days (June 12) - from a presumed fill of 100 ppt. Finally, on June 23, the bag filled in Huntsville was tested again and found to contain less than 5 ppt. This shows that the absence of detectable sample in the bags used for the early demonstration was simply a result of the ~ 40 days that passed between their filling and the experimental runs.

Bags that were fill on site at OSU (some under the supervision of the MET representatives) were consistent with the result obtained directly from the Mass Flow Controllers.

(2) The Unknown mixtures:

a. As was expected, the earlier demonstration showed that substantial reactions took place in the sample bulb mixtures. Thus, there is no unambiguous test that simply compares the gases that were introduced into the bulbs with the gases detected by MACS. The report of the demonstration showed that were there significant modifications from the original fills due to these reactions. However, it also showed that MACS could unambiguously demonstrate that observed gases came from the mixture bulbs, not from MACS cell contamination. This was done by the simple expediency of introducing different amounts of sample from the mixture bulb and showing that the concentrations measured by MACS scale with the amount of sample. As noted in the main body of this report, this same procedure was adopted here as well, but in a more quantitative way.

However, MACS cannot judge *intent*. It is scientifically possible that some of the small concentrations that we detect and label 'trace' were intentionally placed in the bulbs at the time of their filling.

b. Results for mixture #2 and mixture #3

Table **2** shows the results for Unknown Mixture #2. While the results are similar to that of Mixture #1, there were clearly more chemical reactions in this mixture. Although gas 106 (pyridine) and 6 (CH_3SH) passed both of our threshold tests, this was largely due to a generous definition of concentration range associated with 'small' chemical reaction because their concentrations are down by about a factor of 5 from the other 'full fill' species. Additionally, gases 2 (CH_3OH) and 11 (C_2H_3Cl) are clearly present, but at a concentration down by a somewhat larger factor. On the MET form, these gases were listed as 'trace'. Clearly, there were more reaction in sample 2 and there is something of a continuum as you go from the lower

Unknown 2; 1 mtorr 9 mtorr air
6/24/08 13:51

Code	Name	LSQ	ERR	FoM	Result 1	Result 2
104	Hydrogen Cyanide (HCN)	0.000115	0.000012	9.7		
103	Cyanogen Chloride (ClCN)	-0.000005	0.000009	0.6		
21	Cyanogen Bromide (BrCN)	0.000015	0.000012	1.2		
24	Acetonitrile (CH_3CN)	0.000249	0.000020	12.3		
19	Carbonyl Sulfide (OCS)	0.107775	0.000280	385.2	0.1078	0.1078
22	Methyl Fluoride (CH_3F)	0.000891	0.000056	15.9		
25	Methyl Chloride (CH_3Cl)	0.092827	0.000202	459.9	0.0928	0.0928
9	Acrylonitrile (C_2H_3CN)	-0.000190	0.000077	2.5		
12	Sulfur Dioxide (SO_2)	0.095918	0.000257	372.6	0.0959	0.0959
15	Dichloromethane (CH_2Cl_2)	0.000089	0.000097	0.9		
29	Methyl Iodide (CH_3I)	0.000240	0.000112	2.1		
26	Methyl Bromide (CH_3Br)	0.000048	0.000113	0.4		
8	Difluoromethane (CH_2F_2)	0.000184	0.000152	1.2		
49	Ethylene Oxide (C_2H_4O)	0.082768	0.000294	281.2	0.0828	0.0828
52	Trifluoromethane (CHF_3)	0.137283	0.000392	350.3	0.1373	0.1373
34	Acrolein (C_3H_4O)	-0.000311	0.000160	1.9		
63	Propionitrile (C_2H_5CN)	0.000120	0.000143	0.8		
106	Pyridine (C_5H_5N)	0.015251	0.000146	104.1	0.0153	0.0153
13	1,1 Difluoroethene (CH_2CF_2)	-0.000082	0.000246	0.3		
58	Vinyl Fluoride (C_2H_3F)	0.070425	0.000287	245.8	0.0704	0.0704
11	Vinyl Chloride (C_2H_3Cl)	0.010919	0.000271	40.3	0.0109	
35	Oxetane (C_3H_6O)	0.099304	0.000408	243.2	0.0993	0.0993
54	1,1,1 Trifluoroethane ($C_2H_3F_3$)	0.000114	0.000214	0.5		
23	Propyne (C_3H_4)	0.062817	0.000384	163.7	0.0628	0.0628
62	Carbonyl Fluoride (COF_2)	-0.000858	0.000488	1.8		
36	Thietane ($(CH_2)_3S$)	0.105900	0.000575	184.2	0.1059	0.1059
6	Methyl mercaptan (CH_3SH)	0.016827	0.000607	27.7	0.0168	0.0168
31	Methyl isocyanate (CH_3NCO)	-0.000821	0.000525	1.6		
2	Methanol (CH_3OH)	0.002385	0.000466	5.1	0.0024	
57	Thionyl fluoride (F_2SO)	-0.000275	0.000586	0.5		
48	Vinyl bromide (CH_2CHBr)	-0.000741	0.000546	1.4		
101	1,2 dichloroethane ($C_2H_4Cl_2$)	0.004289	0.000864	5.0		
					0.9004	0.8871

Table 2. Results from Unknown Mixture #2.

concentration 'yes' gases to the 'trace' gases.

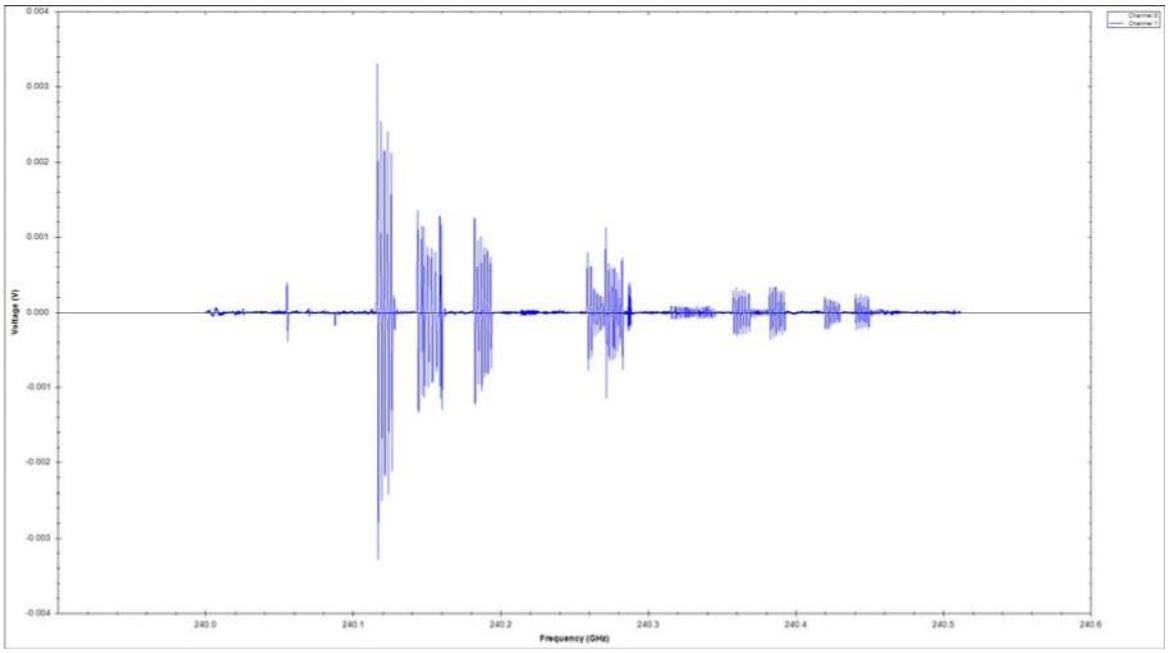

Snippets from mixture 2

Table **3** shows the results for Unknown Mixture #3. Again, there are a number of gases that are clearly present in concentrations consistent with a full fill, but two others that are also clearly present: 25 (CH_3Cl) and 12 (SO_2). Unlike sample 2, these trace gases have significantly smaller concentrations than the 'yes' gases.

For both of these mixtures, analyses of the higher gas pressures were also done. These measurements provide additional verification of these results – usually by showing a much larger concentration because of the larger gas fill from the mixture bulbs. Included in this class are gas 25 (CH_3Cl) and gas 2 (SO_2) from sample #3. While the chemistry that could produce CH_3Cl seems plausible, chemistry to produce SO_2 is less obvious (but any number of reactions could remove SO_2 if it were one of the original 'full fill' gases). However this is a real result - the increased strength that came from a larger fill of gas from unknown mixture #3 clearly shows that the sample is comes from the mixture bulb, not an impurity in our system.

Unknown 3; 1 mtorr 9 mtorr air
6/23/2008 16:44:04 PM

Code	Name	LSQ	ERR	FOM	Result 1	Result 2
104	Hydrogen Cyanide (HCN)	0.073047	0.000188	388.4	0.0730	0.0730
103	Cyanogen Chloride (ClCN)	0.159923	0.000242	659.7	0.1599	0.1599
21	Cyanogen Bromide (BrCN)	0.212470	0.000339	626.9	0.2125	0.2125
24	Acetonitrile (CH_3CN)	0.116772	0.000197	593.9	0.1168	0.1168
19	Carbonyl Sulfide (OCS)	0.000141	0.000048	2.9		
22	Methyl Fluoride (CH_3F)	0.000012	0.000060	0.2		
25	Methyl Chloride (CH_3Cl)	0.003433	0.000067	51.5	0.0034	
9	Acrylonitrile (C_2H_3CN)	0.115649	0.000244	473.8	0.1156	0.1156
12	Sulfur Dioxide (SO_2)	0.008199	0.000101	81.0	0.0082	
15	Dichloromethane (CH_2Cl_2)	-0.000062	0.000098	0.6		
29	Methyl Iodide (CH_3I)	0.000101	0.000113	0.9		
26	Methyl Bromide (CH_3Br)	0.000297	0.000113	2.6		
8	Difluoromethane (CH_2F_2)	-0.000018	0.000152	0.1		
49	Ethylene Oxide (C_2H_4O)	-0.000204	0.000169	1.2		
52	Trifluoromethane (CHF_3)	0.000713	0.000182	3.9		
34	Acrolein (C_3H_4O)	0.001084	0.000159	6.8		
63	Propionitrile (C_2H_5CN)	0.118905	0.000294	404.0	0.1189	0.1189
106	Pyridine (C_5H_5N)	-0.000090	0.000144	0.6		
13	1,1 Difluoroethene (CH_2CF_2)	0.001366	0.000247	5.5		
58	Vinyl Fluoride (C_2H_3F)	0.000463	0.000251	1.8		
11	Vinyl Chloride (C_2H_3Cl)	-0.000022	0.000270	0.1		
35	Oxetane (C_3H_6O)	0.000134	0.000316	0.4		
54	1,1,1 Trifluoroethane ($C_2H_3F_3$)	0.000149	0.000214	0.7		
23	Propyne (C_3H_4)	0.001014	0.000342	3.0		
62	Carbonyl Fluoride (COF_2)	0.000274	0.000490	0.6		
36	Thietane ($(CH_2)_3S$)	-0.000456	0.000500	0.9		
6	Methyl mercaptan (CH_3SH)	0.000771	0.000605	1.3		
31	Methyl isocyanate (CH_3NCO)	0.085035	0.000605	140.5	0.0850	0.0850
2	Methanol (CH_3OH)	0.059406	0.000490	121.3	0.0594	0.0594
57	Thionyl fluoride (F_2SO)	0.138215	0.000720	192.0	0.1382	0.1382
48	Vinyl bromide (CH_2CHBr)	-0.001295	0.000548	2.4		
101	1,2 dichloroethane ($C_2H_4Cl_2$)	0.003836	0.000860	4.5		
					1.0911	1.0794

Table 3. Results from Unknown Mixture #3.

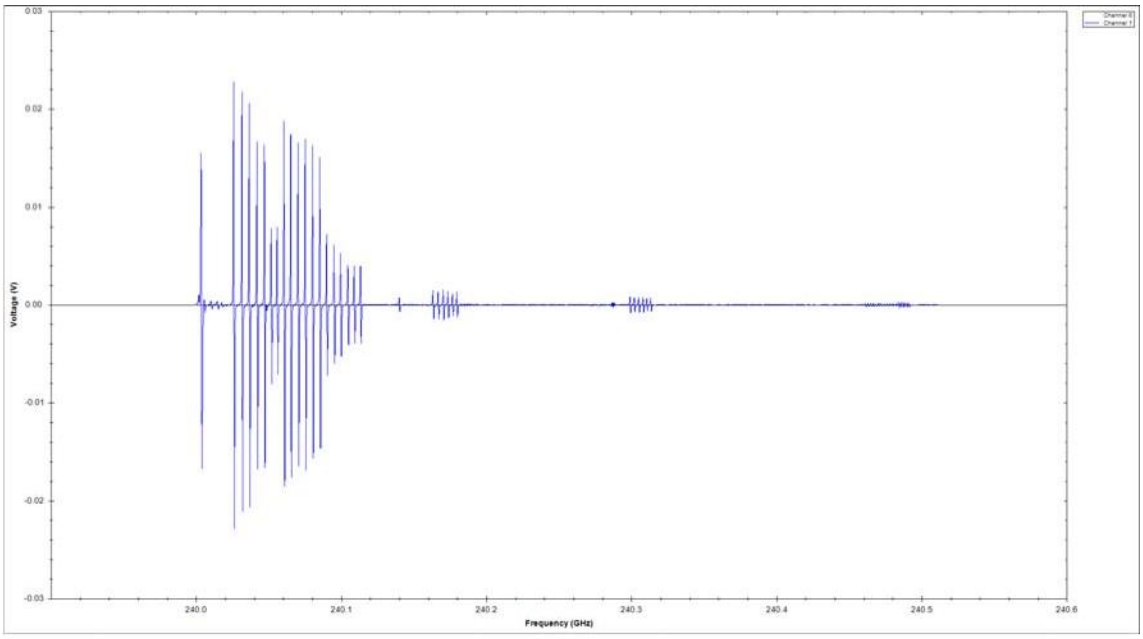

Snippets from Mixture 3

Appendix C. MET Report Forms

We have tried to be careful, but we are concerned that with the very large number of transcriptions required to fill out all of the forms that we may still have a clerical error. If there are discrepancies, the fundamental data are the LSQ and FM columns in the tables in the main body.

Phase I MACS Test Results

Please provide images of each spectrum measured in addition to completing the following tables. For selectivity results an image with all 32 snippets is requested and the individual spectrum for each molecule is not required.

Selectivity Test Results for Measured Sample Mixtures

Please fill in the following table with results measured with the MACS on the 3 sample mixtures labeled "Sample 1, Sample 2, and Sample 3" prepared at OSU. Protocol from preliminary tests was "yes" the molecule was detected, "no" the molecule was not detected, or "trace". For molecules labeled trace please explain in an attached paragraph the justification for trace classification and the threshold levels used. **Please see discussion in main text for Mixture 1 and in Appendix B for Mixtures 2 and 3.**

Library Molecule	**Mixture 1**	**Mixture 2**	**Mixture 3**
	D*	D	D
Sulfur Dioxide (SO_2)	Y	Y	T
Carbonyl Sulfide (OCS)	N	Y	N
Hydrogen Cyanide (HCN)	T	N	Y
Cyanogen Bromide (BrCN)	N	N	Y
Cyanogen Chloride (ClCN)	N	N	Y
Trifluoromethane (CHF_3)	Y	Y	N
Difluoromethane (CH_2F_2)	N	N	N
Dichloromethane (CH_2Cl_2)	N	N	N
Methyl Fluoride (CH_3F)	Y	N	N
Methyl Chloride (CH_3Cl)	N	Y	T
Methyl Bromide (CH_3Br)	Y	N	N
Methyl Iodide (CH_3I)	Y	N	N
1,1 Difluoroethene (CH_2CF_2)	Y	N	N
Acetonitrile (CH_3CN)	Y	N	Y
Vinyl Fluoride (C_2H_3F)	Y	Y	N
Vinyl Chloride (C_2H_3Cl)	N	T	N
1,1,1 Trifluoroethane ($C_2H_3F_3$)	N	N	N
Ethylene Oxide (C_2H_4O)	N	Y	N
1,2 dichloroethane ($C_2{}^{H}{}_4C^{l}{}_2$)	Y	N	N
Acrylonitrile (C_2H_3CN)	Y	N	Y

Propyne (C_3H_4)	N	Y	N
Acrolein (C_3H_4O)	Y	N	N
Propionitrile (C_2H_5CN)	Y	N	Y
Oxetane (C_3H_6O)	N	Y	N
Pyridine (C_5H_5N)	N	Y	N
**Carbonyl Fluoride (COF_2)	T	N	N
**Methanol (CH_3OH)	N	T	Y
**Thietane ($(CH_2)_3S$)	N	Y	N
**Methyl mercaptan (CH_3SH)	N	Y	N
**Methyl isocyanate (CH_3NCO)	N	N	Y
**Thionyl fluoride (F_2SO)	N	N	Y
**Vinyl bromide (CH_2CHBr)	Y	N	N

** Molecules added after dry run test

Selectivity Test Results for Synthetic Spectra

Please fill in the following table with results measured with the MACS on the 7 synthetic spectra labeled as shown in the table below. Protocol from preliminary tests was "yes" the molecule was detected, "no" the molecule was not detected, or "trace". For molecules labeled trace please explain in an attached paragraph the justification for trace classification and the threshold levels used. Where possible, please include a record of the signal strength for all molecules in each spectrum. **Please see fit results in main text for Mixture 1 and in Appendix B for Mixtures 2 and 3 for measured partial pressures in mTorr.**

Library Molecule	**Test 1**				**Test 2**		
	03_25a	**03_25b**	**04_03_V2**	**04_07_V2**	**06_05_A**	**06_05_B**	**06_05_C**
Sulfur Dioxide (SO_2)	Y	Y	N	N	Y	N	N
Carbonyl Sulfide (OCS)	Y	Y	N	Y	Y	N	Y
Hydrogen Cyanide (HCN)	Y	Y	N	T	Y	Y	N
Cyanogen Bromide (BrCN)	Y	Y	N	N	Y	Y	N
Cyanogen Chloride (ClCN)	Y	Y	Y	Y	Y	Y	N
Trifluoromethane (CHF_3)	Y	Y	N	N	Y	N	N
Difluoromethane (CH_2F_2)	Y	Y	N	N	Y	N	Y
Dichloromethane (CH_2Cl_2)	Y	Y	N	N	Y	N	N
Methyl Fluoride (CH_3F)	Y	Y	N	N	Y	Y	Y
Methyl Chloride (CH_3Cl)	Y	Y	N	N	Y	N	N
Methyl Bromide (CH_3Br)	Y	Y	N	N	Y	N	N
Methyl Iodide (CH_3I)	Y	Y	N	Y	Y	N	Y
1,1 Difluoroethene (CH_2CF_2)	Y	Y	N	Y	Y	N	N
Acetonitrile (CH_3CN)	Y	Y	T	T	Y	T	T
Vinyl Fluoride (C_2H_3F)	Y	Y	N	N	Y	Y	N
Vinyl Chloride (C_2H_3Cl)	Y	Y	N	Y	Y	Y	N
1,1,1 Trifluoroethane $_{(C2H3F3)}$	Y	Y	Y	Y	Y	Y	N
Ethylene Oxide (C_2H_4O)	Y	Y	Y	N	Y	Y	N

1,2 dichloroethane $_{(C2H4Cl2)}$	N	N	N	N	Y	Y	Y
Acrylonitrile (C_2H_3CN)	Y	Y	N	Y	Y	Y	N
Propyne (C_3H_4)	Y	Y	N	Y	Y	Y	N
Acrolein (C_3H_4O)	Y	Y	Y	Y	Y	N	N
Propionitrile (C_2H_5CN)	Y	Y	N	Y	Y	N	N
Oxetane (C_3H_6O)	Y	Y	N	Y	Y	N	Y
Pyridine (C_5H_5N)	Y	Y	N	Y	Y	Y	N
**Carbonyl Fluoride (COF_2)	N	N	N	N	Y	N	N
**Methanol (CH_3OH)	N	N	N	N	Y	N	N
**Thietane ($(CH_2)_3S$)	N	N	N	N	Y	N	N
**Methyl mercaptan (CH_3SH)	N	N	N	N	Y	N	N
**Methyl isocyanate (CH_3NCO)	N	N	N	N	Y	Y	N
**Thionyl fluoride (F_2SO)	N	N	N	N	Y	Y	N
**Vinyl bromide (CH_2CHBr)	N	N	N	N	Y	N	Y

** Molecules added after dry run test

Sensitivity Test Results for Tedlar Bags prepared by WSD

For sensitivity test results, please report the concentration of acetonitrile and deuterated acetonitrile measured in tedlar bag A or B. For the sensitivity test with an unknown molecule, labeled C, please report the molecule detected and the estimated concentration. Please include the procedure used for both sensitivity measurements.

Sample Label	Molecule	Concentration	Sampling Time
Bag "A"	Acetonitrile	-	-
Bag "A"	Deuterated Acetonitrile	52 (2) ppt	4 min
Bag "C"	CH3CN (0.24 mtorr) CH3OH (0.024 mtorr)	159 ppb (16 ppb)	4 min

Although the strong signals of the main isotope in Bag "A", would make the measurement straightforward, to protect the integrity of our measurement we do not observe the main isotope (if we did, we could then calculate the deuterated concentration even if the system were not particularly sensitive).

In Bag "C" we detect CH_3CN and CH_3OH at the pressure shown in the second column. However, the sorbent efficiency for CH_3OH has not been measured. If it were the same for CH_3OH as for CH_3CN, its concentration would be 16 ppb. Since we do not expect this sorbent to be especially efficient for CH_3OH, we expect that 16 ppb is a serious underestimate. Thus, we list this for completeness, but in parentheses to indicate that it is an estimate. We note, that this efficiency would not be hard to establish.

We used the same sampling procedures for these measurements as for previous runs that used the sorbents. However, since the samples could have been any of the 31 gases, we used the analysis procedures that we used for the mixtures of gases.

We note that above we observed a significant decrease in the sample concentration in the bags as a function of time.

Appendix A11.2

Determination of ROC Performance

Purpose. The MACS1 system is intended to deliver high ROC performance. However, ROC data cannot be directly measured for systems that operate in the high performance regime, that is, with high PD and low PFA. In general, these parameters are inferred from statistics related to the system operation. The purpose of this report is to prove that the MACS1 system is compliant with the contractual targets of PD=0.9999 and PFA=0.0001. This information was supplied to the MET.

Methodologies and Results. First, MACS is an assessment oriented system that produces a tabulated output of chemical species (and ultimately complexes of such species denoting products and processes). It is not a bell ringer style detector, and furthermore, the environment that completely influences each ROC curve can be very complex and quite varied. Ordinary ROC detection theory has its roots in radar. The precepts of this historic foundation are still relevant to the MACS system, which is indeed a receiver that detects and RF signal under a host of conditions, some environmental some of system origin. The core commodities are (1) whatever provides signal intensity; and (2) overall noise. The system provides both and can maximize S/N for particular conditions. Each ROC point (i.e., PD, PFA) can be obtained by estimates based on several techniques. We will employ a conservative estimate in a classical calculation based on amplitude detection theory applied to the spectral line "targets" or the absence thereof to determine conservative ROC values for the MACS1 sensitivity testing with 100 ppt concentrations from air at the input to the SAPM. The MET-produced the test species (acetylnitrile) lines (10) were used to render the computation of a conservative probability of false alarm for a detection probability set by the amplitude threshold to yield PD=0.9999.

To actually determine the operation of the system as a true detector the classical approach is utilized. Here we observe the noise and the signal (in the noise), and utilize the S+N and N-only distributions, integrating each from +infinity back to some amplitude threshold level (denoted DT=detection threshold). Due to the nature of our current system, the noise in the usable detection channels is either 1st or 2nd derivative. The resulting noise is essentially Gaussian, which facilitates the calculation. While there are energetic constraints that clip the tails of any real physical system's probability functions, the results are only improved by so doing, and as will be shown, the results are acceptable without the extensive study needed to determine and mathematically represented truncated noise.

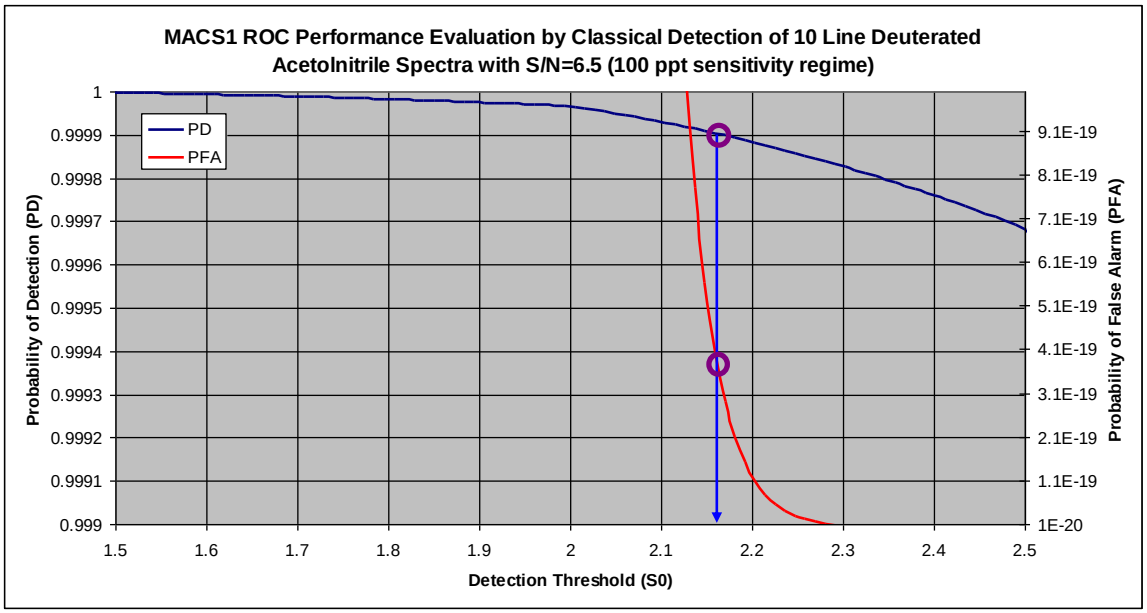

The inset figure gives the results of independently computed 10 line spectra for the 100 ppt regime with S/N=6.5. Note that each of the lines must be detected (that is the individual line PDs are multiplied together) as will be illustrated below.

The to MACS lines are thus detected like10 radar pulses and are mathematically modeled the same way. We begin by computing the integral of the N+S ("the PD") distribution from infinity to the detection threshold (DT). We then set the DT to the value corresponding to the system design point for PD (here, 0.9999). This instance is DT=2.16. Note that 10 lines are included. Then, we integrate the N ("the PFA") distribution to the same DT. This is a simple procedure:

$$PD_i = \int_{+\infty}^{DT} \frac{e^{-\frac{(x-S)^2}{2\sigma^2}}}{\sqrt{2\pi\sigma^2}} dx \tag{30}$$

Is the PD for each line and we have overall PD for the ensemble of lines:

$$PD = \prod_{i=1}^{NL} PD_i \tag{31}$$

For the PFA likewise we have:

$$PFA_i = \int_{+\infty}^{DT} \frac{e^{-\frac{x^2}{2\sigma^2}}}{\sqrt{2\pi\sigma^2}} dx \tag{32}$$

And

$$PFA = \prod_{i=1}^{NL} PFA_i \qquad (33)$$

Where NL=10 and S/N taken as Signal, S to noise, σ; for the data used, S=6 and σ=1. The tabular results for PD and PFA were used to extract the region of interest shown in the figure. We locat the threshold that will assure PD>0.9999 and then use the dame DT value to locate the corresponding PFA. In the figure it is apparent that the PFA of the system is approximately 3.9X10-19. This is not surprising. But both these values are actually somewhat better in practice.

So we gain from classical detection theory that MACS 1 can operate at within the desired ROC bounds. The further reduction of noise within the system, as well as system noise contributors (not electronic noise) are continuing objects for improvement, however, the sensitivity test data has thus been used to affirm the necessary performance.

Final Comment. We have calculated these parameters from many vantages. This one is selected because of its relative clarity. Still, the reader is advised to reflect that in this relatively simple model, the *detection* is registered if S+N>DT for all 10 lines. The lines are not infinitely narrow and the MACS system may have dozens of data points that complete the depiction of a spectral line. One can also include each of these points in the more complicated model. The result will be that you get a *higher* PD. Similarly, for noise to replicate the "detector" we have created in this paper, all 10 lines must appear. Since in actuality there are many more data points that can be included (again due to the line width), we can generate a more sophisticated estimate. But it will still give better results than we are listing. Since we have far exceeded the required performance, there is no advantage in further computations.

Appendix A11.3

Summary of MAG Contacts

JPEO-CBD, ECBC

Contact: Joe Maniaci (DARPA SETA) → Curt Wilhide (JPEO CBD)
Date: 5/26/05 -
Notes: Joe/FP interacted with Dave Cullin several years ago on MACS. Cullin has since left JPEO. Joe later set up meetings with Curt Wilhide, which never occurred. Curt indicated willingness to involve Ed Wack (Director here for Future Acquisitions).

Contact: Chris Ball (Battelle) → Raphael Moon (ECBC) → Fran D'Amico (ECBC)
Date: 8/22/07 – 8/28/07
Notes: Raphael wanted to involve D'Amico in MACS. Fran does a lot of T&E and ground truth field testing of many different sensors. He may be able to provide context with respect to requirements and performance of other, competitive sensor systems. Fran indicated willingness to participate in MAG. Bruce Jezek (Battelle Sr. Market Mgr., former Army) used to supervise Fran and says he is a good guy.

Contact: Chris Ball (Battelle) → Alan Samuels (ECBC)
Date: 10/30/07
Notes: Alan accepted an invitation to be a member of MACS. Alan is focused mainly on CW agents as well as byproducts and related species. He also recommends involving atmospheric chemists to better understand environmental degradates.

Contact: Keith Reiss (ST) → Alan Samuels (ECBC) → James Savage (???)
Date: 11/23/07
Notes: Alan contacted Savage to get additional information/reports on CW agent degradation products that are conducive to detection by MACS.

Contact: Joe Maniaci (DARPA SETA) and Alan Samuels (ECBC) → COL Mark Malatesta, LTC Gregory Green, Tim Ganguly (JPEO CBD)
Date: 1/8/08
Notes: Meeting at PM Guardian involving FP, Joe, and Alan to discuss requirements and interest in MACS. Alan is to follow up on MANSCEN and NORTHCOM, possible JCTD interest, and improvements over ACADA.

Contact: Alan Samuels (ECBC) → Nancy Kammerer (ECBC), Robert Eckhaus (RDECOM), Arne Johnson (ECBC), John Harris (ECBC), Joseph Lovrich (NBC Contamination Avoidance), Randy Young (NBC Contamination Avoidance)
Date: 2/29/08
Notes: Discussed possible fits for MACS technology. Alan introduced the technology via e-mail. Requested information on targeted capabilities, requirements, etc. to help steer Phase 2. Intend to share technology requirements with FP. Response from Eckhaus, Lovrich. Sent JCAD requirements.

Contact: Joe Maniaci (DARPA SETA) → Raphael Moon (ECBC) → Richard Floyd (JPEO CBD)
Date: 3/11/08
Notes: Raphael has made contact with and has been trying to set up a meeting with Floyd re: transition programs.

Contact: Joe Maniaci (DARPA SETA) → Marisa Lalekos (JPEO CBD, Schafer Corp.)
Date: 3/16/08
Notes: Marisa contacted Joe with questions about maturity of MACS and transition plan. Joe trying to set up meeting with her, Curt Wilhide, and Rich Floyd.

Other DoD Agencies

Contact: Chris Ball (Battelle) → Kathy Macdonald (DARPA SOCOM liaison)
Date: 8/22/07-12/7/07
Notes: Kathy indicated willingness to identify potential MAG participants from SOCOM. She thinks there is a community of potential users with a variety of missions. She has sent information to Frank Patten directly.

Contact: Keith Reiss (ST) → Joe Maniaci (DARPA SETA) → Jim Morgan (DARPA SETA) → Col. Timothy Tritch (DARPA Army liaison)
Date: 2/8/08
Notes: Tritch is interested in bomb making, cluttered environments. Has concerns about sorbents being ruined by saturation, residues on internal piping, system corruption. Sees complex signature recognition as only advantage for MACS. Interested in taggants. Tritch was invited, but did not attend, Laura's meeting on 1/28/08 at DARPA. Morgan attended the meeting, and asked about jamming and being jammed. Subsequent meeting involving Keith, Joe, Tritch, and Morgan. Morgan indicated that we should talk to Bill Forrester (ret. Army Col, Booz Allen, Chemical Materials Agency)and Jim Genovese (civ. Scientist ECBC, R&T directorate). Alan has taken lead on making these contacts. Also recommended we talk to DARPA PM Michael Pagels re: Posse program that may be synergistic to MACS.

Contact: Laura Vandenberg (DARPA SETA) → David Kearney, Michael Whittaker (NSWDG)
Date: 12/22/07-1/28/08
Notes: Were contacted by Laura and invited to attend meeting on 1/28/08 (did not attend).

Contact: Laura Vandenberg (DARPA SETA) → Scott Burns (DIA), Chris Tipple (Director of Laboratory Operations, DIA/DTK)
Date: 12/22/07-1/28/08
Notes: Were contacted by Laura and invited to attend meeting on 1/28/08. Both attended.

Contact: Laura Vandenberg (DARPA SETA) → Chris Cunningham (20th Support Command)
Date: 12/22/07-1/28/08
Notes: Attended Laura's meeting on 1/28/08. Is involved with hands-on material collection with limited time (5 min-1 hr). Experience with portable FTIR and Raman, etc. Concerned about battery operation and ruggedization. Typical detections are low ppm. Cited M256 test kit.

Contact: Laura Vandenberg (DARPA SETA) → Paul Benda (Director, CBRNE Directorate, PFPA), Christina Murata (Chief Science Officer, CBRNE Directorate, PFPA)
Date: 12/22/07-1/28/08
Notes: Benda attended Laura's meeting on 1/28/08. He exited early but left Laura a page of notes. He asked about chlorine and looked skeptical over idea of indirect detection.

Contact: Laura Vandenberg (DARPA SETA) → (CBIRF)
Date: 12/22/07
Notes: Were contacted by Laura and invited to attend meeting on 1/28/08 (did not attend).

Intelligence Community

Contact: Chris Ball (Battelle) → Paul J., Rich P., Mark D. (XXX)
Date: 7/25/07-12/31/07
Notes: This organization may be very interested in MACS. Paul has tried to engage management to see if they can find a way to assist the MAG. Rich has offered suggestions on sensor requirements for field use. Mark (management) has expressed some interest in the technology.

Contact: Chris Ball (Battelle) → Dick Garr (Battelle, Special Programs Market Sector) → Donald Ferris (AFTAC/TMK)
Date: 8/7/07
Notes: Dick spoke with Ferris regarding possible participation on MAG. Ferris indicated he was willing and able.

Contact: Keith Reiss (ST) → Chris Ball (Battelle) → Tom M. (XXX)
Date: 12/6/07
Notes: We've made repeated attempts to engage Tom via phone and e-mail. We intend to invite him to be a MAG participant.

Contact: Keith Reiss (ST) → Pat Hughes (L3) → Barbara Sanderson, Peter Bythrow (DIA)
Date: 7/1/02
Notes: Keith met Barbara at CMO. They have offered to assist with moving things forward with DARPA (pre-MACS). They seemed very interested in the technology.

Contact: Chris Ball (Battelle) → Charmaine Gilbreath, Todd Hawley (DIA, National Signatures Program)
Date: 4/18/07
Notes: NSP is interested in following the progress of MACS and on future signature development as it pertains to their signature library products. NSP is facilitating establishment of THz signature library. They have direct ties to JIEDDO and HME detection programs.

Other Non-DoD Agencies

Contact: Chris Ball (Battelle) → Dave Clark (Battelle) → Mark Hoover (Senior Scientist, NIOSH Nanotechnology and Division of Respiratory Disease Studies)
Date: 7/16/07
Notes: Hoover: "The topic of direct-reading methods for chemicals is certainly of great interest to NIOSH. And as we know from the recent NIOSH terrorism preparedness and emergency response project that you and I collaborated on regarding the state-of-art for chemical and biological sensors, understanding the user community needs and providing a strong science base for methods testing and validation is key." Recommended MAG participation of Anita Schill, PhD, Interim Assoc. Director for Science.

Contact: Chris Ball (Battelle) → Dave Clark (Battelle) → Rebecca Blackmon (nee Lankey) (TSWG)
Date: 8/28/07
Notes: Rebecca is a recognized expert in air pollution emission analysis. TSWG would be a good candidate for the MAG because it represents agencies across Government and addresses multi-agency requirements. Rebecca indicated willingness to participate in MAG.

Contact: Keith Reiss (ST) → Chris Ball (Battelle) → John Bosch (EPA)
Date: 10/30/07
Notes: John accepted an invitation to be a member of MACS. John is involved with new emission monitoring technologies and their national policy applications. He also has good contacts in DoD who do environmental monitoring.

Contact: Keith Reiss (ST) → Chris Ball (Battelle) → Ken Baicar (FBI)
Date: 11/5/07
Notes: Ken accepted an invitation to be a member of MACS.

Contact: Henry Everitt (AMRDEC) → Geoff Ling (DARPA) → Geoffrey Ginsburg (Duke)
Date: 11/13/07
Notes: Discussed MACS in the context of breath analysis for early detection of disease onset. Ginsburg has a seedling project on the subject.

Appendix A11.4

MAG Questionnaire and Responses

Mission Adaptable Chemical Sensor (MACS) Advisory Group (MAG) Questionnaire

Name	_____	Phone	_____
Agency	_____	Fax	_____
Office	_____	E-mail	_____
Address	_____		

The intention of this questionnaire is to gauge interest in the MACS sensor technology and to focus system requirements for subsequent development phases. Please answer the following questions to the best of your knowledge. If you have any questions, please contact:

- Keith Reiss – phone: 703-385-2750 x111, e-mail: kreiss@smarttransitions.com
- Chris Ball – phone: 614-424-6502, e-mail: ballc@battelle.org
- Laura Vanderberg – phone: 757-897-3539, e-mail: laura.vanderberg@jhuapl.edu
- Joe Maniaci – phone: 703-797-4558, e-mail: jmaniaci@sainc.com

☐ The requested information is sensitive/classified. Please contact me to discuss secure information transfer options.

Interest in MACS development

Please characterize your organization's interest in MACS

☐ Interested in the continued development of the MACS technology
☐ Potential user of the technology
☐ Potential transition partner/funding source for technology development/transition
☐ Interested in funding additional development
☐ Interested in performing or supporting tests of prototype or field systems
☐ Other _____

Sensing mission type

Please identify the types of missions that would benefit from MACS technology

☐ MASINT collection and analysis
☐ Fixed site protection
☐ WMD forensic analysis
☐ Medical diagnosis
☐ Field test support
☐ Security threat detection
☐ Contamination avoidance
☐ Pollution monitoring
☐ Battlefield characterization
☐ Laboratory chemical analysis
☐ IED detection
☐ Industrial process monitoring
☐ Other _____

Target materials
Please identify classes and chemical targets and provide specific examples

- ☐ Toxic industrial chemicals
- ☐ TIC/CWA precursors or degradates
- ☐ Typical trace atmospheric constituents
- ☐ Expired breath chemicals
- ☐ Nuclear/radiological and related materials
- ☐ Chemical warfare agents
- ☐ Standard industrial chemicals
- ☐ Biological materials, proteins, agents
- ☐ Explosives and related materials
- ☐ Environmental pollutants

Specify chemicals of interest:_____
_____

Detection sensitivity
Please specify chemical detection sensitivity specifications

- ☐ > ppm
- ☐ 10 ppb – 1 ppm
- ☐ 100 ppt – 10 ppb
- ☐ 1 ppt – 100 ppt

Detection selectivity
Please characterize the desired performance for detecting multiple materials

- ☐ Detect >30 target materials simultaneously
- ☐ Detection of several chemicals simultaneously
- ☐ Detection of single chemicals
- ☐ Detect in the presence of cluttered environment (battlefield, urban)

Response time
Please identify the response time requirement for a single measurement cycle: sample acquisition, spectral interrogation, analysis, report

- ☐ > 10 minutes
- ☐ 5 – 10 minutes
- ☐ 1 – 5 minutes
- ☐ < 1 minute

System size, weight
Please identify the size and weight requirements for a future MACS system

- ☐ Fixed installation, vehicle mounted (> 1 ft^3, >50 lbs)
- ☐ Vehicle, air mounted (½ ft^3 – 1 ft^3, 25 – 50 lbs)
- ☐ Man-portable (< ½ ft^3, < 25 lbs)

System power
Please specify the power source requirements

- ☐ External power (AC line, vehicle battery)
- ☐ Internal power (battery)

Mission duration

Please specify the typical duration of a single sensor mission

- ☐ Months
- ☐ Weeks
- ☐ Days
- ☐ 12-24 hours
- ☐ 6-12 hours
- ☐ 3-6 hours
- ☐ 1-3 hours
- ☐ < 1 hour
- ☐ Continuous operation
- ☐ Sporadic operation

Ruggedness/waterproof

Please indicate desired level of ruggedness for a fielded MACS system

- ☐ Waterproof
- ☐ Water resistant
- ☐ Easily packaged in waterproof container
- ☐ Withstands drop from 6 ft onto cement floor
- ☐ Withstands off-road ride in truck bed or high speed boat
- ☐ Withstands off-road ride in truck bed or high speed boat when adequately packaged

Technical expertise of potential operator

Please indicate the desired education level of a potential operator of a fielded MACS system

- ☐ No technical background or training
- ☐ Layman operator
- ☐ Trained technician
- ☐ Advanced science/engineering degree

Production volume

Please indicate how many MACS units could, in the future, be purchased to meet mission needs

- ☐ > 1000
- ☐ 100-1000
- ☐ 10-100
- ☐ < 10
- ☐ Willing to field several prototype instruments for preliminary field use

Current detector technology

Please list detectors currently used by your organization to meet mission requirements

_____
_____
_____
_____
_____

Additional requirements

Please identify any additional requirements not addressed in this questionnaire

_____

_____

_____

_____

_____

Mission Adaptable Chemical Sensor (MACS) Advisory Group (MAG) Questionnaire

Name Tony Szalkowski Phone 703 735 2617
Agency NGA Fax
Office DARPA Liaison Team E-mail SzalkowA@NGA.MIL
Address
Also Contact Fred Schwarze (NGA Liaison @ DARPA) 571-218-4795

The intention of this questionnaire is to gauge interest in the MACS sensor technology and to focus system requirements for subsequent development phases. Please answer the following questions to the best of your knowledge. If you have any questions, please contact:

- Keith Reiss – phone: 703-385-2750 x111, e-mail: kreiss@smarttransitions.com
- Chris Ball – phone: 614-424-6502, e-mail: ballc@battelle.org
- Laura Vanderberg – phone: 757-897-3539, e-mail: laura.vanderberg@jhuapl.edu
- Joe Maniaci – phone: 703-797-4558, e-mail: jmaniaci@sainc.com

☐ The requested information is sensitive/classified. Please contact me to discuss secure information transfer options.

Interest in MACS development

Please characterize your organization's interest in MACS

☐ Interested in the continued development of the MACS technology
☒ Potential user of the technology
☐ Potential transition partner/funding source for technology development/transition
☐ Interested in funding additional development
☐ Interested in performing or supporting tests of prototype or field systems
☐ Other _____

Sensing mission type

Please identify the types of missions that would benefit from MACS technology

☒ MASINT collection and analysis
☐ Fixed site protection
☐ WMD forensic analysis
☐ Medical diagnosis
☐ Field test support
☐ Security threat detection
☐ Other _____
☐ Contamination avoidance
☐ Pollution monitoring
☒ Battlefield characterization
☐ Laboratory chemical analysis
☐ IED detection
☐ Industrial process monitoring

Target materials

Please identify classes and chemical targets and provide specific examples

☐ Toxic industrial chemicals
☐ TIC/CWA precursors or degradates
☒ Typical trace atmospheric constituents
☐ Expired breath chemicals
☐ Nuclear/radiological and related materials
☒ Chemical warfare agents
☐ Standard industrial chemicals
☒ Biological materials, proteins, agents
☒ Explosives and related materials
☐ Environmental pollutants

Specify chemicals of interest: _____

Ruggedness/waterproof

Please indicate desired level of ruggedness for a fielded MACS system

- ☐ Waterproof
- ☐ Water resistant
- ☐ Easily packaged in waterproof container
- ☐ Withstands drop from 6 ft onto cement floor
- ☐ Withstands off-road ride in truck bed or high speed boat
- ☐ Withstands off-road ride in truck bed or high speed boat when adequately packaged

Technical expertise of potential operator

Please indicate the desired education level of a potential operator of a fielded MACS system

- ☑ No technical background or training
- ☐ Layman operator
- ☐ Trained technician
- ☐ Advanced science/engineering degree

Production volume

Please indicate how many MACS units could, in the future, be purchased to meet mission needs

- ☐ > 1000
- ☐ 100-1000
- ☐ 10-100
- ☐ < 10
- ☐ Willing to field several prototype instruments for preliminary field use

Current detector technology

Please list detectors currently used by your organization to meet mission requirements

_____

_____

_____

_____

_____

Additional requirements

Please identify any additional requirements not addressed in this questionnaire

_____

_____

_____

_____

_____